Journal of Inorganic and General Chemistry

ZAAC

Zeitschrift für anorganische und allgemeine Chemie

18
2016

"Thick and thin Multifaceted Properties of Layered Materials"
Abstracts of the 18. Conference of the GDCh Division
Solid State Chemistry and Materials Research Innsbruck,
Austria September 19–21, 2016

www.zaac.wiley-vch.de

ISSN 0044-2313 · Vol. 642 · Iss. 18 · September, 2016

WILEY-VCH

Journal of Inorganic and General Chemistry

ZAAC

Zeitschrift für anorganische und allgemeine Chemie

Editors

Prof. Dr. Thomas F. Fässler
Technische Universität München
Lichtenbergstr. 4
85748 Garching (Germany)
E-Mail: zaac@lrz.tum.de

Prof. Dr. Thomas M. Klapötke
Ludwig-Maximilians-Universität
Butenandtstraße 5–13
81377 München (Germany)
E-Mail: zaac@cup.uni-muenchen.de

Prof. Dr. Christian Limberg
Humboldt-Universität zu Berlin
Institut für Chemie
Brook-Taylor-Straße 2
12489 Berlin (Germany)
E-Mail:
christian.limberg@chemie.hu-berlin.de

Publisher

Editorial Office
Dr. Sabrina Turba
Wiley-VCH Verlag GmbH & Co. KGaA
Boschstr. 12
69469 Weinheim (Germany)
Phone: + 49-6201-606-574
Fax: + 49-6201-606-331
E-Mail: zaac-office@wiley-vch.de

All matters concerning processing of manuscripts once they have been accepted should be addressed to Dr. Sabrina Turba.

Manuscript Submission

www.editorialmanager.com/zaac

Homepage

www.zaac.wiley-vch.de

Wiley Online Library
wileyonlinelibrary.com

International Advisory Board

Evgeny V. Antipov, Moscow (Russian Federation)
Johannes Beck, Bonn (Germany)
Wolfgang Bensch, Kiel (Germany)
Eugenio Coronado, Valencia (Spain)
Stefanie Dehnen, Marburg (Germany)
Hans-Jörg Deiseroth, Siegen (Germany)
Frank T. Edelmann, Magdeburg (Germany)
Claus Feldmann, Karlsruhe (Germany)
Dieter Fenske, Karlsruhe (Germany)
Helmer Fjellvag, Oslo (Norway)
Song Gao, Beijing (China)
Bernd Harbrecht, Marburg (Germany)
Sjoerd Harder, Erlangen (Germany)
Evamarie Hey-Hawkins, Leipzig (Germany)
Christoph Janiak, Düsseldorf (Germany)
Cameron Jones, Monash (Australia)
Peter C. Junk, Townsville (Australia)
Mercouri Kanatzidis, Evanston, IL (USA)
Rhett Kempe, Bayreuth (Germany)
Peter Klüfers, München (Germany)
Rüdiger Kniep, Dresden (Germany)
Robert L. LaDuca, East Lansing, MI (USA)
Sven Lidin, Lund (Sweden)
Antoine Maignan, Caen (France)
Thomas Maschmeyer, Sydney (Australia)
Gerd Meyer, Köln (Germany)
Gordon J. Miller, Ames, IA (USA)
Srinivasan Natarajan, Bangalore (India)
Reinhard Nesper, Zürich (Switzerland)
Rainer Pöttgen, Münster (Germany)
Peter. W. Roesky, Karlsruhe (Germany)
Matthew J. Rosseinsky, Liverpool (UK)
Michael Ruck, Dresden (Germany)
Masahiro Sadakane, Hiroshima (Japan)
Manfred Scheer, Regensburg (Germany)
Thomas Schleid, Stuttgart (Germany)
Wolfgang Schnick, München (Germany)
Hansgeorg Schnöckel, Karlsruhe (Germany)
Won-Kyung Seok, Seoul (Korea)
Konrad Seppelt, Berlin (Germany)
Christian Serre, Versailles (France)
Dirk Steinborn, Halle/S. (Germany)
Douglas W. Stephan, Toronto (Canada)
Werner Uhl, Münster (Germany)
Michael Veith, Saarbrücken (Germany)
Mathias S. Wickleder, Oldenburg (Germany)

ZAAC was founded in 1892 by G. Krüss (1895†) and continued by

R. Lorenz (1895–1929), G. Tammann (1904–1938), W. Biltz (1930–1943), W. Klemm (1939–1965), E. Zintl (1939–1941), O. Hönigschmid (1941–1942), R. Fricke (1942–1950), W. Hieber (1942–1945), U. Hofmann (1942–1945), R. Schwarz (1942–1958), G. Rienäcker (1947–1988), J. Goubeau (1959–1980), H. Schäfer (1966–1980), G. Fritz (1981–1997), R. Hoppe (1981–1997), L. Kolditz (1989–1990), W. Hanke (1990–2008), W. Bronger (1997–2006), K. Dehnicke (1997–2007), M. Jansen (2007–2014).

Corrected Galley Proofs

Galley proofs will be sent to the authors with a reprint order form. The authors are asked to send back the corrected galley proofs within the given time limit to the **Editorial Office**. Otherwise the Imprimatur for the publication will be given by the Editors.

Production/Reprints

Stefanie Labonte
Phone: + 49-6201-606-138
Fax: + 49-6201-606-331
E-Mail: slabonte@wiley.com

Marketing

Monika Silz
Phone: + 49-6201-606-458
E-Mail: msilz@wiley.com

Advertising

Marion Schulz
Phone: +49-6201-606-565
Fax: +49-6201-606-550
E-Mail: mschulz@wiley.com

Copyright Permission

Bettina Loycke
Phone: + 49-6201-606-280
Fax: + 49-6201-606-332
E-Mail: rightsde@wiley.com

Editorial Director

Dr. Carina S. Kniep
Phone: + 49-6201-606-308
E-Mail: stm-journals@wiley-vch.de

Publishers

Wiley-VCH Verlag GmbH & Co. KGaA
P. O. Box 10 11 61
69451 Weinheim (Germany)
Phone: + 49-6201-606-400
Fax: + 49-6201-606-184
Homepage: www.wiley-vch.de

Subscriptions

Customer Service
Phone: +49-6201-606-400
Fax: +49-6201-606-184
www.wileycustomerhelp.com

Courier Services

Boschstraße 12, 69469 Weinheim, Germany

Publication: 24 issues per year

© 2016 Wiley-VCH Verlag GmbH & Co. KGaA, Weinheim

GDCh

Gesellschaft Deutscher Chemiker

Fachgruppe Festkörperchemie
und Materialforschung

18. Vortragstagung

Dick und dünn: facettenreiche Eigenschaften von Schichtmaterialien

19. – 21. September 2016
Innsbruck, Österreich

www.gdch.de/fmf2016

Liebe Mitglieder der Fachgruppe Festkörperchemie und Materialforschung,

die Fachgruppe Festkörperchemie und Materialforschung der GDCh trifft sich dieses Jahr in der wunderschönen Stadt Innsbruck zur Jahrestagung. Als Vorsitzender der Fachgruppe begrüße ich Sie herzlich zu dieser Veranstaltung. Das lokale Organisationskomitee unter Leitung von Hubert Huppertz hat die Tagung hervorragend vorbereitet.

Im Fokus von „Dick und dünn: facettenreiche Eigenschaften von Schichtmaterialien“ stehen die Synthese und Eigenschaften sehr dünner Schichtmaterialien, welche in den letzten Jahren in den Fokus der Festkörperchemie und Materialforschung geraten sind. Die fünf Plenarvorträge bilden das breite und attraktive Gebiet von Schichtmaterialien in hervorragender Weise ab. Mit den Hauptvortragenden J. Goldberger, Frau B. V. Lotsch, D. C. Johnson, J. Breu und T. Heine konnten international ausgewiesene Experten gewonnen werden. Die Fachgruppe wird zum ersten Mal die Rudolf-Hoppe-Vorlesung vergeben und M. Wickleder wird die Laudatio halten. Ein weiterer Höhepunkt stellt die Verleihung des H. C. Starck-Promotionspreises für Anorganische Festkörperchemie durch Herrn Dr. Schnitter dar. Zusätzlich werden wieder die besten Poster prämiert.

Lassen Sie sich von der bei der Tagung angebotenen Vielfalt anorganischer Festkörperchemie und Materialforschung inspirieren, frischen Sie alte Kontakte auf und knüpfen Sie neue. Genießen Sie die Zeit in Innsbruck, nicht nur wissenschaftlich, sondern auch gesellschaftlich.

In diesem Sinne viel Spaß bei der Tagung!

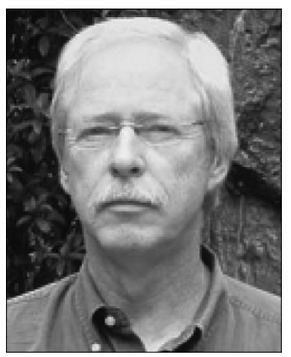

Ihr **Wolfgang Bensch**, Kiel

 © 2016 Wiley-VCH Verlag GmbH & Co. KGaA, Weinheim

Journal of Inorganic and General Chemistry
ZAAC
Zeitschrift für anorganische und allgemeine Chemie

Tagungsheft

„Dick und dünn: facettenreiche Eigenschaften von Schichtmaterialien“
Beiträge zur 18. Vortragstagung der GDCh Fachgruppe
Festkörperchemie und Materialforschung

“Thick and thin – Multifaceted Properties of Layered Materials”
Abstracts of the 18. Conference of the GDCh Division
Solid State Chemistry and Materials Research

Invited Lectures

J. Goldberger, M. Arguilla, S. Jiang, N. Cultrara* ..... **997** — Two-Dimensional Materials from van der Waals Zintl Phases

*B. V. Lotsch** ..... **998** — 2D or not 2D? Two-Dimensional Nanostructures for Sensing and Energy Storage

*D. C. Johnson** ..... **999** — Trapping Metastable Solids via Designed Precursors

*J. Breu** ..... **1000** — Why Melt Synthesis is a Game Changer for Clays

*T, Heine** ..... **1001** — Quantenconfinement: eine alternative Methode zum Design funktionaler zweidimensionaler Kristalle

Oral Presentations

V. Hlukhyy, T. F. Fässler* ..... **1003** — Structural Instability in Layered $BaNi_2Ge_2$ and Influence of VEC on the Distortion of the $ThCr_2Si_2$-Type

*R. Hanus, X. Guo, G. Li, G. J. Snyder, W. G. Zeier** ..... **1003** — Structural Origin of the Band Convergence in Skutterudite $CoSb_3$

*F. Stegemann, O. Janka** ..... **1004** — The Crystal Structure of $BaPt_2Al_5$

F. Jach, S. I. Brückner, A. Ovchinnikov, M. Bobnar, A. Isaeva, M. Groh, E. Brunner, P. Höhn, M. Ruck* ..... **1004** — The Acetonitrilide Anion CCN^{3-}

*D. Hermann, H. Schwartz, U. Ruschewitz** ..... **1005** — MOFs as Hosts for *Pi*-Conjugated Molecules

*T. Wehner, M. Schneider, K. Mandel, G. Sextl, K. Müller-Buschbaum** ..... **1006** — Multifunctional Core/Shell-Structures of Luminescent MOFs and Superparamagnetic Fe_3O_4/SiO_2 Microparticles

*K. Hofmann, N. Kalyon, B. Albert** ..... **1007** — Sheets of Six-Membered Rings in Borides and Boride Carbides: Honeycomb, Chair, Boat, or a Combination Thereof

 © 2016 WILEY-VCH Verlag GmbH & Co. KGaA, Weinheim

CONTENTS

A. Weiz, A. Isaeva,, W. Van den Broek, J. Biskupek, U. Kaiser, T. Doert, M. Ruck* ..... **1007** — Bismuth−Oxide Nanotubes

*K. M. Freitag, H. Kirchhain, L. van Wüllen, T. Nilges** ..... **1008** — Electrospun Solid Electrolytes for Lithium Ion Batteries

*M. Oschatz, S. Kaskel** ..... **1008** — Carbide-Derived Carbons with Hierarchical Pore Architecture as Electrochemical Energy Storage Materials

A. Egger, N. Schrödl, W. Sitte* ..... **1009** — Cr-Poisoning of La_2NiO_{4+} in Solid Oxide Cells

T. Lunkenbein, E. Frei, J. Schumann, M. Behrens, M. G. Willinger, R. Schlögl* ..... **1009** — Local Information Powers Heterogeneous Catalysis Research: TEM Reveals a Layered ZnO in Industrial Relevant $Cu/ZnO/Al_2O_3$ Catalyst

T. Götsch, M. Stöger-Pollach, A. Menzel, E. Bertel, S. Penner* ..... **1010** — The Crystallography and Electronic Structure of YSZ Thin Films

S. Ebbinghaus, N. Quandt, T. Walther* .... **1010** — Spin Coating of Multiferroic Composite Thin Films

*R. R. Zimmermann, M. Siebert, R. Dittmeyer, M. Armbrüster** ..... **1011** — Films of Intermetallic Compounds Prepared by DC Magnetron Sputtering

*S. Krüger, C. Wickleder** ..... **1011** — Red Emission of Eu^{2+} Ions Doped in Oxides and Zirconates as Promising New Candidates for Future LEDs

*D. Bichler** ..... **1012** — Narrow Band Emitting Red Phosphor $Sr(Sr,Ca)Si_2Al_2N_6:Eu^{2+}$

O. Oeckler, L. Neudert, P. Schultz, D. Durach, W. Schnick* ..... **1013** — Komplexe Silicatstrukturen in Mikrodomänen von Lumineszenzmaterialien

*C. Feldmann** ..... **1014** — Graphitic Carbon Dots: Synthesis and Rare-Earth-Based Luminescence

A. Petzold, S. Mascotto, G. Goerigk, D. Clemens, B. Kayaalp, J. Scholz, A. Juhl, M. Fröba, M. Ballauff* ..... **1014** — Distribution of Sulfur in Carbon-Sulfur Nanocomposites Analyzed by Small-Angle Scattering Methods

*G. Heymann** ..... **1015** — Binary Palladium Selenides from Multianvil High-Pressure Experiments

*J. Schneider, R. Schwaiger, S. Baumann, T. Berger, G. Bourret O. Diwald** ..... **1015** — Size Effects in MgO Cube Hydration and Dissolution

H. A. Höppe, S. G. Jantz, K. Förg, A. Kirchhain, P. Gross* ..... **1016** — Layered $Ba[B_4O_6F_2]:Eu$ − On Some New Silicate-Analogous Compounds

*K. F. Ortega, C. Lüttmann, D. Rein, F. Özcan, M. Behrens** ..... **1016** — Layered Double Hydroxides as Precursors for Mixed Metal and Mixed Metal Oxide Catalysts

A. Ovchinnikov, M. Bobnar, Y. Prots, H. Borrmann, J. Sichelschmidt, Y. Grin, P. Höhn** ..... **1017** — Layered Alkaline-Earth Metal Nitridomanganates: Synthesis, Crystal Structures and Physical Properties

*N. C. Hildebrandt, A. Blößer, R. Marschall** ..... **1018** — Mesostructured Layered Perovskites for Solar Energy Conversion

 © 2016 WILEY-VCH Verlag GmbH & Co. KGaA, Weinheim

Posters

*M. Ertl, J. Moir, G. Ozin, J. Breu** ..... **1019** Ferrihydrite Outperforms Haematite in Electrochemical Water Oxidation

*C. Habel, J. Breu** ..... **1019** Verbesserte Heliumbarrieren durch Schichtsilikat-Nanokomposit Filme

*M. Stöter, S. Gödrich, S. Rosenfeldt, G. Papastavrou, J. Breu**..... **1020** Conversion of Bilayers into Janus Monolayers

*A. Edenharter, M. Schöttle, J. Breu** ..... **1020** Topotactic Al-Pillaring of a well characterized Synthetic Fluorohectorite

*T. Martin, J. Fleissner, W. Milius, J. Breu**..... **1021** Polymorphie des Luminols

*K. Ament, S. Förster, J. Breu** ..... **1021** Ordered Intercalation of Nanoparticles into the Interlayer Space of Clay

*T. Martin, T. Gorelik, D. Greim, C. Butterhof, U. Kolb, J. Senker, J. Breu** **1022** Polymorphie des Konservierungsmittels Natriumbenzoat (E211)

E. Doblhofer, J. Schmid, M. Suntinger, H. Bargel, C. Hugenschmidt, J. Breu, T. Scheibel* ..... **1022** Going Green: Spider Silk-Nanoclay Composites for Sustainable Flexible Food Packaging

*K. Förg, H. A. Höppe** ..... **1023** The Borophosphate $(NH_4)_2[B_2P_3O_{11}(OH)]$

M. Petrik, W. Hornfeck* ..... **1023** Packings of Sphere Packings − An Unexplored Path to New Structures

M. Niedermaier, A. Gheisi, J. Bernardi, O. Diwald* ..... **1024** Functionalization of Oxide Nanocrystals and Composites with Transition Metal Ions

*O. Pecher, B. Mausolf, V. Peters, K. Lamberts, A. Korthaus, F. Haarmann** **1024** Local Atomic Order in $M(Al_{1-x}Ga_x)_4$ *with M = Sr, Ba*

*B. Kayaalp, Y. Lee, A. Kornowsky, S. Gross, S. Mascotto**..... **1025** Cooperative Assembly Synthesis of Mesoporous $SrTiO_3$ with Enhanced Photocatalytic Activity

*J. Scholz, Y. Lee, A. Meyer, S. Mascotto** ..... **1025** Crystallization Studies of Perovskite Oxides Confined in Nanopores

*Y. Chen, R. Kriegel, G. Beier, D. C. A. Ivarsson, M. Greiner, T. Keilhauer, M. Armbrüster**..... **1026** An in situ XPS Study of Intermetallic ZnPt in Methanol Steam Reforming

A. Zeugner, A. Isaeva, M. Kaiser, T. Doert, M. Ruck* ..... **1027** Crystal Growth of the New Topological Insulator Bi_2TeI

*R. Lauenstein, C. M. Hamm, C. S. Birkel**..... **1027** Solid State Microwave Synthesis of Ti_2SnC MAX Phase

*C. M. Hamm, C. S. Birkel** ..... **1028** Field Assisted Synthesis of M_2AlC (M = Ti, V, Cr) MAX Phases

 © 2016 WILEY-VCH Verlag GmbH & Co. KGaA, Weinheim

CONTENTS

M. Oschatz, K. P. de Jong*	**1028**	Support Effects on Iron Catalysts for the Direct Production of Lower Olefins from Synthesis Gas
I. Hartenbach, Th. Schleid, S. Strobel*	**1029**	Two Modifications of $Dy_2[MoO_4]_3$
*D. Vitzthum, K. Wurst, H. Huppertz**	**1029**	Synthesis and Crystal Structure of the New High-Pressure Indium Borate $In_{19}B_{34}O_{74}(OH)_{11}$
T. Jahn, I. Weimann, J. Feller, Z. Žák*	**1030**	Phase Analysis on the Quasi-Ternary System $CuO/Fe_2O_3/V_2O_5$ and Characterization of $Cu_4FeO(VO_4)_3$
*J. G. Heck, C. Feldmann**	**1030**	Inorganic-Organic Hybrid Nanoparticles for Drug Delivery and Optical Imaging
T. Zhang, T. Doert, M. Ruck*	**1031**	Synthesis of Metal Sulfides from a Deep Eutectic Solvent Precursor
A. Ritscher, M. Schlosser, A. Pfitzner, M. Lerch*	**1031**	Detaillierte Untersuchung des mechanochemischen Prozesses zur Synthese von CZTS (Kesterit)
*Simon D. Kloß, W. Schnick**	**1032**	Two Polymorphs of $RE_2P_3N_7$ Nitridophosphates
*E.-M. Bertschler, W. Schnick**	**1032**	Li_4PN_3: A High-Pressure Polymorph of $Li_{12}P_3N_9$
B. Anke, T. Bredow, M. Lerch*	**1033**	Gezielte Beeinflussung der optischen Bandlücke von $Ba_3Ta_5O_{15}$
B. Anke, M. Rohloff, A. Fischer, M. Lerch*	**1033**	Verbesserung der photokatalytischen Eigenschaften von $BiVO_4$ durch partielle O/F-Substitution
*M. K. Schmitt, K. Wurst, H. Huppertz**	**1034**	Extending the Field of Nickel Borates *via* High-Pressure Synthesis
*D. Friedrich, M. Schlosser, A. Pfitzner**	**1034**	$CsGaS_2$-*mC*64 − A Low-Temperature Polymorph of $CsGaS_2$
T. Lüdtke, M. Lerch*	**1035**	Synthese und Kristallstruktur neuer Oxidnitride vom Bixbyit-Typ
*S. Bauer, A. Pfitzner**	**1035**	$Cu_7PSe_{5.1}Te_{0.9}$, A New Mixed Chalcogenide Argyrodite
M. Baumgartner, T. Nilges, R. Weihrich*	**1036**	On the Electronic Properties of Low Dimensional Phosphorous Allotropes
*D. Rudolph, Th. Schleid**	**1036**	Eu_2H_3I: A New Hydride Iodide with Divalent Europium
*G. Behrendt, H. Kohlmann**	**1037**	Hydrogenation Reaction Pathways in the System $Li_3N-MgH_2-H_2$ by *in situ* Neutron Diffraction and *in situ* Thermal Analysis
*V. Zimmermann, M. S. Wickleder**	**1037**	Intercalated HNO_3 Molecules in $RE(CH_3SO_3)_3 \cdot HNO_3$ (RE = Sm, Tb)
*P. Strobel, W. Schnick**	**1038**	Luminescence Tuning in Red Emitting $Ca_2Li_2[Mg_2Si_2N_6]:Eu^{2+}$
*F. Lissner, Th. Schleid**	**1038**	B-$La_4N_2S_3$: A Second Modification of Lanthanum(III) Nitride Sulfide
E. Heppke, S. Eickholt, A. Maheshwari, H.-D. Wiemhöfer, M. Lerch*	**1039**	Züchtung und elektrochemische Charakterisierung von Cerdioxid-basierten Einkristallen

 © 2016 WILEY-VCH Verlag GmbH & Co. KGaA, Weinheim

*N. Pienack, H. Terraschke, W. Bensch** ..... **1040** *In-situ* Crystallization Cell: Developments and First Results of the Model System $Al(acac)_3$

M. Elsner, I. Weimann, J. Feller, Žák ..... **1040** Electrochemical and Structural Properties of $Ag_4Fe_5O_2(PO_4)_5$ as well as Phase Diagram $Ag_2O/Fe_2O_3/P_2O_5$

*J. Jung-König, C. Feldmann** ..... **1041** Nanoskalige Carbonat-Hohlkugeln

*P. Wagatha, W. Schnick** ..... **1041** Structure and Luminescence Properties of $Ca_{(20-x)}Li_{(8+2x)}[Al_{39}N_{55}]:Eu^{2+}$

S. Berendts, J.-P. Eufinger, I. Valov, J. Janek, M. Lerch* ..... **1042** Die elektrische Leitfähigkeit von Zirconiumnitridoxid-Einkristallen bei niedrigen Temperaturen

C. Logemann, M. S. Wickleder* ..... **1042** Au^{III}-Chalcogenates: $NaAu(SeO_4)_2$, $AgAu(SeO_4)_2$, and $Au(OH)(SO_4)$,

*P. Gross, H. A. Höppe** ..... **1043** From Columns to Layers: Tailoring the Crystal Structure Topology of Alkaline Earth Isocyanurate-Hydrates by Tuning Stoichiometry and pH

*M. Glätzle, O. Janka, R. Pöttgen, H. Huppertz** ..... **1044** High-Pressure Synthesis, Single-Crystal Structure, and Magnetic Properties of Tb_3O_5

*L. Rößner, R. Kriegel, M. Armbrüster** .... **1045** Stability of ZnPd in Aqueous Media

*K. V. Dorn, Th. Schleid, I. Hartenbach** ..... **1045** $Tb_3Cl_3[WO_6]$: The Final Member in a Series of Lanthanoid(III) Chloride Oxidotungstates(VI) Bearing Trigonal Prismatic $[WO_6]^{6-}$ Units

*F. M. Kleeberg, L. W. Zimmermann, Th. Schleid** ..... **1046** $[Pb_4(OH)_4(H_2O)_4][B_{10}H_{10}]_2 \cdot 2H_2O$: A Basic Lead(II) Decahydro-*closo*-Decaborate Hydrate

*M. Weber, P. Kitschke, M. Mehring** ..... **1046** Microwave-Assisted Synthesis of Bismuth(III) Oxides Containing Sulfur and Selenium

*R. Fritzsche, M. Mehring** ..... **1047** Deposition of Thin Germanium Films on Flexible Substrates

*M. Hofmann, B. Büchter, M. Mehring** ... **1047** Preparation of -Bi_2O_3 Films by Ultrasonic Spray Coating of Bismuth Oxido Clusters and their Photocatalytic Activity under Visible Light

*L. Neudert, M. Scheel, S. Schwarzmüller, O. Oeckler** ..... **1048** Struktur-Eigenschafts-Beziehungen von Verbindungen im System Ge/Sn/Sb/In/Te

*C. Logemann, V. Zimmermann, J.-H. Bölte, M. S. Wickleder** ..... **1048** Disulfato-Metallates

*C. Kolb, M. S. Wickleder** ..... **1049** New Triflimidates as Precursors for Electrochemistry

S. Orthmann, M. Lerch* ..... **1049** Synthese und strukturelle Charakterisierung einer neuen Phase im System Sc-Nb-O-N

*M. Vilsmeier, M. Samandarsangari, A. Pfitzner** ..... **1050** Synthesis of Halocuprate(I) Double Layers with Methenamine

*L. Neumeier, C. Feldmann** ..... **1050** Synthese und Charakterisierung carboxylatbasierter anorganisch-organischer Hybridnanopartikel

 © 2016 WILEY-VCH Verlag GmbH & Co. KGaA, Weinheim

CONTENTS

O. Reckeweg, C. Funk, F. J. DiSalvo, Th. Schleid* ..... **1051** New Insights into $Eu_3[BO_3]_2$

R. Kriegel, M. Armbrüster ..... **1052** EMF of ZnPd at 25 ΘC

*C. Funk, J. Köhler, Th. Schleid** ..... **1053** A New Tetragonal Tungsten-Bronze Structured Compound: $CsEu_2Ta_5O_{15}$

*S. G. Jantz, H. A. Höppe** ..... **1054** The Borate Fluoride $Sn_3[B_3O_7]F$

*V. Rein, C. Feldmann** ..... **1054** Nanoporous Mg_3N_2

*J. Peilstöcker, E. Günes, O. Falkenbach, E. Müller, Mathias S. Wickleder** ..... **1055** Synthesis of Nanostructured, Cadmium-Doped ZnSb and Investigation of the Thermoelectric Properties

*A. Egeberg, C. Feldmann** ..... **1055** Synthesis of Base Metal Nanoparticles using Amine Solvents

*Y.-C. Chen, C. Feldmann** ..... **1056** Near-infrared Triggered Photoactivity of Plasmonic $Au@H_xK_{4-x}Nb_6O_{17}$ Photocatalysts with Biomimetic Nanopeapod Geometry

*D. D. Zimmermann, Th. Schleid** ..... **1057** B-Type CeOF and a Correction for *Zachariasen*·s Tetragonal Crystal Structure of -LaOF

*M. E. Bohem, Th. Schleid** ..... **1058** The Luminescence Properties of $Eu_2O[SiO_4]$ and $Eu_{4.667}O[SiO_4]_3$

*H. Schwartz, U. Ruschewitz** ..... **1059** MOFs as "Solid Solvents" for Spiropyrans

A. Amon, L. G. Akselrud, M. Bobnar, M. Avdeev, R. Gumeniuk, A. Leithe-Jasper, J. Grin* ..... **1059** A New Superconducting Beryllium Platinide

*V. K. Gramm, U. Ruschewitz** ..... **1060** Three New Anhydrous Acetylenedicarboxylates

*M. Werker, U. Ruschewitz** ..... **1060** On the Way to New Ternary Alkali Metal Transition Metal Acetylides

*M. B. Dérghon, C. Feldmann** ..... **1061** Synthesis and Characterization of Barium Thiosulfate Nanoparticles

*S. Schönegger, H. Huppertz** ..... **1061** Synthesis and Characterization of the Lead Borate $Pb_6B_{12}O_{21}(OH)_6$

A.-L. Hansen, W. Bensch* ..... **1062** Chalcogenide-Based Thermoelectric Materials − Microstructure and Thermoelectric Performance

*S. Haumann, R. Weihrich** ..... **1062** Synthesis and Self-Assembly of Cobalt and Nickel Nanoparticles

*U. Pachmayr, S. Kamusella, H.-H. Klauss, D. Johrendt** ..... **1063** Effect of Cobalt Substitution in the Ferromagnetic Superconductor $[(Li_{0.8}Fe_{0.2})OH]FeSe$

*S. Peschke, S. Vogel, D. Johrendt** ..... **1063** Re-Emergence of Superconductivity in $La_{1x}RE_xFeAsO_{0.8}F_{0.2}$ *(RE= Pr−Sm)*

*J. Stahl, L. Neudert, O. Oeckler, D. Johrendt** ..... **1064** $Fe_{2.3}GeTe$ − A New Layered Ferromagnetic Telluride

 © 2016 WILEY-VCH Verlag GmbH & Co. KGaA, Weinheim

*R. Heinemann, P. Schmidt** ..... **1064** Thermodynamic Analysis of Crystal Growth of Zinc Oxide

G. Gramm, G. Fuhrmann, H. Schottenberger, H. Huppertz* ..... **1065** Novel Inorganic Red Pigments Based on Tetragonal -Bi_2O_3

M. Perz, E. Bucher, W. Sitte* ..... **1065** Long-Term Electrochemical Characterization of Thin-Film SOFC Cathodes of $La_{0.6}Sr_{0.4}CoO_{3-}$

*M. Wels, P. Schmidt** ..... **1066** Crystal Growth of Ternary Phases with Homogeneity Range: Modeling and Experiments

S. Bräuchle, K. Wurst, H. Huppertz* ..... **1067** Synthesis and Structural Characterization of $Ca_{12}Ge_{17}B_8O_{58}$

M. van Megen, G. J. Reiss, W. Frank* ..... **1068** Hexane-1,6-diammonium Hexane-1,6-bis(hydrogen phosphonate) − Another Salt with a Herringbone Motif Layer-Like Structure

*C. Schulz, Subrata C. Roy, M. Weber, K. Wittich, R. Glaum, F. Rosowski** ..... **1069** Selective Alkane Oxidation on Catalysts $(V_{1-x}M_x)OPO_4$ *(M: Mo, W)*

*K. Wittich, Subrata C. Roy, C. Schulz, F. Rosowski, R. Glaum** ..... **1070** Multinary Tungsten Phosphates with ReO_3 Structure Type: Synthesis and Catalyst Behavior

*S. W. Prömper, W. Frank** ..... **1070** Orthorhombic Lithium Tetrachloroaluminate and Lithium-bis(pentamethylbenzenium)-tris(tetrachloroaluminate)

*O. Janka, Th. Schleid** ..... **1071** *C*-Type $LaTaO_4$ − A New Polymorph

*E. Selb, G. Heymann** ..... **1071** On the Road to Pyrite-Type PdS_2 and $PdSe_2$ at High Pressures

*D. Schildhammer, G. Fuhrmann, L. L. Petschnig, M. Kogler, H. Schottenberger, H. Huppertz** ..... **1072** Cubically Stabilized $CeO_2-Er_6MoO_{12}$ and $CeO_2-Yb_6MoO_{12}$ Solid Solutions

*A.-M. Tsirigoni, L. R. Arana, P. Lindenberg, H. Terraschke** ..... **1073** *In-situ* Monitoring of Calcium Phosphate Phase Transitions: a Spectroscopic Approach

*P. Polzin, I. V. Eliani, H. Terraschke** ..... **1073** Characterizing the Crystallization Kinetics of *Ln*(2,2-Bipyridine)$_2$(NO$_3$)$_3$ (*Ln* = Eu, Tb) by New *in-situ* Luminescence Analysis Technique

*P. Lindenberg, L. Ruiz Arana, N. Heidenreich, H. Terraschke** ..... **1074** Polymorphism and *in-situ* Detection of Reaction Intermediates on Eu(1,10-Phenanthroline)$_2$(NO$_3$)$_3$

P. Höhn, M. Bobnar, W. Schnelle, M. Fix, A. Jesche* ..... **1074** $Li_2Sr[Li_{0.5}Fe_{0.5}N]_2$ and Isotypic Phases: mm-Sized Single Crystals with Large Single-Ion Magnetic Anisotropy

M. Pathak, M. Bobnar, W. Schnelle, P. Höhn, Y. Grin* ..... **1075** $Li_{16}Sr_6M_6N$ (*M* = Ge, Sn, Pb) − Cubic Tetrelide-Nitrides with an Ordered Ir_4Sc_{11} Type Structure

*T. Rothenaigner, A. Pfitzner** ..... **1075** $Li_2Ag_7Sb_3S_9$ − A Compound in the Quasi-Binary System Li_3SbS_3 − Ag_3SbS_3

*S. Greiner, Th. Schleid** ..... **1076** ScCl[SeO_3]: The Chloride Oxoselenate(IV) of the Smallest Rare-Earth Metal

J. O. Binder, R. Pinedo, D. Weber, K. Weldert, M. S. Friedrich, W. Zeier, J. Janek* ..... **1077** Fluorine-Doped Layered Cathode Materials

 © 2016 WILEY-VCH Verlag GmbH & Co. KGaA, Weinheim

CONTENTS

D. Wiedemann, A. Franz* ..... **1077** Making the Most of Neutron-Diffraction Data: Lithium Diffusion Pathways in Ramsdellite-Like $Li_2Ti_3O_7$

A. Werwein, H. Kohlmann, S. Raseale* ... **1078** Synthesis of New Lanthanide Hydride Oxides *Ln*HO (*Ln* = Sm, Gd, Ho, Er)

*L. Akselrud, A. Wosylus, R. Castillo, B. Wahl, T. Doert, U. Schwarz** ..... **1078** Modulated Vacancy Ordering in $SrGe_{6-x}$

 © 2016 WILEY-VCH Verlag GmbH & Co. KGaA, Weinheim

10.1002/zaac.201603001

Two-Dimensional Materials from van der Waals Zintl Phases

Joshua Goldberger,*[a] Maxx Arguilla,[a] Shishi Jiang,[a] and Nicholas Cultrara[a]

Keywords: Topochemistry, Graphane Analogues, Zintl Phases

Two-dimensional materials have generated considerable research interest over the past decade, in part because of the new physical phenomena that emerge in these atomically thin framework, as well as their potential for impacting diverse sets of technologies including electronics, optoelectronics, sensing, and catalysis. Here, we will discuss the synthesis structure. One of the major lessons of these studies is that the surrounding environment, the substrate flatness, and the local dielectric constant can significantly influence the properties and reactivity of these single/few-atom thick materials. Establishing 2D crystals in which the framework and immediate chemical environment can be modified via covalent functionalization gives a powerful handle towards designing novel properties.

In this presentation, we will describe our recent success in the creation of hydrogen and organic-terminated group 14 graphane analogues, from the topochemical deintercalation of precursor Zintl phases, such as $CaGe_2$ (**Figure 1**).[1–4] We will compare the effectiveness of different topochemical methods to maximize the degree of organic termination in germanane materials. We will demonstrate that the interplay between the size and electron-withdrawing nature of the ligand can be rationally chosen to tune the electronic structure and band gap.[5,6] Additionally, we will describe our recent efforts on the creation and properties of Sn-containing graphane derivatives in order to access the quantum spin Hall phenomena predicted to occur in these materials. [7]

Finally, we will describe a new class of intermetallic Zintl phases held together by van der Waals bonding that can be directly exfoliated onto various substrates. For example, we demonstrate the synthesis, exfoliation and characterization of $NaSn_2As_2$. By combining the theoretical band structure, the Angle-Resolved Photoemission measurements and electronic transport, we show that bulk $NaSn_2As_2$ is semimetallic with nominally p-type conduction. $NaSn_2As_2$ can also be thinned down to few- to single-layer thicknesses either via mechanical exfoliation using Scotch tape or liquid phase exfoliation,. This material represents the first member of a large family of van der Waals Zintl phase derivatives that have varying degrees of spin-orbit coupling, and electronic and magnetic properties, making them promising 2D building blocks for a variety of electronic and spintronic applications.

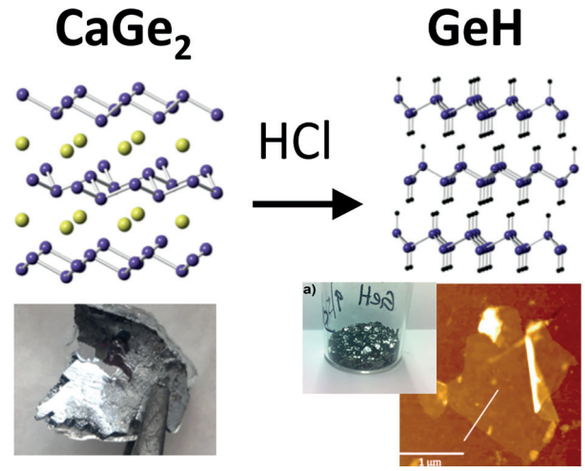

Figure 1. Topotactic transformation of $CaGe_2$ crystals to GeH, a germanium graphane analogue.

[1] E. Bianco, S. Butler, S. Jiang, O. D. Restrepo, W. Windl, J. E. Goldberger, *ACS Nano* **2013**, *7*, 4414–4421.
[2] S. Jiang, E. Bianco, J. E. Goldberger, *J. Mater. Chem. C* **2014**, *2*, 3185-3188.
[3] W. Amamou, P. M. Odenthal, E. J. Bushong, D. J. O′Hara, Y. K. Luo, J. van Baren, I. Pinchuk, Y. Wu, A. S. Ahmed, J. Katoch, M. W. Bockrath, H. W. K. Tom, J. E. Goldberger, R. K. Kawakami, *2d Materials* **2015**, *2*.
[4] J. R. Young, B. Chitara, N. D. Cultrara, M. Q. Arguilla, S. Jiang, F. Fan, E. Johnston-Halperin, J. E. Goldberger, *J. Phys. Condens. Matter* **2016**, *28*, 034001–034001.
[5] S. Jiang, M. Q. Arguilla, N. D. Cultrara, J. E. Goldberger, *Acc. Chem. Res.* **2015**, *48*, 144-151.
[6] O. D. Restrepo, R. Mishra, J. E. Goldberger, W. Windl, *J. Appl. Phys.* **2014**, *115*, 033711.
[7] M. Q. Arguilla, S. Jiang, B. Chitara, J. E. Goldberger, *Chem. Mater.* **2014**, *26*, 6941–6946.

* Prof. Dr. J. Goldberger
E-Mail: goldberger@chemistry.ohio-state.edu
[a] Department of Chemistry and Biochemistry
The Ohio State University
100 W. 18th Ave.
Columbus, OH 43210, USA

 © 2016 WILEY-VCH Verlag GmbH & Co. KGaA, Weinheim

10.1002/zaac.201603002

2D or not 2D? Two-Dimensional Nanostructures for Sensing and Energy Storage B. V. Lotsch*

Bettina V. Lotsch,*[a]

Keywords: 2D materials, exfoliation, $RuCl_3$, antimony phosphate, lithium solid electrolytes

The discovery of graphene, along with the early achievements of soft chemistry and nanotechnology, has led to a resurgence of interest in layered materials, which display a virtually unlimited source of 2D materials of all stripes. The operation of classical and quantum size confinement effects in dimensionally reduced materials offers a unique basis for accessing new properties and reactivity profiles distinct from their bulk counterparts. In addition, the combination of different 2D materials to form superlattices with synergistic properties is the next step forward to access complex heterostructures which are not only key elements in miniaturized devices, but, if scalable, offer new design principles for bulk "artificial solids" with properties engineered on the nanoscale.

We describe the synthesis, characterization and properties of three selected classes of 2D materials and highlight their potential for applications in energy storage and sensing.

We describe the first 2D halide system, $RuCl_3$ nanosheets, which are obtained by reductive intercalation of lithium into α-$RuCl_3$. Re-oxidation of the turbostratically restacked nanosheets provides a tool to manipulate the magnetic properties of $RuCl_3$, which can serve as a quasi 2D model for Kitaev-Heisenberg physics in spin ½ honeycomb magnets.[1]

We further demonstrate the potential of the swellable layered antimony phosphates $H_3Sb_3P_2O_{14}$ and $HSbP_2O_8$ as stimuli-responsive materials for vapor sensing. The exfoliated 2D nanosheets were cast into thin films and integrated in resistive and photonic humidity sensors. Owing to their fast response times and ultrahigh sensitivity to the humid atmosphere of a finger, 1D Photonic Crystals composed of $H_3Sb_3P_2O_{14}$ and oxide nanoparticles provide a new concept for optical touchless positioning interfaces which enable contact-less tracking of finger motion with direct optical feedback.[2,3]

While research into chalcogenide nanosheets has mainly focused on their suitability as electrode materials in batteries and supercapacitors, we have recently discovered the first ultrafast lithium solid electrolyte in the Li-Sn-S system. $Li_{0.6}[Li_{0.2}Sn_{0.8}S_2]$ is composed of layers comprising edge-sharing Li/SnS6 octahedra, interleaved with both tetrahedrally and octahedrally coordinated Li ions, and shows a Li ion conductivity σ_{NMR} of 9.3 10^{-3} S/cm at RT, which puts it *en par* with the best lithium solid electrolytes.[4] Exfoliation – restacking of the nanosheets gives rise to compositionally modified nanosheet thin films with unparalleled in-plane Li ion conductivities.

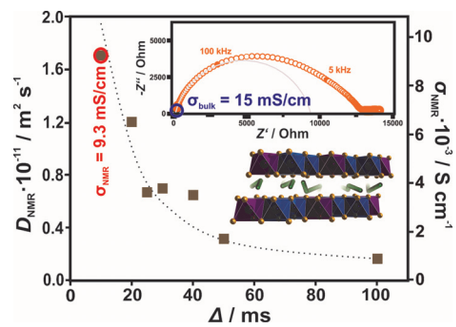

Figure 1. PFG-NMR measurements and impedance spectroscopy of the new superionic Li solid electrolyte $Li_{0.6}[Li_{0.2}Sn_{0.8}S_2]$.[4]

[1] D. Weber, L.M. Schoop, V. Duppel, J.M. Lippmann, J. Nuss, B.V. Lotsch, *NanoLetters* **2016**, DOI:10.1021/acs.nanolett.6b00701.
[2] K. Szendrei, P. Ganter, O. Sánchez-Sobrado, R. Eger, A. Kuhn, B.V. Lotsch, *Adv. Mater.* **2015**, *27*, 6341–6348.
[3] K. Szendrei, P. Ganter, B.V. Lotsch, *submitted*.
[4] T. Holzmann, L. M. Schoop, M. N. Ali, I. Moudrakovski, G. Gregori, J. Maier, R. J. Cava, B. V. Lotsch, *Energy Environ. Sci.* **2016**, DOI: 10.1039/c6ee00633g.

* Prof. Dr. B. V. Lotsch
E-Mail: b.lotsch@fkf.mpg.de
[a] Max-Planck-Institut für Festkörperforschung, Heisenbergstraße 1, 70569 Stuttgart
[b] Department Chemie, LMU München, Butenandtstraße 5-13, 81377 München, Germany

 © 2016 WILEY-VCH Verlag GmbH & Co. KGaA, Weinheim

10.1002/zaac.201603003

Trapping Metastable Solids via Designed Precursors

David C. Johnson*[a]

Keywords: synthesis, dichalcogenides, layered compounds

The search for new inorganic solid state compounds depends on finding conditions where a new compound is thermodynamically stable or avoiding thermodynamic products while forming a metastable product. Amorphous precursors can be used as reaction intermediates to trap metastable products. Precursors can be prepared with nanoarchitectures corresponding to that of targeted compounds and the nanoarchitecture can be maintained during self assemble at low annealing temperatures. This approach differs from traditional approaches, which depend on facile diffusion. The inherent small diffusion distances combined with low diffusion rates at low temperatures prevent the precursor from exploring large areas of the energy landscape.

It is expected that a large number of solid-state inorganic compounds remain undiscovered.[1] There is a desire to discover them as some may have unprecedented physical properties important for both existing and future applications. The search for them, however, has been limited by synthetic challenges. Brewer[2] outlined the synthetic challenges due to both reaction kinetics and thermodynamics, especially for metastable compounds and compounds that are only thermodynamically stable at low or very high temperatures. Schaffer[3] categorized solid-state reactions into two general categories. One is where reactants have high mobility via high temperature, high defect concentrations, facile surface diffusion, or the use of fluids as the transport media. In this regime, binary compounds tend to form as reaction intermediates, so ternary and higher order compounds must be more thermodynamically more stable than a mix of the elements and binary compounds under the reaction conditions in order to be discovered. The other category is the set of reactions in which the nature of the products is determined by existing structural elements or lattice defects of the reactants - referred to as "soft chemistry".[4] The rate of number of new compounds being discovered would be increased by the development of new synthesis approaches and a more general understanding of reaction mechanisms.

The concept of energy landscapes provides a global perspective of potential compounds, as they contain both local free energy maxima as well as the global free energy minima found in traditional phase diagrams.[1] The different pathways between energy minima provide a framework to imagine and rationalize potential reaction mechanisms. Not many energy landscapes have been calculated, however, so the challenge for experimentalists is to imagine compositions and structures that might be local free energy minima and also a viable synthesis route to the targeted compound. Unfortunately, the general design rules to access local free energy minima are not known.

Conceptually, a homogeneous amorphous solid is a useful reaction intermediate to explore energy landscapes, as no long-range diffusion is required to form a product with the same composition as the precursor. At low temperatures, the atoms are not able to move far or explore much area on an energy landscape. If the amorphous solid is poised above a local free energy minima, low temperature annealing might allow the self-assembly of the kinetic product. This diffusion constrained synthesis approach is distinct from the reaction pathways described by Schaffer,[3] potentially providing kinetic access to a different suite of compounds. The amorphous state can generally be accessed through low temperature interdiffusion of repeating sequences of ultrathin elemental layers. The layer thicknesses and layer sequence can be used as parameters to avoid the nucleation of stable binary compounds, resulting in the formation of new binary compounds and in the formation of ternary compounds without the formation of binary compounds as intermediates.[5]

Imagining potential kinetically stable compounds, we thought intergrowths of two or more known structures would be likely local free energy minima because some intergrowth compounds, such as the misfit layered compounds,[6] are thermodynamically stable compounds containing with a single dichalcogenide plane alternating with a bilayer of a rock salt structured compound. It is reasonable that a series of compounds with varying thickness of each constituent might be local free energy minima. The challenge is to figure out how to prepare these compounds. Our approach is to prepare amorphous precursors containing the approximate composition modulation of the targeted compound. Low temperature annealing of these precursors results in the self assembly of many new compounds containing two or more interleaved structures, including structural isomers that contain the same number of layers of each constituent arranged in distinct sequences. With just 2 constituent layers, and confining ourselves to 20 or less layers in the repeating structure, over 60,000 distinct layer sequences are possible. With 3 constituent layers, the number grows to over 130 million and with 4 constituents the number explodes to over 35 billion.[7]

Acknowledgments

DCJ acknowledges support from the National Science Foundation under grant DMR-1266217.

[1] M. Jansen, *Angew. Chem. Int. Ed.* **2002**, *41*, 3746–3766.
[2] L. Brewer, *J. Chem. Ed.* **1958**, *35*, 153–156.
[3] H. Schäfer, *Angew. Chem. Int. Ed. Engl.* **1971**, *10*, 43–50.
[4] A. Stein, S. W. Keller, T. E. Mallouk, *Science* **1993**, *259*, 1558–1564.
[5] M. D. Anderson, J. O. Thompson, D. C. Johnson, *Chem. Mater*, **2013**, *25*, 3996–4002.
[6] G. A. Wiegers, *Prog. Solid. St. Chem*, **1996**, *24*, 1–139.
[7] a) M. Esters, M. Alemayehu, Z. Jones, N. T. Nguyen, M. D. Anderson, C. Grosse, S. Fischer, D. C. Johnson, *Angew. Chem. Int. Ed.* **2015**, *54*, 1130–1134; b) N. S. Gunning, J. Feser, M. Beekman, D. G. Cahill, D. C. Johnson, *J. Am. Chem. Soc.*, **2015**, *137*, 8803–8809.

* Professor David C. Johnson
E-mail: davej@uoregon.edu
[a] Department of Chemistry and Materials Science Institute
University of Oregon
Eugene, Oregon, USA

 © 2016 WILEY-VCH Verlag GmbH & Co. KGaA, Weinheim

10.1002/zaac.201603004

Why Melt Synthesis is a Game Changer for Clays

Josef Breu*[a]

Keywords: 2D materials, hectorites, MOPS, ordered heterostructures, nanocomposites

The intrinsically anisotropic bonding in layered materials on one side enables a vivid intracrystalline reactivity that allows for post synthetic functionalization via ion exchange or intercalation and drives the hype on two-dimensional (2D) materials in general. On the the other side, anisotropic bonding is responsible for frequent planar defects that hamper structural characterization and allow for a great deal of hand-waving in the 2D community. The situation is even worsened for insulator materials like clay minerals where a permanent charge arises from isomorphous substitution. Any deviations from an ideal solid solution situation will then consequently lead to heterogeneities in charge density that in turn gives rise to a non-uniform intracrystalline reactivity and random interstratification because cooperativity of intracrystalline reactions is essentially limited to two dimensions. In summary very little structural information is available for clay minerals and their intercalation compounds.

Syntheses from the melt at temperatures well above 1,000 K gives rise to hectorites with tuneable and homogeneous intracrystalline reactivities.[1–3] With these materials defects can be reduced to a level where a more detailed look at structural features becomes available and where post synthetic functionalization via topotactic ion exchange gives rise to new types of 2D materials. For instance, by pillaring with molecular cations microporous hybrid materials (MOPS) are obtained that may be used for gas separation and enantiodiscrimination.[4–6] Spontaneous delamination by osmotic swelling may be enabled, where continuum electrostatic repulsion separates stacks into individual layers with utmost precision to layer separations > 30 nm.[7] Diluting these gels yields 1 nm thick, transparent, and highly flexible[8,9] platelets with aspect ratios of up to 20000 that when compounded into polymer matrices give rise to much improved mechanical reinforcement,[10,11] flame retardancy[12,13] and gas barrier properties.[14–16]

Utterly controlling homogeneity, moreover, allows for synthesis of regular heterostructures[17] that may be delaminated into double stacks with any kind of functional molecules sandwiched between two clay layers. This way emitters may e.g. be oriented[18] in a quasi-epitaxial way allowing for polarized emission[19] or the ordered heterostacks may be turned into Janus platelets.[20]

[1] M.W. Möller, U.A. Handge, D.A. Kunz, T. Lunkenbein, V. Altstädt, J. Breu, *ACS Nano* **2010,** *4*, 717–724.
[2] H. Kalo, M.W. Möller, D.A. Kunz, J. Breu, *Nanoscale*, **2012,** *4*, 5633–5639.
[3] S. J. You, D.A. Kunz, M. Stöter, H. Kalo, B. Putz, J. Breu, A. V. Talyzin, *Angew. Chem. Int. Ed.* **2013,** *52*, 3891–3895.
[4] A. Baumgartner, K. Sattler, J. Thun, J. Breu, *Angew. Chem. Int. Ed.* **2008,** *47*, 1640–1644.
[5] M. Herling, H. Kalo, S. Seibt, R. Schobert, J. Breu, *Langmuir* **2012**, *28*, 14713–14719.
[6] M. Herling, J. Breu, *Z. Anorg. Allg. Chem.* **2014**, *640*, 547–560.
[7] M. Stöter, S. Rosenfeldt, J. Breu, *Annu. Rev. Mater. Res*. **2015**, *45*, 129–51.
[8] M. Stöter, D. A. Kunz, M. Schmidt, D. Hirsemann, H. Kalo, B. Putz, J. Senker, J. Breu, *Langmuir* **2013**, *29*, 1280–1285.
[9] D. A. Kunz, J. Erath, D. Kluge, H. Thurn, B. Putz, A. Fery, J. Breu, *ACS Appl. Mater. & Interf.*, **2013**, *5*, 5851–5855.
[10] M. Ziadeh, B. Fischer, J. Schmid, V. Altstädt, J. Breu, *Polymer* **2014,** *16*, 3770-3781.
[11] J. Hausner, M. Ziadeh, B. Fischer, H. Kalo, J. Schmid, R. Kunz, V. Altstädt, J. Breu, *Comp. Sci. Technol.* **2015,** *114*, 34-41.
[12] M.R. Schütz, H. Kalo, T. Lunkenbein, J. Breu, C.A. Wilkie, *Polymer* **2011,** *52*, 3288–3294.
[13] J. Hausner, B. Fischer, M. Stöter, A. Edenharter, J. Schmid, R. Kunz, S. Rosenfeldt, V. Altstädt, J. Breu, *Polymer Deg. Stab.* **2016**, *128*, 141–148.
[14] M. W. Möller, T. Lunkenbein, H. Kalo, M. Schieder, D. A. Kunz, J. Breu, *Adv. Mater.* **2010,** *22*, 5245–5249.
[15] M. W. Möller, D. A. Kunz, T. Lunkenbein, S. Sommer, A. Nennemann, J. Breu, *Adv. Mater.* **2012**, *24*, 2142–2147.
[16] D.A. Kunz, J. Schmid, P. Feicht, J. Erath, A. Fery, J. Breu, *ACS Nano* **2013**, *7*, 4275–4280.
[17] M. Stöter, B. Biersack, N. Reimer, M. Herling, N. Stock, R. Schobert, J. Breu, *Chem. Mater.* **2014**, *26*, 5412−5419.
[18] D.A. Kunz, M.J. Leitl, L. Schade, J. Schmid, B. Bojer, U. T. Schwarz, G. A. Ozin, H. Yersin, J. Breu, *Small* **2015**, *11,* 792–796.
[19] M. Stöter, B. Biersack, S. Rosenfeldt, M. J. Leitl, H. Kalo, R. Schobert, H. Yersin, G. A. Ozin, S. Förster, J. Breu, *Angew. Chem. Int. Ed.* **2015**, *54*, 4963–4967.
[20] M. Stöter, S. Gödrich, P. Feicht, S. Rosenfeldt, H. Thurn, J. W. Neubauer, M. Seuss, P. Lindner, H. Kalo, M. Möller, A. Fery, S. Förster, G. Papastavrou, J. Breu, *Angew. Chem. Int. Ed.* **2016**, DOI: 10.1002/anie.201601611.

* Prof. Dr. J. Breu
E-Mail: josef.breu@uni-bayreuth.de
[a] Lehrstuhl für Anorganische Chemie I
Universität Bayreuth
Universitätsstr. 30
95447 Bayreuth, Germany

 © 2016 WILEY-VCH Verlag GmbH & Co. KGaA, Weinheim

10.1002/zaac.201603005

Quantenconfinement: eine alternative Methode zum Design funktionaler zweidimensionaler Kristalle

Thomas Heine*[a,b]

Keywords: 2D-Kristalle, Dichtefunktionaltheorie, Übergangsmetalldichalcogenide, topologische Isolatoren

Die Entdeckung des Graphens öffnete das neue Forschungsfeld: 2005 prägten Novoselov, Geim und Mitarbeiter den Begriff zweidimensionale (2D) Kristalle.[1] Die Bedeutung dieser Materialien für die Elektronik wurde durch die Demonstration eines Transistors auf einer MoS_2-Monolage durch Kis und Mitarbeiter unterstrichen.[2] Coleman, Nicolosi und Mitarbeiter kategorisierten eine Vielzahl von Lagenmaterialien, die exfoliiert und hinsichtlich ihrer Eigenschaften als 2D-Kristalle untersucht werden können.[3] In meiner Arbeitsgruppe wurde die Diversität der elektronischen Eigenschaften von 2D-Kristallen betont,[4] die Stoffklasse umfasst neben Metallen, Halbleitern und Nichtleitern auch neuartige Phasen wie z.B. topologische Isolatoren.

Eine sehr ausgeprägte Eigenschaft der 2D-Kristalle ist die Respons zum Quantenconfinement. Mit einer Dicke von nur wenigen Atomlagen und mit chemisch inaktiver Oberfläche vereinen diese Materialien die Eigenschaften von Kristallen (in 2 Dimensionen) und Molekülen (in der 3. Dimension). Sowohl die Interlagenwechselwirkung als auch die Präsenz externer elektrischer, magnetischer oder mechanischer Spannungsfelder können die Eigenschaften der 2D-Kristalle maßgeblich ändern. Darüber hinaus hängt bei den verbreiteten 2H-Phasen die Symmetrie von der Anzahl der Kristalllagen ab, was qualitative Konsequenzen auf die Spinpolarisation der Materialien hat.

Im ersten Teil des Vortrags werde ich mich auf Materialien mit besonders starkem Quantenconfinement konzentrieren, insbesondere auf Edelmetalldichalcogenide wie PdS_2, dessen Monolage halbleitend, Doppellage jedoch metallisch ist.[5] Daher könnte sich das Material für besonders energiesparende Transistoren eignen, da Elektrode und Halbleiter in einem Kristallgitter vereint sind (Abb. 1).[6] Weitere Beispiele sind III-VI-Verbindungen wie GaSe, wo eine sehr hohe Zustandsdichte an der Fermikante erreicht werden kann.

Besonders interessant sind Interlagenwechselwirkungen, bei denen sich die Symmetrie des Systems ändert. So weisen die 2H-Übergangsmetalldichalcogenide TX_2 (T=Mo, W, X=S, Se) eine signifikante Spinaufspaltung in der Monolage auf, die in der Doppellage verschwindet. Das Verschwinden der Spinaufspaltung beruht auf der Inversionssymmetrie der Doppellage.[7] Durch äußeren Symmetriebruch, z.B. durch ein elektrisches Feld, lässt sich nun eine schaltbare Spinaufspaltung realisieren.[8]

Im zweiten Teil des Vortrags werde ich das Phänomen der 2D topologischen Isolatoren (TI) erläutern. Nach einer Einführung, die auch auf die experimentellen Herausforderungen in der Entwicklung von 2DTI eingeht und in der die theoretischen Grundlagen für den Quanten-Spin-Hall-Effekt, der die 2DTI charakterisiert, erläutert, werde ich anhand von Beispielen zeigen, wie Computer-gestütztes Materialdesign von 2DTI mit großen Bandlücken möglich ist. Ich werde insbesondere auf Allotrope bekannter 2D-Kristalle eingehen, sowie auf deren Funktionalisierung, die eine wichtige Rolle für die Realisierung von 2DTI spielen kann.[9,10]

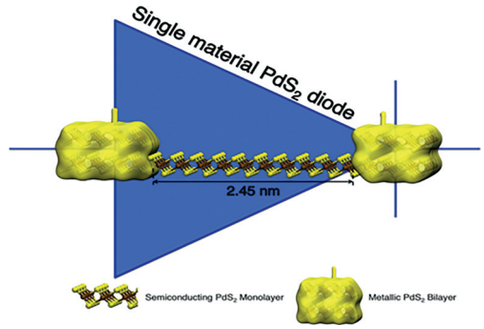

Abbildung 1. Funktionsprinzip einer Diode in einem Einkristallgitter: die Elektroden bestehen aus der metallischen PdS_2-Doppellage, die die halbleitende PdS_2 Monolage kontaktieren.

[1] K. S. Novoselov, D. Jiang, F. Schedin, T. J. Booth, V. V. Khotkevich, S. V. Morozov, A. K. Geim, *Proc. Natl. Acad. Sci. U. S. A.* **2005,** *102,* 10451–10453.
[2] B. Radisavljevic, A. Radenovic, J. Brivio, V. Giacometti, A. Kis, *Nat. Nanotechnol.* **2011,** *6,* 147–150.
[3] V. Nicolosi, M. Chhowalla, M. G. Kanatzidis, M. S. Strano, J. N. Coleman, *Science* **2013,** *340*, 1420–1438.
[4] P. Miro, M. Audiffred, T. Heine, *Chem. Soc. Rev.* **2014,** *43,* 6537–6554.
[5] P. Miro, M. Ghorbani-Asl, T. Heine, *Angew. Chem., Int. Ed.* **2014,** *53,* 3015–3018.
[6] M. Ghorbani-Asl, A. Kuc, P. Miró, T. Heine *Adv. Mater.* **2016,** *28,* 853–856.
[7] N. Zibouche, A. Kuc, J. Musfeldt, T. Heine, *Ann. Phys. (Berlin)* **2014,** *16,* 11251–11255.
[8] N. Zibouche, P. Philipsen, A. Kuc, T. Heine, *Phys. Rev. B* **2014**, 90125440.
[9] Y. Ma, Y. Dai, L. Kou, T. Frauenheim, T. Heine, *Nano Lett.* **2015**, *15*, 1083–1089.
[10] Y. Ma, L. Kou, X. Li, Y. Dai, T. Heine, *NPG Asia Mater.* **2016**, *8,* e264.

* Prof. Dr. T. Heine
E-Mail: thomas.heine@uni-leipzig.de
[a] Wilhelm-Ostwald-Institut für Physikalische und Theoretische Chemie
Universität Leipzig
Linnéstr. 2
04103 Leipzig, Germany
[b] Department of Physics and Earth Science
Jacobs University Bremen
28759 Bremen, Germany

 © 2016 WILEY-VCH Verlag GmbH & Co. KGaA, Weinheim

10.1002/zaac.201604001

Structural Instability in Layered $BaNi_2Ge_2$ and Influence of VEC on the Distortion of the $ThCr_2Si_2$-Type

Viktor Hlukhyy,*[a] and Thomas F. Fässler[a]

Keywords: $ThCr_2Si_2$-type, germanides, phase transition

The intermetallic compound $BaNi_2Ge_2$ similarly to iron based high temperature superconductors of the 122 composition[1] is subject of an orthorhombic-to-tetragonal structural phase transition. $BaNi_2Ge_2$ was prepared by arc-melting mixtures of the elements under an argon atmosphere. Single crystals were obtained by special heat treatment in welded tantalum ampoule. Differential thermal analysis of $BaNi_2Ge_2$ showed a reversible phase transition at ca. 480°C. In-situ temperature-dependent synchrotron powder diffraction studies revealed that below 480°C the crystal structure of $BaNi_2Ge_2$ is orthorhombic (own structure type, space group *Pnma*, a = 8.3852(4) Å, b = 11.3174(8) Å, c = 4.2902(9) Å at 30°C) and above 510°C the high temperature phase belongs to tetragonal $ThCr_2Si_2$-type structure (space group *I4/mmm*, a = 4.2664(1) Å, c = 11.2537(3) Å at 510°C).[2] This LT ↔ HT phase transition around 480°C is associated with the distortion of the [NiGe] layer in LT-modification. The LMTO band structure calculations performed for both orthorhombic and the tetragonal structure hint for a higher stability of the orthorhombic LT-$BaNi_2Ge_2$ modification. The influence of the valence electron concentration (VEC) on the structure stability of two-dimensional representatives of the $ThCr_2Si_2$ type is studied. The increase of the electron number in AeT_2X_2 (T = transition metal; X = As, Ge, Si) along with the symmetry reduction gradually distorts the square net of T-atoms of the tetragonal phase.

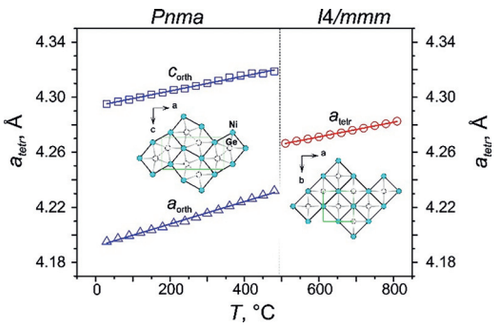

Figure 1. Temperature-dependent evolution of the unit cell parameters in $BaNi_2Ge_2$ associated with the distortion of the [NiGe] layer.

[1] J. Paglione, R. L. Greene, *Nat. Phys.*, **2010**, *6*, 645–658.
[2] V. Hlukhyy, A. Senyshyn, D. Trots, T. F. Fässler, *HASYLAB Ann.Rep.* **2007**, *1*, 1021.

* Dr. V. Hlukhyy
E-Mail: viktor.hlukhyy@lrz.tum.de
[a] Department Chemie, Technische Universität München, Lichtenbergstr. 4, 85747 Garching, Germany

10.1002/zaac.201604002

Structural Origin of the Band Convergence in Skutterudite $CoSb_3$

Riley Hanus,[a] Xingyu,[a] Guodong Li,[a] G. Jeffrey Snyder,[a] and Wolfgang G. Zeier*[b]

Keywords: thermoelectrics, band convergence, skutterudites

Engineering the electronic band structures of certain materials can increase the thermoelectric efficiency of a material, due to an increase in band degeneracy at the band edges. As the band structure of a material is deeply linked to the underlying chemical bonds,[1,2] changing bonding interactions has shown to be most effective in engineering the band degeneracy of thermoelectric materials. Successful strategies include changing the orbital overlap in PbTe via doping,[1] or through chemical pressure exerted on the ligand field splitting in quaternary chalcopyrites and Zintl phases.[3,4]
Skutterudite $CoSb_3$, a well known thermoelectric material, has recently been shown to exhibit band convergence at elevated temperatures when heavily doped.[5] In this study, we aim to explain the observance of the experimentally observed changes in the thermoelectric transport from a chemical and structural point of view. We present temperature dependent synchrotron diffraction data, showing differences in the thermal expansion coefficient of local bonds in the structure. Using the experimentally obtained temperature dependent structural information, density functional theory is employed to assess the changes in the band structure with temperature. These experimental and computational results reveal connections between bonding interactions and electronic structure, providing explanation for observed changes in thermoelectric transport. In addition, we will show how n-type doping in this system alters the bonding situation and the structure due to population of anti-bonding bands. This study shows the direct effect of chemical bonding and orbital population on the structure and transport of thermoelectric materials.

[1] W. G. Zeier, A. Zevalkink, Z. M. Gibbs, G. Hautier, M. G. Kanatzidis, G. J. Snyder, *Angew. Chem. Int. Ed.* **2016**, doi:10.1002/anie.201508381.
[2] W. G. Zeier, J. Schmitt, G. Hautier, U. Aydemir, Z. M. Gibbs, C. Felser, G. J. Snyder, *Nat. Mater. Rev.* **2016**, 16032.
[3] W. G. Zeier, H. Zhu, Z. M. Gibbs, G. Ceder, W. Tremel, G. J. Snyder, *J. Mater. Chem. C* **2014**, *2*, 10189–10194.
[4] J. Zhang, L. Song, G. K. H. Madsen, K. F. F. Fischer, W. Zhang, X. Shi, B. B. Iversen, *Nat. Commun.* **2016**, *7*, 10892.
[5] Y. Tang, Z. M. Gibbs, L. Agapito, G. Li, H.-S. Kim, M. B. Nardelli, S. Curtarolo, G. J. Snyder, *Nat. Mater.* **2015**, *14*, 1223–1228.

* Dr. Wolfgang G. Zeier
E-Mail: Wolfgang.G.Zeier@phys.chemie.uni-giessen.de
[a] Department of Materials Science and Engineering, Northwestern University, Evanston IL 60208, USA
[b] Physikalisch-Chemisches Institut, Justus-Liebig-University Gießen, Heinrich-Buff-Ring 17, 25392 Giessen, Germany
[c] School of Science, Wuhan University of Technology, Wuhan, China

 © 2016 WILEY-VCH Verlag GmbH & Co. KGaA, Weinheim

10.1002/zaac.201604003

The Crystal Structure of $BaPt_2Al_5$

Frank Stegemann[a] and Oliver Janka*[a]

Keywords: Intermetallics, Alkaline Earth, Aluminum

Ternary alkali or alkaline earth metal containing aluminum compounds of the late transition metals (group 10 and 11) have been scarcely investigated[1]. With $SrPt_2Al_2$[2], $Sr_2Pd_4Al_5$[3] and $Ba_3Pt_4Al_4$[4] we have recently added the first compounds to the respective *EA*-*T*-Al systems. During attempts to synthesize additional compounds we were able to obtain single crystals of $BaPt_2Al_5$. This compound crystallizes in the orthorhombic crystal system with space group *Immm* and lattice parameters of a = 420.78(2), b = 728.44(4) and c = 1043.84(7) pm. The compound is isostructural to $PrNi_2Al_5$. The Pt and Al atoms from a network; the Ba atoms reside in cavities. Due to the low transition metal content of the framework no homoatomic Pt bonds are found, however a significant amount of Al–Al interactions are observed. During the structure refinement, unusually large anisotropic displacement parameters were observed for the Al2 atoms, which exhibit a low coordination number (2+8 fold) according to $Al2@Pt_2Al1_8$ in the shape of a 2-fold capped cuboid (Fig. 1). Attempts to synthesize the isostructural iridium compound resulted in the formation of $BaIr_4Al_{11}$ showing similar atomic arrangements.

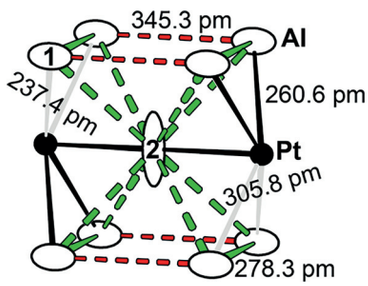

Figure 1. Coordination environment of the Al2 atoms in the crystal structure of $BaPt_2Al_5$.

[1] P. Villars, K. Cenzual, Pearson′s Crystal Data: Crystal Structure Database for Inorganic Compounds (on DVD), ASM International®, Materials Park, Ohio, USA **Release 2015/2016**.
[2] R.-D. Hoffmann, F. Stegemann, O. Janka *Z. Kristallogr.* **2015**, *231*, 127–142.
[3] F. Stegemann, C. Benndorf, R. S. Touzani, B. P. T. Fokwa, O. Janka, *Eur. J. Inorg. Chem.* **2016**, *2016*, 1108–1114.
[4] F. Stegemann, C. Benndorf, T. Bartsch, R. S. Touzani, M. Bartsch, H. Zacharias, B. P. T. Fokwa, H. Eckert, O. Janka ,*Inorg. Chem.* **2015**, *54*, 10785–10793.

* Dr. Oliver Janka
E-Mail: ocjanka@uni-muenster.de
[a] Westfälische Wilhelms-Universität Münster
Institut für Anorganische und Analytische Chemie
Corrensstrasse 28/30
48149 Münster, Germany

10.1002/zaac.201604004

The Acetonitrilide Anion CCN^{3-}

Franziska Jach,*[a,b] Stephan I. Brückner,[a] Alexander Ovchinnikov,[b] Matej Bobnar,[b] Anna Isaeva,[a] Matthias Groh,[a] Eike Brunner,[a] Peter Höhn,*[b] and Michael Ruck[a,b]

Keywords: Acetonitrilide, tantalum, nitridometalate

The new CO_2-isoelectronic acetonitrilide anion CCN^{3-} (Figure 1) is stabilized in the solid state matrix of the metal-rich compound $Ba_5[Ta^VN_4][C_2N]$.[1] Single crystals were obtained from a solution of Ba and NaCN in liquid Na via reaction with the Ta ampoule. The atomic structure of CCN^{3-} was confirmed by single-crystal X-ray diffraction data, 2D NMR experiments and Raman measurements on ^{13}C-, ^{15}N-, and $^{13}C^{15}N$-labelled samples. Vibrations and corresponding isotopic shifts were analyzed using quantum-chemical calculations. Hydrolysis of $Ba_5[TaN_4][C_2N]$ results in H_3CCN (acetonitrile).
In contrast to acetonitrile and its partially deprotonated anions in Li[PhHCCN] and Li_2[*R*CCN] (R = H, Me_3Si),[2] the hydrogen-free CCN^{3-} anion exhibits a weaker C–N bond and a stronger C–C bond as indicated by bond lengths, vibrational frequencies and an increased NMR coupling constant J_{CC} as well as computed delocalization indices. Rather than forming a localized C–C single bond and a C≡N triple bond, the electron pairs are shifted towards two double bonds, indicating an intermediate state between the mesomeric formulas $[C–C{\equiv}N]^{3-} \leftrightarrow [C{=}C{=}N]^{3-}$, in analogy to the pair cyanamide/carbodiimide.

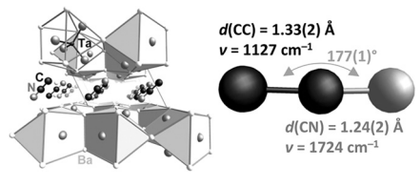

Figure 1. Left: Crystal structure of $Ba_5[Ta^VN_4][C_2N]$ ($C2/m$, a = 12.0177(3) Å, b = 10.9165(3) Å, c = 9.3430(3) Å, β = 117.467(1)°), viewed along [010]. Right: CCN^{3-} anion with bond lengths and valence vibrational frequencies.

[1] F. Jach, M. Groh, P. Höhn, M. Ruck, *Z. Anorg. Allg. Chem.* **2014**, *640*, 2359.
[2] a) R. Enjalbert, J. Galy, *Acta Crystallogr., Sect. B* **2002**, *58*, 1005–1010; b) T. Shimanouchi, *Tables of Molecular Vibrational Frequencies Consolidated Vol. I*, National Bureau of Standards, **1972**, 84; c) G. A. Gornowicz, R. West, *J. Am. Chem. Soc.* **1971**, *93*, 1714–1720; d) G. Boche, M. Marsch, K. Harms, *Angew. Chem. Int. Ed. Engl.* **1986**, *25*, 373–374; e) W. Zarges, M. Marsch, K. Harms, G. Boche, *Chem. Ber.* **1989**, *122*, 1307–1311.

* F. Jach
E-Mail: jach@cpfs.mpg.de
[a] Technische Universität Dresden, Fachrichtung Chemie und Lebensmittelchemie, 01062 Dresden, Germany
[b] Max-Planck-Institut für Chemische Physik fester Stoffe, Nöthnitzer Straße 40, 01187 Dresden, Germany

 © 2016 WILEY-VCH Verlag GmbH & Co. KGaA, Weinheim

10.1002/zaac.201604005

MOFs as Hosts for *Pi*-Conjugated Molecules

Daniela Hermann,[a] Heidi Schwartz,[a] and Uwe Ruschewitz*[a]

Keywords: metal-organic frameworks (MOFs), organic memory devices, organic solar cells, *pi*-conjugated molecules

The photo-switching properties of *pi*-conjugated molecules like azobenzenes (AZO), spiropyrans (SP) / merocyanines (MC) or dithienylethenes (DTE) are well established in solution, but mainly hindered in the crystalline materials due to sterical restrictions. With respect to possible applications e.g. as organic memory devices (OMEMs) we have started to explore the potential of metal-organic frameworks (MOFs) as crystalline host materials for the embedment of such *pi*-conjugated molecules. Within the MOF's pores the guest molecules are spatially separated from each other so that in most cases very good photo-switching properties are observed. Some of them are even improved compared to a solution of the molecular switch.[1]

In this presentation we will show how structural investigations on polycrystalline materials can be used to get a first insight into the underlying host-guest interactions (Figure 1). These results are nicely confirmed by IR spectroscopy, as the IR signals of the OH groups of MOFs of the MIL series show a significant shift indicating strong interactions. For the spiropyran / merocyanine switching systems we observed a remarkable influence of the MOF pores on their photochromic properties. This resembles the behaviour of these molecules in solution so that MOFs might be considered as "solid solvents" for such *pi*-conjugated molecules.

Finally, we will present our first attempts to incorporate such systems into real devices like organic solar cells (OPVs) or organic memory devices (OMEMs). These investigations were conducted in close cooperation with the Meerholz group at Cologne University (Physical Chemistry). Devices based on thin films of MIL-68(In) as well as SURMOFs based on HKUST-1 provided by the Heinke group (KIT, Karlsruhe) will be compared.

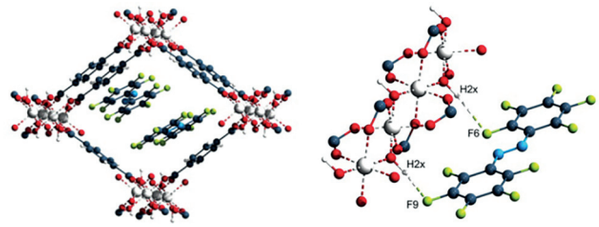

Figure 1. pf-AZO@MIL-53(Al): crystal structure (left) and hydrogen bonding interactions (right).

[1] D. Hermann, H. Emerich, R. Lepski, D. Schaniel, U. Ruschewitz, *Inorg. Chem.* **2013**, *52*, 2744–2749.

* Prof. Dr. U. Ruschewitz
E-Mail: uwe.ruschewitz@uni-koeln.de
[a] Institute of Inorganic Chemistry
University of Cologne
Greinstraße 6
50939 Köln, Germany

 © 2016 WILEY-VCH Verlag GmbH & Co. KGaA, Weinheim

10.1002/zaac.201604006

Multifunctional Core/Shell-Structures of Luminescent MOFs and Superparamagnetic Fe_3O_4/SiO_2 Microparticles

Tobias Wehner,[a] Michael Schneider,[b] Karl Mandel,[b] Gerhard Sextl,[b] and Klaus Müller-Buschbaum*[a]

Keywords: composites, metal organic frameworks (MOFs), superparamagnetism, sensing

Composite materials can combine attractive properties of both components[1]. Core/shell particles of lanthanide containing MOFs such as $2_\infty[Ln_2Cl_6(bipy)_3]\cdot 2bipy$ and microparticles of Fe_3O_4 in a silica matrix have been successfully generated via mechanochemical synthesis of the MOF in the presence of the particles or mechanochemical coating of the particles with the MOF[2]. The resulting composite particles share the initial properties of both components being both, luminescent from the intrinsic MOF luminescence and superparamagnetic from the Fe_3O_4 nanoparticles. This uncommon combination can be shown to be used for an expansion of the sensing concept with MOF luminescence: So far, small molecules have been sensed mainly by from the gas phase[3]. We can now show that the composite particles are suitable to detect molecules such as water or oxygen from liquids by signal augmentation. The sensing of molecules can thereby be carried out in large volumes of liquid phases with only small amount of the sensing device.

The MOF luminescence is used for the sensing process itself by a luminescence change upon analyte interaction, whereas the superparamagnetism of the core allows for collecting the composite particles subsequent to sensing. It is thereby responsible for the strong signal augmentation based on magnetic separation followed by signal read-out.

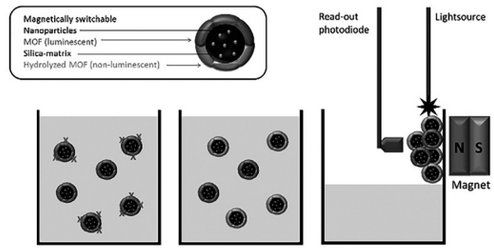

[1] P. Lu, J.-L. Zhang, Y.-L. Liu, D.-H. Sun, G.-X. Liu, G.-Y. Hong, J.-Z. Ni, *Talanta* **2010**, *82*, 450–457.
[2] T. Wehner, K. Mandel, M. Schneider, G. Sextl, K. Müller-Buschbaum, *ACS Appl. Mater. Interfaces* **2016**, *8*, 54455–54462.
[3] K. Müller-Buschbaum, F. Beuerle, C. Feldmann, *Microporous Mesoporous Mater.* **2015**, *216*, 171–199.

* Prof. Dr. K. Müller-Buschbaum
E-Mail: k.mueller-buschbaum@uni-wuerzburg.de
[a] Institut für Anorganische Chemie, Universität Würzburg, Am Hubland, 97074 Würzburg, Germany)
[b] Fraunhofer Institut für Silicatforschung ISC, Neunerplatz 2, 97082 Würzburg, Germany

 © 2016 WILEY-VCH Verlag GmbH & Co. KGaA, Weinheim

10.1002/zaac.201604007

Sheets of Six-Membered Rings in Borides and Boride Carbides: Honeycomb, Chair, Boat, or a Combination Thereof

Kathrin Hofmann,[a] Nalan Kalyon,[a] and Barbara Albert*[a]

Keywords: Borides; Boride carbides; Crystal structure

Due to their favorable materials properties like superconductivity[1], hardness[2], high melting points, and magnetism[2], borides and boride carbides with layered structures are in the focus of our interest. At the same time these compounds exhibit a very diverse structural chemistry which will be discussed, emphasizing on structures with sheets of condensed six-membered boron and boron/carbon rings. On the basis of X-ray and neutron powder data we were able to show that 1) the structures of the diborides of Re, Ru, and Os contain puckered sheets of condensed B_6-rings comparable to the chair- and boat conformation of cyclohexane[3], whereas it is well known for the early transition metal diborides like MnB_2 and CrB_2 to crystallize in the AlB_2-type with planar boron sheets, 2) Mo_2B_4 and W_2B_4 contain both, planar and puckered (chair-conformation) boron layers[4] and 3) in Ru_2B_3 and Os_2B_3 isolated boron atoms can be found besides puckered sheets of B_6-rings in chair conformation[5]. Recent investigations show that the formation of full solid solutions without gap is neither possible for the compounds $Re_{1-x}Mn_xB_2$[6] nor $Cr_{1-x}Mn_xB_2$ [2], suggesting that more factors besides the size of the metal cation influence the formation of these compounds.

Boride carbides exist in an even larger variety of B/C sheets with different ring sizes, but for structural and electronic reasons planar six-membered B/C-rings can only be obtained with small metal atoms, like Li in LiBC[7] and Be in BeB_2C_2 [8]. The arrangement of the B/C-layers is different in both compounds. The structure of LiBC can be derived from the AlB_2-type; BeB_2C_2 is structurally related to graphite.

[1] M. Kayhan et al., *Solid State Sci.* **2012** *14*, 1656–1659.
[2] N. Kalyon, planned PhD thesis, TU Darmstadt.
[3] M. Frotscher, M. Hölzl, B. Albert, *Z. Anorg. Allg. Chem.* **2010**, *636*, 1783–1786.
[4] M. Frotscher et al., *Z. Anorg. Allg. Chem.* **2007**, *633*, 2626–2630.
[5] M. Froscher A. Senyshyn, B. Albert, *Z. Anorg. Allg. Chem.* **2012**, *638*, 2078–2080.
[6] A. Knappschneider, PhD thesis, TU Darmstadt, 2014.
[7] M. Wörle et al., *Z. Anorg. Allg. Chem.* **1995**, *621*, 1153–1159.
[8] K. Hofmann et al., *Angew. Chem.* **2008**, *120*, 2333–2336.

* Prof. Dr. B. Albert
E-Mail: albert@ac.chemie.tu-darmstadt.de
[a] Eduard-Zintl-Institute of Inorganic and Physical Chemistry, Technische Universität Darmstadt
Alarich-Weiss-Straße 12
D-64287 Darmstadt

10.1002/zaac.201604008

Bismuth–Oxide Nanotubes

Alexander Weiz,*[a] Anna Isaeva,[a] Wouter Van den Broek,[b] Johannes Biskupek,[c] Ute Kaiser,[c] Thomas Doert,[a] and Michael Ruck[a,d]

Keywords: Bismuth oxide, Nanotube, TEM, Solvent-mediated synthesis

The reaction of BiOI with *n*-butyllithium in *n*-hexane yields a grey powder that contains elemental bismuth and two bismuth oxide iodides, BiOI and Bi_5O_7I, as identified by X-ray powder diffraction analysis.

An SEM study of the reaction product reveals nanotubes (up to 500 nm in length, ca. 7 nm in diameter) that mainly reside on top or at the sides of rectangular platelets (Figure 1a) as well as partially agglomerated irregular-shaped nanoparticles. The platelets are identified as Bi_5O_7I by TEM and EDX experiments (C_S-corrected FEI Titan, 80 kV). The nanotubes show the same periodicity and thus structural resemblance to Bi_5O_7I (Figure 1b), whereas the EDX analysis yields an approximate composition of Bi_2O_3.

Based on these results, a structure model of the nanotubes was constructed by rolling up a two-dimensional fragment of the Bi_5O_7I structure and replacing the iodine ions by hydroxide in order to maintain electroneutrality (Figure 1c). The theoretical HRTEM image [1] (f = 90 nm, t = 6.7 nm) for the model matches the experimentally observed one very well (Figure 1d).

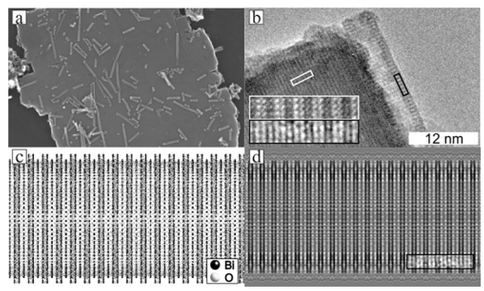

Figure 1. a: SEM image of the nanotubes on a Bi_5O_7I platelet; **b:** an HRTEM image of a nanotube and a Bi_5O_7I platelet (unit cell outlined in white); the periodicity of the platelet and the nanotube are highlighted juxtaposed in the inset; **c:** a structure model of the nanotube; **d:** a theoretical HRTEM image of the nanotube model.

[1] P. A. Stadelmann. JEMS – EMS Java Version, 2004.

* Alexander Weiz, M.Sc.
E-Mail: Alexander.Weiz@chemie.tu-dresden.de
[a] Department of Chemistry and Food Chemistry, TU Dresden, D-01062 Dresden, Germany
[b] Structure Research and Electron Microscopy Group, Humboldt University Berlin, D-12489 Berlin, Germany
[c] Electron Microscopy Group of Material Science, Ulm University, D-89081 Ulm, Germany
[d] Max Planck Institute for Chemical Physics of Solids, D-01187 Dresden, Germany

 © 2016 WILEY-VCH Verlag GmbH & Co. KGaA, Weinheim

10.1002/zaac.201604009

Electrospun Solid Electrolytes for Lithium Ion Batteries

Katharina M. Freitag,[a] Holger Kirchhain,[b] Leo van Wüllen,[b] and Tom Nilges*[a]

Keywords: solid state electrolytes, lithium ion batteries

In order to overcome the security risks of lithium ion batteries resulting from flammability and leakage of liquid electrolytes, solid electrolytes are a promising alternative.[1] Electrospinning as a tool for energy materials design and application seems to be a promising method for membrane synthesis.[2].

Herein, the electrospinning synthesis and characterization of composite solid state polymer electrolytes for lithium ion batteries in the system Polyethylene oxide (PEO) and conductive additives is reported. Electrospinning is a simple and fast synthesis method to produce ultra-thin membranes which can be punched up and directly assembled in batteries.

Different compositions of polymer matrix and additives were tested. All membranes were subject to a detailed material characterization using SEM, X-ray diffraction, differential scanning calorimetry, impedance spectroscopy, cyclic voltammetry, and solid state NMR spectroscopy.[3]

SEM images showed a membrane structure containing of sub micrometer fibers. Impedance experiments showed ionic conductivities up to ~10^{-4} S/cm at room temperature and low activation energies (< 40 kJ/mol). These results were also confirmed by solid state NMR spectroscopy. Activation energies for ion hopping are consistent with the data derived from impedance spectroscopy. Furthermore, we will report on the stability of selected membranes against Lithium metal by CV measurements. The physical properties are positively influenced by electrospun membranes compared to bulk material. Obviously, electrospinning in combination with defined additives beneficial on the ion mobility within the fibers.

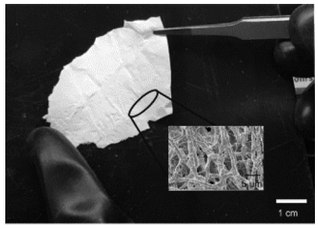

Fig. 1: Electrospun membrane and SEM image.

[1] J. G. Kim, B. Son, S. Mukherjee, N. Schuppert, *J. Power Sources* **2015**, *282*, 299–322.
[2] J.-W. Jung, C.-L. Lee, S. Yu, I-D. Kim, *J. Mater. Chem. A* **2016**, 4, 703–750.
[3] K. M. Freitag, H. Kirchhain, T. Nilges, L. van Wüllen, **2016**, submitted.

* Prof. Dr. T. Nilges
E-Mail: tom.nilges@lrz.tu-muenchen.de
[a] Technical University of Munich, Department of Chemistry, Lichtenbergstr. 4, 85747 Garching b. München, Germany
[b] University of Augsburg, Institute of Physics, Universitätsstr. 1, 86159 Augsburg, Germany

10.1002/zaac.201604010

Carbide-Derived Carbons with Hierarchical Pore Architecture as Electrochemical Energy Storage Materials

Martin Oschatz[a] and Stefan Kaskel*[b]

Keywords: electrical double-layer capacitor, Li-S battery, nanoporous carbide-derived carbon, electrodes

Electrochemical energy storage in batteries and electrochemical capacitors is crucial for the efficient utilization of alternative energy sources and for powering of mobile devices. In such energy storage applications, nanoporous carbon materials are important electrode components due to their high specific surface area (SSA) and electric conductivity.

Especially carbide-derived carbons (CDCs) with hierarchical pore architectures are promising materials due to their high surface area provided by well-defined micropores with diameters < 2 nm and efficient mass transport by a pore system of larger meso- or macropores. CDCs are typically microporous materials produced by high-temperature chlorine treatments of carbides, leading to the formation of pores by removal of metal- or semi-metal atoms.[1] The generation of hierarchical pore structures requires the use of structure-directing agents,[2] sol-gel methods,[3] or sacrificial templates[4] in combination with polycarbosliane polymers as silicon carbide precursors. The transport pore system can be shaped prior to chlorine treatment and the porous silicon carbide is then transferred to hierarchical CDC by silicon removal in a conformal way.

CDCs with hierarchical pore structure provide SSAs close to 3000 m^2/g and internal pore volumes of up to 8 cm^3/g, depending on the applied synthesis method. Li-S batteries with CDC electrodes achieve specific capacities up to 600 $mAh/g_{electrode}$ and EDLCs making use of CDC electrodes can achieve 250 F/g.

[1] V. Presser, M. Heon , Y. Gogotsi, *Adv. Funct. Mater.* **2011**, *21*, 810–833.
[2] M. Oschatz, L. Borchardt, M. Thommes, K. A. Cychosz, I. Senkovska, N. Klein, R. Frind, M. Leistner, V. Presser, Y. Gogotsi, S. Kaskel, *Angew. Chem. Int. Ed.* **2012**, *51*, 7577–7580.
[3] M. Oschatz, W. Nickel, M. Thommes, K. A. Cychosz, M. Leistner, M. Adam, G. Mondin, P. Strubel, L. Borchardt, S. Kaskel, *J. Mater. Chem. A* **2014**, *2*, 18472–18479.
[4] M. Oschatz, J. T. Lee, H. Kim, W. Nickel, L. Borchardt, W. I. Cho, C. Ziegler, S. Kaskel, G. Yushin, *J. Mater. Chem. A* **2014**, *2*, 17649–17654.

* Prof. Dr. S. Kaskel
E-Mail: stefan.kaskel@chemie.tu-dresden.de
[a] Inorganic Chemistry and Catalysis, Debye Institute of Nanomaterials Science, Utrecht University, Universiteitsweg 99, 3584 CG Utrecht, The Netherlands
[b] Institute for Inorganic Chemistry, Technical University Dresden, Bergstraβe 66, 01069 Dresden, Germany

 © 2016 WILEY-VCH Verlag GmbH & Co. KGaA, Weinheim

10.1002/zaac.201604011

Cr-Poisoning of $La_2NiO_{4+\delta}$ in Solid Oxide Cells

Andreas Egger,*[a] Nina Schrödl,[a] and Werner Sitte[a]

Keywords: Cr-poisoning, nickelate, SOFC, SOEC

High-temperature steam electrolysis (HTSE) offers a way for highly efficient water splitting if thermal coupling to existing heat sources is available. HTSE technology is based on solid oxide electrolyser cells (SOECs), whose degradation rates are currently roughly one order of magnitude higher than for their galvanic counterpart, i.e. solid oxide fuel cells (SOFCs)[1]. In this work the mixed ionic-electronic conducting ceramic $La_2NiO_{4+\delta}$ (LNO) is characterised as electrode material for high temperature electrolyser and fuel cells where special emphasis is put on the chromium tolerance of the material[2]. Resistance to chromium poisoning is an important aspect for SOEC and SOFC air electrodes due to the presence of Cr-sources such as metallic interconnects in the stack[3]. The effects of Cr-poisoning are investigated on densely sintered LNO samples as well as on symmetrical cells with porous LNO electrodes under both anodic and cathodic polarisation. Long-term investigations performed on dense samples at 800°C show the formation of detrimental Cr-containing secondary phases on the LNO surface in the presence of a Cr-source in humid atmospheres. Investigations of porous electrodes under similar conditions show a pronounced increase of the cell impedance with time, which is largely attributed to degradation processes at the SOFC cathode side. Moreover, results from analytical post-test investigations of oppositely polarised electrode layers confirm higher Cr-contaminations on the SOFC air electrode.

[1] M.A. Laguna-Bercero, *J. Power Sources* **2012**, *203*, 4–16.
[2] A. Egger, N. Schrödl, W. Sitte, *Faraday Discuss.* **2015**, *182*, 379 – 391.
[3] S.P. Jiang, X. Chen, *Int. J. Hydrogen Energy* **2014**, *39*, 505–531.

* Dr. A. Egger
E-Mail: andreas.egger@unileoben.ac.at
[a] Montanuniversitaet Leoben
Chair of Physical Chemistry
Franz-Josef-Straße 18
8700 Leoben, Austria

10.1002/zaac.201604012

Local Information Powers Heterogeneous Catalysis Research: TEM Reveals a Layered ZnO in Industrial Relevant $Cu/ZnO/Al_2O_3$ Catalyst

Thomas Lunkenbein,*[a] Elias Frei,[a] Julia Schumann,[a] Malte Behrens,[b] Marc G. Willinger,[a] and Robert Schlögl[a]

Keywords: methanol synthesis, TEM, catalysis

In a simplified picture a heterogeneous catalyst can be described as a high energy material, which is composed of two important parts: bulk and surface. The bulk is defined by a crystal and electronic structure as well as defect concentration, and reflects the real structure of the catalyst. It stabilizes the active surface. Although information on the real and surface structure can be obtained by integral methods, local fluctuations from the ideal structure, which are essential for the catalytic performance, of the catalyst composition may be overlooked.[1,2] This highlights the significance of transmission electron microscopy (TEM) for the local description of heterogeneous catalysts.

Here, we focus on a local TEM description of a $Cu/ZnO/Al_2O_3$ catalyst for methanol synthesis. Our observations tackle a detailed investigation of the real- and mesostructure of the catalyst as well as the formation of a special layered polymorph of ZnO on top of the Cu nanoparticles after reductive activation.[2,3] In addition, we will highlight the evolution of this metastable layered ZnO polymorph from minutes to months.

In conclusion, the results demonstrate the power of local TEM investigation in heterogeneous catalysis research.

[1] T. Lunkenbein, F. Girgsdies, A. Wernbacher, J. Noack, G. Auffermann, A. Yasuhara, A. Klein-Hoffmann, W. Ueda, M. Eichelbaum, A. Trunschke, R. Schlögl, M.G. Willinger, *Angew. Chem. Int. Ed.* 2015, *54*, 6828–6831.
[2] T. Lunkenbein, J. Schumann, M. Behrens, R. Schlögl, M.G. Willinger, *Angew. Chem. Int. Ed.* 2015, *54*, 4544–4548.
[3] M. Behrens, F. Studt, I. Kasatkin, S. Kühl, M. Hävecker, F. Abild-Pedersen, S. Zander, F. Girgsdies, P. Kurr, B.L. Kniep, M. Tovar, R.W. Fischer, J.K. Nørskov, R. Schlögl, *Science* 2012, *336*, 893–897.

* Dr. T. Lunkenbein
E-Mail: lunkenbein@fhi-berlin.mpg.de
[a] Fritz-Haber-Institut der Max-Planck-Gesellschaft, Abteilung für Anorganische Chemie
Faradayweg 4-6
14195 Berlin, Germany
[b] Universität Duisburg-Essen, Fakultät für Chemie und CENIDE
Universitätstr.7
45141 Essen, Germany

 © 2016 WILEY-VCH Verlag GmbH & Co. KGaA, Weinheim

10.1002/zaac.201604013

The Crystallography and Electronic Structure of YSZ Thin Films

Thomas Götsch,*[a] Michael Stöger-Pollach,[b] Alexander Menzel,[a] Erminald Bertel,[a] and Simon Penner[a]

Keywords: Thin films, Electron microscopy, Electron diffraction, Electronic structure, YSZ

Employing unsupported yttria-stabilized zirconia (YSZ) thin films (25 nm) with varying yttria contents, we investigated the influence of the amount of Y_2O_3 on the crystallography and electronic structure. Details of the preparation are given elsewhere.[1]

Even though the distinction between tetragonal and cubic YSZ polymorphs using diffraction techniques is almost impossible, we were able to distinguish them by calculating the lattice parameter *c* from selected area diffraction patterns. If this unit cell height is plotted as a function of the yttria-content (see Figure 1a), a stagnation of this parameter can be witnessed from 8 to 20 mol% Y_2O_3. However, because an increased amount of the larger ion (Y^{3+}) is present, the unit cell volume has to increase, which can only be explained if the unit cell is expanding in *a* and *b* directions, i.e. a phase transformation from the tetragonal to cubic crystal structure takes place.

Using EELS and UPS, electronic properties such as the band gaps (Figure 1b) were measured that show a very similar discontinuity between 8 and 20 mol% Y_2O_3, indicating the influence of both the degree of substitution by Y^{3+}, as well as the crystal structure.

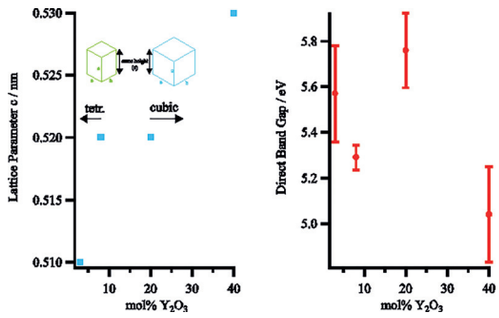

Figure 1. (a) Unit cell height, (b) direct band gaps.

[1] T. Götsch et al., *AIP Adv.* **2016,** *6,* 025119.

* T. Götsch
E-Mail: thomas.goetsch@uibk.ac.at
[a] Institute of Physical Chemistry
University of Innsbruck
Innrain 80–82
6020 Innsbruck, Austria
[b] University Service Center for Transmission Electron Microscopy,
Vienna University of Technology
Wiedner Hauptstraße 8–10
1040 Vienna, Austria

10.1002/zaac.201604014

Spin Coating of Multiferroic Composite Thin Films

Stefan Ebbinghaus,*[a] Norman Quandt,[a] and Till Walther[a]

Keywords: Multiferroics, Thin Films, Composites, Perovskites, Spinels

Multiferroic composites showing magnetoelectric coupling have attracted high interest for their potential applications for example in sensors or multistate data memories. Especially the system $BaTiO_3/CoFe_2O_4$ has been intensively studied and composites of different connectivities (0-3, 2-2, 1-3) have been prepared applying various preparation techniques.

We report on solution based synthesis approaches for preparing thin film composites of $BaTiO_3$ in combination with various ferrite spinels MFe_2O_4 (e.g. M = Co, Ni). Thin films were obtained via spin coating of DMF/HOAc-solutions on platinum coated silicon wafers in the form of bilayers[1], sandwich structures[2] or alternating multilayers. The synthesis was monitored by TGA and XRD and the final composites were investigated via SEM, EDX, AFM, Raman- and IR-spectroscopy. In addition polarization loops as well as magnetic and magnetoelectric measurements were carried out.

To obtain well-crystalline composite films with high-quality interfaces a sequence of different drying, calcination and crystallization steps had to be applied. Each coating step leads to a reproducible film thickness of about 25 nm. Thus, films of various thicknesses and/or stacking sequences can be easily prepared by applying the respective number of coating steps. AFM investigations revealed low surface roughnesses of ca. 4 nm. Polarization loops prove ferroelectricity and in turn the formation of the tetragonal $BaTiO_3$ modification.

Surprisingly, magnetic anisotropy was observed for many of the films. The orientation of the magnetic easy axis of $CoFe_2O_4$ was found to depend on the substrate. When the $CoFe_2O_4$ layer is grown on $BaTiO_3$ its magnetic easy axis is oriented parallel to the film surface. In contrast, the easy axis is perpendicular to the surface when $CoFe_2O_4$ is directly grown on the Pt-coated silicon wafer.

[1] N. Quandt *et al.*, *J. Solid State Chem.* **2016**, *223*, 82–89
[2] T. Walther *et al.*, *J. Eur. Ceram. Soc.* **2016**, *36*, 559–565.

* Prof. Dr. S. Ebbinghaus
E-Mail: stefan.ebbinghaus@chemie.uni-halle.de
[a] Martin Luther University Halle-Wittenberg,
Institute of Chemistry, Kurt-Mothes-Str. 2.
06120 Halle/Saale, Germany

 © 2016 WILEY-VCH Verlag GmbH & Co. KGaA, Weinheim

10.1002/zaac.201604015

Films of Intermetallic Compounds Prepared by DC Magnetron Sputtering

René R. Zimmermann,[a,c] Martin Siebert,[b] Roland Dittmeyer,[b] and Marc Armbrüster*[a]

Keywords: catalysis, gallium, intermetallic, palladium, sputtering

The intermetallic compound $GaPd_2$ is a highly active, selective and stable catalyst material for the selective hydrogenation of acetylene.[1] Bulk $GaPd_2$ possesses an extremely low specific surface area. Therefore $GaPd_2$ nanoparticles where successfully synthesized but here, the effort is quite high.[2]
DC magnetron sputtering from a self-made intermetallic sputter target was applied as a very efficient method for the production of thin intermetallic $GaPd_2$ films. Slabs of polished steel, Si (111) and borosilicate glass were taken as substrates for the film growth.
The single-phase nature of as-prepared samples was proven by X-ray diffraction. Scanning electron microscopy and energy dispersive X-ray spectroscopy confirmed homogeneity and chemical composition of the sputtered layers. The specific catalytic activity of these thin films in the selective hydrogenation of acetylene is increased by a factor of ca. 5000 compared to bulk $GaPd_2$ without affecting the selectivity to ethylene.

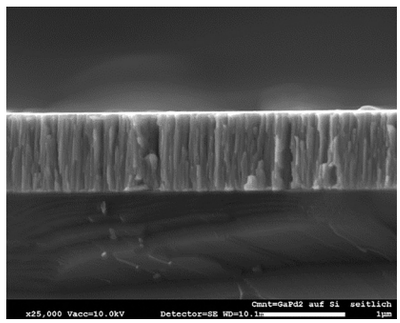

Figure 1. Intermetallic $GaPd_2$ layer sputtered on Si.

[1] M. Armbrüster, R. Schlögl, Yu. Grin, *Sci. Technol. Adv. Mater.* **2014**, *15*, 034803.
[1] M. Armbrüster, G. Wowsnick, M. Friedrich et al., *J. Am. Chem. Soc.* **2011**, *133*, 9112–9118.

* Prof. Dr. Marc Armbrüster
E-Mail: marc.armbruester@chemie.tu-chemnitz.de
[a] Max Planck Institute for Chemical Physics of Solids
01187 Dresden, Germany
[b] Karlsruhe Institute of Technology
Institute for Micro Process Engineering
76344 Eggenstein-Leopoldshafen, Germany
[c] Faculty of Natural Sciences, Institute of Chemistry
Materials for Innovative Energy Concepts
Technische Universität Chemnitz
09107 Chemnitz, Germany

10.1002/zaac.201604016

Red Emission of Eu^{2+} Ions Doped in Oxides and Zirconates as Promising New Candidates for Future LEDs

Sascha Krüger[a] and Claudia Wickleder*[a]

Keywords: Eu^{2+}, luminescence, oxides, zirconates

Recently, the development of new red phosphors became more and more important due to the environmental considerations and the accompanying research in designing novel LEDs[1]. One common method is to coat a blue light emitting GaN-Chip with a yellow phosphor such as $Y_3A_{l5}O_{12}:Ce^{3+}$ (YAG:Ce^{3+})[2], but additional low energy emitting phosphors are necessary to obtain satisfying light quality. The current aim is to find host lattices for Eu^{2+} in which the d-f-transition can be excited by the blue GaN-Chip followed by a low energy emission, which is a real challenge! For this purpose, oxides are a promising choice because of their thermal stability, nontoxicity and general low-energy emission of Eu^{2+} ions doped in these compounds due to the high impact of the nephelauxetic effect and crystal field splitting. The respective materials are, however, not well investigated due to difficult preparation.
SrO and CaO doped with Eu^{2+} are already known[3,4], but with low quality of the samples and low efficiency of the luminescence. For the first time, however, the preparation without reduction in H_2 atmosphere but by direct doping with EuO in Ta ampoules is reported here. Moreover, $CaZrO_3$ and $SrZrO_3$ doped with Eu^{2+} will be presented for the first time, which are extremely advantageous because they are air and long-time stable and excitable even in the blue-green region, which is important for energy-saving devises. All the described phosphors show band emission in the red range of the visible spectrum, which can be assigned to the typical 5d-4f transitions of Eu^{2+}.
As expected, the Ca-based compounds emit at lower energies than the Sr ones, because of the higher crystal field splitting. At room temperature, CaO:Eu^{2+} emits at 13620 cm^{-1} (734 nm) without observation of any Eu^{3+} impurities. SrO:Eu^{2+} shows luminescence at 15540 cm^{-1} (644 nm). The emission of $CaZrO_3:Eu^{2+}$ and $SrZrO_3:Eu^{2+}$ can be found in a similar region to the binary oxides which can be explained by similar first coordination spheres and bond lengths of the host lattices. However, the second coordination sphere differs significantly. Based on that, $CaZrO_3:Eu^{2+}$ emits at 15270 cm^{-1} (654 nm), whereas $SrZrO_3:Eu^{2+}$ shows luminescence at 16230 cm^{-1} (616 nm).

[1] P. Pust, P. J. Schmidt, W. Schnick, *Nat. Mat.*, **2015**, *14*, 454–458.
[2] P. Schlotter, R. Schmidt, J. Schneider, *Appl. Phys. A,* **1997**, *64*, 417–418.
[3] N. Yamashita, *J. Lumin.,* **1993**, *59*, 195–199.
[4] N. Yamashita, *J. Electrochem. Soc.,* **1993**, *140*, 840–843.

* Prof. Dr. C. Wickleder
wickleder@chemie.uni-siegen.de
[a] University of Siegen
Adolf-Reichwein-Straße 2
57068 Siegen, Germany

 © 2016 WILEY-VCH Verlag GmbH & Co. KGaA, Weinheim

10.1002/zaac.201604017

Narrow Band Emitting Red Phosphor $Sr(Sr,Ca)Si_2Al_2N_6:Eu^{2+}$

Daniel Bichler*[a]

Keywords: crystal structure, conversion phosphor, narrow band

For LED lighting applications the search for narrow band, red emitting phosphor materials is a very important task to raise the efficiency of modern phosphor converted LEDs (pc-LEDs). One of the most widespread conversion phosphors for red emission today is Eu-activated $(Ca,Sr)AlSiN_3$[1]. However its broad emission band (FWHM > 85 nm) prohibits highest efficiencies[2].

We discovered the alumo-nitrido-silicate $Sr(Sr_{1-x}Ca_x)Si_2Al_2N_6$. Surprisingly, despite its chemical composition being similar to $(Ca,Sr)AlSiN_3$ it does not crystalize in the same space group $Cmc2_1$[3], but in the monoclinic space group $P2_1$. Compared to $(Ca,Sr)AlSiN_3$, the monoclinic symmetry permits the formation of an ordered Sr-site which is ideal for activation with Eu^{2+}.

Eu-activated samples of $Sr(Sr_{1-x}Ca_x)Si_2Al_2N_6$ show efficient emission in the red spectral region with internal quantum efficiencies > 95 %. The emission can be tailored in a wide spectral region by varying x and the activator concentration. The narrow emission bandwidth (FWHM = 74-79 nm) allows the minimization of IR-losses and thus the design of pc-LEDs with more than 15% efficiency increase compared to typical state-of-the-art LEDs.

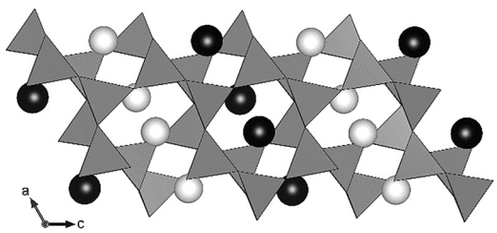

Figure 1. Crystal structure of $Sr(Sr_{1-x}Ca_x)Si_2Al_2N_6$along [010].

[1] H. Watanabe, K. Naoto, *J. Alloys Compd.* **2009**, *475*, 434–439.
[2] M. Mikami, H. Watanabe, K. Uheda, S. Shimooka, Y. Shimomura, T. Kurushima, N. Kijima, *IOP Conference Series: Materials Science and Engineering* **2009**, 1012002.
[3] F. Ottinger, **2004**, Dissertation, ETH Zürich.

* Dr. D. Bichler
E-Mail: d.bichler@osram.com
[a] OSRAM GmbH
CI AT MAT PH SYN
Mittelstetter Weg 2.
86830 Schwabmünchen, Germany

 © 2016 WILEY-VCH Verlag GmbH & Co. KGaA, Weinheim

10.1002/zaac.201604018

Komplexe Silicatstrukturen in Mikrodomänen von Lumineszenzmaterialien

Oliver Oeckler,*[a] Lukas Neudert,[b] Peter Schultz,[a] Dajana Durach,[b] and Wolfgang Schnick[b]

Keywords: Nitridosilicate, Elektronenmikroskopie, Synchrotronstrahlung, Fehlordnung

(Oxo-)Nitridosilicate von Erdalkali- und Seltenerdmetallen stellen wichtige Lumineszenzmaterialien dar. Mit der Kationenkombination La/Ba wurden besonders komplizierte Kristallstrukturen wie die von $La_{11}Si_{13}N_{27.636}O_{1.046}:Ce^{3+}$ oder $La_6Ba_3[Si_{17}N_{29}O_2]Cl$ erhalten.[1,2] Noch komplexere Strukturen finden sich in mikrokristallinen heterogenen Präparaten. Dort treten sie in gerichtet verwachsenen Domänen innerhalb nur wenige Mikrometer großer Kristallite auf. Mittels Elektronenbeugung wurden einkristalline Domänen identifiziert und deren Strukturen dann durch Beugung mikrofokussierter Synchrotronstrahlung[3] aufgeklärt. $Ba_{8-x}La_{18+x}Si_{43}N_{80-x}O_{1+x}$ ($x \approx 0$; $P\bar{6}$; $a = 17.45$, $c = 22.63$ Å; $R1 = 0.05$, $wR2 = 0.13$) ist durch ein ungewöhnliches unterbrochenes Netzwerk aus ecken- und kantenverknüpften $Si(O,N)_4$-Tetraedern und tetreaederfremde Anionen gekennzeichnet (Abb. 1). Es ist über schichtartige Teilstrukturen, die ähnlich auch einer stärker fehlgeordneten Phase mit ähnlicher Zusammensetzung und Struktur vorkommen, mit dieser verwachsen. Die beiden Verbindungen unterscheiden sich in der Anordnung und Verknüpfung der Tetraeder sowie der chemischen Formel. Bei Dotierung mit Ce^{3+} weisen sie unter UV-Licht gelbgrüne Lumineszenz auf.

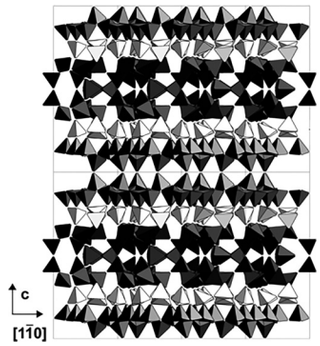

Abbildung 1. Kristallstruktur von $Ba_{8-x}La_{18+x}Si_{43}N_{80-x}O_{1+x}$

[1] D. Durach, P. Schultz, O. Oeckler, W. Schnick, *Inorg. Chem.* **2016**, *55*, 3624–3629.
[2] D. Durach, F. Fahrnbauer, O. Oeckler, W. Schnick, *Inorg. Chem.* **2015**, *54*, 8727–8732.
[3] F. Fahrnbauer, T. Rosenthal, T. Schmutzler, G. Wagner, G. B. M. Vaughan, J. P. Wright, O. Oeckler, *Angew. Chem. Int. Ed.* **2015**, *54*, 10020–10023.

* Prof. Dr. O. Oeckler
E-Mail: oliver.oeckler@gmx.de
[a] Universität Leipzig, Fakultät für Chemie und Mineralogie
Scharnhorststr. 20, 04275 Leipzig, Germany
[b] LMU München, Department Chemie
Butenandtstr. 5-13, 81377 München, Germany

 © 2016 WILEY-VCH Verlag GmbH & Co. KGaA, Weinheim

10.1002/zaac.201604019

Graphitic Carbon Dots: Synthesis and Rare-Earth-Based Luminescence

Claus Feldmann*[a]

Keywords: Carbon dots, layers, polyol synthesis, luminescence

Carbon dots (C-dots) – graphitic, layered carbon nanoparticles (<10 nm) – recently have attracted much attention owing to their fascinating physical properties and their wide range of potential applications, including bioimaging, optoelectronics, and catalysis[1]. In contrast to heavy-metal-based quantum dots (Q-dots), C-dots offer the advantages of absence of toxic heavy-metal elements, high chemical stability, high water dispersibility, and absence of blinking. In comparison to molecular fluorescent dyes, they show broader excitation spectra and low photobleaching[1].

This presentation addresses the synthesis of C-dots via most simple heating of polyols (e.g., glycerol, diethylene glycol, polyethylene glycol) at 180–230 °C[2,3]. Dehydration and carbonization of the polyols are supported by Lewis-acidic, oxophilic metal salts (e.g., $MgCl_2$, $ZnCl_2$). The as-prepared C-dot suspensions show intense blue emission with high quantum yield (50%)[3]. Aqueous suspensions show excellent colloidal stability and particle diameters of 3-5 nm at narrow size distribution[3]. Upon modification with Tb^{3+} or Eu^{3+}, the C-dots show efficient energy transfer after blue-LED excitation to Tb^{3+}/Eu^{3+} with characteristic line-type green or red emission and high quantum yields of 86/75%[3].

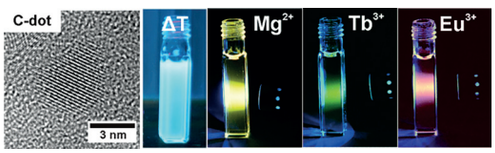

Figure 1. Polyol synthesis of C-dots: TEM image of single C-dot and emission of C-dots after heating (blue) and after modification with Mg^{2+} (yellow), d) Tb^{3+} (green), Eu^{3+} (red) (excited via blue-light LED, λ_{exc} = 465 nm).

[1] S. Y. Lim, W. Shen, Z. Gao, *Chem. Soc. Rev.* **2015**, *44*, 362 (Review).
[2] a) C. Feldmann, H. O. Jungk, *Angew. Chem. Int. Ed.* **2001**, *40*, 359; b) P. Schmitt, N. Brem, S. Schunk, C. Feldmann, *Adv. Funct. Mater.* **2011**, *21*, 3037; c) H. Dong, Y.-C. Chen, C. Feldmann, *Green Chem.* **2015**, *17*, 4107 (Review).
[3] a) H. Dong, A. Kuzmanoski, D. M. Gößl, R. Popescu, D. Gerthsen, C. Feldmann, *Chem. Commun.* **2014**, *50*, 7503; b) H. Dong, M. Roming,C. Feldmann, *Part. Part. Syst. Charact.* **2015**, *32*, 467; c) H. Dong, A. Kuzmanoski, C. Feldmann, *Chem. Commun.* **2016**, *submitted*.

* Prof. Dr. C. Feldmann
E-Mail: claus.feldmann@kit.edu
[a] Institute of Inorganic Chemistry, Karlsruhe Institute of Technology (KIT), Engesserstraße 15, 76131 Karlsruhe, Germany

10.1002/zaac.201604020

Distribution of Sulfur in Carbon-Sulfur Nanocomposites Analyzed by Small-Angle Scattering Methods

Albrecht Petzold,[a] Simone Mascotto,*[b] Günther Goerigk,[a] Daniel Clemens,[a] Bugra Kayaalp,[b] Jonas Scholz,[b] Anika Juhl,[b] Michal Fröba,[b] and Matthias Ballauff[a]

Keywords: (Lithium-sulfur batteries, small-angle scattering, porous carbon)

The analysis of the distribution of sulfur in nanoporous carbon hosts using small-angle scattering of x-ray and neutrons (SAXS and SANS) is here presented. Ordered porous CMK-8 carbon was used as host matrix and gradually filled with sulfur (20-50% wt.) via melt impregnation[1]. Thanks to the match between the electron densities of carbon and sulfur, the porous nanocomposites present two-phase systems and the filling of the host material can be precisely followed by SAXS. The analysis using the Porod parameter and the chord-length distribution (CLD) approach determined the specific surface areas and the filling mechanism of sulfur, respectively[2]. Moreover, using SANS the behavior of sulfur in the carbon matrix in the presence of a liquid phase, which might simulate the battery electrolyte, can be addressed. In the case of neutron scattering sulfur and carbon have different scattering length densities. The imbibition of the nanocomposites with liquids, which possess the same scattering contrast as carbon, enables the separation of the contribution of sulfur phase. Hence, valuable information on sulfur-carbon-solvent interactions can be gained. Thus, SAXS and SANS provide comprehensive characterization of the sulfur in porous carbon and valuable information for deeper understanding of cathode materials of lithium-sulfur batteries.

[1] X. Ji, K. Lee, L. Nazar, *Nature Materials* **2009**, *6*, 500–506.
[2] A. Petzold, A. Juhl, J. Scholz, B. Ufer, G. Goerigk, M. Fröba, M. Ballauff, S. Mascotto, *Langmuir* **2016**, 32, 27800–2786.

* JProf. Dr. Simone Mascotto
E-Mail: simone.mascotto@chemie.uni-hamurg.de
[a] Helmholtz-Zentrum Berlin
Hahn-Meitner Platz 1
14109 Berlin, Germany
[b] Institut für Anorganische und Angewandte Chemie
Universität Hamburg
Martin-Luther-King Platz 6
20146 Hamburg, Germany

 © 2016 WILEY-VCH Verlag GmbH & Co. KGaA, Weinheim

10.1002/zaac.201604021

Binary Palladium Selenides from Multianvil High-Pressure Experiments

Gunter Heymann*[a]

Keywords: high-pressure, selenides, palladium, crystal structure

Chalcogenide compounds of transition-metals show a broad range of semiconducting and metallic behaviors, tunable by physical and chemical methods [1]. High-pressure, in contrast to chemical composition and temperature, is one of the less frequently used parameters to modify properties, or even crystal structures. We were able to isolate single crystals of two new compounds, Pd_5Se_4 and Pd_9Se_7, synthesized under high-pressure/high-temperature conditions of 9.5 GPa and 1200 °C. Single crystal structure analyses for Pd_5Se_4 indicated the space group $C222_1$ with the following lattice parameters and refinement results: $a = 544.82(4)$, $b = 1124.08(7)$, $c = 1023.29(7)$ pm, $R1 = 0.0377$, $wR2 = 0.0646$, $GooF = 1.092$. The compound Pd_9Se_7 (Figure 1) crystallizes orthorhombic F-centered in the space group $Fdd2$ with lattice parameters and refinement results of $a = 3647.9(2)$, $b = 541.7(1)$, $c = 1116.5(1)$ pm, $R1 = 0.0256$, $wR2 = 0.0490$, and $GooF = 1.055$. Interestingly, the binary phases show a structural analogy to the ternary lithium transition-metal sulfides $Li_2M_3S_4$ (M = Pd, Pt) [2] from our group.

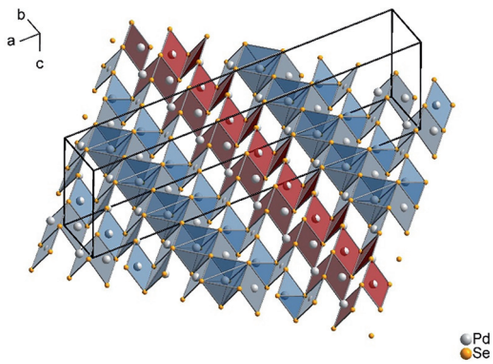

Figure 1. Layer of the Pd_9Se_7 crystal structure.

[1] a) H. Wang, H. Yuan, S. Sae Hong, Y. Li, Y. Cui, *Chem. Soc. Rev.* **2015**, *44*, 2664-2680; b) M. Ghorbani-Asl, A. Kuc, P. Miró, T. Heine, *Adv. Mater.* **2016**, *28*, 853–856.
[2] G. Heymann, O. Niehaus, H. Krüger, P. Selter, G. Brunklaus, R. Pöttgen, *J. Solid State Chem.* **2016**, *in press*.

* Gunter.Heymann
E-Mail: Gunter.Heymann@uibk.ac.at
[a] Institut für Allgemeine, Anorganische und Theoretische Chemie
Universität Innsbruck
Innrain 80-82
6020 Innsbruck, Austria

10.1002/zaac.201604022

Size Effects in MgO Cube Hydration and Dissolution

Johannes Schneider,[a] Ruth Schwaiger,[b] Stefan Baumann,[c] Thomas Berger,[a] Gilles Bourret,[a] and Oliver Diwald*[a]

Keywords: nanomaterials in the ambient, thin films of water, dissolution and recrystallization

The stability of oxide nanomaterials plays an important role during materials processing and storage. In particular interactions of water with the oxide surface are of high interest. The water can hereby originate from a processing solvent or is physisorbed due to contact with the ambient. We prepared MgO nanoparticles via chemical vapor synthesis and larger MgO cubes by Mg combustion in air. Both powders are subsequently annealed and oxidized under high vacuum conditions to achieve a dehydroxylated surface. The nanocubes are characterized by a small particle size d ≤ 10 nm whereas the larger MgO cubes have a size distribution in the range 10 nm ≤ d ≤ 1000 nm. Electron microscopy in conjunction with X-ray diffraction is applied to study the dissolution of MgO and formation of $Mg(OH)_2$. Two dissolution mechanisms were found: I) faster dissolution of (110) planes leading to truncation of the cubes and II) (100) and (110) dissolve with the same rate but much slower than in I). For the smaller nanocubes full particle dissolution is reached during the first stage[1].
In addition helium ion microscopy was applied to investigate the influence of physisorbed water on an indium substrate on the MgO cubes. Significant particle growth indicates the formation of $Mg(OH)_2$ and the truncation of cube edges and corners was observed. By pre-drying the indium foil before pressing the MgO on it, no such effect can be observed[2].

[1] S. O. Baumann, J. Schneider, A. Sternig, D. Thomele, S. Stankic, T. Berger, H. Groönbeck, O. Diwald, *Langmuir* **2015**, *31*, 2770−2776.
[2] R. Schwaiger, J. Schneider, G. R. Bourret, O. Diwald, *Beilstein J. Nanotechnol.* **2016**, *7*, 302–309.

* Prof. Dr. Oliver Diwald
E-Mail: oliver.diwald@sbg.ac.at
[a] Department of Chemistry and Physics
Paris-Lodron Universität Salzburg
Hellbrunnerstraße 34/III
5020 Salzburg, Austria
[b] nstitute for Applied Materials
Karlsruhe Institute of Technology
Hermann-von-Helmholz-Platz 1
76344 Eggenstein-Leopoldshafen, Germany
[c] Institute of Particle Technology
Friedrich-Alexander Universitaät Erlangen-Nuürnberg
Cauerstraße 4
91058 Erlangen, Germany

 © 2016 WILEY-VCH Verlag GmbH & Co. KGaA, Weinheim

10.1002/zaac.201604023

Layered $Ba[B_4O_6F_2]$:Eu – On Some New Silicate-Analogous Compounds

Henning A. Höppe,*[a] Stephan G. Jantz,[a] Katharina Förg,[a] Arno Kirchhain,[a] and Peter Gross[a]

Keywords: barium, gadolinium, borate, sulphate, phosphate, europium

Silicate-analogous materials comprise tetrahedral basic building units and thus provide host structures suited for luminescent applications. This contribution focusses on three new silicate-analogous compounds. Besides the first alkaline-earth fluorooxoborate $Ba[B_4O_6F_2]$ ($P2_1/n$, a = 663.84(2) pm, b = 767.33(3) pm, c = 1133.85(4) pm, β = 91.281(2)°), the first alkaline-earth and rare-earth borosulphates $Ba[B_2S_3O_{13}]$ and $Gd_2[B_2S_6O_{24}]$[1] the highly interesting ammonium borophosphate $(NH_4)_2[B_2P_3O_{11}(OH)]$ (a = 450.9(3) pm, b = 1449.0(2) pm, c = 1640.1(2) pm, $P2_12_12_1$) will be presented and discussed with respect to their syntheses and within structure systematics of borosulphates[2], borophosphates[3] and fluorooxoborates[4].

Besides the crystal structures of these new compounds also initial results of the optical properties of the doped compounds $Ba[B_4O_6F_2]$:Eu and $Gd_2[B_2S_6O_{24}]$:Eu will be discussed.

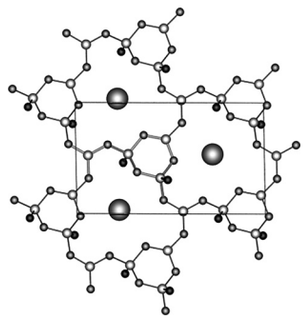

Figure 1. Fluorooxoborate layers in $Ba[B_4O_6F_2]$ (F black, O dark grey, B white, Ba large grey spheres).

[1] P. Gross, A. Kirchhain, H. A. Höppe, *Angew. Chem. Int. Ed.* **2016**, *55*, 4353-4355, *Angew. Chem.* **2016**, *128*, 4426–4428.
[2] H. A. Höppe, K. Kazmierczak, M. Daub, K. Förg, F. Fuchs, H. Hillebrecht, *Angew. Chem.* **2012**, *124*, 6359–6362; *Angew. Chem. Int. Ed.* **2012**, *51*, 6255–6257; M. Daub, K. Kazmierczak, P. Gross, H. A. Höppe, H. Hillebrecht, *Inorg. Chem.* **2013**, *52*, 6011–6020.
[3] B. Ewald, Y.-X. Huang, R. Kniep, Z. Anorg. Allg. Chem. **2007**, *633*, 1517–1540; K. Förg, H. A. Höppe, *Z. Anorg. Allg. Chem.* **2015**, *641*, 1009.
[4] G. Cakmak, J. Nuss, M. Jansen, *Z. Anorg. Allg. Chem.* **2009**, *635*, 631-636; T. Pilz, H. Nuss, M. Jansen, *J. Solid State Chem.* **2012**, *186*, 104–108.

* Prof. Dr. H. A. Höppe
E-Mail: henning.hoeppe@physik.uni-augsburg.de
[a] Institut für Physik, Universität Augsburg, Universitätsstraße 1, 86135 Augsburg, Germany

10.1002/zaac.201604024

Layered Double Hydroxides as Precursors for Mixed Metal and Mixed Metal Oxide Catalysts

Klaus Friedel Ortega,[a] Christian Lüttmann,[a] Denise Rein,[a] Faith Özcan,[a] and Malte Behrens*[a]

Keywords: Layered double hydroxides, heterogeneous catalysis, co-precipitation, thermal decomposition, ammonia decomposition

Layered double hydroxides (LDHs) or hydrotalcite-like materials of the general form $M^{II}_{1-x}M^{III}_x(OH)_2(CO_3)_{x/2}\cdot yH_2O$ are layered compounds, in which the composition of the brucite-like cationic layers $[M^{II}_{1-x}M^{III}_x(OH)_2]^{x+}$ exhibit a great flexibility with regard to their composition[1]. Many different divalent and trivalent metal cations, M^{II} and M^{III}, can be incorporated into the layers, among them numerous transition metals that possess interesting catalytic properties in various reactions solid catalysts ($Fe^{2+/3+}$, Co^{2+}, Ni^{2+}, Cu^{2+}, Pd^{2+}) or metal cations that act as catalyst promoters (Al^{3+}, Zn^{2+}, Mg^{2+}, Ga^{3+}). Thus, the synthesis of LDH precursors with controlled composition allows a systematic study of solid catalysts with a largely unaltered microstructure. The microstructure is determined by the hexagonal platelet-like morphology of the LDH precursors, which can be preserved to a large extent when forming the final catalysts from the precursor.

We have studied the co-precipitation and thermal treatment of various LDH precursors containing the above mentioned species as active metals or promoters[2-4]. Combining thorough characterization of the resulting materials with careful catalytic testing allows to establish robust relationships of structure and activity. For example, we were recently able to show that ex-LDH α-Fe/MgO/Ga_2O_3 is more active in the ammonia decomposition reactions than α-Fe/MgO/Al_2O_3 likely due to the in-situ nitridation of gallium oxide. Ga was also an efficient promoter of Ni- and Pd-based ex-LDH catalysts due to the formation of the intermetallic compounds Ni_3Ga and Pd_2Ga, respectively. These were found to be more active in the hydrogenation of CO_2 to methanol than the elemental metals.

[1] M. Behrens, *Catal. Today* **2015**, *246*, 46–54.
[2] S. Kühl, A. Tarasov, S. Zander, I. Kasatkin, M. Behrens, *Chem. Eur. J.* **2014**, *13*, 3782–3792.
[3] A. Ota, J. Kröhnert, G. Weinberg, I. Kasatkin, E.L. Kunkes, D. Ferri, F. Girgsdies, N. Hamilton, M. Armbrüster, R. Schlögl, M. Behrens, *ACS Catal.* **2014**, *4*, 2048–2059.
[4] K. Mette, S. Kühl, H. Düdder, K. Kähler, A. Tarasov, M. Muhler, M. Behrens, *ChemCatChem* **2014**, *6*, 100–104.

* Prof. Dr. M. Behrens
E-Mail: malte.behrens@uni-due.de
[a] Universität Duisburg-Essen, Fakultät für Chemie & Center for Nanointegration Duisburg-Essen (CENIDE), Universitätsstr. 7
45141 Essen, Germany

 © 2016 WILEY-VCH Verlag GmbH & Co. KGaA, Weinheim

10.1002/zaac.201604025

Layered Alkaline-Earth Metal Nitridomanganates: Synthesis, Crystal Structures and Physical Properties

Alexander Ovchinnikov,*[a] Matej Bobnar,[a] Yurii Prots,[a] Horst Borrmann,[a] Jörg Sichelschmidt,[a] Yuri Grin,[a] and Peter Höhn*[a]

Keywords: layered structures, magnetism, nitrides

Ternary phases comprising 0*D*[1] or 1*D*[2] building blocks are known in the *AE*–Mn–N systems. Here we report on three new layered *AE* nitridomanganates. Their crystal structures possess hexagonal nets of *AE* and Mn atoms coordinated by nitrogen. Due to short Mn–Mn distances within the layers, extended networks of metal-metal interactions are realized, leading to quenching of magnetism.

In $\mathbf{Ca_{12}[Mn_{19}N_{23}]}$ (space group *P*3, *a* = 11.8130(1) Å, *c* = 5.58976(7) Å, *Z* = 1), one Mn atom per formula unit carries a magnetic moment, hallmarked by a significant orbital contribution. The occurrence of the localized magnetism is caused by a peculiar arrangement of these particular Mn atoms, which do not participate in the Mn–Mn interactions. In contrast, the remaining Mn atoms are involved in such interactions and do not accommodate unpaired electrons, being non-magnetic.

In $\mathbf{Sr_{25}[Mn_{42}N_{50}]}$ (space group *P*, *a* = 17.9754(6) Å, *c* = 5.7935(2) Å, *Z* = 1), all Mn atoms appear to be chemically bound. As a result, no intrinsic localized magnetism is observed in this phase.

The most structurally complex compound from this family is $\mathbf{Ca_{133}[Mn_{216}N_{260}]}$ (space group *P*, *a* = 39.477(1) Å, *c* = 5.5974(2) Å, *Z* = 1). Its crystal structure comprises building modules found in both above-mentioned phases. Thus, the nitridomanganate layer can be divided into the following parts: $[Mn_{216}N_{260}]^{266-} = 3[Mn_{20}N_{24}]^{24-} + [Mn_{42}N_{50}]^{50-} + 6[Mn_{19}N_{23}]^{24-}$, where the last two fragments represent the structural building blocks of the two related nitridomanganates. Unpaired electrons reside only on the Mn atoms of the last block, analogous to that in $Ca_{12}[Mn_{19}N_{23}]$. Consequently, six manganese atoms per formula unit of $Ca_{133}[Mn_{216}N_{260}]$ demonstrate a localized magnetic behaviour.

[1] a) A. Tennstedt, C. Röhr, R. Kniep, *Z. Naturforsch.* **1993**, *48b*, 794–796. b) A. Tennstedt, C. Röhr, R. Kniep, *Z. Naturforsch.* **1993**, *48b*, 1831–1834. c) D. H. Gregory, M.G. Barker, P. P. Edwards, D. J. Siddons, *Inorg. Chem.* **1995**, *34*, 5195–5198. d) J. K. Bendyna, P. Höhn, R. Kniep, *Z. Kristallogr. – New Cryst. Struct.* **2008**, *223*, 185–186.

[2] A. Ovchinnikov, W. Schnelle, Yu. Grin, P. Höhn, *Z. Anorg. Allg. Chem.* **2014**, *640*, 2360.

* A. Ovchinnikov
E-Mail: Alexander.Ovchinnikov@cpfs.mpg.de
* Dr. P. Höhn
E-Mail: Peter.Hoehn@cpfs.mpg.de
[a] Max-Planck-Institut für Chemische Physik fester Stoffe, Nöthnitzer Straße 40, 01187 Dresden, Germany

 © 2016 WILEY-VCH Verlag GmbH & Co. KGaA, Weinheim

10.1002/zaac.201604026

Mesostructured Layered Perovskites for Solar Energy Conversion

Nils C. Hildebrandt,[a] André Blößer,[a] and Roland Marschall*[a]

Keywords: photocatalysis, layered perovskites, composites, electrospinning

Layered perovskites are a very interesting class of materials for photocatalytic water splitting. Their interlayer spaces can incorporate water, thus providing a higher number of active sites for photocatalysis,[1] and also facilitate homogenous doping from the gas phase.[2]

Moreover, structuring semiconductor oxides on the nanoscale to improve photocatalytic activity has gained increasing attention in recent years. One strategy is the synthesis and *in-situ* formation of semiconductor multiphase or multicomponent heterojunctions to reduce charge carrier recombination *via* vectorial charge transfer in photocatalytic reactions. For example, a three-component composite consisting of the layered perovskite $Ba_5Ta_4O_{15}$ with $Ba_3Ta_5O_{15}$ and $BaTa_2O_6$ shows superior overall water splitting without any co-catalyst over Rh-modified $Ba_5Ta_4O_{15}$.[3]

Photocatalyst nanofibers can be of advantage compared to particulate systems, exhibiting a high aspect ratio and surface area for good photocatalytic activity, however being usually thick enough to avoid band gap increase due to quantum confinement. We have prepared nanofibers of the complex layered perovskite photocatalysts $Ba_5Ta_4O_{15}$, $Ba_5Ta_2Nb_2O_{15}$ and $Ba_5Nb_4O_{15}$ via electrospinning. The formation mechanism of the nanofibers was investigated in detail. Superior photocatalytic activity for hydrogen generation and overall water splitting was found compared to simple powder samples,[4] and the influence of fiber thickness on the activity was investigated.

[1] F. E. Osterloh, *Chem. Mater.* **2008**, *20*, 35–54.
[1] R. Marschall, L. Wang, *Catal. Today* **2014**, *225*, 111–135.
[1] J. Soldat, R. Marschall, M. Wark, *Chem. Sci.* **2014**, *5*, 3746–3752.
[4] N. C. Hildebrandt, J. Soldat, R. Marschall, *Small* **2015**, *11*, 2051–2057.

* Dr. R. Marschall
E-Mail: roland.marschall@phys.chemie.uni-giessen.de
[a] Physikalisch-Chemisches Institut, Justus-Liebig-Universität Gießen
Heinrich-Buff-Ring 17
35392 Gießen, Germany

 © 2016 WILEY-VCH Verlag GmbH & Co. KGaA, Weinheim

10.1002/zaac.201605001

Ferrihydrite Outperforms Haematite in Electrochemical Water Oxidation

Michael Ertl,[a] Jonathan Moir,[b] Geoffrey Ozin,*[b] and Josef Breu,*[a]

Keywords: ferrihydrite, haematite, water splitting

Note: J. Moir and M. Ertl contributed equally to this work.

In order for solar and wind energy to fill the gap arising from the declining availability of fossil fuels, and considering the difficulty in storing primary forms of energy such as heat or electricity, renewable, chemical energy carriers are essential. Electrochemical water splitting is a promising, carbon-free solution for harnessing and storing excess energy in hydrogen and oxygen bonds. However, decreasing the overpotential for this process using stable and Earth-abundant catalysts is an ongoing global research endeavor. With iron being the fourth most abundant element in the Earth's crust, an efficient iron-based catalyst is highly desirable. In this work, we report on the electrochemical activity of ferrihydrite – a rare, but naturally-occurring mineral of iron – for the oxygen evolution reaction (OER). Thin films of ferrihydrite used as anodes for electrochemical water oxidation were found to have significantly higher exchange current densities than thin films of haematite prepared from the same precursor. A 200 mV decrease in overpotential was observed for the high-surface area ferrihydrite material compared to its haematite derivative, and the increased activity was correlated to changes in morphology and surface area as measured using high-resolution transmission electron microscopy and N_2 adsorption isotherms.

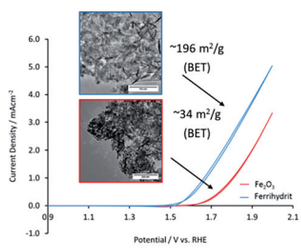

Figure 1. Cyclic voltammograms for ferrihydrite and haematite as OER catalysts in 1.0 M NaOH using a Ag/AgCl reference electrode, a Pt wire counter electrode and a scan rate of 20 mV/s.

* Prof. Dr. G. Ozin
E-Mail: gozin@chem.utoronto.ca
* Prof. Dr. J. Breu
E-Mail: josef.breu@uni-bayreuth.de
[a] Lehrstuhl für Anorganische Chemie I
Universität Bayreuth
Universitätsstr. 30
95447 Bayreuth, Germany
[b] Department of Chemistry
University of Toronto
80 St. George Street
M5S3H6 Toronto, ON, Canada

10.1002/zaac.201605002

Verbesserte Heliumbarrieren durch Schichtsilikat-Nanokomposit Filme

Christoph Habel[a] and Josef Breu*[a]

Keywords: Heliumbarriere, Schichtsilikat-Nanokomposite, *lighter-than-air*-Fahrzeuge, Barrierematerialien

Nanokompositmaterialien weisen ausgeprägte, neuartige Eigenschaften auf. Von Interesse sind hierbei im Besonderen mechanische, Flammschutz-, aber vor allem auch die Gasbarriereeigenschaften der hergestellten Nanokomposite. Ein besonderes Augenmerk bei den sogenannten Schichtsilikat-Polymer-Nanokompositen liegt im Bereich von Lebensmittelverpackungen besonders auf den verbesserten Barrierewerten gegenüber Wasserdampf und Sauerstoff.[1] Darüber hinaus sind ebenfalls Barrierematerialien gegenüber industriell genutzter Gase, wie z.B. Helium, ein aufstrebender Forschungsbereich. Mögliche Anwendungen finden sich vor allem bei *ligther-than-air*-Fahrzeugen wieder.[2]

Da die Durchlässigkeit von Matrizen gegenüber Gasen sowohl von der Diffusivität, als auch von der Löslichkeit der Gasmoleküle in der Polymermatrix, beeinflusst wird, ist in dieser Arbeit eine geeignete Polymermatrix (Polyvinylalkohol) und ein synthetischer Hectorit als Füllstoff, kombiniert worden. Dieser Hectorit weist eine hohe Homogenität und ein Aspektverhältnis von ~20.000 auf.[3] Dadurch ist es gelungen, ein transparentes, flexibles und wasserbasiertes Barrierematerial herzustellen, welches die Heliumtransmissionsrate (GTR, Gastransmissionsrate) einer 36 µm-PET-Substratfolie um einen Faktor von 10^3 verbessert.

[1] D. A. Kunz, J. Schmid, P. Feicht, J. Erath, A. Fery, J. Breu, *ACS Nano* **2013**, *7*[5] 4275–4280.
[2] K. McDaniels et al., *Cubic Tech Corp. Arizona* **2009**.
[3] M. Stöter, D. A. Kunz, M. Schmidt, D. Hirsemann, H. Kalo, B. Putz, J. Senker, J. Breu, *Langmuir* **2013**, *29* 1280–1285.

* Prof. Dr. J. Breu
E-Mail: josef.breu@uni-bayreuth.de
[a] Universität Bayreuth
Universitätsstraße 30
95440 Bayreuth, Deutschland

 © 2016 WILEY-VCH Verlag GmbH & Co. KGaA, Weinheim

10.1002/zaac.201605003

Conversion of Bilayers into Janus Monolayers

Matthias Stöter,[a] Sebastian Gödrich,[b] Sabine Rosenfeldt,[c] Georg Papastavrou,[b] and Josef Breu*[a]

Keywords: Bilayer, Janus particles, Monolayer, 2D materials

Distinct chemical and physical properties of the two different basal surfaces of Janus platelets offer directionality, which allows for complex self-assembly.[1] Typically the symmetry of inorganic particles is broken by immobilization of particles at a second phase (template or interface) followed by selective modification of one particle hemisphere.[1–2] Here we present a novel synthesis approach which does not require an immobilization step.

Ordered heterostructures of layered materials where interlayers with different reactivities strictly alternate in stacks[3] offer predetermined slippage planes that provide a precise route for the preparation of bilayer materials.[4] We use this route for the synthesis of a novel type of reinforced layered silicate bilayer which is 15% stiffer than the corresponding monolayer.[5] Triggering cleavage of those bilayers by gentle osmotic swelling gives access to a generic toolbox for an asymmetrical modification of inorganic monolayers. Only two simple steps applying arbitrary commercial polycations are needed to obtain Janus–type monolayers as bulk material.[5]

[1] A. Walther, A. H. E. Müller, *Chem. Rev.* **2013**, *113,* 5194–5261.
[2] J. H. Liu, G. N. Liu, M. M. Zhang, P. C. Sun, H. Y. Zhao, *Macromolecules* **2013**, *46*, 5974–5984.
[3] M. Stöter, B. Biersack, N. Reimer, M. Herling, N. Stock, R. Schobert, J. Breu, *Chem. Mater.* **2014,** *26*, 5412–5419.
[4] M. Stöter, B. Biersack, S. Rosenfeldt, M. J. Leitl, H. Kalo, R. Schobert, H. Yersin, G. A. Ozin, S. Förster, J. Breu, *Angew. Chem. Int. Ed.* **2015,** *54*, 4963–4967.
[5] M. Stöter, S. Gödrich, P. Feicht, S. Rosenfeldt, H. Thurn, J. W. Neubauer, M. Seuss, P. Lindner, H. Kalo, M. Möller, A. Fery, S. Förster, G. Papastavrou, J. Breu, J. *Angew. Chem. Int. Ed.* **2016**, doi:10.1002/anie.201601611

* Prof. Dr. Josef Breu
E-Mail: josef.breu@uni-bayreuth.de
[a] Lehrstuhl für Anorganische Chemie I, Universität Bayreuth
Universitätsstraße 30
95440 Bayreuth, Germany
[b] Lehrstuhl für Physikalische Chemie II, Universität Bayreuth
Universitätsstraße 30
95440 Bayreuth, Germany
[c] Lehrstuhl für Physikalische Chemie I, Universität Bayreuth
Universitätsstraße 30
95440 Bayreuth, Germany

10.1002/zaac.201605004

Topotactic Al-Pillaring of a well characterized Synthetic Fluorohectorite

Andreas Edenharter,[a] Marius Schöttle,[a] and Josef Breu*[a]

Keywords: Pillared clay, Al_{13}-Keggin polyoxocation, clay

Synthetic Na-Fluorohectorite used in this work has an exceptionally homogeneous layer charge distribution, which allows for controlled separation of adjacent layers by osmotic swelling. This way interlayer distances > 100 nm may easily be realized, a separation which is magnitudes larger than the diameter of the ε-Keggin-type Al13-Ions (≈ 1nm, $[AlO_4Al_{12}(OH)_{24}(OH_2)_{12}]^{7+}$), the oligocation predominantly present in the pillaring solution at pH = 5. While conventional cation exchange is kinetically hindered, diffusion of Al_{13}-Ions into the highly swollen synthetic clay allows for a fast synthesis of highly ordered Al-pillared Clays (Al-PILC) in a matter of minutes and minimizes the degree of acid activation unavoidable at pH = 5. This way, a highly ordered Al-PILC with a rational d-spacing of 18.9 Å and a coefficient of variation of 3.7 % of the *00l*-series is obtained. Furthermore, the material shows a high thermal stability with a d(*001*)-value of 18.5 Å and 17.4 Å at 450 °C and 650 °C, respectively. Air-drying produced a microporous material with a high surface area (> 460 m^2/g) and very little interparticle mesopores. Reliable and exact investigations into composition and structure of the Al-PILC are facilitated by the superb charge homogeneity, phase purity and the absence of aluminum in the starting clay material.

* Prof. Dr. J. Breu
E-Mail: josef.breu@uni-bayreuth.de
[a] Lehrstuhl für Anorganische Chemie I
Universität Bayreuth
Universitätsstr. 30
95447 Bayreuth, Germany

 © 2016 WILEY-VCH Verlag GmbH & Co. KGaA, Weinheim

10.1002/zaac.201605005

Polymorphie des Luminols

Thomas Martin,[a] Juliane Fleissner,[a] Wolfgang Milius,[a] and Josef Breu*[a]

Keywords: Polymorphie, Crystal Engineering, Kristallstruktur-analyse, Röntgendiffraktometrie, Luminol

Für seinen Einsatz in der Kriminalistik zur Spurensuche und dem Nachweis selbst geringster Mengen von Blut weltbekannt, zeigt kommerziell erhältliches Luminol (5-Amino-2,3-dihydro-1,4-phthalazinedione) keine Übereinstimmung mit einer bereits bekannten Kristallstruktur[1] (Form I). Es konnte gezeigt werden, dass es sich bei dem vermarkteten Produkt um ein Polymorph (Form II) von Luminol handelt. Durch die Optimierung der Kristallwachstumsbedingungen konnte hier letztendlich eine Verbesserung der Kristallinität dieser neuen Form erreicht und die Strukturlösung ermöglicht werden. Da beide Formen des Luminols sich lediglich in der Stapelung von, aus Trimeren des Amid-Hydroxyimin-Tautomers von Luminol aufgebauten Schichten unterscheiden, stellen sie ein seltenes Beispiel für Polytypie[2] in einer rein organischen Verbindung dar. Untersuchungen zur thermodynamischen Beziehung zeigten eine lösungsvermittelte Umwandlung der neuen Form II zur bereits bekannten Form I des Luminols und somit deren Metastabilität bei Raumtemperatur.

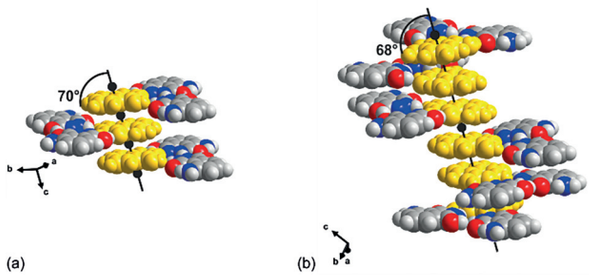

Abbildung 1. Verschobene Stapelung von Luminol-Trimeren in benachbarten Schichten in Luminol Form I (a) und Form II (b). Gelbe Moleküle liegen auf einer Inversionszentren (●) verbindenden Achse.

[1] H. H. Paradies, Berichte der Bunsengesellschaft für Phys. Chemie **1992**, 96, 1027–1031.
[2] International Union of Crystallography (IUCr), "Online Diktionary of Crystallography: Polytypism," zu finden unter: http://reference.iucr.org/dictionary/Polytypism, **2015**.

* Prof. Dr. J. Breu
E-Mail: josef.breu@uni-bayreuth.de
[a] Lehrstuhl für Anorganische Chemie I
Universität Bayreuth
Universitätsstr. 30
95447 Bayreuth, Germany

10.1002/zaac.201605006

Ordered Intercalation of Nanoparticles into the Interlayer Space of Clay

Kevin Ament,[a] Stefan Förster,[b] and Josef Breu*[a]

Keywords: Palladium, Nanoparticles, Clay, Intercalation

Highly active catalysts require an ordered structure that allows for an efficient mass transport and high specific surface area. These criteria can be achieved by the ordered intercalation of small nanoparticles into the interlayer space of clay materials where the nanoparticles act as pillars and reactive catalysts.
In this work, preformed palladium nanoparticles are intercalated into the interlayer space of synthetic hectorite. Small Pd nanoparticles are first synthesized via reduction of a Pd(II) precursor in water.[1] The interlayer space of the swellable hectorite is fine-tuned by the addition of a defined amount of water to facilitate the intercalation of these nanoparticles. This route enables a complete loading of the silicate lamellae. The intercalated nanoparticles are well stabilized, retain their size and are well ordered between the lamellae of the clay as evidenced by a rational *00l*-series of the PXRD pattern and by cross section TEM (Fig.1).

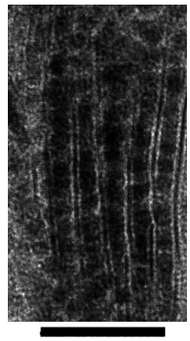

Figure 1. Cross section TEM of palladium nanoparticles in the interlayer of hectorite. The scale bar represents 20 nm.

[1] K. A. Flanagan, J. A. Sullivan, H. Müeller-Bunz, *Langmuir* **2007**, *23*, 12508–12520.

* Prof. Dr. J. Breu
E-Mail: josef.breu@uni-bayreuth.de
[a] Anorganische Chemie I
Universität Bayreuth
Universitätsstraße 30
95440 Bayreuth, Germany
[b] Physikalische Chemie I
Universität Bayreuth
Universitätsstraße 30
95440 Bayreuth, Germany

 © 2016 WILEY-VCH Verlag GmbH & Co. KGaA, Weinheim

10.1002/zaac.201605007

Polymorphie des Konservierungsmittels Natriumbenzoat (E211)

Thomas Martin,[a] Tatiana Gorelik,[b] Dominik Greim,[c] Christian Butterhof,[a] Ute Kolb,[b] Jürgen Senker,[c] and Josef Breu*[a]

Keywords: Polymorphie, Crystal Engineering, Kristallstruktur-analyse, Röntgendiffraktometrie, Elektronenbeugung

Natriumbenzoat (NaBz) fällt bei der technischen Kristallisation als teilkristallines Produkt an. Die Kristallisation zu der strukturell bereits charakterisierten Form I kann thermisch (420 °C) induziert werden.[1] Ein, bei niedrigerer Temperatur (350 °C) kristallisierendes Polymorph des NaBz (Form II) konnte mittels Elektronen- und Röntgenpulverdiffraktotion strukturell charakterisiert werden. Beide Formen des NaBz zeichnen sich durch eine Art Mikrophasensegregation aus und bilden nahezu hexagonale Packungen von micellartigen Bändern aus. Form II unterscheidet sich von Form I durch die Anzahl von NaBz-Einheiten, welche entlang der längeren Hauptachse dieser elliptischen, micellaren Strukturen angeordnet sind (Abb. 1). Die exotherme Umwandlung von NaBz Form II zu Form I im DSC-Experiment und Ergebnisse aus DFT-D Rechnungen zur Energieoptimierung legen eine enantiotrope Phasenbeziehung und eine höhere thermodynamische Stabilität von NaBz Form II gegenüber Form I bei 0 K nahe.

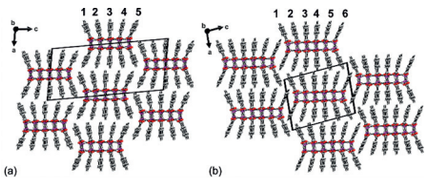

Abbildung 1. Packungsmuster von NaBz Form I (a) und Form II (b). Annähernd hexagonale Packung micellartiger Bänder entlang der jeweiligen b-Achse mit unterschiedlicher NaBz Anzahl entlang der Hauptachse der Bänder.

[1] C. Butterhof, T. Martin, W. Milius, J. Breu, *ZAAC* **2013**, *639*, 2816–2821.

* Prof. Dr. J. Breu
E-Mail: josef.breu@uni-bayreuth.de
[a] Lehrstuhl für Anorganische Chemie I
Universität Bayreuth
Universitätsstr. 30
95447 Bayreuth, Germany
[b] Institut für Physikalische Chemie
Johannes Gutenberg-University Mainz
Welderweg 11,
55099 Mainz, Germany
[c] Lehrstuhl für Anorganische Chemie III
Universität Bayreuth
Universitätsstr. 30
95447 Bayreuth, Germany

10.1002/zaac.201605008

Going Green: Spider Silk-Nanoclay Composites for Sustainable Flexible Food Packaging

Elena Doblhofer,[a] Jasmin Schmid,[b] Magdalena Suntinger,[a] Hendrik Bargel,[a] Christoph Hugenschmidt,[c] Josef Breu,*[b] and Thomas Scheibel[a]

Keywords: Bio-Nanocomposite, Gas Barrier, water-based

Packaged food requires restricted permeability for hydrophobic (O_2, N_2, CO_2) as well as hydrophilic (water vapor) permeates. Environmentally friendly, degradable bio-based polymers are the preferred choice for sustainability reasons, but water vapor barriers made from water-based formulations are a serious challenge. Here, compounding of synthetic sodium hectorite (Na-hec) as filler with aspect ratios of ≈ 20.000 and a designed polycationic spider silk protein (spidroin eADF4(κ16)) as matrix in a water-based formulation achieved all food packaging requirements (e.g. mechanical, optical, and barrier properties). The bio-nanocomposite was 60-fold more efficient than high performance packaging materials like polyvinylidene chloride and 600-fold better than polyethylene terephthalate. The unique combination of high oxygen and water vapour barrier, the processing from aqueous suspensions and its sustainability make the novel spidroin-nanoclay biocomposite highly suitable as a new, green, flexible food packaging material.

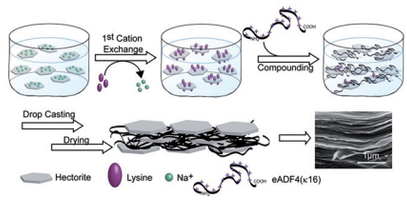

Figure 1. Steps of nanocomposite preparation: 1. Delamination of Na-hec in water. 2. Ion exchange with lysine (Lys). 3. Solution blending of Lys-hec with engineered spidroin eADF4(κ16). 4. Drop casting and drying of the nanocomposite. 5. SEM image of a cross-section of the spidroin-hectorite nanocomposite coating.

* Prof. Dr. J. Breu
E-Mail: josef.breu@uni-bayreuth.de
[a] Lehrstuhl für Biomaterialien
Universität Bayreuth
Universitätsstr. 30
95447 Bayreuth, Germany
[b] Lehrstuhl für Anorganische Chemie I
Universität Bayreuth
Universitätsstr. 30
95447 Bayreuth, Germany
[c] FRM II und Physik-Department E21
Technische Universität München
James-Franck-Straße 1
85748 Garching, Germany

 © 2016 WILEY-VCH Verlag GmbH & Co. KGaA, Weinheim

10.1002/zaac.201605009

The Borophosphate $(NH_4)_2[B_2P_3O_{11}(OH)]$

Katharina Förg[a] and Henning A. Höppe*[a]

Keywords: ammonium, borophosphate, crystal structure

Borophosphates combine both structural properties of borates and phosphates and are furthermore in many cases isoelectronic to silicates[1,2,3]. $(NH_4)_2[B_2P_3O_{11}(OH)]$ was synthesised from $(NH_4)_2HPO_4$, H_3BO_3 and H_3PO_4 (85 %) under hydrothermal conditions. It crystallises in the orthorhombic space group $P2_12_12_1$ (Z = 4, a = 4.509(3) Å, b = 14.490(11) Å, c = 16.401(12) Å, V = 1071.7(14) Å^3, 1682 data, 200 parameters, $R1$ = 0.046, $wR2$ = 0.093, GooF = 1.037, x = 0.05(17)). The polyanion comprises oB vierer-single rings as FBU, which was observed in $(NH_4)_2Mn(II)[B_2P_3O_{11}(OH)_2]Cl$[4] for the first time. NH_4^+ ions are located between the parallel and corrugated borophosphate layers (Figure 1).
Exhibiting a deviation of 0.7 % the structure model shows electrostatic consistency according to the MAPLE concept[5,6,7]. The title compound is stable up to 300 °C.

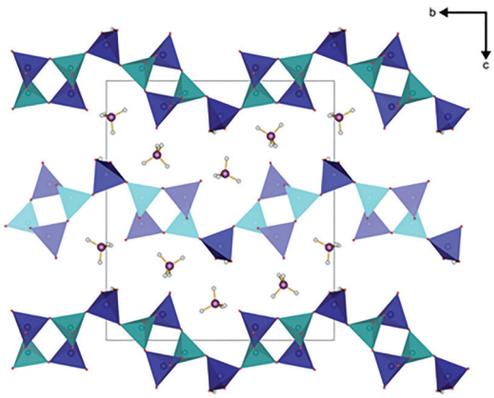

Figure 1. The crystal structure of $(NH_4)_2[B_2P_3O_{11}(OH)]$; phosphate tetrahedra blue, borate tetrahedra turquoise, nitrogen violet, hydrogen white.

[1] B. Ewald, Y.-X. Huang, R. Kniep, *Z. Anorg. Allg. Chem.* **2007**, *633*, 1517–1540.
[2] R. Kniep, G. Gözel, B. Eisenmann, C. Röhr, M. Asbrand, M. Kizilyalli, *Angew. Chem. Int. Ed.* **1994**, *33*, 749–751.
[3] F. Liebau, *Structural Chemistry of Silicates*, Springer Verlag, Berlin Heidelberg, **1985**.
[4] K. Förg, H. A. Höppe, *Z. Anorg. Allg. Chem.* **2015**, *641*, 1009–1015.
[5] R. Hoppe, *Angew. Chem. Int. Ed.* **1966**, *5*, 95–106.
[6] R. Hoppe, *Angew. Chem. Int. Ed.* **1970**, *9*, 25–34.
[7] R. Hübenthal, *MAPLE, Program for the Calculation of the Madelung Part of Lattice Energy*, University of Gießen, Germany, **1993**.

* Prof. Dr. H. A. Höppe
E-Mail: henning.hoeppe@physik.uni-augsburg.de
[a] Institut für Physik, Universität Augsburg
Universitätsstraße 1
86159 Augsburg, Germany

10.1002/zaac.201605010

Packings of Sphere Packings – An Unexplored Path to New Structures

Marek Petrik,*[a] and Wolfgang Hornfeck[b]

Keywords: Crystal structures; quasi-random; random close packing; sphere packings.

Sphere packings – three-dimensional arrangements of equal spheres with at least one uninterrupted path of contacts (bonds) between any two spheres – are prototypes of crystal structures. As such they are well-documented. Fischer, Koch and Sowa have enumerated homogeneous packings[1a] while a comprehensive database by O'Keeffe, Yaghi and coworkers covers heterogeneous ones as well.[1b] Surprisingly, composite sphere packings, or packings of sphere packings, have not been explored. Here two substructures must interpenetrate, contact being established between them without disrupting connectivity within either. This demands a degree of porosity and a symmetry relationship. While (self-) interpenetrating nets are not uncommon, contact between substructures – as observed in the trivial case of two interpenetrating diamond nets – does not occur as a rule. In fact, we now realize that the first nontrivial case of such a packing of sphere packings emerged only recently.[2] This new structure – a combination of the two univariant homogeneous sphere packings 4/3/c1 (**lcv**) and 3/10/c1 (**srs**) in $P4_132$ (213), with parameters $y(12d)$ = 0.1771 and $x(8c)$ = 0.0363 respectively (Figure 1c) – is, furthermore, found to possess a unique property. The density (0.648), the number of contacts per sphere (6) and the radial distribution function all closely mimick random close packing (RCP).[3] In other words it is the first structure which, although perfectly ordered, deserves to be called quasi-random.

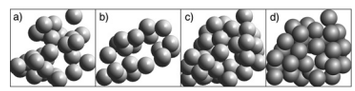

Figure 1. Portions of sphere packings: a) 4/3/c1 (**lcv**); b) 3/10/c1 (**srs**); c) composite of a) and b); d) random close packing after Bernal and Mason.[3a]

[1] a) H. Sowa, *Acta Cryst.* **2016**, *A72*, 357-365 and references therein; b) M. O'Keeffe, M. A. Peskov, S. J. Ramsden, O. M. Yaghi, *Acc. Chem. Res.* **2008**, *41*, 1782–1789.
[2] a) M. Petrik, W. Hornfeck, B. Harbrecht, *Z. Anorg. Allg. Chem.* **2014**, *640*, 2328; b) W. Hornfeck, P. Kuhn, *Acta Cryst.* **2014**, *A70*, 441–447.
[3] a) J. D. Bernal, J. Mason, *Nature* **1960**, *188*, 910-911, fig. 5; b) T. Aste, *J. Phys.: Condens. Matter* **2005**, *17*, S2361–S2390.

* Dipl.-Ing. M. Petrik
E-Mail: petrik@chemie.uni-marburg.de
[a] Department of Chemistry – Harbrecht Group and Centre of Materials Science (WZMW), Philipps University of Marburg
Hans-Meerwein-Str. 4
35043 Marburg, Germany
[b] Institut für Materialphysik im Weltraum, Deutsches Zentrum für Luft- und Raumfahrt (DLR)
51170 Köln, Germany

 © 2016 WILEY-VCH Verlag GmbH & Co. KGaA, Weinheim

10.1002/zaac.201605011

Functionalization of Oxide Nanocrystals and Composites with Transition Metal Ions

Matthias Niedermaier,*[a] Amir Gheisi,[b] Johannes Bernardi,[c] and Oliver Diwald[a]

Keywords: non-equilibrium solids, nanocomposites, metal-oxide nanoparticles

Structure and functional properties of composite metal oxide nanoparticle systems are subject to stability and composition of related surfaces and interfaces. For vapor phase grown non-equilibrium solids, annealing induced ion diffusion provides efficient means to adjust the surface composition and, thus, the functional properties of the material. Insights into the underlying transformation processes, which can be controlled by annealing in different gas atmospheres, are essential for both nanomaterial design and material applications at elevated temperatures.

In the present contribution we will discuss properties and transformation behavior of metal oxide composites, such as Fe–Mg–O or Co–Mg–O nanoparticles, which were prepared by a hybrid chemical vapor synthesis approach using organic transition metal compounds as precursors. In addition to their combustion in the MgO formation flame, we also explored the feasibility of adsorption of transition metal oxides on MgO nanocubes in liquid particle dispersions followed by subsequent annealing in different chemical environments.

We used an integrated characterization approach involving electron microscopy (SEM, TEM), X-ray diffraction (XRD), electron dispersive X-ray spectroscopy (EDX) and Mößbauer spectroscopy to study the ensemble properties of nanoparticle composites, on the one hand, and structure and morphological features of characteristic local structures, on the other. The complex evolution of the composite nanostructures as a result of annealing induced segregation and phase separation was characterized for samples with different thermal processing histories. These can give rise to a variety of material types in the range between nanostructures with bulk and surface admixed transition metal oxides to phase separated systems such as Fe–Mg–O magnesioferrite $MgFe_2O_4$ particles.

* M. Sc. M. Niedermaier
E-Mail: matthias.niedermaier2@sbg.ac.at
[a] Paris Lodron University of Salzburg, Hellbrunnerstrasse 34/III, A-5020 Salzburg, Austria
[b] Friedrich Alexander University, Cauerstr. 4, D-91052 Erlangen, Germany
[c] Vienna University of Technology, Wiedner Hauptstrasse 8-10, A-1040 Vienna, Austria

10.1002/zaac.201605012

Local Atomic Order in $M(Al_{1-x}Ga_x)_4$ with M = Sr, Ba

Oliver Pecher,[a,b,c] Bernhard Mausolf,[a] Volker Peters,[a] Kevin Lamberts,[a] Alexander Korthaus,[a] and Frank Haarmann*[a,b]

Keywords: (DFT, NMR, Intermetallics)

The quasi-binary section of the intermetallic phases MAl_4 and MGa_4 with M = Sr, Ba was characterized by means of X-ray diffraction (XRD), NMR spectroscopy, quantum mechanical (QM) calculations, and differential thermal analysis.

The binary phases crystallize in the $BaAl_4$ type structure with one position for the cations and two for the anions.[1] The corresponding NMR signals are well resolved.[2] The triel element positions are four- (4b) and fivefold (5b) coordinated with next neighbor distances being significantly smaller than in the elements.

The solid solutions $M(Al_{1-x}Ga_x)_4$ with M = Sr, Ba show a minimum of the lattice parameter a, which can be assigned to a preferred occupation of the 4b positions by Al atoms. This is shown by NMR experiments on magnetically aligned crystallites (Figure) and QM calculations of the formation energies. Additional local order of the Al atoms is evident from a structuring of the NMR satellite transition signals (Figure). It can be assigned by QM calculations to Al paring with shorter Al–Al distances than expected for an exclusive statistical occupation of the Al(4b) positions.

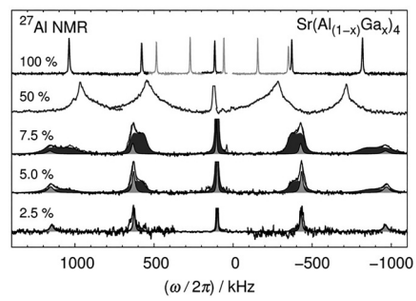

Figure 1. ^{27}Al NMR signals of oriented $Sr(Al_{1-x}Ga_x)_4$. The Al contribution of the anionic sub lattice is given in percentage.

[1] G. Bruzzone, M. L. Fornasini, F. Merlo, *J. Less-Common Met.* **1989**, *154*, 67–77.
[2] F. Haarmann, K. Koch, P. Jeglič, O. Pecher, H. Rosner, Yu. Grin, *Chem. Eur. J.* **2011**, *17*, 7560–7568.

* Dr. F. Haarmann
E-Mail: frank.haarmann@ac.rwth-aachen.de
[a] RWTH Aachen University, Institut für Anorganische Chemie Landoltweg 1, 52074 Aachen, Germany
[b] Max-Planck-Institut für Chemische Physik fester Stoffe Nöthnitzer Straße 40, 01187 Dresden, Germany
[c] University of Cambridge, Department of Chemistry, Lensfield Road CB2 1EW, Cambridge, UK

 © 2016 WILEY-VCH Verlag GmbH & Co. KGaA, Weinheim

10.1002/zaac.201605013

Cooperative Assembly Synthesis of Mesoporous $SrTiO_3$ with Enhanced Photocatalytic Activity

Bugra Kayaalp,[a] Youngjoo Lee,[a] Andreas Kornowsky,[b] Silvia Gross,[c] and Simone Mascotto*[a]

Keywords: (perovskite oxide, mesoporous $SrTiO_3$, photocatalysis)

The synthesis of mesoporous $SrTiO_3$ combining Pechini method[1] and silica hard templating is here presented. The high affinity and intimate mixing between the TEOS precursor and the metal chelating agents fostered the cooperative assembly of the corresponding inorganic and organic polymer.[2] Hence, after calcination and removal of the siliceous phase, highly porous $SrTiO_3$ with interconnected, well defined pores and crystalline pore walls was obtained. Systems with different $SrTiO_3$:SiO_2 molar ratios were prepared. At low concentrations of template only monomeric and oligomeric domains of silica could be formed. Conversely, significant condensation of the siloxane groups and formation of dense domains occurred for concentrations larger than 20%. The porous properties of the final perovskite reproduce very well the structural evolution of the silica in the nanocomposite materials. Only at high concentrations the condensed silica species acted as real template leading to the formation of large surface areas (S_{BET} = 240 m^2/g) with defined pore sizes. Finally, the activity of the mesoporous $SrTiO_3$ systems was demonstrated by exemplary photodegradation tests of methylene blue. The dye conversion progressively increased with the content of silica template up to 7 times than for the corresponding non-porous system, as result of the combined increase of porosity and decrease of crystallite size.

[1] M. Kakihana, T. Okubo, M. Arima, Y. Nakamura, M.Yashima and M. Yoshimura, *J. Sol-Gel Sci. Technol.* **1998**, *12*, 95–109.
[2] Y. Deng, T. Yu, Y. Wan, Y. Shi, Y. Meng, D. Gu, L. Zhang, Y. Huang, C. Liu, X. Wu and D. Zhao, *J. Am. Chem. Soc.* **2007**, *129*, 1690–1697.

* JProf. Dr. Simone Mascotto
E-Mail: simone.mascotto@chemie.uni-hamurg.de
[a] Institut für Anorganische und Angewandte Chemie, Universität Hamburg, Martin-Luther-King Platz 6, 20146 Hamburg, Germany
[b] Institut für Physikalische Chemie, Universität Hamburg, Grindelallee 117, 20146 Hamburg, Germany
[c] Istituto per l'Energetica e le Interfasi, IENI-CNR and INSTM, UdR Padova, via Marzolo, 1, I-35131, Padova, Italy

10.1002/zaac.201605014

Crystallization Studies of Perovskite Oxides Confined in Nanopores

Jonas Scholz,[a] Youngjoo Lee,[a] Andreas Meyer,[b] and Simone Mascotto*[a]

Keywords: (perovskite oxide, crystallization, nanoconfinement)

Perovskite oxides are considered as a very versatile class of materials suitable for a wide range of applications. However, the poor textural properties still limit their functionality. One general strategy to increase their active surface area is to use nanoporous silica either as host matrix to disperse perovskite nanoparticles or as mould for the complete structural replication, i.e. nanocasting.
In both cases the silica is firstly impregnated with the perovskite precursor solution and subsequently treated at high temperature to promote the crystallization of the guest species. However, the formation of crystalline perovskite phase within the pores is not a straightforward process. In the present work we systematically addressed the crystallization of cubic and distorted perovskite structures ($BaZrO_3$, $LaFeO_3$, $LaCoO_3$) in silica matrices with different pore sizes and arrangements. Interestingly, crystal growth occurred only in spherical pores of 12 nm or less organized in a *Fm3m* structure (Figure 1). Combining spectroscopic, diffraction and thermal analyses important insights on the crystallization mechanism of perovskites in nanopores could be achieved.

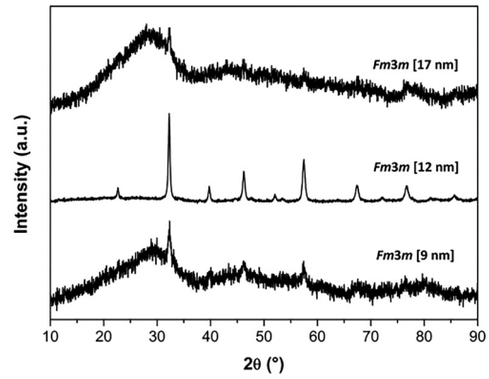

Figure 1. $LaFeO_3$ crystallized in different porous silica hosts

* JProf. Dr. Simone Mascotto
E-Mail: simone.mascotto@chemie.uni-hamurg.de
[a] Institut für Anorganische und Angewandte Chemie, Universität Hamburg, Martin-Luther-King Platz 6, 20146 Hamburg, Germany
[b] Institut für Physikalische Chemie, Universität Hamburg, Grindelallee 117, 20146 Hamburg, Germany

 © 2016 WILEY-VCH Verlag GmbH & Co. KGaA, Weinheim

10.1002/zaac.201605015

An in situ XPS Study of Intermetallic ZnPt in Methanol Steam Reforming

Ying Chen,[a] René Kriegel,[a] Gregor Beier,[b] Dennis C. A. Ivarsson,[a] Mark Greiner,[c] Toni Keilhauer,[a] and Marc Armbrüster*[a]

Keywords: intermetallic compound, methanol steam reforming, ZnPt, X-ray photoelectron spectroscopy

Methanol steam reforming (MSR, $CH_3OH + H_2O \rightarrow 3\ H_2 + CO_2$) is deemed as one of the most promising routes to generate highly pure hydrogen on-board to provide fuel for polymer electrolyte membrane fuel cells [1]. To achieve the high purity of the produced H_2, the performance of the catalyst in MSR reaction, i.e. selectivity and activity, is decisive. Among the potential MSR catalysts are intermetallic compounds (IMCs), which have been attracting more and more interest due to their fascinating catalytic properties [2]. The IMCs ZnPd and InPd have proved to be both active and selective towards CO_2 in MSR [2-4].

ZnPt is isostructural with ZnPd and is supposed to show also interesting catalytic properties. The result from this work proved that ZnPt indeed showed high activity and excellent selectivity in MSR. The dependency of selectivity with chemical composition was similar to that for ZnPd. Zinc-rich ZnPt showed much higher CO_2 selectivity, as shown in Fig. 1. For ZnPd in MSR, the formation of oxidic zinc patches on ZnPd surface has been shown to be the reason for the high selectivity [3]. Different from ZnPd, the formation of oxidic zinc on ZnPt was not detectable by *in situ* near ambient pressure X-ray photoelectron spectroscopy (NAP-XPS) under MSR conditions. Instead, it seems that the formation of a new intermetallic compound is the reason for the high selectivity for zinc-rich ZnPt samples.

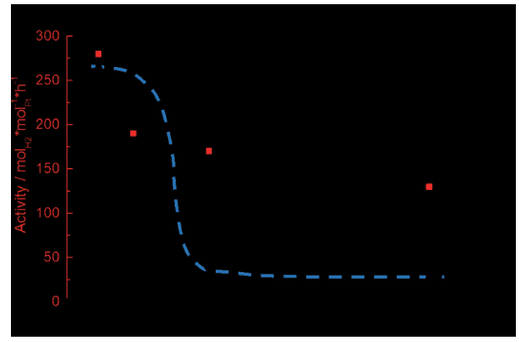

Figure 1. The dependence of CO_2 selectivity and activity of ZnPt on the composition and reaction temperature. The line is a guide to the eye.

[1] G. A. Olah, *Catal. Lett.,* **2004,** *93,* 1-2.
[2] M. Armbrüster, R. Schlögl, Y. Grin, *Sci. Tech. Adv. Mater.,* **2014,** *15,* 034803.
[3] M. Friedrich, S. Penner, M. Heggen, M. Armbrüster, *Angew. Chem. Int. Ed.,* **2013,** *52,* 4389-4392.
[4] D. C. A. Ivarsson, M. Neumann, A. A. Levin, T. Keilhauer, P. Wochner, M. Armbrüster, *Z. Anorg. Allg. Chem.,* **2014,** *640,* 3065–3069

* Prof. Dr. M. Armbrüster
E-Mail: marc.armbruester@chemie.tu-chemnitz.de
[a] Faculty of Natural Sciences, Institute of Chemistry, Materials for Innovative Energy Concepts, Technische Universität Chemnitz, 09107 Chemnitz, Germany
[b] Faculty of Mathematics and Science, Institute for Chemistry and Food Chemistry, Technische Universität Dresden, 01062 Dresden, Germany
[c] Department of Inorganic Chemistry, Fritz-Haber Institute, 14195 Berlin, Germany

 © 2016 WILEY-VCH Verlag GmbH & Co. KGaA, Weinheim

10.1002/zaac.201605016

Crystal Growth of the New Topological Insulator Bi_2TeI

Alexander Zeugner,[a] Anna Isaeva,*[a] Martin Kaiser,[a] Thomas Doert,[a] and Michael Ruck[a,b]

Keywords: topological insulator, single-crystal growth

A topological insulator (TI) is a bulk semiconductor with spin-resolved metallic channels on its surface(s) allowing for dissipationless transport. Recently Bi_2TeI was theoretically predicted to be a weak TI [1] and a topological crystalline insulator (TCI),[2] but no experimental confirmation was obtained due to the lack of large crystals. Three ternary compounds were reported in the Bi-Te-I system: BiTeI, Bi_2TeI and $Bi_4TeI_{1.25}$,[3] of which only the first two were structurally characterized. The BiTeI structure features •**FORMEL unleserlich!!!**• layers, which are separated by van der Waals gaps between tellurium and iodine. Bi_2TeI can be regarded as a heterostructure formed by addition of corrugated Bi-layers to the BiTeI parent structure.

We aimed at the elucidation of the BiTeI-Bi quasi-binary section and crystal growth of the ternary compounds. Combined DSC, PXRD and EDS experiments in the Bi-rich part of the Bi-Te-I system do not confirm $Bi_4TeI_{1.25}$ and reveal a new Bi_3TeI phase instead. Our Rietveld refinement data ($R3m$, $a = 4.413(1)$ Å, $c = 32.201(1)$ Å, $R = 3.7\%$) suggest that Bi_3TeI is built by alternating •**FORMEL unleserlich!!!**• and Bi-layers as proposed for $Bi_4TeI_{1.25}$.[3] Hence BiTeI, Bi_2TeI and Bi_3TeI constitute a family of $(Bi_2)_m(BiTeI)_n$ heterostructures.

We determined the peritectic melting points of Bi_2TeI and Bi_3TeI (449°C and 408°C) and the corresponding liquidus temperatures and thus the suitable temperature ranges for crystal growth. Bi_2TeI crystals (0.3 mm) can be reproducibly grown by annealing of the mixture of Bi, Te and BiI_3 / BiI in the subsolidus region. SEM/EDS and preliminary X-ray diffraction data on the crystals accord with the crystal structure reported earlier.[3] For the first time phase-pure powders of Bi_2TeI and Bi_3TeI were obtained by ball milling and further annealing at 400°C for 3 days, where the product purity strongly depends on the chosen educts.

[1] P. Tang, B. Yan, W. Cao, S.-C. Wu, C. Felser, W. Duan, *Phys. Rev. B* **2014**, *89*, 041409.
[2] I. P. Rusinov, A. Isaeva et al., *Sci. Rep.* **2016**, *6*, 20734.
[3] S. V. Savilov, V. N. Khrustalev, A. N. Kuznetsov, B. A. Popovkin, M. Yu. Antipin, *Russ. Chem. Bull. Int. Ed.* **2005**, *54*, 87–92.

* Dr. A. Isaeva
E-Mail: anna.isaeva@tu-dresden.de
[a] Department of Chemistry and Food Chemistry, TU Dresden, 01062 Dresden, Germany
[b] Max Planck Institute for Chemical Physics of Solids, 01187 Dresden, Germany

10.1002/zaac.201605017

Solid State Microwave Synthesis of Ti_2SnC MAX Phase

Raphael Lauenstein,[a] Christin M. Hamm,[a] and Christina S. Birkel*[a]

Keywords: ((Ti_2SnC, MAX phase, ternary carbide, microwave heating, X-ray diffraction))

Ti_2SnC belongs to the family of the 211 MAX phases with the general formula M_2AX where M is an early transition metal, A is a main group element and X is either carbon or nitrogen. They crystallize in a hexagonal structure consisting of alternating layers of edge-sharing M_6X octahedra and A atoms along the c-axis (Figure 1 lower right). The synthesis of Ti_2SnC usually involves exceptionally long reaction times[1,2] and/or high temperatures.[3] Here, we present a time and energy efficient preparation technique by means of microwave heating. Elemental powders with an excess of tin (Ti:Sn:C 2:1.2:1) are thoroughly ground and subsequently pressed into a dense pellet. The pellet is sealed inside a quartz ampoule and surrounded by 7g of granular graphite that acts as an efficient microwave susceptor. The insulation housing holding the reaction setup is places inside a laboratory microwave oven (Figure 1). The reaction is completed within 30 min (1000 W) whereas a light purple plasma is observed after a few seconds. X-ray diffraction data show that single phase Ti_2SnC is obtained after washing with ~3 molar HCl to remove the excess of tin (Figure 1 upper left). Lattice parameters match those reported in the literature well.[1]

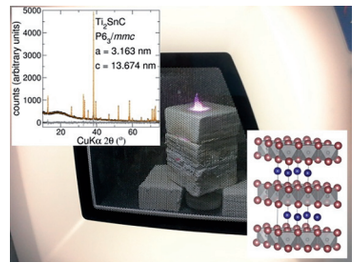

Figure 1: Reaction setup inside a laboratory microwave oven, le Bail fit of X-ray diffraction data (upper left), crystal structure of 211 MAX phase (Ti red, Sn blue, C grey).

[1] W. Jeitschko, H. Nowotny, F. Benesovsky, *Monatshefte für Chemie*, **1963**, *94*, 672–676.
[2] W. Jeitschko, H. Nowotny, F. Benesovsky, *Monatshefte für Chemie*, **1964**, *95*, 431-435.
[3] M. Barsoum, G. Yaroschuk, *Scripta Materialia*, **1997**, *37*, 1583–1591.

* Dr. C. S. Birkel
E-Mail: birkel@ac.chemie.tu-darmstadt.de
[a] Eduard-Zintl-Institut für Anorganische und Physikalische Chemie, Technische Universität Darmstadt, 64287 Darmstadt, Germany

 © 2016 WILEY-VCH Verlag GmbH & Co. KGaA, Weinheim

10.1002/zaac.201605018

Field Assisted Synthesis of M_2AlC (M = Ti, V, Cr) MAX Phases

Christin M. Hamm[a] and Christina S. Birkel*[a]

Keywords: MAX phases, ternary carbides, microwave heating, spark plasma sintering, X-ray diffraction

Ternary carbides that belong to the family of the so called MAX phases are of great interest due to their unique combination of ceramic and metallic characteristics.[1] Usually synthesis techniques are applied that require high reaction temperatures and long reaction times.[2] We prepared MAX phases M_2AlC (M = Ti, V, Cr) in a time and energy efficient way by means of microwave heating. Using graphite as a strong susceptor to the microwave radiation, the compounds can be synthesized within two reaction cycles of 30 minutes (1000 W). For Cr_2AlC, Cr_2Al is first synthesized in a microwave oven starting from Cr and Al powders, and then mixed with carbon to form the desired carbide phase. For Ti_2AlC and V_2AlC, elemental powders are used as starting materials. In all cases a 30% excess of Al is required to account for Al loss during the reaction. Rietveld refiements of X-ray diffraction data show that Cr_2AlC is single-phase while small amounts of additional phases are found in the case of Ti_2AlC and V_2AlC (Figure 1). Refined lattice parameters match those reported in the literature very well.[3] The MAX phases are densified by means of spark plasma sintering (100 MPa, 1000°C, 15 min) in order to enhance the crystalline quality.

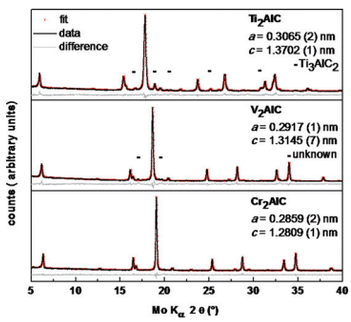

Figure 1. Rietveld refinement of X-ray diffraction data including refined lattice parameters of MAX phases Ti_2AlC, V_2AlC, Cr_2AlC.

[1] M. Radovic, M. Barsoum, *American Ceramic Society Bulletin,* **2013**, *92*, 20–27.
[2] P. Eklund, M. Beckers, U. Jansson, H. Högberg, L. Hultman, *Thin Solid Films*, **2010**, *518*, 1851–1878.
[3] W. Jeitschko, H. Nowotny, F. Benesovsky, *Monatshefte für Chemie*, **1963**, *94*, 672–676.

* Dr. Christina S. Birkel
E-Mail: birkel@ac.chemie.tu-darmstadt.de
[a] Eduard-Zintl-Institut für Anorganische und Physikalische Chemie, Technische Universität Darmstadt, 64287 Darmstadt, Germany

10.1002/zaac.201605019

Support Effects on Iron Catalysts for the Direct Production of Lower Olefins from Synthesis Gas

Martin Oschatz,*[a] and Krijn P. de Jong[a]

Keywords: iron catalysts, Fischer-Tropsch synthesis, lower olefins, ordered mesoporous carbon

Lower olefins (C_2–C_4) are important commodity chemicals which are traditionally produced by steam cracking of naphtha or fluid catalytic cracking of vacuum gas oil. The conversion of synthesis gas to C_2–C_4 olefins with iron catalysts is non-oil based and known as Fischer-Tropsch to olefins process (FTO).[1] Sodium and sulfur can be added as promoters to increase the catalytic activity and the selectivity towards the desired products.[2] Nanostructured materials can be used as supports to disperse and stabilize catalytically active iron particles.[1-3] The chemical and textural properties of the supports can influence the dispersion of iron and promoters as well as the formation of catalytically active iron carbide species. However, the relationship between structure of the supports and the properties of the catalysts remain poorly understood.

We utilize a series of ordered mesoporous (OM) materials as supports for iron-based FTO catalysts with sodium and sulfur as promoters.[3] Whereas hardly reducible iron silicates are formed in case of an OM-silica support during calcination, catalytically active iron carbide particles are present in OM-carbon and OM-silicon carbide-supported catalysts after activation and exposure to synthesis gas. Carbon-supported catalysts show highest activity and selectivity towards lower olefins due to the most efficient distribution of the promoters and the presence of iron nanoparticles with narrow size distribution. The calcination and activation conditions on carbon-supported catalysts and the ratio of promoters are optimized as well, leading to stable FTO catalyst operation for up to 140 h of time on stream at 340°C, 10 bar, H_2/CO = 2, GHSV = 9600 h^{-1}.

[1] H. M. Torres Galvis, K. P. de Jong, *ACS Catal.* **2013**, *3*, 2130−2149.
[2] H. M. Torres Galvis, A. C. J. Koeken, J. H. Bitter, T. Davidian, M. Ruitenbeek, A. I. Dugulan, K. P. de Jong, *J. Catal.* **2013**, *303*, 22–30.
[3] M. Oschatz, W. Lamme, J. Xie, A. I. Dugulan, K. P. de Jong, *ChemCatChem* **2016**, submitted.

* Dr. Martin Oschatz
E-Mail: M.Oschatz@uu.nl
[a] Inorganic Chemistry and Catalysis, Debye Institute of Nanomaterials Science, Utrecht University, Universiteitsweg 99, 3584 CG Utrecht, The Netherlands.

 © 2016 WILEY-VCH Verlag GmbH & Co. KGaA, Weinheim

10.1002/zaac.201605020

Two Modifications of $Dy_2[MoO_4]_3$

Ingo Hartenbach,*[a] Thomas Schleid,[a] and Sabine Strobel[a]

Keywords: Dysprosium, Oxidomolybdates, Crystal Structure, Phase Transition

The *ortho*-oxidomolybdates $RE_2[MoO_4]_3$ of the mid-sized rare-earth elements (RE = Y[1], Gd[2], Tb[3]) crystallize isotypically to each other. At room temperature a paraelectric/paraelastic, orthorhombic modification occurs, while at higher temperatures a ferroelectric/ferroelastic tetragonal phase results. This observation is also true for the title compound; however, crystals of both modifications were obtained at room temperature, albeit from different reactions. The orthorhombic form of $Dy_2[MoO_4]_3$ (*Pba*2; a = 1033.43(3), b = 1033.71(3), c = 1060.99(3) pm; Z = 4; CSD-431083) was yielded from solid-state reactions, comprising Dy_2O_3 and MoO_3 with slow cooling rates, while the tetragonal modification ($P2_1m$; a = 730.80(2), c = 1060.95(3) pm; Z = 2; CSD-431084) resulted from reactions that were rapidly cooled down from the reaction temperature of 850 °C to ambient conditions. The structural relationship between the tetragonal HT- and the orthorhombic LT-phase is described by a *translationengleiche* followed by a *klassengleiche* symmetry reduction according to the *Bärnighausen* tree in **Figure 1**. Both crystal structures feature monocapped trigonal $[DyO_7]^{11-}$ prisms, which fuse together with $[MoO_4]^{2-}$ tetrahedra in a heterocubane-like manner[1].

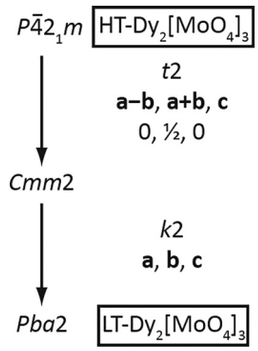

Figure 1. *Bärnighausen* tree of the symmetry reduction from the tetragonal HT- to the orthorhombic LT-modification of $Dy_2[MoO_4]_3$.

[1] S. Laufer, S. Strobel, Th. Schleid, J. Cybinska, A.-V. Mudring, I. Hartenbach, *New. J. Chem.* **2013**, *37*, 1919−1926.
[2] W. Jeitschko, *Acta Crystallogr., Sect. B* **1972**, *28*, 60–76.
[3] S. C. Abrahams, C. Svensson, J. L. Bernstein, *J. Chem. Phys.* **1980**, *54*, 4278−4285.

* Dr. I. Hartenbach
E-Mail: hartenbach@iac.uni-stuttgart.de
[a] University of Stuttgart
Institute for Inorganic Chemistry
Pfaffenwaldring 55
70569 Stuttgart, Germany

10.1002/zaac.201605021

Synthesis and Crystal Structure of the New High-Pressure Indium Borate $In_{19}B_{34}O_{74}(OH)_{11}$

Daniela Vitzthum,[a] Klaus Wurst,[a] and Hubert Huppertz*[a]

Keywords: high-pressure, indium borate, supertetrahedra

In the system In–B–O(–H), there are three compounds known up to now: $InBO_3$[1], $H_2InB_5O_{10}$[2] and its dehydrated equivalent InB_5O_9[2]. All three compounds were synthesized either in autoclaves or at ambient pressure. This motivated us to apply high-pressure conditions to explore the field of indium borates in more detail. With the successful high-pressure synthesis of $In_{19}B_{34}O_{74}(OH)_{11}$, we were able to find the second hydrated indium borate, which is also the first borate showing the structural motif of a T2-supertetrahedron.

The synthesis of $In_{19}B_{34}O_{74}(OH)_{11}$ was carried out under high-pressure/high-temperature conditions of 12.8 GPa and 1100 °C in a Walker-type multianvil apparatus. Its crystal structure was solved and refined based on single-crystal X-ray diffraction data. $In_{19}B_{34}O_{74}(OH)_{11}$ crystallizes in the trigonal space group R-3 (Z = 3) with the lattice parameters a = 1802.49(6), c = 1340.46(5) pm, and V = 0.37716(3) nm^3. The complex structure of $In_{19}B_{34}O_{74}(OH)_{11}$, which could be refined to R-values of R_1 = 0.0195 and wR_2 = 0.0366 (all data), is mainly built up of InO_6 octahedra, corner-sharing BO_4 tetrahedra and hydroxyl groups. Additionally, the structure of $In_{19}B_{34}O_{74}(OH)_{11}$ includes adamantane-like B_4O_{10} groups, which form the above mentioned T2-supertetrahedra.

To conclude, with the synthesis of the second hydrated indium borate $In_{19}B_{34}O_{74}(OH)_{11}$, we were able to expand the substance class of indium borates opening up a promising new field for high-pressure syntheses.

[1] J.R. Cox, D.A. Keszler, *Acta Crystallogr., Sect. C: Struct. Chem.* **1994**, *50*, 1857-1859.
[2] R. Cong, T. Yang, H. Li, F. Liao, Y. Wang, J. Lin, *Eur. J. Inorg. Chem.* **2010**, *2010*, 1703-1709.

* Prof. Dr. H. Huppertz
E-Mail: hubert.huppertz@uibk.ac.at
[a] Institute of General, Inorganic, and Theoretical Chemistry
University of Innsbruck, Innrain 80-82
6020 Innsbruck, Austria

 © 2016 WILEY-VCH Verlag GmbH & Co. KGaA, Weinheim

10.1002/zaac.201605022

Phase Analysis on the Quasi-Ternary System $CuO/Fe_2O_3/V_2O_5$ and Characterization of $Cu_4FeO(VO_4)_3$

Torsten Jahn,[a] Iren Weimann,[a] Jörg Feller,*[a] and Zdirad Žák[b]

Keywords: Phase Diagram $CuO/Fe_2O_3/V_2O_5$; $Cu_4FeO(VO_4)_3$

The investigation of oxide vanadates has the intention to offer a similar class of compounds for an application as cathode material in Lithium batteries like oxide phosphates[1]. Powder samples were prepared from CuO, Fe_2O_3 and V_2O_5 whilst the starting materials were thoroughly milled, placed in porcelain crucibles and using a stepwise heating procedure up to 750 °C for 7 days. Investigations on the sintered samples carried out by X-ray powder diffraction led to the phase diagram at 750 °C depicted in Figure 1.

A new oxide vanadate phase with the formula $Cu_4FeO(VO_4)_3$ could be identified. Single crystals of the new compound were obtained by a melting procedure starting at 800 °C and cooling down to 700 °C with 1 K/min. The obtained product contains agglomerated dark-green needles of the compound. The crystallographic data are presented in Tab. 1.

Furthermore, the new phase has been characterized by DTA, TG and Galvanostatic Discharge.

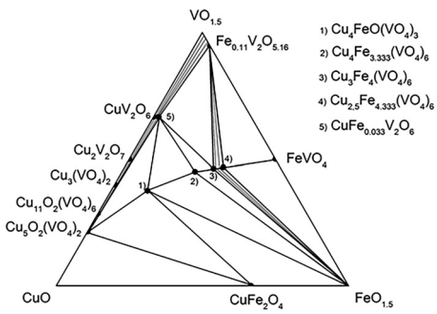

Figure 1. Phase Diagram $CuO/Fe_2O_3/V_2O_5$ at 750 °C.

Table 1. Lattice Constants $Cu_4FeO(VO_4)_3$ (ISCD 428557)

Space group	*a/b/c [Å]*	*V [Å³]*	*z*
P nma	*14.1496(14)*	*1086.66(17)*	*1*
No. 62	*6.7178(6)*		
	11.4320(10)		

[1] T. Traulsen, G. Fehrmann, Th. Hucke, A. Deckert, J. Feller, T. Schuffenhauer, DE 1020110793798 and EP 2548841B1.

* Prof. Dr. J. Feller
E-Mail: feller@htw-dresden.de
[a] Hochschule für Technik und Wirtschaft Dresden
Friedrich-List-Platz 1; 01069 Dresden
[b] Přírodovědecká fakulta Masaryk University
61137 Brno; Kotlářská 2

10.1002/zaac.201605023

Inorganic-Organic Hybrid Nanoparticles for Drug Delivery and Optical Imaging

Joachim G. Heck[a] and Claus Feldmann*[a]

Keywords: luminescence, drug delivery, nanoparticles, inorganic-organic hybrid nanoparticles

Phosphate-based inorganic-organic hybrid nanoparticles are presented that consist of the inorganic cation $[ZrO]^{2+}$ and functional organic anion with a phosphate group. These nanomaterials are easily accessible by a water-based synthesis. They can be promising optical marker or drug containers for application in medicine and molecular biology.

Fluorescent nanoparticlesOptical imaging has emerged as a powerful tool for visualizing whole organisms or single cells (e.g. tumor cells) in life science[1]. In particular for *in vivo* application, new biocompatible contrast agents are required.

As a first example of a new class of inorganic-organic hybrid nanomaterials, ZrO(FMN) (FMN: flavin mononucleotide) shows high biocompatibility and high cell uptake[2]. The dye anion was responsible for bright green emission of the nanoparticles under UV and blue-light excitation.This concept is extended to blue and far red emission: ZrO(PUFP) (PUFP: phenylumbellipherone phosphate) and ZrO(RP) (RP: resorufin phosphate)[3].

Nanoparticles as drug delivery systemsIn contrast to systemic drug administration, nanoparticular drug delivery systems can effectively reduce side-effects. Different material concepts are known for drug delivery with nanoparticles. Drugs are attached on the surface (e.g., Au, SiO_2) or encapsulated in matrix materials (e.g., polymers, liposomes, CNTs, SiO_2).

In order to obtain drug-loaded phosphate-based inorganic-organic hybrids, phosphate ester prodrugs are used[3]. These nanoparticles can be loaded with up to 85 wt-% of drugs against inflammation, bacterial infection, rheumatism, arthritis, multiple sclerosis or cancer. The respective drug is delivered within several hours or days under physiological conditions.

Both properties fluorescence and drug delivery can be combined to bimodal hybrid nanomaterials that can be used for diagnosis and therapy, simultaneously.

[1] J. G. Fujimoto, D. Farkas, *Biomedical Optical Imaging*, Oxford University Press, Oxford, **2009**.
[2] M. Roming, H. Lünsdorf, K. E. J. Dittmar, C. Feldmann, *Angew. Chem. Int. Ed.* **2010**, *49*, 632–637.
[3] J. G. Heck, J. Napp, S. Simonato, M. Lange, J. Mollmer, R. Staudt, F. Alves, C. Feldmann, *J. Am. Chem. Soc.* **2015**, *137*, 7329–7336.

* Prof. Dr. C. Feldmann
E-Mail: claus.feldmann@kit.edu
[a] Institut für Anorganische Chemie
Karlsruher Institut für Technologie (KIT)
Engesserstr. 15
76131 Karlsruhe

 © 2016 WILEY-VCH Verlag GmbH & Co. KGaA, Weinheim

10.1002/zaac.201605024

Synthesis of Metal Sulfides from a Deep Eutectic Solvent Precursor

Tao Zhang,[a] Thomas Doert,*[a] and Michael Ruck[a,b]

Keywords: Metal sulfides, Deep eutectic solvent

Deep eutectic solvents (DESs) are acknowledged as a new class of ionic liquid analogue solvents[1]. They are generally synthesized by mixing a quaternary ammonium halide salt like choline chloride with a metal salt or hydrogen-bond donor. DESs have recently received increasing attention in the synthesis of advanced functional nanomaterials, including metals, metal oxides, metal chalcogenides, open-framework structures and carbons[2]. In our current work, a new DES was designed by stirring choline chloride (ChCl) and thioacetamide (TAA) in a molar ratio of 1:2 at 70 °C until a homogeneous liquid was formed. This ChCl/TAA system DES was used to synthesize a series of metal sulfides by adding metals salts, such as Bi_2S_3 nanowires or cube-shaped PbS crystals. The powder XRD patterns and SEM images of these metal sulfides are shown in Fig. 1 and Fig. 2, respectively. The general use of ChCl/TAA as sulfur source has been proven by synthesizing other metal sulfides such as Sb_2S_3, ZnS, CuS, CdS and Ag_2S. Thus, ChCl/TAA can serve as an all-in-one solvent-reactant-template or deep eutectic solvent precursor.

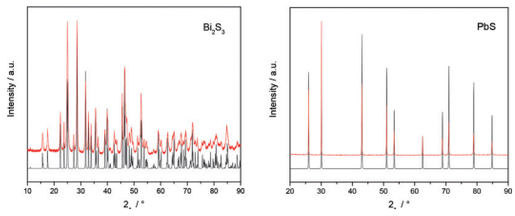

Figure 1 Measured (red) and calculated (black) X-ray powder diagrams of synthesized metal sulfides.

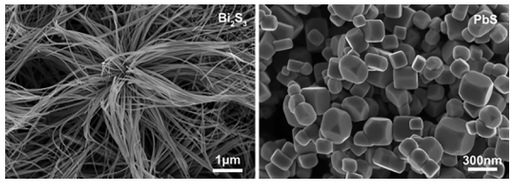

Figure 2 SEM images of synthesized metal sulfides.

[1] E. L. Smith, A. P. Abbott and K. S. Ryder, *Chem. Rev.* **2014**, *114*, 11060–11082.
[2] A. Abo-Hamad, M. Hayyan, M. A. AlSaadi, M. A. Hashim, *Chem. Eng. J.* **2015**, *273*, 551–567.

* Prof. Dr. T. Doert,
E-Mail: thomas.doert@tu-dresden.de
[a] Department of Chemistry and Food Chemistry, Dresden University of Technology, 01062 Dresden, Germany.
[b] Max Planck Institute for Chemical Physics of Solids, 01187 Dresden, Germany.

10.1002/zaac.201605025

Detaillierte Untersuchung des mechanochemischen Prozesses zur Synthese von CZTS (Kesterit)

Anna Ritscher,*[a,b] Marc Schlosser,[c] Arno Pfitzner,[c] and Martin Lerch[a]

Keywords: Kesterit, Mechanochemische Synthese, *in situ* HT-Röntgenpulverbeugung, Rietveld-Verfeinerung

Die Halbleiterverbindung Cu_2ZnSnS_4 (CZTS) gilt aufgrund ihrer physikalischen Eigenschaften (optische Bandlücke = 1.5 eV, Absorptionskoeffizient ~10^{-4} cm^{-1}) als viel verprechendes Material für Absorberschichten in zukünftigen Dünnschicht-solarzellen[1–3]. Diese liegt bei 25 °C im tetragonalen Kesterit-Typ (Raumgruppe $I\bar{4}$) vor[4].
In dieser Arbeit wurde der von uns neu entwickelte mechanochemische Syntheseprozess[5] zur Herstellung phasenreiner CZTS Pulver umfangreich untersucht. Die Umsetzung der zugehörigen binären Sulfide in einer Planeten-kugelmühle wurde durch Röntgenpulverbeugungsuntersuchungen detailliert verfolgt. Nach etwa 150 Minuten sind nur noch Reflexe von Kesterit zu beobachten. Für die Kristallitgröße des gemahlenen Pulvers konnte nach 3 Stunden ein Wert von 10 nm bestimmt werden.
Darüber hinaus wurde das Kristallisationsverhalten des gemahlenen Vorläufers mit Hilfe von *in situ* Hochtemperatur-Röntgenbeugungsmessungen im Temperaturbereich von 300–500 °C untersucht. Eine signifikante Unordnung der Kationen (Cu/Zn und Sn) wurde bei 500 °C beobachtet, die nach langsamem Abkühlen auf Raumtemperatur mit einer Rate von 60 $K \cdot h^{-1}$ stark verringert ist.
Diese Arbeit wurde von der MatSEC (Materials for Solar Energy Conversion) Graduiertenschule des Helmholtz Zentrums Berlin (HZB) gefördert.

[1] S. Siebentritt, S. Schorr, *Prog. Photovol: Res. App.* **2012**, *20*, 512–519.
[2] S. Chen, X.G. Gong, A. Walsh, S.-H. Wei, *Appl. Phys. Lett.* **2009**, *94*, 041903/1–041903/3.
[3] J.J. Scragg, P.J. Dale, L.M. Peter, G. Zoppi, I. Forbes, *Phys. Status Solidi B* **2008**, *245*, 1772–1778.
[4] S.R. Hall, J.T. Szymanski, J.M. Stewart, *Can. Mineral.* **1978**, *16,* 131–137.
[5] A. Ritscher, J. Just, O. Dolotko, S. Schorr, M. Lerch, *J. Alloys Compd.* **2016**, *670,* 289–296.

* Anna Ritscher M.Sc.
E-Mail: anna.ritscher@campus.tu-berlin.de
[a] Inst. f. Chemie, Technische Universität Berlin
Straße des 17.Juni 135
10623 Berlin, Germany
[b] Abteilung Kristallographie, Helmholtz-Zentrum Berlin
Hahn-Meitner-Platz 1
14109 Berlin, Germany
[c] Inst. f. Anorganische Chemie, Universität Regensburg,
Universitätsstr. 31
93040 Regensburg, Germany

 © 2016 WILEY-VCH Verlag GmbH & Co. KGaA, Weinheim

10.1002/zaac.201605026

Two Polymorphs of $RE_2P_3N_7$ Nitridophosphates

Simon D. Kloß[a] and Wolfang Schnick*[a]

Keywords: High-pressure, High-temperature, Nitrides, Rare-earth, Metathesis

The elusive class of rare-earth nitridophosphates has found a potent method of synthesis. Recently, high-pressure metathesis produced the first example, $LiNdP_4N_8$, which opened the study of this completely uncharted materials class.[1] Striving for layered, chain-, ring- and, ortho-nitridophosphates, we developed a unified approach to access all kinds of rare-earth nitridophosphates by expanding the crude reaction scheme used for $LiNdP_4N_8$:

$$x\ RE\mathrm{F}_3 + y\ \mathrm{LiPN}_2 + z\ \mathrm{Li}_3\mathrm{N} \rightarrow RE_x\mathrm{P}_y\mathrm{N}_{y+z} + 3x\ \mathrm{LiF}$$

The high-pressure (up to 5 GPa) and high-temperature (up to 1350 °C) conditions were achieved with the multi-anvil technique using a 1000 t hydraulic press. The degree of condensation (ratio of P:N) can be tuned between ½ and ¼ by addition of Li_3N. As a proof of principle we present two modifications of the layered nitridophosphates $RE_2P_3N_7$ (RE = La, Ce, Pr, Nd, Sm, Eu, Ho, Yb); one crystallizes in the tetragonal melilite structure type (SG $P\text{-}42_1m$, a = 7.4915(7) Å, c = 5.1880(7) Å, Z = 2), the other in the monoclinic $Ba_2CuSi_2O_7$-type (SG $C2/c$, a = 7.8006(3) Å, b = 10.2221(3) Å, c = 7.7798(3) Å, β = 111.299(1)°, Z = 4, Figure 1). Previously unknown[2], the latter is a high-pressure modification of the melilite-type.

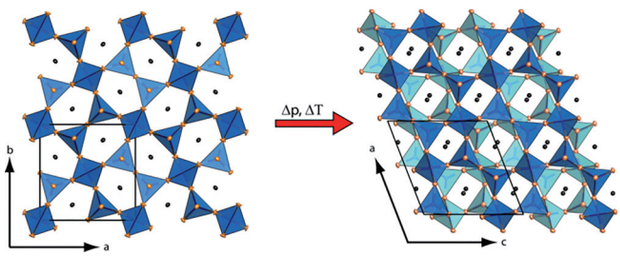

Figure 1. Melilite-type $Pr_2P_3N_7$ (left) transitions to the monoclinic $Ba_2CuSi_2O_7$-type at high pressure (5 GPa) and ca. 1250 °C.

[1] S. D. Kloß, W. Schnick, *Angew. Chem. Int. Ed.* **2015**, *54*, 11250–11253; *Angew. Chem.* **2015**, *127*, 11402–11405.
[2] M. Ardit, M. Dondi, M. Merlini, G. Cruciani, *Phys. Chem. Miner.* **2011**, *39*, 199–211.

* Prof. Dr. W. Schnick
E-Mail: wolfgang.schnick@uni-muenchen.de
[a] Department of Chemistry, University of Munich (LMU), Butenandtstraße 5-13, 81377 Munich, Germany

10.1002/zaac.201605027

Li_4PN_3: A High-Pressure Polymorph of $Li_{12}P_3N_9$

Eva-Maria Bertschler[a] and Wolfgang Schnick*[a]

Keywords: High-pressure; Multi anvil; Nitrides; Phosphorus

$Li_{12}P_3N_9$ (Cc, Z = 4, a = 12.1089(3), b = 7.6588(2), c = 9.7212(2) Å, β = 90.897(2)°) was synthesized by reaction of Li_3N and P_3N_5 in tantalum crucibles at 800 °C.[1] It contains non-condensed *dreier*-rings[2,3] made up of three vertex-sharing PN_4 tetrahedra isoelectronic to $[Si_3O_9]^{6-}$.[1] Applying the multi anvil technique we were able to obtain the high-pressure polymorph Li_4PN_3, the first lithium nitridophosphate with infinite chains. Li_4PN_3 ($Pccn$, Z = 8, a = 9.6394(4), b = 11.8357(9), c = 4.8553(3) Å) was synthesized from $Li_{12}P_3N_9$ at 6 GPa and 820 °C. The high-pressure polymorph exhibits vertex-sharing PN_4 tetrahedra running parallel to [001] with a chain periodicity of two. The $[PN_3]^{4-}$ chains in Li_4PN_3 are similar to those in Zn_2PN_3,[4] and Mg_2PN_3.[5] Temperature dependent X-ray powder diffraction indicates that Li_4PN_3 transforms back to $Li_{12}P_3N_9$ above 650 °C. Furthermore, the density of Li_4PN_3 (ρ = 2.416 g/cm^3) is about 7 % higher than that of $Li_{12}P_3N_9$ (ρ = 2.235 g/cm^3), suggesting that Li_4PN_3 is a high-pressure polymorph of $Li_{12}P_3N_9$.

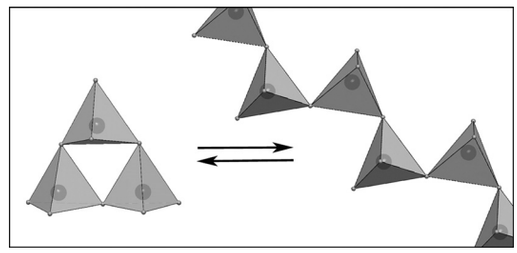

Figure 1. $[P_3N_9]^{12-}$ ring in $Li_{12}P_3N_9$ (left) and chain in Li_4PN_3 (right).

[1] W. Schnick, Angew. Chem. 1993, 105, 846-858; *Angew. Chem. Int. Ed. Engl.* **1993**, *32*, 806–818.
[2] F. Liebau, *Structural Chemistry of Silicates*; Springer-Verlag Berlin, **1985**.
[3] The term dreier ring was coined by Liebau and is derived from the German word "drei". A dreier ring comprises three tetrahedra centers.
[4] S.J. Sedlmaier, M. Eberspächer, W. Schnick, Z. Anorg. Allg. Chem. 2011, 637, 362–367.
[5] V. Schultz-Coulon, W. Schnick, Z. Anorg. Allg. Chem. 1997, 623, 69–74.

* Prof. Dr. W. Schnick
E-Mail: wolfgang.schnick@uni-muenchen.de
[a] Department of Chemistry, University of Munich (LMU) Butenandtstrasse 5–13, 81377 Munich, Germany.

 © 2016 WILEY-VCH Verlag GmbH & Co. KGaA, Weinheim

10.1002/zaac.201605028

Gezielte Beeinflussung der optischen Bandlücke von $Ba_3Ta_5O_{15}$

Björn Anke,*[a] Thomas Bredow,[b] and Martin Lerch[a]

Keywords: Kristallstruktur, Quantenchemische Rechnungen, Oxidnitride, Synthese

Als *Band gap engineering* wird üblicherweise das gezielte Verändern der Bandlücke bezeichnet. Eine Variante besteht darin, das Valenzband durch die partielle Substitution von Sauerstoff mit Stickstoff zu beeinflussen und dadurch die Bandlücke zu verringern.[1]
Formal ausgehend vom gemischtvalenten Oxid $Ba_3Ta_5O_{15}$[2] haben wir den Stickstoffgehalt durch reine Anionensubstitution ($Ba_3Ta_5O_{14}N$[3]) und gekoppelte Kationen-Anionensubstitution ($Ba^{2+}/O^{2-} \rightarrow La^{3+}/N^{3-}$) bis zum $LaBa_2Ta_5O_{13}N_2$ erhöht. Der Stickstoff- und Sauerstoffgehalt der neuen Verbindung wurde mittels Heißgasextraktion bestimmt. Alle drei Verbindungen kristallisieren im tetragonalen Wolframbronze Strukturtyp. Die optische indirekte Bandlücke verkleinerte sich wie erwartet von 2.80 eV für $Ba_3Ta_5O_{14}N$ auf 2.77 eV für $LaBa_2Ta_5O_{13}N_2$. Quantenchemische Berechnungen mit Hybriddichtefunktionalen bestätigen diesen Trend. Die berechnete Bandlücke wird signifikant von der Anionenkonfiguration beeinflusst.
Diese Arbeit wird von der DFG im Rahmen des SPP 1613 gefördert.

[1] M. Jansen, H. P. Letschert, *Nature*, **1999**, *404*, 980–982.
[2] C. R. Feger, R. P. Ziebarth, *Chem.Mater.*, **1995**, *7*, 373–378.
[3] B. Anke, T. Bredow, J. Soldat, M. Wark, M. Lerch, *J. Solid State Chem.* **2016**, *233*, 282–288.

* Björn Anke
E-Mail: B.Anke@TU-Berlin.de
[a] Technische Universität Berlin
Straße des 17. Juni 115
10623 Berlin, Germany
[b] Universität Bonn
Beringstraße 4
53115 Bonn, Germany

10.1002/zaac.201605029

Verbesserung der photokatalytischen Eigenschaften von $BiVO_4$ durch partielle O/F-Substitution

Björn Anke,*[a] Martin Rohloff,[a,b] Anna Fischer,[b] and Martin Lerch[a]

Keywords: Photokatalyse, Bismutvanadat, O/F-Substitution, Wasseroxidation

In den letzten Jahren hat der n-Halbleiter Bismutvanadat ($BiVO_4$) große Aufmerksamkeit erregt, was besonders den photokatalytischen Eigenschaften geschuldet ist. Diese werden durch viele Faktoren beeinflusst, so zeigen die 3 verschiedenen Modifikationen von $BiVO_4$ unterschiedliche photokatalytische Aktivitäten bei der Wasseroxidationsreaktion.
Eine gängige Strategie zur Beeinflussung der photokatalytischen Aktivität ist die partielle Substitution der Kationen mit üblicherweise aliovalenten Ionen. Im Gegensatz dazu wird hier ein Anionensubstitutions-Konzept vorgestellt, bei dem eine partielle Substitution von Sauerstoff durch Fluor realisiert wird. Wir entwickelten hierfür ein neues Verfahren basierend auf einer Feststoff-Gas-Reaktion mit getrennten Reaktanten bei Normaldruck in einer Inertgas-Atmosphäre.
Zur Untersuchung der photokatalytischen Eigenschaften wurden aus reinem und fluorhaltigem $BiVO_4$ mittels elektrophoretischer Abscheidung und nachfolgender Kalzinierung Elektroden hergestellt und die katalytische Aktivität bzgl. Wasseroxidation elektrochemisch untersucht. Erste Ergebnisse zeigen einen positiven Effekt der O/F-Substitution.
Diese Arbeit wird von der DFG im Rahmen des SPP 1613 gefördert.

* Björn Anke
E-Mail: B.Anke@TU-Berlin.de
[a] Technische Universität Berlin
Straße des 17. Juni 115
10623 Berlin, Germany
[b] Albert-Ludwigs-Universität Freiburg
Albertstraße 21
79104 Freiburg, Germany

 © 2016 WILEY-VCH Verlag GmbH & Co. KGaA, Weinheim

10.1002/zaac.201605030

Extending the Field of Nickel Borates *via* High-Pressure Synthesis

Martin K. Schmitt,[a] Klaus Wurst,[a] and Hubert Huppertz*[a]

Keywords: nickel borates, high-pressure, crystal structures

When comparing the systems Fe–B–O(–H), Co–B–O(–H), and Ni–B–O(–H), it is striking that the number of published high-pressure borates in each system decreases from five (Fe-borates), to four (Co-borates), to two (Ni-borates). Since the transition metals Fe, Co, and Ni have similar chemical properties and thus often form isotypic compounds, one would also expect that a similar number of corresponding transition metal borates exist. Therefore, the small number of already known nickel borates motivated us to further investigate the system Ni–B–O(–H).

Within this system, six compounds are known so far. Three hydrous phases and three anhydrous phases. Two of these anhydrous compounds were formed during high-pressure experiments at 7.5 GPa/680 °C (HP-NiB_2O_4)[1] and 7.5 GPa/1150 °C (β-NiB_4O_7)[2], respectively.

Here, we present the crystal structures of another four nickel borates synthesized at elevated pressures using a Walker-type multianvil apparatus. The compositions, reaction conditions, and space groups are listed in Table 1.

Table 1. Compositions, reaction conditions, and space groups of the new nickel borates.

Composition	p /GPa	T /°C	Crucible	Space group
$NiB_3O_5(OH)$	3.5	750	h-BN	$P2_1/c$
"$Ni_3B_{18}O_{32}$" a)	5	750	h-BN	P-62m
γ-NiB_4O_7	5	900	h-BN	$P6_522$
$Ni_6B_{22}O_{39} \cdot H_2O$	5	900	Pt	$Pmn2_1$

a) The exact composition could not be determined yet.

[1] Knyrim, J. S.; Roessner, F.; Jakob, S.; Johrendt, D.; Kinski, I.; Glaum, R.; Huppertz, H., *Angew. Chem. Int. Ed.* **2007**, *46*, 9097–9100.
[2] Knyrim, J. S.; Friedrichs, J.; Neumair, S.; Roessner, F.; Floredo, Y.; Jakob, S.; Johrendt, D.; Glaum, R.; Huppertz, H., *Solid State Sci.* **2008**, *10*, 168–176.

* Prof. Dr. H. Huppertz
E-Mail: hubert.huppertz@uibk.ac.at
[a] Institute of General, Inorganic, and Theoretical Chemistry, University of Innsbruck, Innrain 80-82, 6020 Innsbruck, Austria

10.1002/zaac.201605031

$CsGaS_2$-*mC*64 – A Low-Temperature Polymorph of $CsGaS_2$

Daniel Friedrich,[a] Marc Schlosser,[a] and Arno Pfitzner*[a]

Keywords: Crystal Structure, Layered Compound, Cesium Thiogallate

During our explorative investigations of group 13 chalcogenometallates,[1-4] we obtained a new low-temperature polymorph of $CsGaS_2$. The crystal structure of $CsGaS_2$-*mC*64 was determined by single-crystal X-ray diffraction. The title compound crystallizes in the monoclinic space group $C2/c$ (No. 15) with a = 10.5718(6) Å, b = 10.5708(6) Å, c = 16.0847(8) Å, β = 99.445(4)°, V = 1773.1(2) Å^3, and Z = 16. The anionic substructure of $CsGaS_2$-*mC*64 consists of layers of vertex sharing supertetrahedral Ga_4S_{10}-units composed of four corner-sharing GaS_4 tetrahedra penetrated by the cesium cations (Figure 1).

Thermal analysis revealed an irreversible phase transition to the known phase $CsGaS_2$-*mC*16[4] at temperatures above 600°C.

The compound was further characterized by using Raman- and diffuse-reflectance spectroscopy. The results of DFT calculations are in good agreement with the experimental data.

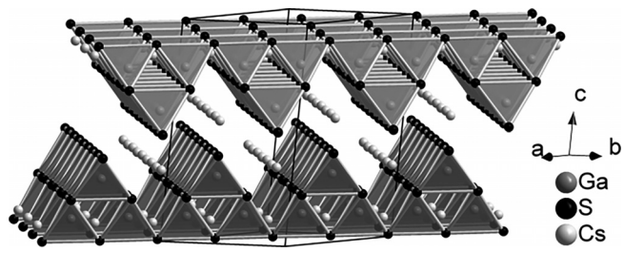

Figure 1. Section of the crystal structure of $CsGaS_2$-*mC*64 showing the corner-sharing Ga_4S_{10} supertetraedra.

[1] D. Friedrich, M. Schlosser, A. Pfitzner, *Z. Anorg. Allg. Chem.* **2014**, *640*, 826–829.
[2] D. Friedrich, F. Pielnhofer, M. Schlosser, R. Weihrich, A. Pfitzner, *Chem. Eur. J.* **2015**, *21*, 1811–1817.
[3] V. Winkler, M. Schlosser, A. Pfitzner, *Z. Anorg. Allg. Chem.* **2015**, *641*, 549–556.
[4] D. Friedrich, M. Schlosser, A. Pfitzner, *manuscript submitted*.
[5] D. Schmitz, W. Bronger, *Z. Naturforsch.* **1975**, *30b*, 491–493.

* Prof. Dr. A. Pfitzner
E-Mail: arno.pfitzner@chemie.uni-regensburg.de
[a] Institut für Anorganische Chemie
Universität Regensburg
Universitätsstraße 31
93040 Regensburg, Germany

 © 2016 WILEY-VCH Verlag GmbH & Co. KGaA, Weinheim

10.1002/zaac.201605033

Synthese und Kristallstruktur neuer Oxidnitride vom Bixbyit-Typ

Tobias Lüdtke,*[a] and Martin Lerch[a]

Keywords: Bixbyit, Oxidnitride

Im quaternären System Ta-Zr-O-N sind Verbindungen mit Baddeleyit- bzw. Anosovitstruktur bekannt[1]. Jetzt konnten phasenreine Oxidnitride mit kubischer Bixbyitstruktur (Raumgruppe $Ia\bar{3}$) für die Ta:Zr Verhältnisse von 2:1, 1:1 und 1:2 synthetisiert werden. Die Darstellung erfolgte durch Ammonolyse entsprechender amorpher Ta/Zr-Oxide bei Flussraten von 10–20 L/h NH_3 im Temperaturbereich zwischen 1023 und 1173 K für 12 h. Durch Variation der Synthesebedingungen ist es möglich, Phasen mit unterschiedlichen N/O-Verhältnissen (7,75–0,92) zu synthetisieren. Im Falle der für den Bixbyit-Typ idealen Zusammensetzung A_2X_3 sollte für ein Kationenverhältnis von 1:1 eine reine Nitridverbindung mit der Formel $TaZrN_3$ gebildet werden. Die synthetisierte Phase mit dem höchsten Stickstoffanteil weist jedoch die Summenformel $TaZrO_{0,4}N_{3,1}$ auf. Aufgrund einer partiellen Besetzung der für A_2X_3 leeren 16*c* Lage erlaubt die Bixbyitstruktur, die als 2×2×2 Überstruktur des Fluorit-Typs beschrieben werden kann, das Auftreten von Verbindungen mit Anionenüberschuss der Art A_2X_{3+x} ($x<1$).

Der Gitterparameter *a* variiert durch die unterschiedlichen N/O-Verhältnisse in den dargestellten Phasen zwischen Werten von 995,2 und 1007,9 pm. Der Parameter *x* der 24*d* Kationenposition, der als Maß für die Abweichung von der Fluoritstruktur betrachtet werden kann, wird dadurch ebenfalls beeinflusst. Eine Ordnung der Kationen konnte nicht festgestellt werden. Vergleichbare Phasen sind auch im System Sc-Ta-O-N bekannt[2].

Diese Arbeit wird von der DFG im Rahmen des SPP 1415 gefördert.

[1] J. Grins, P.-O. Käll, G. Svensson, *J. Mater. Chem.* **1994**, *4*, 1293–1301.
[2] A. Stork, H. Schilling, C. Wessel, H. Wolff, A. Börger, C. Baehtz, K.-D. Becker, R. Dronskowski, M. Lerch, *J. Solid State Chem.* **2010**, *183*, 2051–2058.

* Tobias Lüdtke
E-Mail: tobias.luedtke@tu-berlin.de
[a] Institut für Chemie, Technische Universität Berlin
Straße des 17. Juni 135
10623 Berlin, Germany

10.1002/zaac.201605034

$Cu_7PSe_{5.1}Te_{0.9}$, A New Mixed Chalcogenide Argyrodite

Severin Bauer[a] and Arno Pfitzner*[a]

Keywords: Argyrodite, Conductor

The compound $Cu_7PSe_{5.1}Te_{0.9}$ was prepared by solid state synthesis. It crystallizes in the space group $F43m$ (No. 216), $Z = 4$, with $a = 10.1605(2)$ Å, and $V = 1048.91(6)$ Å^3. The chemical composition and the crystal structure are characteristic for the argyrodite family [1,2]. A fcc lattice is formed by a mixed site of tellurium and selenium. Half of the tetrahedral sites therein also show this mixed occupancy. Tetrahedral anions $[PSe_4]^{3-}$ occupy the octahedral holes of the cubic close packing. The copper sites are only partially occupied, and are coordinated by a so called double tetrahedron formed by the anions [2]. No mixing of Se and Te is observed around P.

The total conductivities were determined by impedance measurements at different temperatures. They are $\sigma = 0.30$ S cm^{-1} at 305 K and $\sigma = 0.26$ S cm^{-1} at 573 K, respectively.

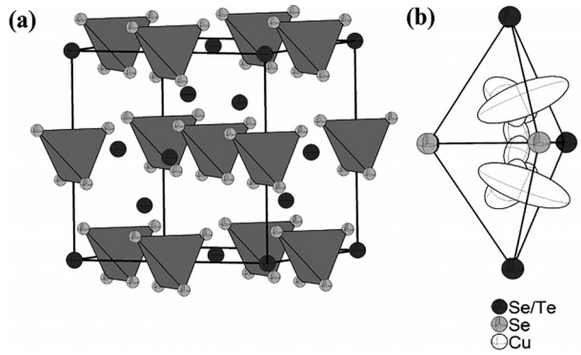

Figure 1. a) anionic PSe_4 tetrahedra in the fcc arrangement of Se/Te and b) double tetrahedron around the copper sites.

[1] W. F. Kuhs, R. Nitsche, K. Scheunemann, *Mater. Res. Bull.* **1979**, *14*, 241.
[2] T. Nilges, A. Pfitzner, *Z. Kristallogr.* **2005**, *220*, 281.

* Prof. Dr. A. Pfitzner
E-Mail: arno.pfitzner@chemie.uni-regensburg.de
[a] Institut für anorganische Chemie, Universität Regensburg
Universitätsstraße 31
93040 Regensburg, Germany

 © 2016 WILEY-VCH Verlag GmbH & Co. KGaA, Weinheim

10.1002/zaac.201605035

On the Electronic Properties of Low Dimensional Phosphorous Allotropes

Maximilian Baumgartner,[a] Tom Nilges,*[a] and Richard Weihrich*[b]

Keywords: (electronic properties, polyphosphides, semiconducting material)

Within recent years fascinating novel 1D allotropes of phosphorous were discovered and compared to the known forms (see Ref.[1]). They include the novel nanorods found by Pfitzner[2] that consist of single P chains that are related to those known for Hittorf's and Ruck's fibrous P[3]. For all known allotropes, namely white, red, violet and black P, strong relations of crystal and electronic structures are obvious. The electronic properties of black phosphorous and $P_{1-x}As_x$ are intensively investigated, as they change upon exfoliation to single and bilayer systems[4]. Within our recent work[1] crystal structure models were identified for two types of phosphorous nanorods [P8]P4(4)[and [P10]P2[and the not yet isolated [P12(4)]P2[.

Herein, we report on details concerning the electronic structures of the nanorod allotropes and changes upon separation into single one-dimensional polymers similarly to the couple black P-phosphorene.

According to the present results all three models exhibit interesting semiconducting properties with bandgaps in a range from 1.0 to 1.1 eV from DFT calculations. Towards single polymers the gap opens to 2.3 and 2.9 eV. The results are confirmed by calculations with different functionals (LDA, PBE, PBE0, HSE06).

[1] F. Bachhuber, J. von Appen, R. Dronskowski, P. Schmidt, T. Nilges, A. Pfitzner, R. Weihrich, *Angew. Chem.,* **2014***, 126,* 11813–11817. *Angew. Chem. Int. Ed.,* **2014***, 53,* 11629–11633.
[2] A. Pfitzner, M. F. Bräu, J. Zweck, G. Brunklaus, H. Eckert, Angew. Chem. **2004**, *116*, 4324-4327; Angew. Chem. Int. Ed. **2004**, *43*, 4228–4231.
[3] M. Ruck, D. Hoppe, B. Wahl, P. Simon, Y. Wang, G. Seifert, Angew. Chem. **2005**, *117*, 7788-7792; Angew. Chem. Int. Ed. **2005**, *44*, 7616–7619.
[4] B. Liu, M. Köpf, A. A. Abbas, X. Wang, Q. Guo, Y. Jia, F. Xia, R. Weihrich, F. Bachhuber, F. Pielnhofer, H. Wang, R. Dhall, S. B. Cronin, M. Ge, X. Fang, T. Nilges, C. Zhou, *Adv. Mater* **2015**, *27*, 4423–4429.

* Prof. Dr. Richard Weihrich
E-Mail: richard.weihrich@mrm.uni-augsburg.de
* Prof. Dr. Tom Nilges
E-Mail: Tom.Nilges@lrz.tu-muenchen.de
[a] TU München, Lichtenbergstr. 4.
85747 Garching, Germany
[b] Universität Augsburg, Institut für Materials Resource Management, Universitätsstr. 1, 86135 Augsburg, Germany

10.1002/zaac.201605036

Eu_2H_3I: A New Hydride Iodide with Divalent Europium

Daniel Rudolph[a] and Thomas Schleid*[a]

Keywords: Europium, Hydrides, Iodides, Crystal Structure

Merohedrically twinned crystals of Eu_2H_3I were obtained by the reaction of europium(II) hydride and iodide in a cesium-iodide flux, while all attempts to reproduce the PbFCl-type EuHI[1] failed. The dark red compound crystallizes in the trigonal space group $P3m1$ (a = 419.36(4) pm, c = 760.65(7) pm, Z = 1; CSD-429401) and is isotypic with the analogous europium(II) hydride chloride[2] and bromide.[3]

In the crystal structure of Eu_2H_3I, the Eu^{2+} cations exhibit a tenfold coordination figure consisting of seven hydride and three iodide anions. The Eu–H distances range from 244 to 279 pm, while the Eu–I bond length is 342 pm. A bond-valence sum of +1.95 for the europium cation supports its divalency.

The crystal structure can be described as a stuffed *anti*-CdI_2-type structure, where the Eu^{2+} cations form a hexagonal closest packing of spheres. The iodide anions occupy every second layer of octahedral holes, while the remaining layers of octahedral interstices are filled with one portion of hydride anions $(H1)^-$. The second kind of hydride anions $(H2)^-$ are located in all the tetrahedral voids of the same europium double layer (Figure 1).

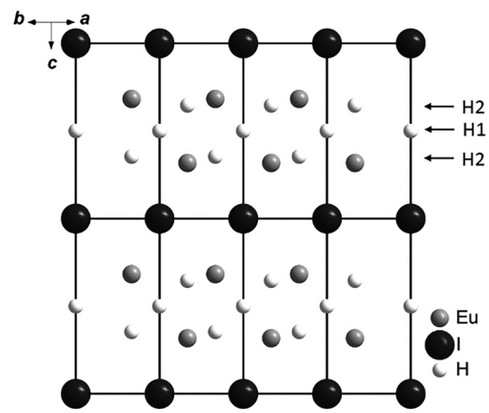

Figure 1. [110]-view at the crystal structure of trigonal Eu_2H_3I.

[1] H. P. Beck, A. Limmer, *Z. Naturforsch.* **1982**, *37b*, 574–578.
[2] O. Reckeweg, F. J. DiSalvo, S. Wolf, Th. Schleid, *Z. Anorg. Allg. Chem.* **2014**, *640*, 1254–1259.
[3] O. Reckeweg, F. A. Weber, B. Blaschkowski, Th. Schleid, *Z. Anorg. Allg. Chem.* **2014**, *640*, 2354–2354.

* Prof. Dr. Th. Schleid,
E-Mail: schleid@iac.uni-stuttgart.de
[a] University of Stuttgart, Institute for Inorganic Chemistry, Pfaffenwaldring 55, 70569 Stuttgart, Germany

 © 2016 WILEY-VCH Verlag GmbH & Co. KGaA, Weinheim

10.1002/zaac.201605037

Hydrogenation Reaction Pathways in the System Li_3N–MgH_2–H_2 by *in situ* Neutron Diffraction and *in situ* Thermal Analysis

Gereon Behrendt[a] and Holger Kohlmann*[a]

Keywords: Hydrogen storage, lithium nitride, lithium amide, magnesium hydride, in situ

The phase diagram Li–Mg–N–H offers ample opportunities for potential hydrogen storage systems. A system of lithium nitride and magnesium hydride was investigated by time-resolved *in situ* methods (thermal analysis, X-ray and neutron diffraction) at temperatures up to 703 K. Equimolar mixtures, both at 1.5 and 9.4 MPa hydrogen gas pressure, react according to $Li_3N + 2\ H_2 \rightarrow LiNH_2 + 2\ LiH$ up to 543 K, as found identically for the pure lithium nitride system, i. e. magnesium hydride does not participate in the reaction. Kinetic observations of this reaction revealed a parabolic time law typical for solid-gas reactions (Fig. 1).[1] At higher temperatures lithium magnesium nitride is formed according to the endothermic reaction $LiNH_2 + MgH_2 \rightarrow LiMgN + 2\ H_2$ at moderate ($\leq$ 1.5 MPa) and via the exothermic reaction $Li_3N + MgH_2 \rightarrow LiMgN + 2\ LiH$ at higher hydrogen gas pressures (5.0 MPa). Mixed imide $Li_2Mg(NH)_2$ is formed when an excess of Li_3N is used in the reaction.
In situ neutron powder diffraction experiments were carried out at the Institut Laue-Langevin in Grenoble, France, at the high flux diffractometer D20 using a sapphire gas pressure cell allowing for the collection of high quality powder diffraction data in time-resolved experiments with a time resolution of two minutes per diffraction pattern.[2] The results were confirmed by *in situ* differential scanning calorimetry (DSC) and *in situ* and *ex situ* X-ray diffraction studies.

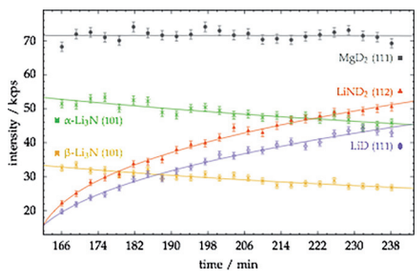

Figure 1. Development of the intensities of individual reflections during an isothermal section (476 K) in the *in situ* neutron powder diffraction experiment on the deuteration of equimolar mixtures of Li_3N and MgD_2.

[1] H. Schmalzried, *Solid State Phenom.* **1997**, *56*, 13–36.
[2] T. C. Hansen, H. Kohlmann, *Z. Anorg. Allg. Chem.* **2014**, *640*, 3044–3063.

* Prof. Dr. H. Kohlmann
E-Mail: holger.kohlmann@uni-leipzig.de
[a] Inorganic Chemistry, University of Leipzig, Johannisallee 29, 04103 Leipzig, Germany

10.1002/zaac.201605038

Intercalated HNO_3 Molecules in $RE(CH_3SO_3)_3{\cdot}HNO_3$ (RE = Sm, Tb)

Vanessa Zimmermann[a] and Mathias S. Wickleder*[a]

Keywords: methanesulfonate, crystal structure, intercalation, nitric acid, adduct

The importance of methanesulfonic acid raised in the last years due to its beneficial properties like low toxicity or environmental compatibility.[1] Besides several application the acid might play also a crucial role in the recycling of rare earth elements.[2] Methanesulfonates of the lanthanides have been investigated especially in form of their solvates but also some anhydrous species are known.[3] Most of the latter show layer type structures, for example $Nd(CH_3SO_3)_3$. We were now able to intercalate these layer structure by nitric acid molecules as shown in the crystal structures of $Sm(CH_3SO_3)_3{\cdot}HNO_3$ (CSD 431219) (triclinic, $P1$, Z = 2, a = 496.23(2) pm, b = 1034.13(3) pm, c = 1351.80(5) pm, α = 108.5557(15)°, β = 92.7736(16)°, γ = 92.5971(15)°) and its isotypic terbium congener $Tb(CH_3SO_3)_3{\cdot}HNO_3$ (CSD 431220) (triclinic, $P1$, Z = 2, a = 493.02(4) pm, b = 1023.90(8) pm, c = 1360.42(11) pm, α = 108.691(5)°, β = 92.744(5)°, γ = 92.590(5)°) which were obtained from $Sm(NO_3)_3$ and $Tb(NO_3)_3{\cdot}5H_2O$, respectively. The nitrates were reacted with methanesulfonic acid at 140 °C in sealed glass ampoules. As in the need compounds layers of the composition $RE(CH_3SO_3)_3$ (RE = Sm, Tb) are observed. However, between the layers now molecules of nitric acid are intercalated (Fig. 1).

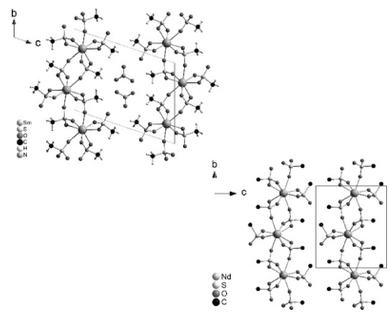

Figure 1. Left: Crystal structure of anhydrous $Nd(CH_3SO_3)_3$ projected onto (100).[3] Right: Crystal structure of $RE(CH_3SO_3)_3{\cdot}HNO_3$ (RE = Sm, Tb) with intercalated nitric acid molecules projected onto (100).

[1] M. D. Gernon, M. Wu, T. Buszta, P. Janney, *Green Chem.* **1999**, *1*, 127–140.
[2] Loser Chemie GmbH (U. Loser. W. Palitzsch), DE102014112952 A1 (March 12, 2015).
[3] M. S. Wickleder, *Chem. Rev.* **2002**, *102*, 2011–2088.

* Prof. Dr. Mathias S. Wickleder
E-Mail: mathias.wickleder@anorg.chemie.uni-giessen.de
[a] Institute of Inorganic and Analytical Chemistry
Justus-Liebig-University Gießen
Heinrich-Buff-Ring 17
35392 Gießen, Germany

 © 2016 WILEY-VCH Verlag GmbH & Co. KGaA, Weinheim

10.1002/zaac.201605039

Luminescence Tuning in Red Emitting $Ca_2Li_2[Mg_2Si_2N_6]:Eu^{2+}$

Philipp Strobel[a] and Wolfgang Schnick*[a]

Keywords: Nitridosilicate, Luminescence, Narrow-Band Red, Metathesis

Eu^{2+}-doped nitridosilicates emerged as outstanding red emitting luminescent materials. Examples are $(Ba,Sr)_2Si_5N_8:Eu^{2+}$ and $M[Mg_3SiN_4]:Eu^{2+}$ (M=Ca-Ba) that are successfully synthesized by solid state metathesis.[1,2]

The novel material $Ca_2Li_2[Mg_2Si_2N_6]:Eu^{2+}$ unifies the most important properties of red phosphors for an application in highly efficient LEDs with high color rendition: Single crystals show thermal and chemical stability as well as a large band gap of the host lattice. Rather narrow band emission in the red spectral region at 638 nm and a fwhm of only 60 nm have been demonstrated.[3] The emission maximum can be shifted towards smaller wavelengths by substitution of Ca by Sr.

Structural features are $[Si_2N_6]^{10-}$ units, which are connected with each other by chains of MgN_4 tetrahedra forming a rigid network. Two crystallographic distinct octahedral spheres are filled with Ca^{2+} respectively two Li^+.[4]

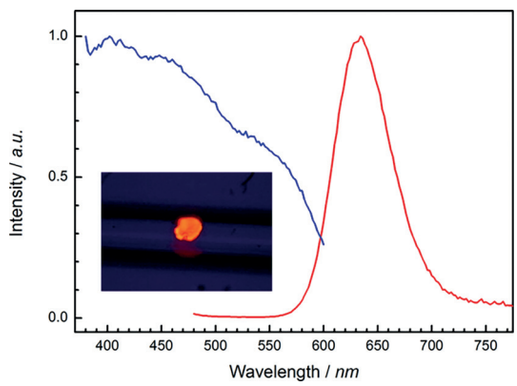

Figure 1. Excitation (blue) and emission spectra (red) of $(Ca,Sr)_2Li_2[Mg_2Si_2N_6]:Eu^{2+}$ (7% Sr).

[1] R. Mueller-Mach, G. Mueller, M. R. Krames, H. A. Höppe, F. Stadler, W. Schnick, T. Juestel, P. Schmidt, *Phys. Stat. Sol. A* **2005**, *202*, 1727–1732.
[2] S. Schmiechen, H. Schneider, P. Wagatha, C. Hecht, P. J. Schmidt, W. Schnick, *Chem.Mater.* **2014**, *26*, 2712–2719.
[3] P. Strobel, V. Weiler, P. J. Schmidt, W. Schnick, *in preparation*.
[4] S. Schmiechen, F. Nietschke, W. Schnick, *Eur. J. Inorg. Chem.* **2015**, 1592–1597.

* Prof. Dr. W. Schnick
E-Mail: wolfgang.schnick@uni-muenchen.de
[a] Department of Chemistry, University of Munich (LMU), Butenandtstraße 5-13, 81377 Munich, Germany

10.1002/zaac.201605040

B-$La_4N_2S_3$: A Second Modification of Lanthanum(III) Nitride Sulfide

Falk Lissner[a] and Thomas Schleid*[a]

Keywords: Lanthanum, Nitrides, Sulfides, Crystal Structure

On orthorhombic $La_4N_2S_3$ (*Pnnm*, Z = 2) the first time was reported in 2006.[1] By the oxidation of lanthanum metal with sulfur and sodium azide (NaN_3) in the presence of lanthanum iodide (LaI_3) and sodium iodide (NaI) as flux, a second modification could be obtained now. The dark brown compound crystallizes mono-clinically in the space group *C*2/*c* with Z = 8 (a = 1820.14(9), b = 1005.42(5), c = 1288.91(6) pm, β = 134.443(3)°, CSD-431099) and is isotypic with the analogous praseodymium nitride sulfide.[2]

Although the density of both modifications shows very small deviations from each other (5.426 g/cm^3 for orthorhombic $La_4N_2S_3$ *vs.* 5.363 g/cm^3 for monoclinic $La_4N_2S_3$) their crystal structures exhibit fundamental differences.

The main structural feature of the denser orthorhombic A-$La_4N_2S_3$ is built up by double chains of edge- and vertex-connected $[NLa_4]^{9+}$ tetrahedra.[1] In contrast, the new monoclinic B-$La_4N_2S_3$ shows layers perpendicular to [001] forming a network of similarly fused $[NLa_4]^{9+}$ tetrahedra, which can be described as a porous sheet consisting of four- and eight-membered rings (Figure 1). Four different La^{3+} cations are coordinated sixfold by 2 N^{3-} and 4 S^{2-} anions (La1 and La3) on the one hand as well as sevenfold by 2 N^{3-} and 5 S^{2-} anions (La2 and La4) on the other.

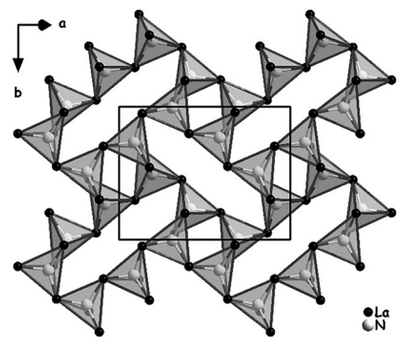

Figure 1. Porous layer of edge- and vertex-sharing $[NLa_4]^{9+}$ tetrahedra spreading out perpendicular to [001] in the monoclinic crystal structure of B-type $La_4N_2S_3$.

[1] F. Lissner, Th. Schleid, *Z. Anorg. Allg. Chem.* **2006**, *632*, 1167–1172.
[2] F. Lissner, Th. Schleid, *Z. Anorg. Allg. Chem.* **2005**, *631*, 427–432.

* Prof. Dr. Th. Schleid
E-Mail: schleid@iac.uni-stuttgart.de
[a] University of Stuttgart
Institute for Inorganic Chemistry
Pfaffenwaldring 55
70569 Stuttgart, Germany

 © 2016 WILEY-VCH Verlag GmbH & Co. KGaA, Weinheim

10.1002/zaac.201605041

Züchtung und elektrochemische Charakterisierung von Cerdioxid-basierten Einkristallen

Eva Heppke,*[a] Sebastian Eickholt,[b] Aditya Maheshwari,[b] Hans-Dieter Wiemhöfer,[b] and Martin Lerch[a]

Keywords: Cerdioxid, Skullschmelz-Verfahren

Cerdioxid-basierte Materialien sind aufgrund ihrer elektrochemischen Eigenschaften von besonderem Interesse[1]. Der Einfluss der Substitution höher- bzw. nieder-valenter Kationen sowie der Ko-Substitution auf die ionische und elektronische Leit-fähigkeit wurde an Cerdioxid-basierten Einkristallen untersucht. Korngrenzeneffekte können somit vernachlässigt und die Bestimmung der Konzentrationen und Beweglichkeit der Ionen und Elektronen im Volumen in den Vordergrund gestellt werden.

Die Cerdioxid-basierten Einkristalle wurden mit Hilfe der Skullschmelz-Technik gezüchtet. Beim Skullschmelzen handelt es sich um ein quasi-tiegelfreies Verfahren, bei dem das Material induktiv über ein Hochfrequenzfeld aufgeschmolzen wird[2]. Dies ermöglicht das Verflüssigen hochschmelzender Verbindungen sowie eine hohe chemische Reinheit und Homogenität der Einkristalle[2].

Cerdioxid-basierte Einkristalle mit folgenden nominellen Zusammensetzungen wurden gezüchtet:

$Ce_{0,97}Pr_{0,03}O_{2-\delta}Ce_{0,82}Pr_{0,15}Ta_{0,03}O_{2-\delta}$
$Ce_{0,82}Pr_{0,15}Nb_{0,03}O_{2-\delta}$
$Ce_{0,35}Zr_{0,40}Y_{0,20}Pr_{0,05}O_{2-\delta}$
$Ce_{0,99}Nb_{0,01}O_{2-\delta}$
$Ce_{0,8}Gd_{0,17}Pr_{0,03}O_{2-\delta}$

Die Einkristalle wurden strukturell mittels Röntgendiffraktometrie untersucht. Über Mikrokontaktmessungen wurde die elektronische Leitfähigkeit ermittelt, die bei Pr-substituierten Einkristallen ein klassisches Polaronen-Hopping zeigt. Die Bestimmung der Gesamtleitfähigkeit erfolgte an polykristallinen Proben mittels Impedanz-Spektroskopie.

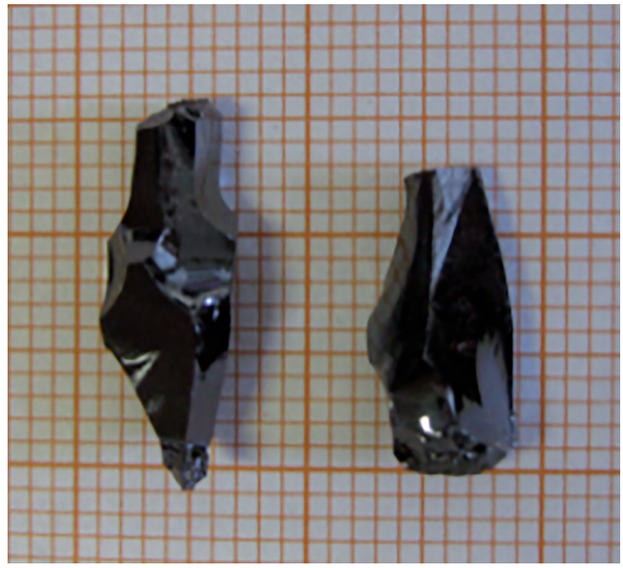

Abb. 1: $Ce_{0,97}Pr_{0,03}O_{2-\delta}$ - Einkristalle

[1] M. Morgensen, N. M. Sammes, G. A. Tompsett, *Solid State Ionics*, **2000**, 29, 62–94.
[2] Yu. S. Kuz'minov, E. E. Lomonova, V. V. Osiko, *Cambridge International Science Publishing Ltd.*, **2008.**

* Eva Heppke, M.Sc.
E-Mail: e.heppke@tu-berlin.de
[a] Technische Universität Berlin
Straße des 17.Juni 135
10623 Berlin, Deutschland
[b] Westfälische Wilhelms-Universität Münster
Corrensstraße 28/30
48149 Münster, Deutschland

 © 2016 WILEY-VCH Verlag GmbH & Co. KGaA, Weinheim

10.1002/zaac.201605042

In-situ Crystallization Cell: Developments and First Results of the Model System $Al(acac)_3$

Nicole Pienack,[a] Huayna Terraschke,[a] and Wolfgang Bensch*[a]

Keywords: Crystallization cell, *in-situ* XRD

In-situ investigations of the crystallization of solids are still necessary for the understanding and the rational synthesis of precursors, intermediates and products with special or even improved properties.[1] With our crystallization cell,[2] the detection and the control of different reaction parameters during chemical reactions in fluid media can be achieved. The modifications of the cell allow *in-situ* experiments with X-ray diffraction (XRD).[2] The crystallization of $Al(acac)_3$ (acac = acetylacetonate) as model system was investigated to demonstrate the performance of the cell. First *in-situ* energy-dispersive X-ray diffraction (EDXRD) experiments were carried out at the beamline F3 (DORIS, DESY). During the crystallization of $Al(acac)_3$ changes of pH value and redox potential could be observed, but a higher concentrated reaction suspension was required for obtaining suitable EDXRD spectra. In subsequent *in-situ* XRD experiments at beamline P07B (PETRA III, DESY) with modified reaction vessels in a special sample holder (Fig. 1) the growth of the Bragg peaks during the crystallization of $Al(acac)_3$ could be detected. The possibility of integrating further methods and/or sensors is highly important while working with synchrotron radiation (Fig. 1). Hence, the potential of the cell was proved to be beneficial for controlling and monitoring several reaction parameters during the crystallization.

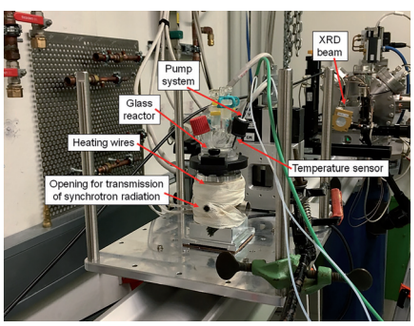

Figure 1. Setup of the modified reaction vessel in the sample holder at the beamline P07B at PETRA III, DESY.

[1] N. Pienack, W. Bensch, *Angew. Chem. Int. Ed.* **2011**, *50*, 2014–2034.[2] H. Terraschke, L. Ruiz Arana, P. Lindenberg, W. Bensch, *Analyst* **2016**, *141*, 2588–2594.

* Prof. Dr. W. Bensch
E-Mail: wbensch@ac.uni-kiel.de
[a] Institut für Anorganische Chemie der Christian-Albrechts-Universität zu Kiel, Max-Eyth-Str. 2, 24118 Kiel, Germany

10.1002/zaac.201605043

Electrochemical and Structural Properties of $Ag_4Fe_5O_2(PO_4)_5$ as well as Phase Diagram $Ag_2O/Fe_2O_3/P_2O_5$

Marcel Elsner,[a] Iren Weimann,[a] Jörg Feller,*[a] and Zdirad Žák[b]

Keywords: Phase Diagram $Ag_2O/Fe_2O_3/P_2O_5$; $Ag_4Fe_5O_2(PO_4)_5$

In order to complete the understanding of electrochemical properties from oxide phosphates, the quasi-ternary system $Ag_2O/Fe_2O_3/P_2O_5$ has been investigated. In accordance to Becht[1] a oxide phosphate phase with the formula $Ag_4Fe_5O_2(PO_4)_5$ occurs. Powder samples of the compound were prepared from $AgNO_3$, Fe_2O_3 and $(NH_4)_2HPO_4$ whilst the starting materials were milled, placed in porcelain crucibles and heated stepwisely up to 800 °C for 5 days. The phase diagram at 800 °C depicted in Figure 1 was the result of the X-ray powder analysis.
Yellow column single crystals from the oxide phosphate were obtained by a melting procedure starting at 800 °C and cooling down to 700 °C with 1 K/min. The compound shows a phase transition from the orthorhombic to the monoclinic system at -74 °C. The lattice constants of the low temperature modification are presented in Tab. 1.
Furthermore, the new phase has been characterized by DTA, TG and Galvanostatic Discharge.

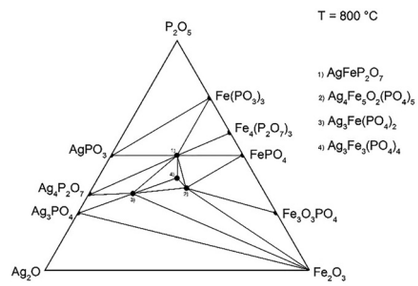

Figure 1. Phase Diagram $Ag_2O/Fe_2O_3/P_2O_5$ at 800 °C

Table 1. Lattice Constants α-$Ag_4Fe_5O_2(PO_4)_5$ (CSD 431199)

Space group	*a/b/c [Å]*	β/°	*V [Å³]*	*z*
P 2 1/n	*17.2458(12)*	110.017(4)	*1763.3(2)*	*4*
No. 14	*6.3071(5)*			
	17.2538(12)			

[1] G. A. Becht, PhD Dissertation, Clemson University, **2008**.

* Prof. Dr. J. Feller
E-Mail: feller@htw-dresden.de
[a] Hochschule für Technik und Wirtschaft Dresden
Friedrich-List-Platz 1; 01069 Dresden
[b] Přírodovědecká fakulta Masaryk University
61137 Brno; Kotlářská 2

 © 2016 WILEY-VCH Verlag GmbH & Co. KGaA, Weinheim

10.1002/zaac.201605044

Nanoskalige Carbonat-Hohlkugeln

Jan Jung-König[a] and Claus Feldmann*[a]

Keywords: Hohlkugel, Nano, Gadolinium, Magnesium, Carbonat

Nanoskalige Gadolinium- und Magnesiumcarbonat-Hohlkugeln wurden über eine neue Syntheseroute aus einer W/O-Mikroemulsion[1] durch Reaktion mit gasförmigem CO_2 synthetisiert. Über STEM-Untersuchungen wurde für Gadoliniumcarbonat-Hohlkugeln ein Durchmesser von 22±4 nm mit Kavitäten von 7,5±1,5 nm gemessen (Magnesiumcarbonat 35±9 nm, 17±5 nm).[2-3] Die Substanzzusammensetzung der amorphen Gadolinium- und Magnesiumcarbonat-Hohlkugeln wurde über XRD und TG-IR bestimmt.

Die Synthese der Gadolinium- und Magnesiumcarbonat-Hohlkugeln wurde unter milden Bedingungen so geführt, dass das Cytostatikum Doxorubicin bei der Bildung der Kugelschale in die Kavität eingeschlossen wurde. Die Freisetzung von Doxorubicin aus den Hohlkugeln liegt unter physiologischen Bedingungen bei mehreren Stunden, bei niedrigerem pH-Wert wird die Freisetzung beschleunigt.

In *in vitro* Zelltests zeigen Gadolinium- und Magnesiumcarbonat-Hohlkugeln in Kooperationen mit *Prof. U. Schepers* (ITG, KIT) ihr Potential als Wirkstofftransporter durch den Einschluss von Doxorubicin. Messungen im magnetischen Wechselfeld in Kooperation mit *Prof. I. Hilger* (Universitätsklinikum Jena) zeigen, dass durch Gadoliniumcarbonat-Hohlkugeln eine Gewebeerwärmung initiiert werden kann.

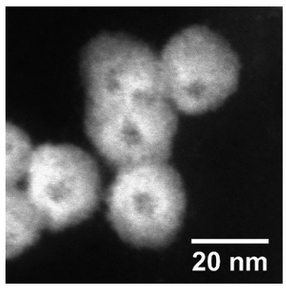

Abbildung 1. HAADF-STEM Abbildung von Gadoliniumcarbonat-Hohlkugeln.

[1] P. Leidinger, R. Popescu, D. Gerthsen, C. Feldmann, *Small.* **2010**, *17*, 1886–1891
[2] J. Jung-König, R. Popescu, C. Seidel, I. Hilger, U. Schepers, D. Gerthsen, C. Feldmann, **2016**, *in Vorbereitung*.
[3] J. Jung-König, R. Popescu, C. Seidel, U. Schepers, D. Gerthsen, C. Feldmann, **2016**, *in Vorbereitung*.

* Prof. Dr. C. Feldmann
E-Mail: claus.feldmann@kit.edu
[a] Institute of Inorganic Chemistry
Karlsruhe Institute of Technology (KIT)
Engesserstr. 15
76131 Karlsruhe, Germany

10.1002/zaac.201605045

Structure and Luminescence Properties of $Ca_{(20-x)}Li_{(8+2x)}[Al_{39}N_{55}]:Eu^{2+}$

Peter Wagatha[a] and Wolfgang Schnick*[a]

Keywords: Nitridoaluminate, Luminescence, Narrow-Band Red, Supertetrahedra

Eu^{2+}-doped nitridoaluminates like $Sr[LiAl_3N_4]:Eu^{2+}$ and $M[Mg_2Al_2N_4]:Eu^{2+}$ (M = Ca–Ba, Eu) that are accessible by high temperature synthesis proved to be extraordinary red emitting luminescent materials.[1,2]

$Ca_{(20-x)}Li_{(8+2x)}[Al_{39}N_{55}]:Eu^{2+}$ is a novel narrow-band red-emitting material with a remarkable crystal structure and outstanding luminescence properties. Single crystals and powder samples exhibit red emission at 645 nm with a fwhm of only 1280 cm^{-1} (54 nm). With increasing Li content, the emission wavelength and conversion efficiencies shift towards higher values.[3]

The crystal structure features vertex sharing T_5 supertetrahedra, forming two interpenetrating diamond-type networks. The networks are interconnected by Al_2N_7-moieties with the Ca and Li counterions occupying the space between the supertetrahedra. $Ca_{(20-x)}Li_{(8+2x)}[Al_{39}N_{55}]:Eu^{2+}$ is structurally closely related to the homeotypic manganate $Na_{26}Mn_{39}O_{55}$.[3,4]

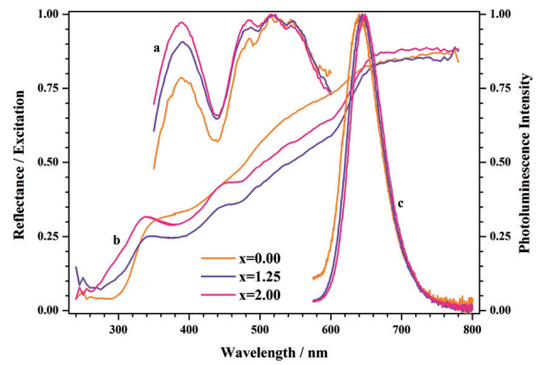

Figure 1. Excitation (a), reflectance (b) and emission spectra (c) of $Ca_{(20-x)}Li_{(8+2x)}[Al_{39}N_{55}]:Eu^{2+}$.

[1] P. Pust, V. Weiler, C. Hecht, A. Tücks, A. S. Wochnik, A.-K. Henß, D. Wiechert, C. Scheu, P. J. Schmidt, W. Schnick, *Nat. Mater.* **2014**, *13*, 891–896.
[2] P. Pust, F. Hintze, C. Hecht, V. Weiler, A. Locher, D. Zitnanska, S. Harm, D. Wiechert, P. J. Schmidt, W. Schnick, *Chem. Mater.* **2014**, *26*, 6113–6119.
[3] P. Wagatha, P. Pust, V. Weiler, A. S. Wochnik, P. J. Schmidt, C. Scheu, W. Schnick, *Chem. Mater.* **2016**, *28*, 1220–1226.
[4] A. Möller, P. Amann, V. Kataev, N. Schittner, *Z. Anorg. Allg. Chem.* **2004**, *630*, 890–894.

* Prof. Dr. W. Schnick
E-Mail: wolfgang.schnick@uni-muenchen.de
[a] Department of Chemistry, University of Munich (LMU),
Butenandtstraße 5-13, 81377 Munich, Germany

 © 2016 WILEY-VCH Verlag GmbH & Co. KGaA, Weinheim

10.1002/zaac.201605046

Die elektrische Leitfähigkeit von Zirconiumnitridoxid-Einkristallen bei niedrigen Temperaturen

Stefan Berendts,*[a] Jens-Peter Eufinger,[b] Ilia Valov,[c] Jürgen Janek,[b] and Martin Lerch[a]

Keywords: Zirconiumnitridoxid, Ionenleitfähigkeit

Aufgrund ihrer hervorragenden Eigenschaften sind Materialien auf Basis von Zirconiumdioxid seit mehreren Jahrzehnten Gegenstand der Forschung und Technik.[1] Die Fähigkeit Sauerstoffionen zu leiten resultiert aus der Präsenz von Sauerstoffleerstellen, die klassisch durch Substitution von Zirconium durch niedervalente Kationen erzeugt werden. Eine weitere Möglichkeit der Erzeugung von Anionenleerstellen bietet die Substitution von Sauerstoff durch Stickstoff.[2] Gering Yttrium-substituierte Zirconiumdioxid-Kristalle, die über das Skull-Schmelz-Verfahren darstellbar sind, können durch eine nachträgliche Nitridierung kubisch stabilisiert werden.[3]
Elektrochemische Unter-suchungen an solchen Kristallen haben gezeigt, dass die ionische Leit-fähigkeit bei niedrigen Temperaturen um eine Größenordnung höher ist als bei den stickstoffreien Kristallen und sogar um zwei Größen-ordnungen höher als bei technisch eingesetztem YSZ (Abb. 1). Dies kann darauf zurückgeführt werden, dass durch den Einbau von Stickstoff ein optimales Anionenleerstellenverhältnis vorhanden und die Aktivierungsenergie für den Ladungstransport, bedingt durch eine minimale Yttrium-Konzentration, gering ist.
Dieses Konzept könnte evtl. auch auf andere multinäre Systeme zur Verbesserung der elektrischen Eigenschaften übertragen werden.

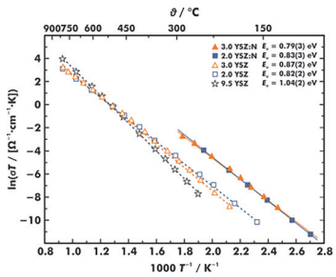

Abbildung 1. Elektrische Leitfähigkeit von Y-Zr-O(-N) Kristallen.

[1] L. Malavasi et al., *Chem. Soc. Rev.* **2010**, *39*, 4370–4387.
[2] M. Lerch et al., *Prog. Solid State Chem.* **2009**, *37*, 81–131.
[3] S. Berendts et al., *J. Cryst. Growth* **2013**, *371*, 28–33.

* Dr. S. Berendts
E-Mail: berendts@tu-berlin.de
[a] TU Berlin, Institut für Chemie, Straße des 17. Juni 135, 10623 Berlin, Germany
[b] JLU Gießen, Physikalisch-Chemisches Institut, Heinrich-Buff-Ring 17, 35392 Gießen, Germany
[c] Research Center Jülich, Peter Grünberg Institute, Electronic Materials (IEM), 52425 Jülich, Germany

10.1002/zaac.201605047

Au^{III}-Chalcogenates: $NaAu(SeO_4)_2$, $AgAu(SeO_4)_2$, and $Au(OH)(SO_4)$,

Christian Logemann,*[a] and Mathias S. Wickleder[a]

Keywords: gold, sulfates, selenates, crystal structure

Ternary gold(III)sulfates of the general formulae $MAu(SO4)_2$ (M = Na-Cs) and $BAu_2(SO_4)_4$ (B = Mg, Sr, Ba) have been successfully prepared by our group in recent years.[1,2] Interestingly, the binary gold sulfate $Au_2(SO_4)_3$ remains still elusive, even if the binary gold(II) sulfate $AuSO_4$ has been reported already in 2001.[3] As a first step towards $Au_2(SO_4)_3$ the here presented basic sulfate $Au(OH)(SO_4)$ (CSD 431173) could be seen. The structure shows the Au^{3+} ion in square planar surrounding of two sulfate groups and two hydroxide ions resulting in infinite chains along the *b*-axis (Figure 1).
For the heavier sulfur congener selenium, reactions using concentrated selenic acid are interesting because this acid can oxidize even elemental gold. In this way the compounds $Au_2(SeO_3)_2(SeO_4)$ and $RbAu(SeO_4)_2$ have been reported some ten years ago.[4,5] Now we present as a continuation the related selenates $NaAu(SeO_4)_2$ (CSD 431172) and $AgAu(SeO_4)_2$ (CSD 431171). Both are isotypic and exhibit anionic chains according to $^1{}_\infty[Au(SeO_4)_{4/2}]^-$ showing gold in square planar surrounding of selenate groups. In contrast to $RbAu(SeO_4)_2$ the resulting $[AuO_4]$- substructures are in staggered arrangement with respect to each other. Moreover, Na^+ and Ag^+ show octahedral coordination of oxygen atoms while tenfold oxygen coordination of Rb^+ was found for $RbAu(SeO_4)_2$.

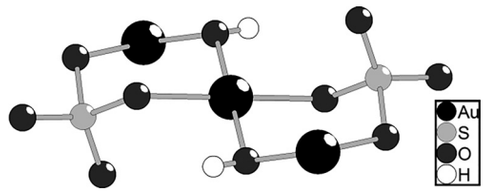

Figure 1. Square planar coordination of Au^{3+} in $Au(OH)(SO_4)$.

[1] a) M. S. Wickleder, O. Büchner, *Z. Naturforsch.*. **2001**, *56b*, 1340–1343; b) M. S. Wickleder, K. Esser, *Z. Anorg. Allg. Chem.* **2002**, *628*, 911–912.
[2] C. Logemann, M. S. Wickleder, *Z. Anorg. Allg. Chem.* **2014**, 640, 11, 2346.
[3] M. S. Wickleder, Z. Anorg. Allg. Chem. 2001, 627, 2112–2114.
[4] M. S. Wickleder, O. Büchner, C. Wickleder, S. el Sheik, G. Brunklaus, H. Eckert, Inorg. Chem. 2004, 43, 5860–5864.
[5] O. Büchner, M. S. Wickleder, Z. Anorg. Allg. Chem. 2004, 630, 1539–1540.

* Prof. Dr. M. S. Wickleder
E-Mail: mathias.wickleder@anorg.chemie.uni-giessen.de
[a] Justus Liebig Universität Gießen
Heinrich-Buff-Ring 17
35392 Gießen, Germany

 © 2016 WILEY-VCH Verlag GmbH & Co. KGaA, Weinheim

10.1002/zaac.201605048

From Columns to Layers: Tailoring the Crystal Structure Topology of Alkaline Earth Isocyanurate-Hydrates by Tuning Stoichiometry and pH

Peter Gross[a] and Henning A. Höppe*[a]

Keywords: Isocyanurate, Crystal growth, Calcium, Strontium, Barium

Inspired by the recently described nonlinear optical properties of alkaline earth cyanurates AE_3[cya]$_2$ (AE = Ca, Sr, Ba; cya = $C_3N_3O_3$), we studied several hydrated alkaline earth isocyanurates. Macroscopic crystals of Ca[H_2cya]$_2$·7H_2O[2], Sr[H_2cya]$_2$·4H_2O, Ca[Hcya]·3.5H_2O, Sr[Hcya]·3H_2O and Ba_3[H_2cya]$_2$[Hcya]$_2$·4H_2O were prepared via careful interdiffusion of aqueous solutions of AECl$_2$ and $Na_3[C_3N_3O_3]$[1] inside a U-tube by varying molar ratios and pH. For the latter four compounds, structure elucidation was performed by single-crystal XRD (Sr[H_2cya]$_2$·4H_2O: $P2_1$, a = 6.4672(2) Å, b = 18.8613(6) Å, c = 10.7532(4) Å, β = 91.080(1)°, Ca[Hcya]·3.5H_2O: $P2_1/c$, a = 7.3451(16) Å, b = 12.251(3) Å, c = 17.141(3) Å, β = 91.883(6)°), Sr[Hcya]•3H_2O: $P2_1/c$, a = 6.5360(3) Å, b = 12.1360(5) Å, c = 18.8657(8) Å, β = 96.345(1)°, Ba_3[H_2cya]$_2$[Hcya]$_2$·4H_2O: $P1$, a = 6.5781(3) Å, b = 9.0411(4) Å, c = 10.2008(4) Å, α = 91.018(2)°, β = 91.770(3)°, γ = 107.134(2)°). While both diprotonated compounds show columns formed by parallel-displaced stacking of hydrogen bonded isocyanurate dimers, the monoprotonated compounds feature layers formed by similar stacking of hydrogen bonded isocyanurate ribbons. The intermediate situation in Ba_3[H_2cya]$_2$[Hcya]$_2$•4H_2O results in corrugated layers of parallel stacked isocyanurate anions with only small displacement.

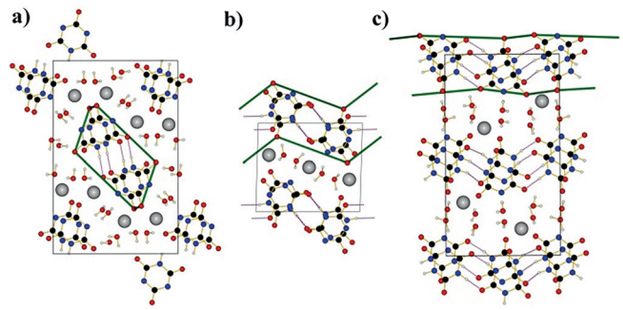

Figure 1. a) Sr[H_2cya]$_2$·4H_2O, **b)** Ba_3[H_2cya]$_2$[Hcya]$_2$·4H_2O and **c)** Sr[Hcya]·3H_2O (EA grey, H white, C black, N blue, O red). The green line indicates the topology.

[1] M. Kalmutzki, M. Ströbele, F. Wackenhut, A. J. Meixner, H.-J. Meyer, *Angew. Chem., Int. Ed.*, **2014**, *53*, 14260–14263.
[2] P. Gross, H. A. Höppe, manuscript in preparation.
[3] A. N. Chekhlov, *Russ. J. Inorg. Chem.* **2006**, *51*, 732–736.

* Prof. Dr. H. A. Höppe
E-Mail: henning.hoeppe@physik.uni-augsburg.de
[a] Institut für Physik
Universität Augsburg.
Universitätsstraße 1
86135 Augsburg, Germany

 © 2016 WILEY-VCH Verlag GmbH & Co. KGaA, Weinheim

10.1002/zaac.201605049

High-Pressure Synthesis, Single-Crystal Structure, and Magnetic Properties of Tb_3O_5

Matthias Glätzle,[a] Oliver Janka,[b] Rainer Pöttgen,[b] and Hubert Huppertz*[a]

Keywords: high pressure, rare earth oxide, crystal structure, magnetic properties

By applying high-pressure/high-temperature conditions of 8 GPa and 1050 °C utilizing a 1000 t press and a Walker-type multianvil device, we were able to obtain single crystals of Tb_3O_5[1] for the first time. This mixed-valent oxide forms dark rust-brown crystals that are stable under standard conditions in air. The synthesis was carried out in a boron nitride crucible using an equimolar mixture of Tb_4O_7 and Tb_2O_3 as the starting materials.

Single-crystal X-ray diffraction analysis showed that Tb_3O_5 crystallizes in the orthorhombic space group *Pnma* ($Z = 4$) with the parameters $a = 979.30(6)$, $b = 670.64(4)$, $c = 604.23(3)$ pm, $V = 0.39683(4)$ nm^3, $R_1 = 0.0160$, and $wR_2 = 0.0371$ (all data).

The crystal structure of Tb_3O_5 shows a strong analogy with oxometalates of the composition MBeRE_2O_5 (M = Ca, Sr, Ba, Eu; RE = rare earth)[2–4]. The two crystallographically independent terbium cations are coordinated by seven and eight oxygen anions, respectively. The Tb1 cation is coordinated in form of a twofold capped trigonal prism. The oxygen atoms O1 show a distorted tetrahedral coordination by the rare-earth cations, while the atoms O2, O3, and O4 are coordinated by five terbium cations in a square pyramidal arrangement. As the formula MBeRE_2O_5 and Tb_3O_5 indicate, the structure of Tb_3O_5 lacks one cation in comparison. In fact, the position of the Be^{2+} cation in MBeRE_2O_5 is not occupied in the Tb_3O_5 structure, and the charge neutrality is achieved by the mixed valence state of terbium, namely Tb^{3+} and Tb^{4+}. This was confirmed by calculations based on bond valence sums as well as magnetic measurements. The effective magnetic moment of 9.21 μ_B perfectly fits the calculated value of 9.18 μ_B for $Tb^{3.33+}$ ($\sqrt{{}^2/_3\cdot(Tb^{3+})^2 + {}^1/_3\cdot(Tb^{4+})^2} = \sqrt{{}^2/_3\cdot(9{,}74\ \mu_B)^2 + {}^1/_3\cdot(7{,}94\ \mu_B)^2}$). Measurements of the magnetic susceptibility at 100 Oe indicate an antiferromagnetic ordering of Tb_3O_5 at 3.6 K.

[1] L.-G. Liu, *Earth Planet. Sci. Lett.* **1980**, *49*, 166–172.
[2] R. Rettich, Hk. Müller-Buschbaum, *Z. Anorg. Allg. Chem.* **1995**, *621*, 562–566.
[3] Hk. Müller-Buschbaum, S. Münchau, *Z. Anorg. Allg. Chem.* **1994**, *620*, 1033–1036.
[4] Hk. Müller-Buschbaum, S. Münchau, *J. Alloys Compd.* **1994**, *206*, 175–178.

* Univ.-Prof. Dr. Hubert Huppertz
E-Mail: Hubert.Huppertz@uibk.ac.at
[a] Leopold-Franzens-Universität Innsbruck
Institut für Allgemeine, Anorganische und Theoretische Chemie
Innrain 80-82, 6020 Innsbruck, Austria
[b] Westfälische Wilhelms-Universität Münster
Institut für Anorganische und Analytische Chemie
Corrensstr. 28/30, 48149 Münster, Germany

 © 2016 WILEY-VCH Verlag GmbH & Co. KGaA, Weinheim

10.1002/zaac.201605050

Stability of ZnPd in Aqueous Media

Leonard Rößner,[a] René Kriegel,[a,b] and Marc Armbrüster*[a]

Keywords: ZnPd, PdZn, electrochemistry, corrosion

Previous results on intermetallic ZnPd in the methanol steam reforming showed excellent catalytic properties of Zn-rich ZnPd which could be attributed to the formation of ZnO on the surface of ZnPd[1]. To understand the corrosion behaviour of ZnPd further, its stability in aqueous KOH was investigated. Single-phase materials with different compositions were synthesised by a vapour-solid reaction. The samples were exposed to aqueous solutions with differing pH values while CVs were recorded. First results for pH = 14 can be seen in Fig. 1.

There are no Zn-related signals visible in the investigated potential range. The peak current density of the Pd^{2+} reduction peak grows on consecutive cycling. While this effect is tiny for an equimolar composition, it is much stronger for Zn-rich and Pd-rich samples. For the latter the 5th cycle shows a Pd^{2+}-reduction peak more negative compared to the former one. This might be due to a greater amount of surface Pd-atoms accessible for redox reactions. With increasing cycle number, the Zn-rich sample de-alloys faster than the Pd-rich, which translates into faster growing reduction peaks with increasing cycle numbers.

We expect the de-alloying behaviour of Zn to change with alteration of the pH-value, due to the formation of different Zn-species in the solution. Whether an oxidic Zn-species is formed will be explored by *in situ*-Raman spectroscopy in the future.

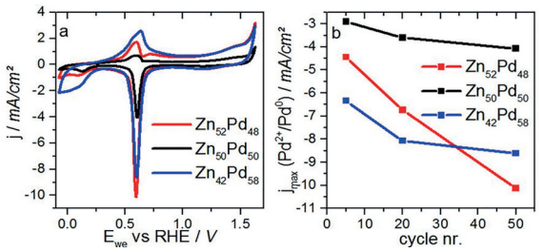

Figure 1: Stability test of ZnPd in 1M KOH (pH = 14) solution. a) CVs of ZnPd; b) peak current vs cycle no. for ZnPd samples; CVs recorded between -0,07 V and 1,63 V; dE/dt = 100 mV/s.

[1] M. Friedrich, S. Penner, M. Heggen, M. Armbrüster, *Angew. Chemie Int. Ed.* **2013**, *52*, 4389.

* Prof. Dr. Marc Armbrüster
E-Mail: marc.armbruester@chemie.tu-chemnitz.de
[a] Faculty of Natural Sciences, Institute of Chemistry, Materials for Innovative Energy Concepts, Technische Universität Chemnitz, 09107 Chemnitz, Germany.
[b] Max-Planck-Institut für Chemische Physik fester Stoffe, Nöthnitzer Straße 40, 01187 Dresden, Germany

10.1002/zaac.201605051

$Tb_3Cl_3[WO_6]$: The Final Member in a Series of Lanthanoid(III) Chloride Oxidotungstates(VI) Bearing Trigonal Prismatic $[WO_6]^{6-}$ Units

Katharina V. Dorn,[a] Thomas Schleid,[a] and Ingo Hartenbach*[a]

Keywords: Lanthanoids, Chlorides, Tungstates, Crystal Structure

The first representative of the $Ln_3Cl_3[WO_6]$ series, $Pr_3Cl_3[WO_6]$, was found in 1970 by *Polyanskaya et al.*[1]. More than a decade later, *Brixner et al.* thoroughly investigated $La_3Cl_3[WO_6]$ and presented lattice constants for the $Ln_3Cl_3[WO_6]$ derivates with Ln = La – Nd, Sm – Gd[2]. Although the existence of the title compound was questioned due to the large coordination number of ten for the Ln^{3+} cations, $Tb_3Cl_3[WO_6]$ now completes the hexagonal series of isotypic lanthanoid(III) chloride oxidotungstates(VI) in space group $P6_3/m$ with the lattice constants a = 908.56(4) pm and c = 524.63(2) pm for Z = 2. Outstanding for this crystal structure are the isolated trigonal prismatic $[WO_6]^{6-}$ units (Fig. 1, *right*), at which all nine edges are capped by one Ln^{3+} each, thereby creating a $^3_\infty\{([WO_6]Ln^e_{9/3})^{3+}\}$ framework (e = edge-sharing) with tube-shaped channels along [001] (Fig. 1, *left*). These channels are lined with Cl^- anions providing octahedral voids, which remain empty in this UCl_3-type related crystal structure.

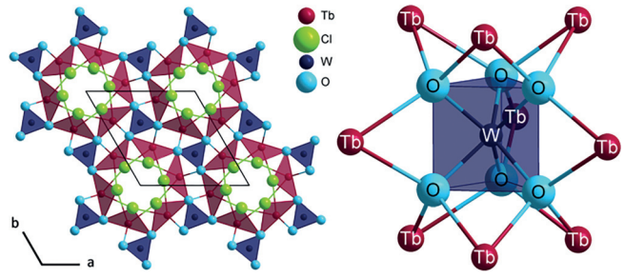

Figure 1: View at the hexagonal crystal structure of $Tb_3Cl_3[WO_6]$ along the c axis showing the isolated $[WO_6]^{6-}$ trigonal prisms (*right*) and the tetracapped trigonal prisms around Tb^{3+} (*left*).

[1] T. M. Polyanskaya, S. V. Borisov, N. V. Belov, *Dokl. Akad. Nauk SSSR* **1969**, *189*, 1043–1046.
[2] L. H. Brixner, H.-Y. Chen, C. M. Foris, *J. Solid State Chem.* **1982**, *44*, 99–107; J. B. Parise, L. H. Brixner, E. Prince, *Acta Crystallogr., Sect. B* **1983**, *39*, 1326–1328.

* Dr. I. Hartenbach
E-Mail: hartenbach@iac.uni-stuttgart.de
[a] University of Stuttgart, Institute for Inorganic Chemistry Pfaffenwaldring 55, 70569 Stuttgart, Germany

 © 2016 WILEY-VCH Verlag GmbH & Co. KGaA, Weinheim

10.1002/zaac.201605052

$[Pb_4(OH)_4(H_2O)_4][B_{10}H_{10}]_2 \cdot 2H_2O$: A Basic Lead(II) Decahydro-*closo*-Decaborate Hydrate

Fabian M. Kleeberg,[a] Lucas W. Zimmermann,[a] and Thomas Schleid*[a]

Keywords: Lead, Basic Salts, Decahydro-*closo*-Decaborates, Hydrates

Salt-like *closo*-borates containing additional hydroxide anions are quite rare in literature. They can be found only in reports about an aluminum- ($[Al_6(OH)_{10}(H_2O)_{14}[B_{12}H_{12}]_4 \cdot 28\ H_2O$[1]) and a bismuth-containing compound ($[Bi_6O_4(OH)_4][B_{12}H_{12}]_3 \cdot 10\ H_2O$[2]). The structure determination of the title compound with single-crystal X-ray diffraction data revealed an orthorhombic structure with *Pbcn* as space group (a = 1311.97(8), b = 1322.83(8) and c = 1562.78(9) pm for Z = 4; CSD-431231). The crystal structure contains Pb^{2+} cations, which build up $[Pb_4(OH)_4(H_2O)_4]^{4+}$ units (Fig. 1, *left*) with a distorted heterocubane-type $[Pb_4(OH)_4]^{4+}$ cluster (d(Pb–O) = 234 – 246 pm) as core, structurally similar to the $[Fe_4S_4]^{n+}$ complexes known as cofactors in enzymatic reactions[3]. Additional interactions between the Pb^{2+} cations and the hydridic hydrogen atoms of the nearest $[B_{10}H_{10}]^{2-}$ clusters with d(Pb–H) = 273 – 295 pm can be found to fill the coordination sphere of Pb^{2+} along with the water molecules of hydration (d(Pb–O) = 278 – 300 pm). These Pb–H distances are in accord with those of other compounds containing suboxidized cations from the 6th period and *closo*-borates, *e.g.* $Pb[B_{12}H_{12}]$ (d(Pb–H) = 274 – 282 pm)[4]. Furthermore the crystal structure contains bicapped square-antiprismatically shaped $[B_{10}H_{10}]^{2-}$ cluster anions, which are responsible for the charge compensation (Fig. 1, *right*).

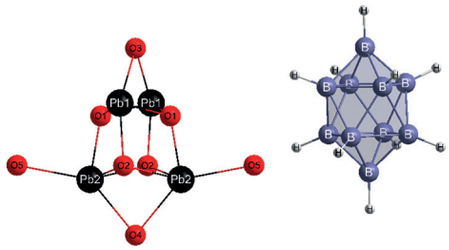

Figure 1. Cationic $[Pb_4(OH)_4(H_2O)_4]^{4+}$ unit (*left*) and $[B_{10}H_{10}]^{2-}$ cluster anion (*right*) of the title compound.

[1] Th. Schölkopf, *Doctoral Thesis*, Univ. Stuttgart, **2011**.
[2] L. W. Zimmermann, Th. Schleid, *Z. Anorg. Allg. Chem.* **2011**, *637*, 1903–1908.
[3] H. Beinert, *J. Biol. Inorg. Chem.* **2000**, *5*, 2–15.
[4] F. M. Kleeberg, L. W. Zimmermann, Th. Schleid, *Z. Anorg. Allg. Chem.* **2014**, *640*, 2352–2352.

* Prof. Dr. Th. Schleid
E-Mail: schleid@iac.uni-stuttgart.de
[a] University of Stuttgart, Institute for Inorganic Chemistry, Pfaffenwaldring 55, 70569 Stuttgart, Germany

10.1002/zaac.201605053

Microwave-Assisted Synthesis of Bismuth(III) Oxides Containing Sulfur and Selenium

Marcus Weber,[a] Philipp Kitschke,[a] and Michael Mehring*[a]

Keywords: Bismuth oxido cluster, δ-Bi_2O_3, Microwave reactor

The high-temperature modification of bismuth(III) oxide δ-Bi_2O_3 exhibits the best oxygen ion conductivity of all polymorphs but the low stability at room temperature is its major drawback.[1,2] By addition of metal oxides such as TeO_2 or Ln_2O_3 (Ln = lanthanoids), the high-temperature modification δ-Phase can be stabilized at room temperature.[3] In case of the chalcogenides, only Te^{4+} is known to form a bismuth(III) oxide with the structure of δ-Bi_2O_3,[4] whereas the combination with sulfur or selenium does not form the high-temperature cubic phase. Bismuth(III) oxides containing chalcogenides are traditionally obtained in solid state reactions at high temperatures and the resulting compounds are expected to be the stable polymorphs.[4–6] We here report on new bismuth(III) oxides with a cubic δ-Bi_2O_3 structure containing sulfur and selenium, respectively, as obtained by the hydrolysis of the bismuth oxido cluster $[Bi_{38}O_{45}(OMc)_{24}(DMSO)_9] \cdot 2DMSO \cdot 7H_2O$ (OMc = $O_2CC_3H_5$)[7] with an aqueous NaOH solution in the presence of several sulfur and selenium sources followed by subsequent heating in a microwave reactor. For example, the formation of cubic $Bi_{14}O_{20}(SO_4)$ (a = 5.5955(6) Å) was confirmed by PXRD and EDX analysis. IR spectroscopy confirms the presence of SO_4^{2-} in the crystal lattice by a strong band at 1060 cm^{-1}. Temperature dependent PXRD studies confirm the metastability of the cubic phase due to the transformation into the reported tetragonal polymorph $Bi_{14}O_{20}(SO_4)$[5], the formation of which was confirmed by PXRD, EDX and elemental analysis. IR spectroscopy confirms the phase transition from the cubic to the tetragonal phase by a shift of the SO_4^{2-} vibration band from 1060 cm^{-1} to 1048 cm^{-1}.

[1] H. A. Harwig, *Z. Anorg. Allg. Chem.* **1978**, *444*, 151–166.
[2] P. Shuk, H. D. Wiemhöfer, U. Guth, W. Göpel, M. Greenblatt, *Solid State Ionics* **1996**, *89*, 179–196.
[3] A. Watanabe, *Solid State Ionics* **1990**, *40–41*, 889–892.
[4] B. Frit, M. Jaymes, G. Perez, P. Hagenmuller, *Rev. Chim. Miner.* **1971**, *8*, 453–461.
[5] M. G. Francesconi, A. L. Kirbyshire, C. Greaves, *Chem. Mater.* **1998**, *10*, 626–632.
[6] H. Oppermann, H. Göbel, H. Schadow, P. Schmidt, C. Hennig, V. Vassilev, I. Markova-Deneva, *Z. Naturforsch.* **1999**, *54b*, 239–251.
[7] L. Miersch, T. Rüffer, M. Mehring, *Chem. Commun.* **2011**, *47*, 6353–6355.

* Prof. Dr. M. Mehring
E-Mail: michael.mehring@chemie.tu-chemnitz.de
[a] Technische Universität Chemnitz
Institut für Chemie, Professur Koordinationschemie
09107 Chemnitz, Germany

 © 2016 WILEY-VCH Verlag GmbH & Co. KGaA, Weinheim

10.1002/zaac.201605054

Deposition of Thin Germanium Films on Flexible Substrates

Ronny Fritzsche[a] and Michael Mehring*[a]

Keywords: Germanium, AFM, AP MO-CVD, Deposition

Fabrication of flexible thin-film transistors[1] as well as optical,[2] and spintronic devices[3] became an important research topic in the last years. Semiconductors and especially germanium has been reported to be a promising candidate for flexible electronic devices due to its high carrier mobility and optical properties.[4]

An atmospheric pressure metalorganic chemical vapor deposition process (AP MO-CVD) of the highly volatile germanes $GeH_2(C_5Me_4H)_2$[5] and $GeH_2(C_5Me_5)_2$ gave Ge-films with tunable thickness between 45 to 500 nm. The deposition rate was varied between 15–135 nm/min and a typical surface roughness of < 1 nm was obtained. The deposition on flexible Kapton® foils, as well as on silicon wafers and float glass in a low temperature process (275–400 °C) was possible as a result of the low decomposition temperatures of the precursors. Characterization with four point probe measurements showed a decrease in resistivity from $1.9 \cdot 10^8$ Ω to $5.1 \cdot 10^7$ Ω with increasing film thickness from 85 nm to 345 nm. RAMAN spectrometry shows a broad band between 220-310 cm^{-1}, which is indicative for amorphous germanium. Weak but characteristic D and G bands at 1350 cm^{-1} and 1600 cm^{-1} are indicative for some carbon impurities, which was ≤ 10 % according to XPS measurements and is comparable to germanium films deposited by the use of $GeH_3(C_5Me_5)$ in a PE CVD process.[6]

The as-deposited germanium films are non-porous and amorphous, and show strong adhesion to the substrates. Highly flexible germanium films with bending radii < 2 mm were obtained on Kapton® foils, which is of great interest for the development of flexible electronic devices.

[1] Y. Liu, H. Zhou, R. Cheng, W. Yu, Y. Huang, X. Duan, *Nano Lett.* **2014**, *14*, 1413–1418.
[2] L. Li, H. Lin, S. Qiao, Y. Zou, S. Danto, K. Richardson, J. D. Musgraves, N. Lu, J. Hu, *Nat Photon* **2014**, *8*, 643–649.
[3] A. Bedoya-Pinto, M. Donolato, M. Gobbi, L. E. Hueso, P. Vavassori, *Appl. Phys. Lett.* **2014**, *104*, 062412.
[4] M. A. Kats, F. Capasso, *Appl. Phys. Lett.* **2014**, *105*, 131108.
[5] K. Dittmar, PhD thesis, University Bielefeld **2002**.
[6] K. Dittmar, P. Jutzi, J. Schmalhorst, G. Reiss, *Chem. Vap. Deposition* **2001**, *7*, 193–195.

* Prof. Dr. M. Mehring
E-Mail: michael.mehring@chemie.tu-chemnitz.de
[a] Technische Universität Chemnitz
Institut für Chemie, Professur Koordinationschemie
09107 Chemnitz, Germany

10.1002/zaac.201605055

Preparation of β-Bi_2O_3 Films by Ultrasonic Spray Coating of Bismuth Oxido Clusters and their Photocatalytic Activity under Visible Light

Max Hofmann,[a] Benjamin Büchter,[a] and Michael Mehring*[a]

Keywords: Bismuth oxido cluster, Ultrasonic spray coating, β-Bi_2O_3, Photocatalysis

The conversion of photon energy into chemical energy has become of interest for photoinduced, environmentally friendly water and air purification by oxidation of organic pollutants. As one promising example, the preparation of β-Bi_2O_3 nanoparticles starting from bismuth oxido clusters provides photocatalysts with high activity. In general, suspensions of semiconductor particles show a higher photocatalytic activity than immobilized photocatalysts, nevertheless, to avoid leaching and a costly phase separating process for potential industrial applications it is essential to establish immobilization approaches for photocatalysts.[3] Therefore, the well-defined and nanoscaled (ca. 2nm) bismuth oxido cluster $[Bi_{38}O_{45}(OMc)_{24}(DMSO)_9]\cdot 2DMSO\cdot 7H_2O$ ($OMc = O_2CC_3H_5$)[4] was deposited on glass substrates by ultrasonic spray coating from solution. The as-deposited layers of the metal oxido cluster were hydrolyzed by a washing procedure using a sodium hydroxide solution and were air-dried at 40 °C. A final heat treatment protocol under argon atmosphere ensures the conversion of the pre-organized precursor to bismuth oxide. Powder X-ray diffraction indicates the formation of phase-pure metastable β-Bi_2O_3. Absorbtion edges around 550 nm and optical band gaps around 2.34 eV were determined by UV-Vis diffuse reflectance spectroscopy. Electron microscopy showed layers with a thickness of ca. 10 µm containing some cracks, which enlarge the effective surface area. Photodegradation experiments using an aqueous Rhodamine B solution (10^{-5} M) under visible light irradiation in the presence of the as-prepared β-Bi_2O_3 film proved its catalytic activity. Moreover, no photocorrosion after 10 h of light illumination was observed the as-deposited β-Bi_2O_3 films.

[1] M. Schlesinger, S. Schulze, M. Hietschold, M. Mehring, *Dalton Trans.* **2013**, *42*, 1047–1056.
[2] M. Schlesinger, M. Weber, S. Schulze, M. Hietschold, M. Mehring, *ChemistryOpen* **2013**, *2*, 146–155.
[3] P. Pichat, *Photocatalysis and Water Purification*, Wiley-VCH, Weinheim, **2013**.
[4] L. Miersch, T. Rüffer, M. Mehring, *Chem. Commun.* **2011**, 47, 6353–6355.

* Prof. Dr. M. Mehring
E-Mail: michael.mehring@chemie.tu-chemnitz.de
[a] Technische Universität Chemnitz
Institut für Chemie, Professur Koordinationschemie
09107 Chemnitz, Germany

 © 2016 WILEY-VCH Verlag GmbH & Co. KGaA, Weinheim

10.1002/zaac.201605056

Struktur-Eigenschafts-Beziehungen von Verbindungen im System Ge/Sn/Sb/In/Te

Lukas Neudert,[a] Manuel Scheel,[a] Stefan Schwarzmüller,[b] and Oliver Oeckler*[b]

Keywords: GST-Materialien, Transmissionselektronenmikroskopie, Realstruktur, Thermoelektrik

Mit In und Sb substituierte Germaniumantimontelluride $(Ge_{1-x}Sn_x)_n(Sb_{1-y}In_y)_2Te_{n+3}$ ($4 \leq n \leq 12$ und $0 \leq x, y \leq 1$) zeigen ausgeprägte Realstruktureffekte, die Einfluss auf die thermoelektrischen Eigenschaften haben.[1] Schnelles Abschrecken aus der Hochtemperaturphase im NaCl-Typ führt für $7 \leq n$ zu unterschiedlich ausgeprägter kurzreichweitiger Ausordnung der Defekte in einer pseudokubischen, metastabilen Modifikation. Bezüglich der Mischkristallbildung Ge/Sn bzw. Sb/In zeigen die Phasen Vegard'sches Verhalten. Transmissionselektronenmikroskopie (TEM) zeigt Nanostrukturen, welche potenziell die Phononstreuung erhöhen.[2] In abgeschrecktem $Ge_2Sn_2SbInTe_7$ liegen Domänen mit einer durch Defektausordnung charakterisierten Überstruktur des NaCl-Typs vor (13*P*-Schichtstruktur, $P\bar{3}m1$). TEM-Untersuchungen (HRTEM und STEM-HAADF) an $Ge_6Sn_6SbInTe_{15}$ zeigen bei der Umwandlung von der pseudokubischen zur stabilen trigonalen Modifikation nanoskalige In-reiche Ausscheidungen. Auch diese Phasen weisen Überstrukturphänomene auf. Die thermoelektrischen Gütefaktoren der quinären Phasen (ZT bei 300 °C: 0.20 für $Ge_6Sn_6SbInTe_{15}$ und 0.18 für $Ge_{3.5}Sn_{3.5}SbInTe_{10}$) liegen in der Größenordnung derjenigen von reinen oder nur mit Sn bzw. In substituierten GST-Materialien zeigen aber eine leichte Verbesserung bei geringen Temperaturen.[2,3] Unterschiede in bestimmten Temperaturbereichen weisen jedoch im Zusammenhang mit strukturellen Änderungen auf ursächliche Mechanismen hin.

[1] T. Rosenthal, M. N. Schneider, C. Stiewe, M. Doeblinger, O. Oeckler, *Chem. Mater.* **2011**, *23*, 4349–4356.
[2] T. Rosenthal, L. Neudert, P. Ganter, J. de Boor, C. Stiewe, O. Oeckler, *J. Solid State Chem.* **2014**, *215*, 231–240.
[3] T. Rosenthal, S. Welzmiller, O. Oeckler, *Solid State Sci.* **2013**, *25*, 118–123.

* Prof. Dr. O. Oeckler
E-Mail: oliver.oeckler@gmx.de
[a] LMU München, Department Chemie
Butenandtstr. 5-13
81377 München, Germany
[b] Universität Leipzig, Fakultät für Chemie und Mineralogie
Scharnhorststr. 20
04275 Leipzig, Germany

10.1002/zaac.201605057

Disulfato-Metallates

Christian Logemann,[a] Vanessa Zimmermann,[a] Jens-Henning Bölte,[b] and Mathias S. Wickleder*[a]

Keywords: disulfates, tetrels, noble metals

Some years ago we presented the *tris*-(disulfato)-silicate anion $[Si(S_2O_7)_3]^{2-}$ exhibiting a silicon atom in octahedral coordination of three chelating disulfate groups.[1] The sixfold silicon coordination by oxoanions is quite unusual even if the structure of the complex has been proposed in 1969.[2] Further studies showed that also other tetravalent metals are well stabilized in form of $[M(S_2O_7)_3]^{2-}$ type complexes (M = Ge, Sn, and Ti).[3] Disulfato-metallates could be also found for the heavier congeners of titanium but in this case the complexes $[M(S_2O_7)_4]^{4-}$ (M = Zr, Hf) are formed showing four chelating disulfate anions. Interestingly, a *tetrakis*-disulfato complex could also been prepared with silicon as a central atom but in this case only half of the disulfate ions are chelating ligands so that the silicon atom is in sixfold coordination again.[3] Stabilization of the complexes was achieved by various counter cations, mostly alkaline metal ions. Very recent investigations showed that also NO^+ and Tl^+ ions may serve for charge balance (CSD 431188-431192). Even divalent main group metals are suitable, for example for the stabilization of the $[M(S_2O_7)_4]^{4-}$ ion in $Pb_2[Si(S_2O_7)_4]$ (CSD 431193). The stability of the above mentioned compounds encouraged us to attempt also the inclusion of untypical tetravalent metals in these complexes. A first success was the preparation of $[Pt(S_2O_7)_3]^{2-}$.[4] Even more exciting is the analogous $[Pd(S_2O_7)_3]^{2-}$ because it is the first oxoanionic compound of tetravalent palladium. Interestingly, the preparation is only successful if XeF_2 is added as an oxidizer.[5] We hope that this elaborated approach will lead to further fascinating compounds, e.g. complexes containing tetravalent osmium and iridium.

[1] C. Logemann, T. Klüner, M. S. Wickleder, *Chem. Eur. J.* **2011**, *17*, 758–760.
[2] E. Thilo, A. Winkler, *Z. Anorg. Allg. Chem.* **1969**, *360*, 180–184.
[3] a) C. Logemann, D. Gunzelmann, T. Klüner, J. Senker, M. S. Wickleder, *Chem. Eur. J.* **2012**, *18*, 15495–15503; b) C. Logemann, J. Witt, D. Gunzelmann, J. Senker, M. S. Wickleder, *Z. Anorg. Allg. Chem.* **2012**, *638*, 2053–2061; c) C. Logemann, K. Rieß, M. S. Wickleder, *Chem. Asian J.* **2012**, *7*, 2912–2920.
[4] J. Bruns, O. Niehaus, R. Pöttgen, M. S. Wickleder, *Z. Anorg. Allg. Chem.* **2015**, *641*, *6*, 1002–1008.
[5] J. Bruns, D. van Gerven, T. Klüner, M. S. Wickleder, *Angew. Chem. Int. Ed.* **2016**, DOI: 10.1002/anie.201601767.

* Prof. Dr. M. S. Wickleder
E-Mail: mathias.wickleder@anorg.chemie.uni-giessen.de
[a] Justus Liebig Universität Gießen
Heinrich-Buff-Ring 17
35392 Gießen, Germany
[b] Carl-von-Ossietzky Universität Oldenburg
Carl-von-Ossietzky-Str. 9-11
26121 Oldenburg, Germany

 © 2016 WILEY-VCH Verlag GmbH & Co. KGaA, Weinheim

10.1002/zaac.201605058

New Triflimidates as Precursors for Electrochemistry

Claudia Kolb[a] and Mathias S. Wickleder*[a]

Keywords: metal triflimidates, noble metal triflimidate adducts, crystal structure

Various compounds containing the triflimid anion, $[N(CF_3SO_2)_2]^-$ or $[NTf_2]^-$, are used as catalysts and in electrochemistry e.g. in batteries[1] or as precursors for ionic liquids[2].

We could obtain a solvent-free $Ag[NTf_2]$ (CCDC 1475430) which shows a layer structure and its 2-ethylpyridine derivative $[Ag(NC_7H_9)_2][NTf_2]$ (CCDC 1475873) with linearly surrounded Ag^+ ions and only minor coordinative contributions of the $[NTf_2]^-$ ion. Contrastingly, a strong triflimid coordination via the bridging nitrogen atom is observed in the complexes $[Pd(NTf_2)_2(H_2O)_2]$ (CCDC 1436912) and $[Pd(NTf_2)_2(HAc)_2]$ (HAc = acetic acid) (CCDC 1476026). The Pd^{2+} ions is in almost perfect square planar coordination (Fig. 1) in both compounds.

We were also able to characterize the structure of $Pb[NTf_2]_2$ (CCDC 1475896), with three-dimensional Pb^{2+} linkage.

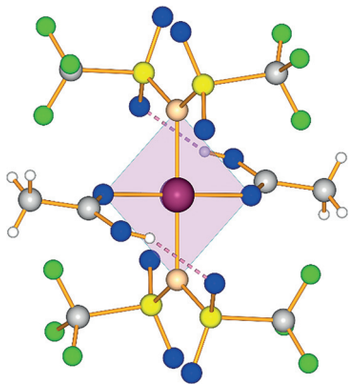

Figure 1 Molecular structure of $[Pd(NTf_2)_2(HAc)_2]$.

[1] S. Antoniotti, V. Dalla, E. Dunach, *Angew. Chem.* **2010**, *122*, 8032–8060; *Angew. Chem. Int. Ed.* **2010**, *49*, 7860–7888.
[2] Financial support of the DFG within the priority program SPP 1708 is gratefully acknowledged.

* Prof. Dr. M. S. Wickleder
E-Mail: Mathias.Wickleder@anorg.Chemie.uni-giessen.de
[a] Institute of Inorganic and Analytical Chemistry, JustusLiebigUniversity of Gießen
Heinrich-Buff-Ring 17
35392 Gießen, Germany

10.1002/zaac.201605059

Synthese und strukturelle Charakterisierung einer neuen Phase im System Sc-Nb-O-N

Steven Orthmann,*[a] and Martin Lerch[a]

Keywords: Nioboxidnitride, Röntgenbeugung, Synthese, Ammonolyse, Fluorit-Struktur

In den letzten Jahren haben Oxidnitride als Farbpigmente[1] und Photokatalysatoren[2] großes Interesse erweckt. Ausgehend von verschiedenen Niob-Scandium-Mischoxiden werden von uns seit einigen Jahren die Möglichkeiten der Darstellung der korrespondierenden Oxidnitride untersucht. Nachdem kürzlich eine Verbindung der Zusammensetzung $ScNb_4O_7N_3$ (Rutilstruktur) synthetisiert wurde[3], konnte nun auch eine hellbeige Phase mit Fluoritstruktur dargestellt werden.

Zur Synthese wurden Niob- und Scandiumcitrat-Lösungen mit Ethylenglycol als Komplexbildner gemischt und bei 200 °C polymerisiert. Nach anschließender Calcinierung bei 400 °C konnte ein röntgenamorphes, farbloses Oxidpulver erhalten werden, welches dann in einem Rohrofen drei Stunden bei 700 °C mit einer Gasmischung aus 10 $L \cdot h^{-1}$ Ammoniak und 0,03 $L \cdot h^{-1}$ Sauerstoff behandelt wurde.

Die Kristallstruktur wurde mit Hilfe der Rietveld-Methode verfeinert und ergab eine statistische Verteilung der Kationen sowie eine Unterbesetzung der Anionenposition (Raumgruppe *Fmm*). Die Stickstoff/Sauerstoff-Analyse erfolgte durch Heißgasextraktion. Es ergab sich eine Zusammensetzung von $Sc_2NbO_{5,11}N_{0,35}\square_{0,54}$. Vergleichbare Verbindungen mit Wolfram wurden bisher von Marchand et al.[4], Diot et al.[5] und Tessier et al.[6] beschrieben.

[1] M. Jansen, H. P. Letschert, Nature 2000, 404, 27, 980–982.
[2] K. Maeda, K. Domen, *J. Phys. Chem. C* **2007**, 111, 7851–7861.
[3] S. Orthmann, M. Lerch, *Z. Anorg. Allg. Chem.* **2014**, 640, 2349.
[4] R.Marchand, P. Antoine, Y. Laurent, *J. Solid State Chem.* **1993**, 107, 34–38.
[5] N. Diot, O. Larcher, R. Marchand, J.Y. Kempf, P. Macaudière, *J. Alloy. Compd.* **2001**, 323-324, 45–48.
[6] F. Tessier, P. Maillard, E. Orhan, F. Cheviré, *Mater. Res. Bull.* **2010**, 45, 97–102.

* Steven Orthmann
E-Mail: steven.orthmann@mailbox.tu-berlin.de
[a] Institut für Chemie
Technische Universität Berlin
Straße des 17. Juni 115
10623 Berlin, Germany

 © 2016 WILEY-VCH Verlag GmbH & Co. KGaA, Weinheim

10.1002/zaac.201605060

Synthesis of Halocuprate(I) Double Layers with Methenamine

Max Vilsmeier,[a] Mozhgan Samandarsangari,[a] and Arno Pfitzner*[a]

Keywords: Halocuprate(I), Methenamine, Luminescence

The halocuprate(I) $[C_6H_{12}N_4(CH_3)]\ ^2{}_\infty[(C_6H_{12}N_4)Cu_5Br_6]$ was synthesized at roomtemperature in an aqueous KBr solution and characterized by single crystal X-ray diffraction. The compound crystallizes monoclinic with a = 16.6200(4) Å, b = 9.4517(2) Å, c = 18.3575(4) Å, β = 108.590(2)° V = 2733.3(1) Å^3, and Z = 4 in the space group *C2/m* (No.12). The complex anion forms a honeycomb shaped double layer built by methenamine and $[Cu_5Br_6]$- clusters. Four of the Cu(I) ions form $CuBr_3L$ tetrahedra (L = methenamine) whereas one Cu(I) ion is coordinated trigonal planar by Br, thus terminating the anionic network to layered growth. Further the double layers are separated by dimers of mono-methylated methenamonium cations, which are connected via N···H – C hydrogen bonds. They are located in the cavities of two honeycomb layers. The whole arrangement resembles pillared clays[1].The compound shows an intensive orange fluorescence with a strong red shift upon cooling[2].

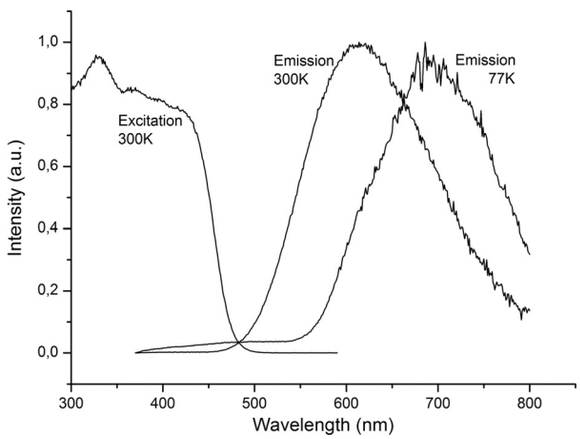

Figure 1.

[1] M. M. Herling, H. Kalo, S. Seibt, R. Schobert, J. Breu, *Zeitschrift* **2012**, *28*, 14713–14719.
[2] S. Maderlehner, M. J. Leitl, H. Yersin, A. Pfitzner, *Dalton Trans.* **2015**, *44*, 19305–19313.

* Prof. Dr. A. Pfitzner
E-Mail: arno.pfitzner@chemie.uni-regensburg.de
[a] Institut für anorganische Chemie, Universität Regensburg
Universitätsstraße 31
93040 Regensburg, Germany

10.1002/zaac.201605061

Synthese und Charakterisierung carboxylatbasierter anorganisch-organischer Hybridnanopartikel

Lilli Neumeier[a] and Claus Feldmann*[a]

Keywords: Anorganisch-organische Hybride, Nanomaterialien

Die Nanotechnologie spielt in der Medizin sowohl in der Diagnostik (z.B. Fluoreszenzmarker) als auch in der Therapie (z.B. Wirkstofftransport, Magnetothermie) eine zunehmende Rolle.[1]

Die hier beschriebenen anorganisch-organischen Hybridnanopartikel sind Verbindungen, die durch direkte Fällung eines anorganischen Kations und eines organischen Anions entstehen. Als Anionen können beispielsweise Fluoreszenzfarbstoffe oder medizinische Wirkstoffe eingesetzt werden. Diese müssen über funktionelle Gruppen verfügen, die in Gegenwart eines Metallkations eine schwerlösliche Verbindung eingehen. Die anorganisch-organischen Hybride zeichnen sich durch ihre einfache, meist wasserbasierte Synthese, Biokompatibilität und hohen Massenanteil an Fluoreszenzfarbstoff beziehungsweise Wirkstoff aus. Bislang wurden in der Literatur phosphat[2]- und sulfonatbasierte[3] Hybridnanopartikel beschrieben.

Ziel ist es, die Klasse der anorganisch-organischen Hybridnanopartikel um neue, carboxylatbasierte Substanzen zu erweitern. Als Kationen kommen z.B. Cu^{2+} oder Ag^+ in Frage. Eingesetzte Fluoreszenzfarbstoffe und Wirkstoffe werden dabei im Hinblick auf eine spätere Anwendbarkeit in der Medizin und anderen Bereichen gewählt.

[1] V. Wagner, A. Dullaart, A.-K. Bock, A. Zweck, *Nat. Biotechnol.* **2006**, *24*, 1211–1217.
[2] J. Heck, J. Napp, S. Simonato, J. Moellmer, M. Lange, H. Reichardt, R. Staudt, F. Alves, C. Feldmann, *J. Am. Chem. Soc.* **2015**, *137*, 7329–7336.
[3] M. Poß, J. Napp, O. Niehaus, R. Pöttgen, F. Alves, C. Feldmann, *J. Mater. Chem. C* **2015**, *3*, 3860–3868.

* Prof. Dr. C. Feldmann
E-Mail:claus.feldmann@kit.edu
[a] Institut für Anorganische Chemie
Karlsruher Institut für Technologie
Engesserstraße 15
76131 Karlsruhe, Germany

 © 2016 WILEY-VCH Verlag GmbH & Co. KGaA, Weinheim

10.1002/zaac.201605062

New Insights into $Eu_3[BO_3]_2$

Olaf Reckeweg,*[a] Christian Funk,[b] Francis J. DiSalvo,[a] and Thomas Schleid[b]

Keywords: Divalent Europium, Oxoborates, Crystal Structure

Europium(II) *ortho*-oxoborate was reported a while ago[1, 2], but the black appearance of the product under consideration usually indicates mixed-valent compounds containing Eu^{2+} *and* Eu^{3+} at the same time. Borothermic reduction of Eu_2O_3 (along with NaBr or KCl serving as flux) yields lemon yellow and transparent single crystals of $Eu_3[BO_3]_2$ forming either needles or triangular platelets. The structure determination revealed that $Eu_3[BO_3]_2$ crystallizes isotypically with $Ca_3[BO_3]_2$[1] and $Sr_3[BO_3]_2$[2] (trigonal, $R3c$, $Z = 6$; LT: $a = 904.73(6)$, $c = 1249.12(8)$ pm, CSD-431170; RT: $a = 906.89(6)$, $c = 1254.03(8)$ pm, CSD-431175; Figure 1). Raman-spectroscopic data confirm the presence of isolated $[BO_3]^{3-}$ triangles. Our structure data resemble earlier reports[3], but differences in the look of the crystals and in the crystallographic coordinates (Table 1) become obvious, when the results are compared in detail. Structural changes seem to occur between 150 and 450 °C. The slight thermochromic effect above 150 °C shifts the color from yellow to orange and a reversible phase transition at 400 °C needs to be checked in the future.

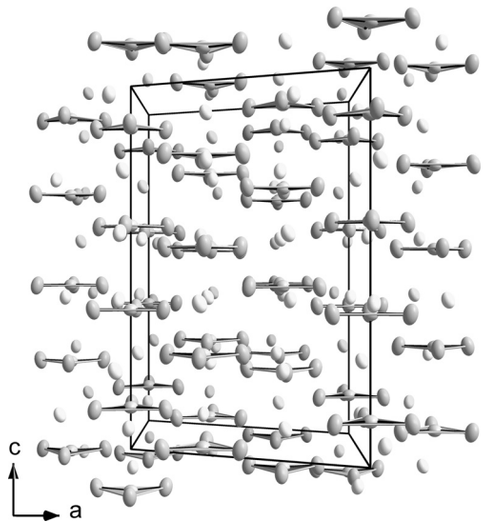

Figure 1: View at the crystal structure of $Eu_3[BO_3]_2$ along [110].

Table 1: Atomic coordinates and U_{eq} values for $Eu_3[BO_3]_2$ at low temperature (**–50 °C**) and at room temperature (*+25 °C*).

Atom	Site	*x / a*	*y / b*	*z / c*	U_{eq} / pm^2
Eu	18*e*	**0.35400(2)** *0.35379(4)*	0	$^1/_4$	**69(1)** *115(2)*
B	12*c*	0	0	**0.1157(4)** *0.1155(6)*	**74(8)** *112(12)*
O	36*f*	**0.1575(3)** *0.1576(4)*	**0.0095(3)** *0.0101(5)*	**0.1143(2)** *0.1142(3)*	**94(4)** *148(6)*

[1] W. Schuckmann, *Neues Jb. Miner. Mh.* **1969**, *3*, 142−144.
[2] A. Vegas, F. H. Cano, S. Garcia-Blanco, *Acta Crystallogr., Sect. B* **1975**, *31*, 1416−1419.
[3] K. Machida, G. Adachi, H. Hata, J. Shiokawa, *Bull. Chem. Soc. Jpn.* **1981**, *54*, 1052–1055.

* Dr. O. Reckeweg
E-Mail: olaf.reykjavik@gmx.de
[a] Baker Laboratory, Department of Chemistry and Chemical Biology, Cornell University, Ithaca, NY 14853-1301, USA
[b] University of Stuttgart, Institute for Inorganic Chemistry, Pfaffenwaldring 55, 70569 Stuttgart, Germany

 © 2016 WILEY-VCH Verlag GmbH & Co. KGaA, Weinheim

10.1002/zaac.201605063

EMF of ZnPd at 25 °C

René Kriegel[a,b] and Marc Armbrüster*[b]

Keywords: Intermetallic compound, ZnPd, PdZn, electromotive force, Thermodynamic measurements

Electromotive force (EMF) measurements on intermetallic ZnPd compounds with different chemical compositions were conducted at room temperature. The ZnPd electrodes were prepared as foils through a vapor-solid reaction of palladium foil and zinc granules, allowing a precise adjustment of the chemical composition. The single-phase nature of the samples was confirmed by powder X-ray analysis and light microscopy. To exclude oxidation and therefore wrong determination of the electrochemical potentials a method was developed to conduct the electrochemical measurements under non-corrosive conditions. Following the investigations of Schwitzgebel[1] the experiments were conducted in inert atmosphere. Corrosion by the electrolyte was avoided using DMF as aprotic solvent. Figure 1 shows the activities of Zn calculated from the preliminary EMF measurements in comparison with values determined from isopiestic methods at 1000 C°[2]. These are the first activities, given for the easily oxidised ZnPd compounds at room temperature.

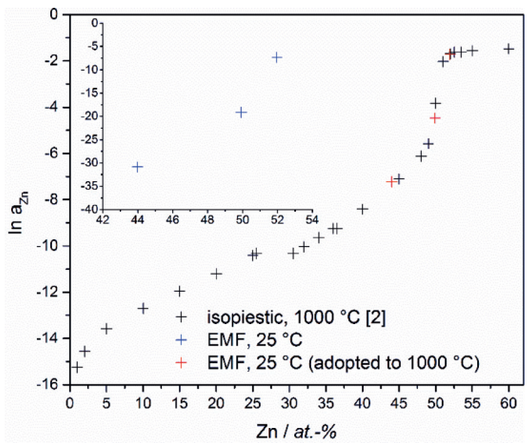

Figure 1. Activities of Zn in ZnPd at different chemical compositions by isopiestic and EMF measurements.

[1] G. Schwitzgebel, *Z. Phys. Chem.*, **1975**, *95*, 15–24.
[2] T.H. Chiang, H. Ipser, Y.A. Chang, *Z. MetaIlkd.*, **1977**, *68*, 141–147.

* Prof. Dr. Marc Armbrüster
E-Mail: marc.armbruester@chemie.tu-chemnitz.de
[a] Max-Planck-Institut für Chemische Physik fester Stoffe, Nöthnitzer Straße 40, 01187 Dresden, Germany
[b] Faculty of Natural Sciences, Institute of Chemistry, Materials for Innovative Energy Concepts, Technische Universität Chemnitz, 09107 Chemnitz, Germany

 © 2016 WILEY-VCH Verlag GmbH & Co. KGaA, Weinheim

10.1002/zaac.201605064

A New Tetragonal Tungsten-Bronze Structured Compound: $CsEu_2Ta_5O_{15}$

Christian Funk,[a] Jürgen Köhler,[b] and Thomas Schleid*[a]

Keywords: Europium, Oxotantalates, Crystal Structures, Magnetic Susceptibility

Out of tungsten oxide in combination with the alkali metals, there is a big variety of compounds and structures known. Most of them are called tungsten bronzes (TB)[1] and occur in four different structure types: perovskite TB ($La_{0.14}WO_3$)[2], tetragonal TB ($Ba_3Nb_5O_{15}$)[3], hexagonal TB (KNb_2O_9)[4], and intergrowth TB[1]. Now it was possible to get access to a new compound of the tetragonal TB representatives, namely $CsEu_2Ta_5O_{15}$, which was synthesized by mixing Li_2O, Eu_2O_3, Ta_2O_5, Ta powder, and CsF and heating the mixture in a Ta crucible in evacuated SiO_2 ampoules to 900 °C for 56 h. Afterwards it was reground and heated in a Ta capsule in a high-frequency furnace for 4 minutes. The black cubes of $CsEu_2Ta_5O_{15}$ crystallize tetragonally in the space group *P4/mbm* with $a = 1236.97(9)$, $c = 385.56(3)$ pm and $c/a = 0.312$ for $Z = 2$. Six oxygen atoms octahedrally surround the Ta atoms and the Cs atoms are located in oxygen cuboctahedra. Not less than fifteen oxygen atoms coordinate europium, but in first sphere, there are just six of them, which form an elongated trigonal prism (d(Eu–O) = 270 and 284 pm). In second sphere, two of the rectangular planes of the prism are capped with four oxygen atoms (d(Eu–O) = 300 – 354 pm), while the remaining one carries only one at a Eu^{2+}–O^{2-} distance of 301 pm. The magnetic susceptibility shows a paramagnetic behavior corresponding well with divalent europium.

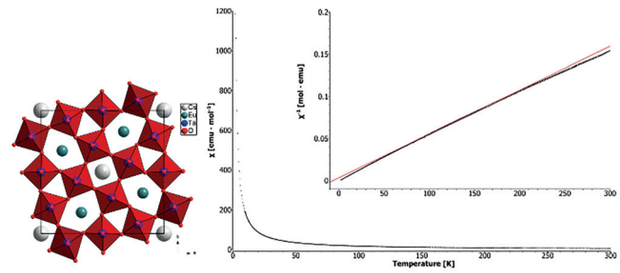

Figure 1. [001]-view at the $CsEu_2Ta_5O_{15}$ structure (*left*) and its magnetic and inverse magnetic susceptibility (*right*).

[1] P. Labbe, *Key Engin. Mater.* **1992**, *68*, 293–339.
[2] P. J. Wiseman, P. G. Dickens, *J. Solid State Chem.* **1976**, *17*, 91–100.
[3] C. R. Feger, R. P. Ziebarth, *Chem. Mater.* **1995**, *7*, 373–378.
[4] H. Y. Chang, T. Sivakumar, K. M. Ok, P. S. Halasyamani, *Inorg. Chem.* **2008**, *47*, 8511–8517.

* Prof. Dr. Th. Schleid
E-Mail: schleid@iac.uni-stuttgart.de
[a] University of Stuttgart, Institute for Inorganic Chemistry, Pfaffenwaldring 55, 70569 Stuttgart, Germany
[b] Max Planck Institute for Solid State Research, Heisenbergstraße 1, 70569 Stuttgart, Germany

 © 2016 WILEY-VCH Verlag GmbH & Co. KGaA, Weinheim

10.1002/zaac.201605065

The Borate Fluoride $Sn_3[B_3O_7]F$

Stephan G. Jantz[a] and Henning A. Höppe*[a]

Keywords: Tin, Borate Fluoride, Crystal Structure

In the course of our systematic investigations on silicate-analogous compounds[1–3], we also focus on fluoro-derivatives of phosphates[4], borates and other oxo-anions. $Sn_3[B_3O_7]F$ was synthesised from SnF_2 and B_2O_3 in a nitrogen flow at 300–400°C. It crystallises in the orthorhombic space group $Pna2_1$ (Z = 4, a = 9.2185(3) Å, b = 7.6970(3) Å, c = 12.2239(4) Å, V = 867.34(5) Å^3, 2426 F_o^2, 127 parameters, $R_1(F^2>2\sigma(F^2))$ = 0.025, $wR2(F^2$ all) = 0.039, GooF = 1.001). The structure (Fig. 1) is built up by $[B_3O_7]^5$- rings and fluoride anions, which was confirmed by $^{11}B\{^{19}F\}$-REDOR-NMR. The three crystallographically different Sn^{2+} -cations are coordinated three- and fourfold by oxygen and fluorine atoms, respectively. With a deviation of 0.2 % the structure is electrostatically consistent in terms of the MAPLE concept[5–7] (MAPLE ($Sn_3[B_3O_7]F$) = 43843 kJ·mol^{-1}, MAPLE (2.5 SnO + 0.5 SnF_2 + 1.5 B_2O_3) = 43754 kJ·mol^{-1}). $Sn_3[B_3O_7]F$ is stable up to 350°C under nitrogen.

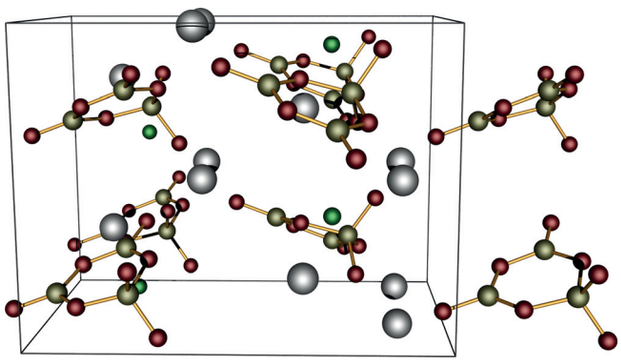

Figure 1. The crystal structure of $Sn_3[B_3O_7]F$. Sn grey, B olive, O red, F green.

[1] P. Gross, A. Kirchhain, H. A. Höppe, *Angew. Chem. Int. Ed.* **2016**, *55*, 4353–4355.
[2] K. Förg, H. A. Höppe, *Z. Anorg. Allg. Chem.* **2015**, *641*, 1009–1015.
[3] H. A. Höppe, S. J. Sedlmaier, *Inorg. Chem.* **2007**, *46*, 3467–3474.
[4] S. G. Jantz, L. van Wüllen, A. Fischer, E. Libowitzky, E. J. Baran, M. Weil, H. A. Höppe, *Eur. J. Inorg. Chem.* **2016,** 1121–1128.
[5] R. Hoppe, *Angew. Chem. Int. Ed.* **1966**, *5*, 95–106.
[6] R. Hoppe, *Angew. Chem. Int. Ed.* **1970**, *9*, 25–34.
[7] R. Hübenthal, MAPLE, Program for the Calculation of the Madelung Part of Lattice Energy, University of Gießen, Germany, **1993**.

* Prof. Dr. H. A. Höppe
E-Mail: henning.hoeppe@physik.uni-augsburg.de
[a] Institut für Physik, Universität Augsburg
Universitätsstraße 1
86159 Augsburg, Germany

10.1002/zaac.201605066

Nanoporous Mg_3N_2

Viktor Rein[a] and Claus Feldmann*[a]

Keywords: Nanoporous nitride, ammonia, liquid crystals, gas sorption

The material class of nitrides attracts significant attention due to outstanding catalytic, mechanical, optical and electronic properties, which further can be modified by nanostructuring.[1–3] Depending on the bonding situation, metal nitrides can be divided into three categories: 1. Ionic nitrides of the alkaline and alkaline earth metals; 2. Covalent nitrides of the late main group elements; 3. Interstitial nitrides of the transition metals. Thereby, ionic nitrides exhibit a strong basic nitride anion, which should be appropriate for chemisorption of acidic gases as for example carbon dioxide.

In our group, we were already able to synthesize several porous covalent as well as transition metal nitrides by using a liquid ammonia based liquid crystalline template (liq-NH_3 LCT).[4]

Here, we now report on the synthesis of nanoporous Mg_3N_2 using the liq-NH_3 LCT. The compound was formed by ammonolysis of di-*n*-butylmagnesium and subsequent annealing in nitrogen flow. It was extensively characterized, especially with regard to the ability of selective CO_2 sorption. In first measurements, thereby, it showed good loading capacities of up to 110 mg g^{-1} (90 bar, 50°C).

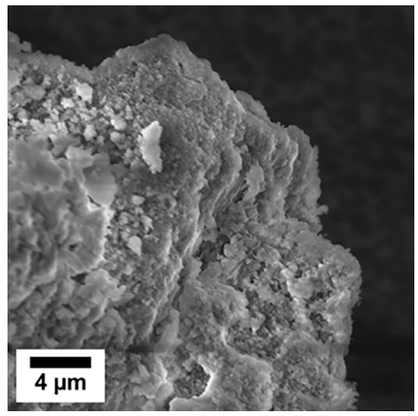

Figure 1. SEM image of nanoporous Mg_3N_2.

[1] C. Giordano, M. Antonietti, *Nano Today* **2011**, *6*, 366.
[2] S. Dong, X. Chen, X. Zhang, G. Cui, *Coord. Chem. Rev.* **2013**, *257*, 1946.
[3] J. Hargreaves, *Coord. Chem. Rev.* **2013**, *257*, 2015.
[4] F. Gyger, P. Bockstaller, D. Gerthsen, C. Feldmann, **2016**, *in preparation*.

* Prof. Dr. C. Feldmann
E-Mail: claus.feldmann@kit.edu
[a] Institute of Inorganic Chemistry, Karlsruhe Institute of Technology (KIT), Engesserstr. 15, 76131 Karlsruhe, Germany

 © 2016 WILEY-VCH Verlag GmbH & Co. KGaA, Weinheim

10.1002/zaac.201605067

Synthesis of Nanostructured, Cadmium-Doped ZnSb and Investigation of the Thermoelectric Properties

Jan Peilstöcker,[a] Ekrem Günes,[a] Oliver Falkenbach,[a] Eckhard Müller,[a,b] and Mathias S. Wickleder*[a]

Keywords: nanostructured, thermoelectrics, zinc antimony, cadmium

ZnSb is an interesting *p*-type thermoelectric compound for the middle temperature range (450 K – 650 K). Besides its relatively high electric conductivity and Seebeck coefficient, ZnSb possesses a low thermal conductivity. Furthermore, both constituent elements are cost-efficient and non-toxic.[1–2] Aim of this work was the synthesis of nanostructured ZnSb by mechanical alloying and doping with different amounts of cadmium to replace the zinc atoms in the lattice and so improve its thermoelectric properties. The synthesized samples were analyzed regarding their structural and thermoelectric properties. After synthesis, X-ray diffractograms and transmission electron microscopy images were taken from the samples. TEM images (Fig. 1) are showing agglomerates, which consisting of smaller particles of 20–50 nm in diameter. Cadmium-doping resulted in little change of the electrical conductivity compared to the undoped material but in an increase of the Seebeck coefficient. The thermal conductivity decreased by cadmium-doping and a figure of merit between 0.6 and 0.75 at 623–650 K was obtained.

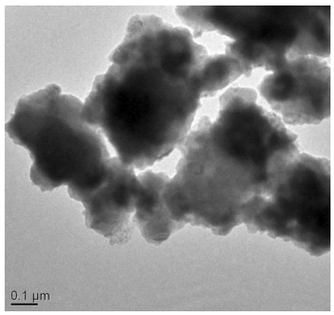

Figure 1. TEM image of the synthesized ZnSb.

[1] C. Okamura, T. Ueda, K. Hasezaki, *Mater. Trans.* **2010**, 5, 860–862.
[2] X. Song, P. H. M. Böttger, O. B. Karlsen, T. G. Finstad, J. Taftø, *Phys. Scr.* **2012**, T148, 014001-1–014001-6.

* Prof. Dr. M. S. Wickleder
E-Mail: Mathias.S.Wickleder@Anorg.Chemie.uni-giessen.de
[a] Institute of Inorganic and Analytical Chemistry, Justus-Liebig-University Gießen
Heinrich-Buff-Ring 17
35392 Gießen, Germany
[b] Institute of Materials Research, German Aerospace Center (DLR)
51170 Cologne, Germany

10.1002/zaac.201605068

Synthesis of Base Metal Nanoparticles using Amine Solvents

Alexander Egeberg[a] and Claus Feldmann[a]*

Keywords: Base Metal Nanoparticles, Amines

The high number of surface atoms, and consequently, a high reactivity is one property assigned to metal nanoparticles (MNP). In case of base MNP this effect is further reinforced. Synthesis and handling are challenging due to oxidation and agglomeration of the particles.
Organic radicals, generated by electron-transfer reactions of alkali metals provide extremely strong reducing agents without the need of decomposition of toxic, volatile and expensive metallorganic precursors. Base MNP were synthesized via reduction of simple metal chlorides using sodium naphthalenide ([NaNaph]) in ethereal solvents.[1] Amines are known to be more resistant to reduction than ethers.[2] Furthermore amines exhibit coordinating properties which make them well suitable for an application in the synthesis of MNP. The aim of this work is to expand the concept of reduction of metal salts in ethers to amines as solvent. Metal halides such as $FeCl_3$ and WCl_6 are used as cheap and uncomplex precursors. This oxygen-free synthesis could open ways to produce MNP, which are not accessible via the most common synthetic methods.

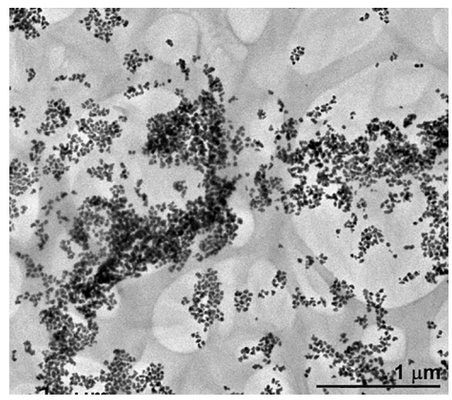

Figure 1. Ni^0-nanoparticles synthesized in oleylamine.[3]

[1] J. L. Dye, *Acc. Chem. Res.* **2009**, *42*, 1564-1572.
[2] C. Schöttle, P. Bockstaller, R. Popescu, D. Gerthsen, C. Feldmann, *Angew. Chem.* **2015**, *127*, 10004-10008.
[3] A. Egeberg, *master thesis, KIT*, Karlsruhe, Germany, **2015**.

* Prof. Dr. C. Feldmann
E-Mail: claus.feldmann@kit.edu
[a] Institut für Anorganische Chemie
Karlsruher Institut für Technologie (KIT)
Engesserstr. 15, Geb. 30.45
76131 Karlsruhe, Germany

 © 2016 WILEY-VCH Verlag GmbH & Co. KGaA, Weinheim

10.1002/zaac.201605069

Near-infrared Triggered Photoactivity of Plasmonic Au@$H_xK_{4-x}Nb_6O_{17}$ Photocatalysts with Biomimetic Nanopeapod Geometry

Ying-Chu Chen[a] and Claus Feldmann*[a]

Keywords: Nanopeapods, near infrared, photocatalyst, surface plasmon resonance, 3D Schottky barrier

It has been more and more frequently reported that engineering materials in a biomimic configuration could endow the objects with exceptional properties to fulfill human wish for millennia.[1–2] Driven by the above concept, this study puts forward a geometric approach of fabricating plasmonic photocatalysts in a peapod-analogous arrangement (Figure 1).[3] Nanoscale Au antennas unidirectionally resided inside a tubular semiconductor successfully yielded a broadband photocatalyst that not only absorbed visible but also near-infrared (NIR) light. The enhancement in light harvesting ability was formulated by the specific di-/multipole interactions originated from the peapodded pattern subduing the surface plasmon resonance (SPR) over extended wavelength region. Moreover, a proof-of-concept photocatalytic dye degradation has manifested these Au NP-loaded nanopeapods bearing superior photoactivity under simulated sunlight consisting more than 90 % of visible and NIR light. The results in this study proved that this peculiar peapod-mimic configuration successfully brought a broadband photoactivity to plasmonic Au@$H_xK_{4-x}Nb_6O_{17}$ photocatalysts.

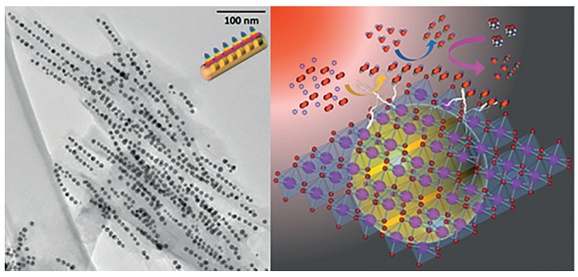

Figure 1. TEM image highlights the peapod-analogous geometry of plasmonic Au@$H_xK_{4-x}Nb_6O_{17}$ photocatalyst (left panel). Schematic photocatalysis principle of Au@$H_xK_{4-x}Nb_6O_{17}$ nanopeapods under NIR illumination (right panel).

[1] N. Savage, *Nature* **2015**, *519*, S7-S9.
[2] J. Gould, *Nature* **2015**, *519*, S2-S3.
[3] Y. C. Chen, C. Feldmann, in preparation.

* Prof. Dr. C. Feldmann
E-Mail: claus.feldmann@kit.edu
[a] Institut für Anorganische Chemie
Karlsruhe Institute of Technology (KIT)
Engesserstr. 15
76131 Karlsruhe

 © 2016 WILEY-VCH Verlag GmbH & Co. KGaA, Weinheim

10.1002/zaac.201605070

B-Type CeOF and a Correction for *Zachariasen*'s Tetragonal Crystal Structure of *β*-LaOF

Dirk D. Zimmermann[a] and Thomas Schleid*[a]

Keywords: Cerium, Oxide Fluorides, *Zachariasen*, *Bond-Valence* Calculations

Cerium(III) oxide fluoride (CeOF) emerged in its B-type structure as a side-product during attempts to synthesize quaternary cerium(III) oxide fluoride chalcogenides[1]. Electron-beam microprobe investigations proved that this compound is a ternary representative, only including oxide and fluoride. B-CeOF crystallizes tetragonally in the space group *P*4/*nmm* with the lattice parameters a = 406.84(3) and c = 578.19(4) pm with c/a = 1.421 for Z = 2. In these systems there are three different polymorphs known with a cubic, a tetragonal and a trigonal structure[2–4]. The tetragonal *M*OF phases were already known, but only mentioned by *Zachariasen* for the yttrium and lanthanum examples[5]. With the help of a B-CeOF single crystal of supreme quality, we were now able to recognize a significant difference for the interatomic distances of oxide and fluoride anions to the Ce^{3+} cations ($d(Ce^{3+}–O^{2–})$ = 245 pm (4×), $d(Ce^{3+}–F^{–})$ = 255 pm (4×)). *Bond-valence* calculations that we have performed indicate that *Zachariasen*'s refinement for both anionic positions ($O^{2–}$ and $F^{–}$) are falsely reversed for the tetragonal *β*-LaOF case (CSD-30622).

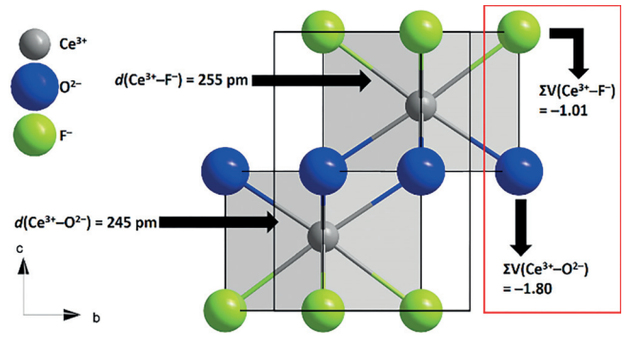

Figure 1. Extended unit cell with marked $Ce^{3+}–O^{2–}$ and $Ce^{3+}–F^{–}$ distances as consequence of *bond-valence* calculations for the determined oxide and fluoride positions in B-type CeOF.

Table 1: Fractional atomic coordinates for B-type CeOF.

Atom	Site	*x/a*	*y/b*	*z/c*	U_{eq} / pm^2
Ce	2*c*	$^1/_4$	$^1/_4$	0.26503(12)	172(4)
O	2*b*	0	0	0	172(19)
F	2*a*	$^3/_4$	$^1/_4$	0	502(29)

[1] D. D. Zimmermann, H. Grossholz, S. Wolf, O. Janka, A. C. Müller, Th. Schleid, *Z. Anorg. Allg. Chem.* **2015**, *641*, 1926–1933.
[2] W. Klemm, H. A. Klein, *Z. Anorg. Allg. Chem.* **1941**, *248*, 167–171.
[3] O. Janka, *Dissertation*, Univ. Stuttgart **2010**, 73–124.
[4] S. E. Dutton, D. Hirai, R. J. Cava, *Mater. Res. Bull.* **2012**, *47*, 714–718.
[5] W. H. Zachariasen, *Acta Crystallogr.* **1951**, *4*, 231–236.

* Prof. Dr. Th. Schleid
E-Mail: schleid@iac.uni-stuttgart.de
[a] University of Stuttgart, Institute for Inorganic Chemistry, Pfaffenwaldring 55, 70569 Stuttgart, Germany

 © 2016 WILEY-VCH Verlag GmbH & Co. KGaA, Weinheim

10.1002/zaac.201605071

The Luminescence Properties of $Eu_2O[SiO_4]$ and $Eu_{4.667}O[SiO_4]_3$

Monika E. Bohem[a,b] and Thomas Schleid*[b]

Keywords: Europium, Luminescence, Inorganic Pigments

Eu^{3+} is a useful activator ion for red-emitting phosphors and other applications[1]. Various studies focus on the luminescence properties of Eu^{3+}-doped host lattices, *e.g.* of the *apatite*-type structure[2], whereas compounds containing europium in other stoichiometric compositions gain much less attention. Single phase $Eu_2O[SiO_4]$ and $Eu_{4.667}O[SiO_4]_3$ were synthesized via solid-state reactions of the binary oxide components and their luminescence spectra have been comparatively studied. Single crystals of $Eu_2O[SiO_4]$ show the lattice parameters a = 913.72(8), b = 712.64(6), c = 676.25(6) pm, β = 107.673(3)° for the monoclinic space group $P2_1/c$ and Z = 4. The *apatite*-type oxosilicate $Eu_{4.667}O[SiO_4]_3$ crystallizes hexagonally in the space group $P6_3/m$ with Z = 2[3] and the lattice parameters a = 944.76(8), c = 690.83(6) pm. The notable peculiarity of both compounds is the additional oxygen within the structure, besides the oxosilicate-forming $[SiO_4]^{4-}$ tetrahedra, being coordinated by Eu^{3+} exclusively. The respective O^{2-} position is surrounded by a tetrahedral arrangement in $Eu_2O[SiO_4]$, whereas its coordination number reduces in $Eu_{4.667}O[SiO_4]_3$, since O^{2-} now centers plane $(Eu^{3+})_3$ triangles. The interatomic distance variation between the Eu^{3+} and O^{2-} plays a crucial role for the crystal field strength and therefore has an influence on the spectroscopic properties. In both cases, the $^5D_0 \rightarrow {}^7F_2$ transitions are the dominant emissions, which only occur when Eu^{3+}ioccupies sites without an inversion center[4]. The high sensitivity of Eu^{3+} luminescence to changes in the local environment leads to a slight variation of the shape in the emission spectra below, regarding the $^5D_0 \rightarrow {}^7F_J$ (J = 0, 1, 2, 3, 4) transitions.

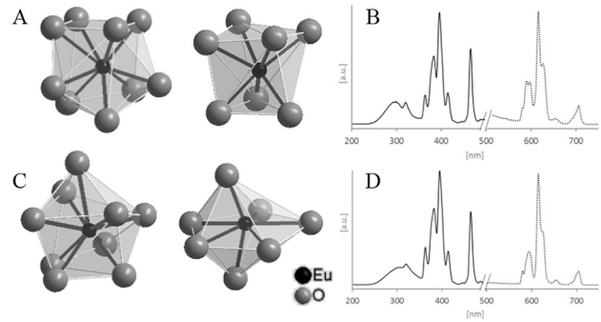

Figure 1.

[1] H. Shen, R. Liu, M. Yang, J. Zhou, Y. Gu, H. Yang, W. Wang, D. Xu, *Phys. Status Solidi* **2013 A**, *9,* 1839–1845.
[2] D. Kim, D. Park, N. Oh, J. Kim, E. D. Jeong, S.-J. Kim, S. Kim, J.-C. Park, *Inorg. Chem.* **2015**, *54,* 1325–1336.
[3] I. Hartenbach, Th. Schleid *Z. Kristallogr.,* S24, **2006**, 169.
[4] G. H. Dieke, Spectra and Energy Levels of Rare Earth Ions in Crystals, John Wiley & Sons, New York, **1969**.

* Prof. Dr. Th. Schleid
E-Mail: schleid@iac.uni-stuttgart.de
[a] Fraunhofer Institute for Manufacturing Engineering and Automation IPA, Allmandring 37, 70569 Stuttgart, Germany
[b] Institute for Inorganic Chemistry, University of Stuttgart, Pfaffenwaldring 55, 70569 Stuttgart, Germany

 © 2016 WILEY-VCH Verlag GmbH & Co. KGaA, Weinheim

10.1002/zaac.201605072

MOFs as "Solid Solvents" for Spiropyrans

Heidi Schwartz[a] and Uwe Ruschewitz*[a]

Keywords: metal-organic frameworks (MOFs), optical data storage devices, photochromism, spiropyran

In solution spiropyrans show photoswitching properties, which are typically hindered in the crystalline materials. With respect to possible applications as photoswitches in optical data storage devices we have started to embed spiropyrans in metal-organic frameworks (MOFs). It has already been shown for several azobenzenes that after the embedment in MOFs the switching properties of these azobenzenes are maintained or even improved.[1] In our initial experiments different (colorless) MOFs were chosen as host materials because of their fitting pore sizes and well-defined crystalline structures; 1′,3′,3′-trimethyl-6-nitrospiro[1(2H)-benzopyrane-2,2′-indoline] (**SP-1**) was used as the photochromic guest. Accordingly different guest@MOF systems were synthesized with MIL-68(In), MIL-68(Ga), MIL-53(Al), MOF-5 and HKUST-1 as host matrices.

In solution spiropyrans show, depending on the polarity of the solvent, colors from pink (polar solvent) to blue (non-polar solvent) after irradiation with UV light.[2] When embedded in MOFs, we found that the spiropyrans show a similar behavior so that the MOFs might be considered as "solid solvents". Photoswitching is reversible by irradiation with daylight or upon heating.

But for possible applications it is a severe drawback of many MOFs that their chemical and thermal stability is limited. Therefore we have recently started to use porous interpenetrated zirconium–organic frameworks (PIZOFs)[3] as a new class of host materials with high thermal and chemical stability. In cooperation with the *Godt* (Bielefeld) and the *Behrens* (Hannover) groups, our first investigations concentrated on PIZOF-2 as an exemplary model system for the whole series. PIZOF-2 was loaded with **SP-1** and successful embedment was proven by XRPD. Remarkably, after loading the deep-colored merocyanine isomer **MC-1** is already formed inside the MOF's pores without UV irradiation.

[1] D. Hermann, H. Emerich, R. Lepski, D.Schaniel, U. Ruschewitz, *Inorg. Chem.* **2013**, *52*, 2744–2749.
[2] S. Scarmagnani, PhD thesis,*University of Dublin*, **2010**.
[3] A. Schaate, P. Roy, R. T. Preuße, S. J. Lohmeyer, A. Godt, P. Behrens, *Chem. Eur. J.* **2011**, *17*, 9320–9325.

* Prof. Dr. U. Ruschewitz
E-Mail: uwe.ruschewitz@uni-koeln.de
[a] Institute of Inorganic Chemistry
University of Cologne
Greinstraße 6
50939 Köln, Germany

10.1002/zaac.201605073

A New Superconducting Beryllium Platinide

Alfred Amon,*[a] Lev G. Akselrud,[b] Matej Bobnar,[a] Maxim Avdeev,[c] Roman Gumeniuk,[d] Andreas Leithe-Jasper,[a] and Juri Grin[a]

Keywords: (Beryllium, Platinum, Complex metallic alloy, Superconductor)

Beryllium displays a manifold structural chemistry in its intermetallic compounds[1]. Electron deficiency and a high degree of covalency in beryllium-rich compounds yield interesting structural motifs where radii differences can lead to large coordination spheres.

We report on a new beryllium-rich compound in the Pt-Be system, which was indexed from X-ray powder diffractometry as a face-centered cubic cell with a=15.8832(2) Å. The strong contrast in scattering power between platinum and beryllium and the large number of atoms per unit cell posed a challenge during structure solution. The unfavorable synthesis conditions prohibited the growth of single crystals, therefore the structure was solved using a combination of synchrotron and neutron powder diffraction. The contrast variation of scattering cross sections between Pt and Be was advantageously exploited to refine the crystal structure in the space group type $F\bar{4}3m$.

The structure can be described in terms of several clusters, composed of concentrical polyhedral shells, which show different ordering of Pt and Be atoms.

It constitutes a new member in the class of large unit cell complex metallic alloys and can be seen as a superstructure of the known γ-brass phase, as it was also described in the Cu-Sn system[2,3].

Furthermore we observed a transition into a superconducting state.

[1] G.V. Samsonov, *Uspekhi Khimii* **1966**, *35*, 779–882.
[2] A. Westgren, G. Phragmen, *Z. Anorg. Allg. Chem.* **1928**, *175*, 80–89.
[3] L. Arnberg, A. Jonsson, S. Westman, *Acta Chem. Scand.* **1976**, *A30*, 187–192.

* Alfred Amon
E-Mail: alfred.amon@cpfs.mpg.de
[a] Max-Planck Institut für Chemische Physik fester Stoffe, Nöthnitzer Str. 40, 01187 Dresden, Germany
[b] Department of Inorganic Chemistry, Ivan Franko National University of Lviv, 6 Kyryla i Mephodiya Street, Lviv 79005, Ukraine
[c] Bragg Institute, Australian Nuclear Science and Technology Organisation, Private Mail Bag 1, Menai, NSW 2234, Australia
[d] Tech Univ Bergakad Freiberg, Inst Expt Phys, Leipziger Str 23, D-09596 Freiberg, Germany

 © 2016 WILEY-VCH Verlag GmbH & Co. KGaA, Weinheim

10.1002/zaac.201605074

Three New Anhydrous Acetylenedicarboxylates

Verena K. Gramm[a] and Uwe Ruschewitz*[a]

Keywords: coordination polymers, acetylenedicarboxylates, synchrotron powder diffraction data

From high-resolution synchrotron powder diffraction data we were able to solve and refine the crystal structures of two new anhydrous alkali metal acetylenedicarboxylates, namely Na_2ADC and Cs_2ADC. Anhydrous coordination polymers with acetylenedicarboxylate as bridging ligand have only been known for alkaline earth metals[1] as well as thallium[2] and lead[3]. But for alkali metals no such compounds have been published up to now.

Na_2ADC crystallizes in the monoclinic space group $P2_1/a$ (no. 14, Z = 4), whereas Cs_2ADC crystallizes in space group $C2/c$ (no. 15, Z = 8). The crystal structures are shown in Figure 1. Both compounds were obtained by dehydration of their respective hydrates, $Na_2ADC{\cdot}4H_2O$[4] and $Cs_2ADC{\cdot}H_2O$[5].

As SrADC shows negative thermal expansion,[1a)] we also investigated the thermal expansion of Na_2ADC and Cs_2ADC via temperature-dependent powder diffraction. Due to the similar ionic radii of Sr^{2+} and Eu^{2+} we have aimed at synthesizing EuADC as well. Starting from elemental europium in liquid ammonia or from $EuBr_2$ a crystalline powder was obtained revealing that EuADC crystallizes isostructurally to SrADC ($I4_1/amd$, no. 141, Z = 4).

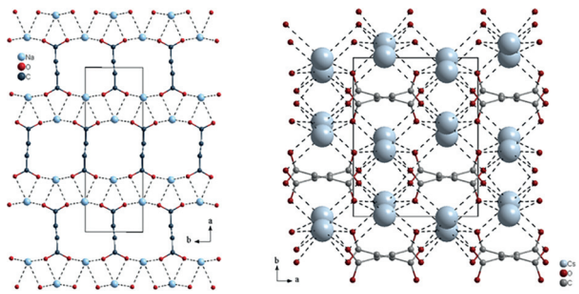

Figure 1. Packing diagrams of Na_2ADC (left) and Cs_2ADC (right) in a view along [001].

[1] a) F. Hohn, I. Pantenburg, U. Ruschewitz, *Chem. Eur. J.* **2002**, *8*, 4536–4541; b) I. Stein, U. Ruschewitz, *Z. Anorg. Allg. Chem.* **2010**, *636*, 400–404.
[2] R. Ahlers, U. Ruschewitz, *Solid State Sci.* **2009**, *11*, 1058–1064.
[3] A. Schuy, I. Stein, U. Ruschewitz, *Z. Anorg. Allg. Chem.* **2010**, *636*, 1026–1031.
[4] H. Billetter, I. Pantenburg, U. Ruschewitz, *Z. Naturforsch.* **2004**, *59b*, 903–909.
[5] I. Stein, U. Ruschewitz, unpublished results.

* Prof. Dr. Uwe Ruschewitz
E-Mail: uwe.ruschewitz@uni-koeln.de
[a] Institute of Inorganic Chemistry
University of Cologne
Greinstr. 6
50939 Cologne, Germany

10.1002/zaac.201605075

On the Way to New Ternary Alkali Metal Transition Metal Acetylides

Melanie Werker[a] and Uwe Ruschewitz*[a]

Keywords: acetylide, alkali metal, cadmium, synchrotron powder diffraction

Many ternary alkali metal transition metal acetylides have been reported for d^{10} configured metals like Pd(0), Pt(0), Cu^+, Ag^+ and Au^+.[1] In all of them a linear coordination of the d^{10} metal by end-on bound acetylide anions is found. Switching to Cd^{2+} and Zn^{2+} as transition metals ions a tetrahedral coordination sphere is expected and the formation of 3D networks is conceivable.

One approach for the synthesis of such ternary alkali metal zinc/cadmium acetylides is to use alkali metal tetraethinylozincates and -cadmates[2] as precursors according to:

(1) $A_2M(C_2H)_4 \rightarrow A_2M(C_2)_2 + 2\,C_2H_2$ (A = Na-Cs, M = Zn, Cd).

A similar route was used for the synthesis of some of the ternary copper, silver and gold acetylides mentioned above. Upon heating $Cs_2Cd(C_2H)_4$[2] at 200 °C in an argon atmosphere $Cs_2Cd(C_2H)_2(C_2)$ was obtained, which can be understood as an intermediate of the proposed synthetic route in eq. (1). The crystal structure of $Cs_2Cd(C_2H)_2(C_2)$ was solved and refined from synchrotron powder diffraction data. It crystallizes in the orthorhombic space group $Cmcm$ (no. 63, $Z = 4$). Two of the four C_2H^- anions are condensed to C_2 dumbbells, which connect the tetrahedra around Cd^{2+} to chains along [100] (Figure 1).

So by heating $Cs_2Cd(C_2H)_2(C_2)$ at temperatures above 200 °C the proposed acetylide $Cs_2Cd(C_2)_2$ according to eq. (1) seems to be achievable. Furthermore, investigations on other alkali metal tetraethinylozincates and -cadmates are planned.

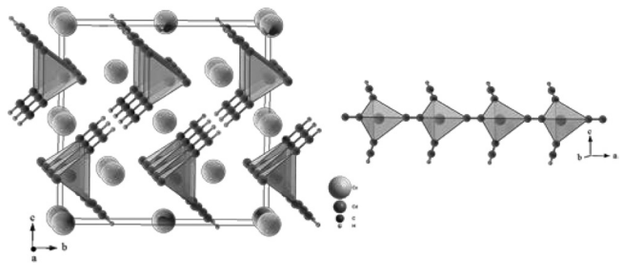

Figure 1. Crystal structure of $Cs_2Cd(C_2H)_2(C_2)$ (left) and chains of connected tetrahedra along the *a* axis (right).

[1] Reviewed in: U. Ruschewitz, *Z. Anorg. Allg. Chem.* **2006**, *632*, 705–719.
[2] U. Cremer, U. Ruschewitz, *Z. Anorg. Allg. Chem.* **2004,** *630,* 337–343.

* Prof. Dr. Uwe Ruschewitz
E-Mail: uwe.ruschewitz@uni-koeln.de
[a] Institute of Inorganic Chemistry
University of Cologne
Greinstr. 6
50939 Cologne, Germany

 © 2016 WILEY-VCH Verlag GmbH & Co. KGaA, Weinheim

10.1002/zaac.201605076

Synthesis and Characterization of Barium Thiosulfate Nanoparticles

Maia Burgués Dérghon[a] and Claus Feldmann*[a]

Keywords: microemulsion, barium thiosulfate, nanoparticles

BaS_2O_3 nanoparticles are prepared for the first time using an inverse microemulsion method. The reaction takes place in the polar micelle phase of a water-in-oil microemulsion, at room temperature. A micellar system is established with an aqueous solution of $Na_2S_2O_3x5H_2O$ as the polar phase and n-dodecane, n-hexanol and cetyltrimethylammonium bromide (CTAB) as the non-polar phase, surfactant and co-surfactant, respectively. An equimolar amount of $BaNO_3$ in water is added to this system under vigorous stirring. The water-to-surfactant molar ratio (ω) is 40. Based on Dynamic Light Scattering (DLS) and Scanning Transmission Electron Microscopy (STEM) analysis, the as-prepared nanoparticles exhibit an average diameter of 17 nm. The composition and phase purity of this nanomaterial is validated with X-ray Diffraction (XRD), Fourier Transform Infrared Spectroscopy (FT-IR), Energy Dispersive X-ray Spectroscopy (EDX) and Thermogravimetric Analysis (TGA). The importance of these nanoparticles lies in their reductant properties and their potential application in the synthesis of metal, metal oxide or metal sulfide nanostructures[1–3]. Different test reactions are used to demonstrate the reactivity of this nanoscale reducing agent.

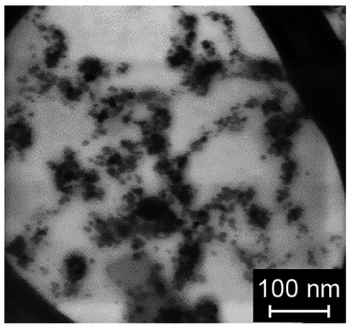

Figure 1. STEM image of BaS_2O_3 nanoparticles.

[1] D. M. H. Buchold, C. Feldmann, *Nano Lett.* **2007**, *7*, 3489–3492.
[2] P. Leidinger, R. Popescu, D. Gerthsen, C. Feldmann, *Nanoscale* **2011**, *3*, 2544–2551.
[3] F. Gyger, A. Sackmann, M. Hübner, P. Bockstaller, D. Gerthsen, H. Lichtenberg, J.-D. Grunwaldt, N. Barsan, U. Weimar, C. Feldmann, *Part. Part. Syst. Charact.* **2014**, *31*, 591–596.

* Prof. Dr. C. Feldmann
E-Mail: claus.feldmann@kit.edu
[a] Karlsruhe Institute of Technology
Institute of Inorganic Chemistry, Engesserstraße 15
76131 Karlsruhe, Germany

10.1002/zaac.201605077

Synthesis and Characterization of the Lead Borate $Pb_6B_{12}O_{21}(OH)_6$

Sandra Schönegger[a] and Hubert Huppertz*[a]

Keywords: hydrothermal synthesis, borate, lead borate, single-crystal structure determination

A lead borate with the composition $Pb_6B_{12}O_{21}(OH)_6$ was synthesized through a hydrothermal synthesis, using lead metaborate in combination with sodium nitrate and potassium nitrate. The compound $Pb_6B_{12}O_{21}(OH)_6$ has been characterized by single-crystal X-ray diffraction and FT-IR spectroscopy.
The compound $Pb_6B_{12}O_{21}(OH)_6$ crystallizes in the trigonal, non- centrosymmetric space group $P3_2$ (no. 145) with the lattice parameters $a = 1176.0(4)$, $c = 1333.0(4)$ pm, and $V = 0.1596(2)$ nm^3. The structure is built up from trigonal planar BO_3 and tetrahedral BO_4 groups forming complex chains. The Pb^{2+} cations are located between neighbouring polyborate chains. The fundamental building block consist of Dreierringe[1] build up from three corner sharing BO_4 tetrahedra and one additional corner sharing BO_3 group connected to this ring. Two corner sharing tetrahedra of two different Dreierringe are also connected to the latter BO_3 group forming an additional Dreierring. A three-fold screw axis is the central axis of each helical chain.
Based on the results of the compound $Pb_6B_{12}O_{21}(OH)_6$, it was possible to correct the structure and composition of the formerly published compound $Pb_6B_{11}O_{18}(OH)_9$.[2]

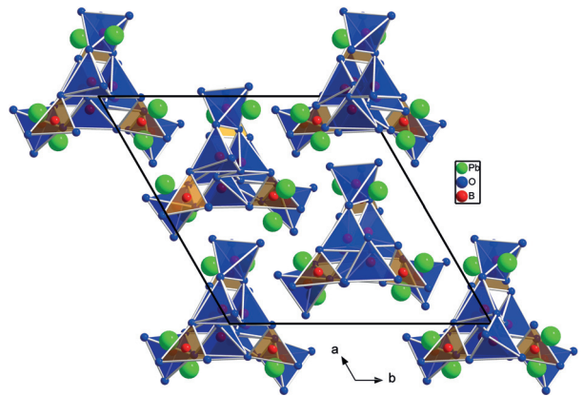

Figure 1.

[1] F. Liebau, *Structural Chemistry of Silicates*, Springer-Verlag, Berlin, **1985**.
[2] Z.-T. Yu, Z. Shi, Y.-S. Jiang, H.-M. Yuan, J.-S. Chen, *Chem. Mater.* **2002**, *14*, 1314–1318.

* Univ.-Prof. Dr. H. Huppertz
E-Mail: Hubert.Huppertz@uibk.ac.at
[a] Institute of General, Inorganic, and Theoretical Chemistry,
University of Innsbruck
Innrain 80-82
A-6020 Innsbruck, Austria

 © 2016 WILEY-VCH Verlag GmbH & Co. KGaA, Weinheim

10.1002/zaac.201605078

Chalcogenide-Based Thermoelectric Materials – Microstructure and Thermoelectric Performance

Anna-Lena Hansen,*[a] and Wolfgang Bensch[a]

Keywords: Thermoelectrics, Layered Materials, Chalcogenides,

A challenging topic of the 21st century is to find renewable and sustainable sources of energy. We need effective ways to convert waste energy back into usable energy in order to use it more efficiently. Common thermoelectric devices are based on toxic and rare elements like Pb, Te or Bi. The very low abundance of elements like Te (0.005 ppm) or Bi (0.05 ppm) in the earth's crust can be regarded as one reason why thermoelectric generators are expensive and only used in niche applications[1]. Our aim is to find new efficient materials following 'guidelines' for thermoelectrics like abundance, availability, toxicity and sustainability. Within the last decade, so-called hierarchical structures attracted more and more attention, representing the interaction of physical phenomena, like *e.g.* phonon scattering on different length-scales (atomic, nano-, micro- and macro-scale) leading to dramatically enhanced performances[2]. Chromium chalcogenides, $CuCrX_2$ (X = S, Se) in particular, have recently attracted attention as promising sustainable and inexpensive thermoelectric materials[3,4]. Our aim is to understand the complex interplay of the microstructure revealed by (*in situ*) X-ray diffraction and their thermoelectric performance. Thermoelectric devices work at elevated temperatures. Consequently, it is crucial to perform temperature dependent *in situ* experiments to track the microstructural evolution. We already demonstrated for telluride based materials that *e.g.* the presence of metastable precipitates massively alters the efficiency of thermoelectric devices[5]. Although very important for developing efficient thermoelectric devices, such systematic investigations are still scarce in scientific literature.

[1] R. Amatya, R. J. Ram, *J. Electron. Mater.*,**2011**, *41*, 1011.
[2] M. G. Kanatzidis, *MRS Bull.*, **2015**, *40*, 687.
[3] S. Bhattacharya, R. Basu, R. Bhatt, S. Pitale, A. Singh, D. K. Aswal, S. K. Gupta, M. Navaneethan, Y. Hayakawa, *J. Mater. Chem. A*, **2013**, *1*, 11289.
[4] G. C. Tewari, T. S. Tripathi, A. K. Rastogi, *J. Electron. Mater.*, **2010**, *39*, 1133.
[5] J. Koenig, M. Winkler, T. Dankwort, A.-L. Hansen, H.-F. Pernau, V. Duppel, M. Jaegle, K. Bartholomé, L. Kienle, W. Bensch, *Dalton Trans*, **2015**, *44*, 2835.

* Anna-Lena Hansen
E-Mail: alhansen@ac.uni-kiel.de
[a] Institut für Anorganische Chemie
Christian-Albrechts-Universität
24118 Kiel, Germany

10.1002/zaac.201605079

Synthesis and Self-Assembly of Cobalt and Nickel Nanoparticles

Sebastian Haumann[a] and Richard Weihrich*[a]

Keywords: Cobalt, Nickel, Nanoparticles, Self-assembly

Cobalt and nickel nanoparticles were synthesized with different reducing agents in a polyol medium and observation of magnetic self-assembly between nearly spherical nanoparticles[1].
In the last years metal nanoparticles attracted interest particularly due to their magnetic properties and use in different applications like data storage, DNA sequencing, drug delivery, biomedical sensors, microelectronics, radiation therapy and catalysis[2,3]. Therein, the synthesis of cobalt and nickel nanoparticles seems very promising from pioneering work[4]. But besides these promising utilizations in everyday life, there are still problems in the production of well-shaped nanoparticles with a certain size and a narrow size distribution. That is why the development of the synthetic routes has to improve constantly with a look at the physical and chemical properties of the nanoparticles.
To understand and improve the processes in the synthesis of cobalt and nickel nanoparticles and the resulting properties, nanometer-scale particles were produced in a typical polyol process. Therefore various solvents, different reducing agents and reaction conditions were investigated with respect to the size shape, and self-organization of the particles. The size and shape of the nanoparticles were determined with the Scherrer-equation out of the powder patterns and scanning electron microscope (SEM) measurements.

[1] S. Haumann, Master Thesis ,Universität Regensburg, **2014**.
[2] J. Park, E. Kang, S. U. Son, H. M. Park, M. K. Lee, J. Kim, K. W. Kim, H.-J. Noh, J.-H. Park, C. J. Bae, J.-G. Park, T. Hyeon, *Adv. Mater.* **2005**, *17*, 429.
[3] O. Santini, A. R. de Moraes, D. H. Mosca, P. E. N. de Souza, A. J. A. de Oliveira, R. Marangoni, F. Wypych, *J. Colloid Interface Sci.* **2005**, *289*, 63.
[4] C. B. Murray, S. Sun, H. Doyle, T. A. Betley, *Mater. Res. Bull.* **2001**, 985.

* Prof. Dr. R. Weihrich
E-Mail: Richard.weihrich@ur.de
[a] University of Augsburg, Institute of Materials Resource Management, Germany

 © 2016 WILEY-VCH Verlag GmbH & Co. KGaA, Weinheim

10.1002/zaac.201605080

Effect of Cobalt Substitution in the Ferromagnetic Superconductor $[(Li_{0.8}Fe_{0.2})OH]FeSe$

Ursula Pachmayr,[a] Sirko Kamusella,[b] Hans-Henning Klauss,[b] and Dirk Johrendt*[a]

Keywords: superconductivity, ferromagnetism, iron selenides

The ferromagnetic superconductor $[(Li_{0.8}Fe_{0.2})OH]FeSe$ ($T_c \approx$ 43 K, $T_C \approx 10$ K) provides a rare opportunity to further investigate the unusual coexistence of superconductivity and ferromagnetism.[1] A recent density functional study predicts a positive effect on superconductivity for a substitution of iron by cobalt in the hydroxide layer, i. e. the hypothetical $[(Li_{0.8}Co_{0.2})OH]FeSe$.[2] A sample with this nominal composition was prepared by hydrothermal synthesis. EDX measurements confirmed 0.2–0.3 cobalt per formula unit as expected, but no superconductivity emerged. ^{57}Fe-Mössbauer spectroscopy identifies two main iron sites, one in the selenide (blue) and one in the hydroxide (magenta) layer (Fig. 1, the anisotropy of the spectrum results from texture). A third doublet (green) indicates that the iron environment in the FeSe layer is slightly disturbed. Thus cobalt has been incorporated in the hydroxide and in the FeSe-layers. The latter probably suppresses superconductivity as known from $Fe_{1-x}Co_xSe$.[3]

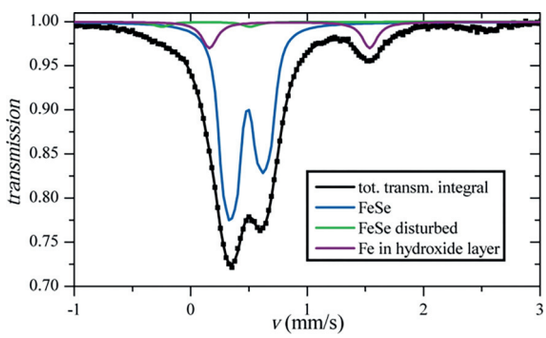

Figure 1. ^{57}Fe-Mössbauer spectrum at 20 K detects two main iron sites and indicates that the FeSe layer is disturbed by cobalt.

[1] U. Pachmayr, F. Nitsche, H. Luetkens, S. Kamusella, F. Brückner, R. Sarkar, H.-H. Klauss, D. Johrendt, *Angew.Chem. Int. Ed.* **2015**, *54*, 293.
[2] W. Chen, C. Zeng, E. Kaxiras, Z. Zhang, *Phys. Rev. B* **2016**, *93*, 064517.
[3] Y. Mizuguchi, F. Tomioka, S. Tsuda, T. Yamaguchi, Y. Takano, *J. Phys. Soc. Jpn.* **2009**, *78*, 074712.

* Prof. Dr. D. Johrendt
E-Mail: johrendt@lmu.de
[a] Department Chemie, Ludwig-Maximilians-Universität München, Butenandtstrasse 5-13 (Haus D)
81377 München, Germany
[b] Institut für Festkörperphysik, Technische Universität Dresden
Helmholtzstrasse 10
01069 Dresden, Germany

10.1002/zaac.201605081

Re-Emergence of Superconductivity in $La_{1-x}RE_xFeAsO_{0.8}F_{0.2}$ (RE= Pr–Sm)

Simon Peschke,[a] Sebastian Vogel,[a] and Dirk Johrendt*[a]

Keywords: iron-based superconductors, rare-earth metals

The discovery of superconductivity in iron arsenides with the tetragonal ZrCuSiAs-type structure such as REFeAsO$_{1-x}$F$_x$ (RE = rare-earth metal) and critical temperatures (T_c) up to 56 K has revived intense search for new superconducting materials.[1] Recently we reported a solid state metathesis reaction which is efficient to prepare polycrystalline LaFeAsO$_{1-x}$F$_x$ ($0 \leq x \leq 0.15$).[2] Using this method, we found superconducting samples with fluoride contents only below 20 %. LaFeAsO$_{0.80}$F$_{0.20}$ is no longer superconducting because of over-doping with electrons. We then used this approach to realize the systematic substitution of lanthanum in LaFeAsO$_{0.80}$F$_{0.20}$ by smaller rare-earth metals (RE = Pr, Nd, Sm). Remarkably, superconductivity re-emerges in the solid solution $La_{1-x}RE_xFeAsO_{0.80}F_{0.20}$ at $x \geq 10$ % in spite of constant electron doping. As shown in Fig. 1, the critical temperature increases power-law-like as soon as the unit cell volume decreases below ≈ 140 Å^3, and reaches 56 K at ≈ 130 Å^3. From this we infer that T_c cannot be controlled alone by the charge carrier density and suggest that structural parameters may play a decisive role.[3]

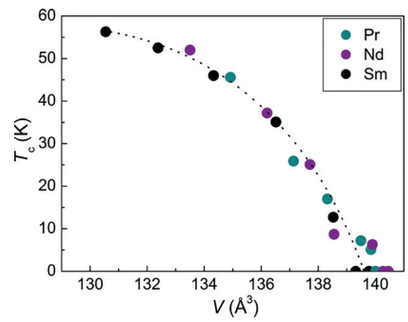

Figure 1. Critical temperature T_c of $La_{1-x}RE_xFeAsO_{0.80}F_{0.20}$ (RE = Pr, Nd, Sm; $0 \leq x \leq 1$) against the unit cell volume.

[1] Y. Kamihara, T. Watanabe, M. Hirano, H. Hosono, *J. Am. Chem. Soc.* **2008**, *130*, 3296.
[2] R. Frankovsky, A. Marchuk, R. Pobel, D. Johrendt, *Solid State Chem.* **2012**, *152*, 632.
[3] F. Nitsche, A. Jesche, E. Hieckmann, Th. Doert, M. Ruck, *Phys. Rev. B.* **2010**, *82*, 134514.

* Prof. Dr. D. Johrendt
E-Mail: johrendt@lmu.de
[a] Department Chemie
Ludwig-Maximilians-Universität München
Butenandtstr. 5–13 (Haus D)
81377 München, Germany

 © 2016 WILEY-VCH Verlag GmbH & Co. KGaA, Weinheim

10.1002/zaac.201605082

$Fe_{2.3}GeTe$ – A New Layered Ferromagnetic Telluride

Juliane Stahl,[a] Lukas Neudert,[a] Oliver Oeckler,[b] and Dirk Johrendt*[a]

Keywords: iron germanium telluride; crystal structure; ferromagnetism; transmission electron microscopy

$Fe_{2.3}GeTe$ was obtained by solid state synthesis and the crystal structure was determined by single crystal X-ray diffraction. The telluride exhibits a new structure type (*Pm*1, a = 398.91(6) pm, c = 1076.6(3) pm) composed of layers stacked along c. FeGe- hexagons sandwiched by additional iron atoms are separated by Te double layers building a van der Waals gap. Similar structural motifs are found in Fe_2Ge and Fe_3GeTe_2.[1,2]
The Fe3 site in the FeGe-hexagons has Fe-vacancies (*sof*(Fe3) = 0.79), while additional electron density between the Te layers indicates iron in the van der Waals gap (*sof*(Fe4) = 0.13). The total iron content of the structure is in accordance with EDX measurements. Diffuse intensity along [001]* was observed with electron diffraction indicating a non-periodic stacking of the $Fe_{2.3}GeTe$ layers. SAED patterns correspond to reciprocal lattice sections based on X-ray data. Magnetic susceptibility measurements indicate ferromagnetic ordering below T_C = 239 K. The Curie-Weiss fit gives an effective moment of $\mu_{eff} = 4.68\ \mu_B$ per iron atom and the ferromagnetic Weiss temperature θ = 236 K. Isothermal magnetization at 1.8 K shows a saturation moment $\mu_{sat} = 1.37\ \mu_B$ at 5 T. The magnetic properties are similar to those of Fe_3GeTe_2.[2]

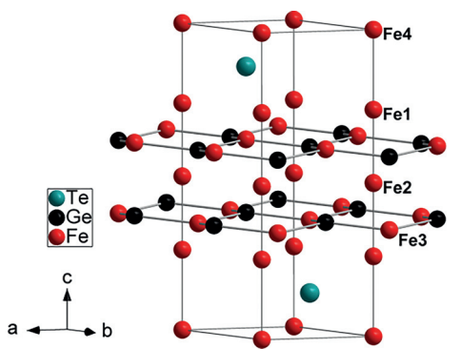

Figure 1.

[1] P. J. Schurer, N. J. G. Hall, A. H. Morrish, *Phys. Rev. B* **1978**, *18*, 4860–4874.
[2] H.-J. Deiseroth, K. Aleksandrov, C. Reiner, L. Kienle, R. K. Kremer, *Eur. J. Inorg. Chem.* **2006**, *8*, 1561–1567.

* Prof. Dr. D. Johrendt
E-Mail: johrendt@lmu.de
[a] Department Chemie, Ludwig-Maximilians-Universität München, Butenandtstrasse 5-13, D-81377 München, Germany
[b] Fakultät für Chemie und Mineralogie, Universität Leipzig, Scharnhorststrasse 20, D-04275 Leipzig, Germany

10.1002/zaac.201605083

Thermodynamic Analysis of Crystal Growth of Zinc Oxide

Robert Heinemann[a] and Peer Schmidt*[a]

Keywords: zinc oxide (ZnO), crystal growth, chemical vapor transport

Chemical vapor transport (CVT[1]) is a suitable method for production of single-crystals of high purity. In order to find proper strategies for CVT various tools of thermodynamic calculations and analysis of solid-gas equilibria are available. Those applications are demonstrated for vapor transport of zinc oxide under addition of phosphorous and water.
The reduction of ZnO and H_2O by P_4(g) likewise a thermite reaction can be predicted by electromotive series of oxides [2] and proofed by application of High-temperature Gas-balance (HTGB[3]). Composition of condensed phases within the system Zn/P/O during vapor transport is shown by calculation and experimental results. Transport modeling using TRAGMIN[4] give access to the existing solid-gas equilibria and relevant transport conditions. Thus, CVT of ZnO via H_2(g) under addition of H_2O and P is found and growth of ZnO single-crystals up to 1,8 mm in size can be achieved (Figure 1).

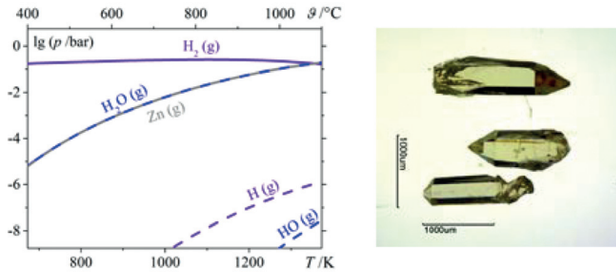

Figure 1. left: calculated solid-gas-equilibria for Zn/P/O/H, right: ZnO single-crystals grown by CVT

[1] M. Binnewies, R. Glaum, M. Schmidt, P. Schmidt, *Chemical Vapor Transport Reactions*, De Gruyter, Berlin, **2012**, ISBN 978-3-11-025465-5.
[2] P. Schmidt, Habilitation TU Dresden **2007**, http://nbn-resolving.de/urn:nbn:de:bsz:14-ds-1200397971615-40549.
[3] P. Schmidt, M. Schöneich, M. Bawohl, T. Nilges, R. Weihrich, *J. Thermal Anal. Calorim.* **2012**, *110*, 1511.
[4] G. Krabbes, W. Bieger, K.-H. Sommer, T. Söhnel, U. Steiner GMIN Version 5.0b, package TRAGMIN for calculations of thermodynamic equilibrium, Dresden, **2008**.

* Prof. Dr. P. Schmidt
E-Mail: Peer.Schmidt@b-tu.de
[a] BTU Cottbus – Senftenberg, Großenhainer Str. 57. 01968 Senftenberg, Germany

 © 2016 WILEY-VCH Verlag GmbH & Co. KGaA, Weinheim

10.1002/zaac.201605084

Novel Inorganic Red Pigments Based on Tetragonal β-Bi_2O_3

Georg Gramm,*[a] Gerda Fuhrmann,[a] Herwig Schottenberger,[a] and Hubert Huppertz[a]

Keywords: Bismuth oxide, β-phase stabilization, red pigments, color coordinates

Novel red inorganic pigments based on the tetragonal β-phase of Bi_2O_3 have been investigated as possible ecological alternatives to currently used materials, which usually contain hazardous elements, such as Cd, Cr or Pb. There are few reports dealing with the coloristic properties of Bi_2O_3 based compounds, but almost all with focus on the stabilized high-temperature δ-modification.[1–3] These materials exhibit promising high red chromaticity values (a* ≈ 30), but due to their concomitant high yellow hues (b* > 35), they are rather orange.
In this work, the synthesis by solid-state reaction and stabilization of the metastable tetragonal β-phase of Bi_2O_3 at room temperature through incorporation of diverse metal cations into the lattice of Bi_2O_3 has been studied. The produced materials were characterized by X-ray powder diffraction and UV-Vis spectroscopy. Depending on the composition, the color of the ß-phases ranged from yellow to orange, with $(Bi_{0.975}Zr_{0.025})_2O_{3\text{-}\delta}$ showing the most vivid orange coloration. Subsequently, the effect of Fe^{3+} doping on the structural and coloristic properties was investigated. The most intense red was achieved with $(Bi_{0.975}Zr_{0.025})_{0.8}Fe_{0.2}]_2O_{3\text{-}\delta}$ having the color coordinates of a* = 31.1 and b* = 25.8. As indicated also by the resulting a*/b*-ratio of 1.2, the new pigments clearly surpass the coloristic performance of the δ-phase based counterparts. Further, they have excellent heat and chemical stability and are suitable even in high-temperature processing.

[1] Wendusu, T. Masui, N. Imanaka, *Chem. Lett.* **2012**, *41,* 1616–1618.
[2] Wendusu, T. Masui, N. Imanaka, *J. Asian Ceram. Soc.* **2014,** *2*, 195–198.
[3] P. Šulková, L. Stránská, E. Proklešková, *J. Therm. Anal. Calorim.* **2013,** *113,* 1203–1208.

* Hubert Huppertz
E-Mail: Hubert.Huppertz@uibk.ac.at
[a] Institut für Allgemeine, Anorganische und Theoretische Chemie, Leopold-Franzens-Universität Innsbruck, Innrain 80–82, 6020 Innsbruck, Austria

10.1002/zaac.201605085

Long-Term Electrochemical Characterization of Thin-Film SOFC Cathodes of $La_{0.6}Sr_{0.4}CoO_{3-\delta}$

Martin Perz,*[a] Edith Bucher,[a] and Werner Sitte[a]

Keywords: solid oxide fuel cell, cathode, thin films, electrical conductivity, electrochemical impedance spectroscopy

The electrochemical characterization of 100 nm to 1 μm thin films of mixed ionic-electronic conducting perovskites as possible cathodes in solid oxide fuel cells has been a topic of many studies[1]. Even though these results are quite promising, long-term degradation effects have hardly been investigated.
In the present work, symmetric cells with thin film electrodes of $La_{0.6}Sr_{0.4}CoO_{3-\delta}$ on $Gd_{0.1}Ce_{0.9}O_{2-\delta}$ electrolytes were fabricated by a sol-gel spin coating deposition technique[2]. The area specific resistance (ASR) of the electrode was characterized by electrochemical impedance spectroscopy (EIS) in ambient air at temperatures up to 700°C. The long-term evolution of the ASR over time was determined in long-term experiments up to 1000h at 700°C.
In a short timeframe the thin film cathodes showed an ASR of 0.1 Ωcm^2 at 700°C, which was significantly lower than the ASR of conventional porous μm-sized cathodes of $La_{0.6}Sr_{0.4}Co_{0.2}Fe_{0.8}O_{3-\delta}$ measured in a previous study[3]. However, after 1000h the ASR was about 7 Ωcm^2, so the long-term degradation of thin film electrodes was significantly faster than of the conventional cathodes shown in[3].
Pre- and post-test analyses by scanning electron microscopy (SEM), transmission electron microscopy (TEM) and X-ray photoelectron spectroscopy (XPS) with elemental depth profiling showed that the degradation of LSC thin films is accompanied by changes in the microstructure and chemical composition.

[1] J. Hayd, *Journal of Power Sources* **2011**, *196*, 7263–7270.
[2] J. Januschewsky, Zeitschrift für Physikalische Chemie **2012**, 226, 889–899.
[3] M. Perz, *Solid State Ionics* **2016**, *288*, 22–27.

* Dipl.-Ing. M. Perz
E-Mail: martin.perz@unileoben.ac.at
[a] Montanuniversitaet Leoben
Franz Josef Strasse 18
8700 Leoben, Austria

 © 2016 WILEY-VCH Verlag GmbH & Co. KGaA, Weinheim

10.1002/zaac.201605086

Crystal Growth of Ternary Phases with Homogeneity Range: Modeling and Experiments

Martin Wels[a] and Peer Schmidt*[a]

Keywords: crystal growth; chemical vapor transport, bismuth selenide, bismuth telluride

Synthesizing crystals of ternary solid solutions M_2Q_3 (M = Bi, Q=Se, Te) with definite composition requires advanced knowledge on the phase relations in the system. By chemical vapor transport[1] the request of homogeneous crystallization can be fulfilled. The experimental scope gets supported by modeling. A phase diagram of the pseudobinary system generated with FactSage[2] (Fig. 1(1)) provides the thermodynamic parameters of the miscibility gap respectively the solid solution. Additionally, these parameters are used to optimize the processes while chemical vapor transport with iodine[3]. The optimum transport conditions of ϑ_{source} = 500 °C and ϑ_{sink} = 450 °C has been applied as for the synthesis of the binary compounds[4]. Both by modeling and experiments the congruent transport can be demonstrated, Fig. 1(2).

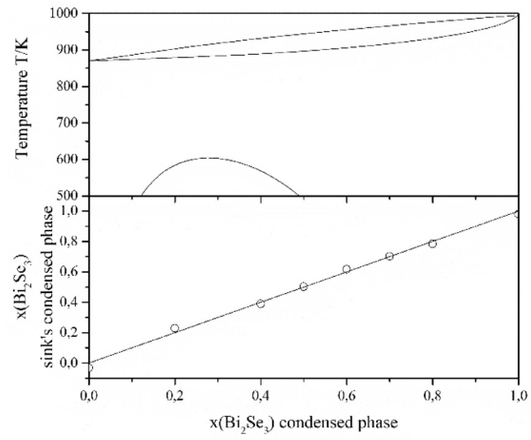

Figure 1. 1) Phase diagram of Bi_2Te_3 – Bi_2Se_3. 2) Calculated composition of sink's condensed phases compared source's condensed phases of Bi_2Q_3

[1] M. Binnewies, R. Glaum, M. Schmidt, P. Schmidt, *Chemical Vapor Transport Reactions*, De Gruyter, Berlin, **2012**, ISBN 978-3-11-025465-5.
[2] C. W. Bale, E. Bélisle, P. Chartrand, S. A. Decterov, G. Eriksson, K. Hack, I. H. Jung, Y. B. Kang, J. Melançon, A. D. Pelton, C. Robelin and S. Petersen, *FactSage Thermochemical Software and Databases – Recent Developments*, Calphad, vol. 33, pp 295–311, 2009.
[3] *GMIN Version 5.0b, package TRAGMIN for calculation of thermodynamic equilibrium*, G. Krabbes, W. Bieger, K.-H. Sommer, T. Söhnel, U. Steiner, Dresden, **2008**.
[4] M. Schöneich, M. Schmidt, P. Schmidt, *Z. Anorg. Allg. Chem.* **2010**, *636*, 1810–1816.

* Prof. Dr. P. Schmidt
E-Mail: peer.schmidt@b-tu.de
[a] BTU Cottbus-Senftenberg, 01958 Senftenberg, Germany

 © 2016 WILEY-VCH Verlag GmbH & Co. KGaA, Weinheim

10.1002/zaac.201605087

Synthesis and Structural Characterization of $Ca_{12}Ge_{17}B_8O_{58}$

Sebastian Bräuchle,*[a] Klaus Wurst,[a] and Hubert Huppertz[a]

Keywords: Solid-state reaction; Calcium borogermanate; Crystal structure; IR spectroscopy

Over the last couple of years, the interest in the class of metal borogermanates is steadily increasing. Borogermanates are known due to their interesting physical properties like nonlinear optical (NLO) properties.[1,2]

$Ca_{12}Ge_{17}B_8O_{58}$ was prepared by high-temperature solid-state synthesis at 1100 °C in a platinum crucible from calcium carbonate, boric acid, and germanium(IV) oxide. The compound crystallizes in the tetragonal crystal system in the space group *P*4 (No. 81) isotypically to $Cd_{12}Ge_{17}B_8O_{58}$[2]. The structure was refined from single-crystal X-ray diffraction data: $a = 15.053(8)$, $c = 4.723(2)$ Å, $V = 1070.2(2)$ Å^3, $R1 = 0.0151$, and $wR2 = 0.0339$ for all data. The crystal structure of $Ca_{12}Ge_{17}B_8O_{58}$ consists of one-dimensional $[Ge_4O_{12}]_n$ chains composed of GeO_4 tetrahedra and GeO_6 octahedra. The chains are interconnected into a $[Ge_4O_{10.5}]_n$ network *via* corner sharing. By additional $[Ge(B_2O_7)_4]^{28-}$ clusters, these units are connected to a three-dimensional $[Ge_{17}B_8O_{58}]^{24-}$ framework. The open structure forms three types of one-dimensional tunnels with five-, six-, and seven-membered rings (MRs) along the *c* axis, where the Ca^{2+} are located in between.

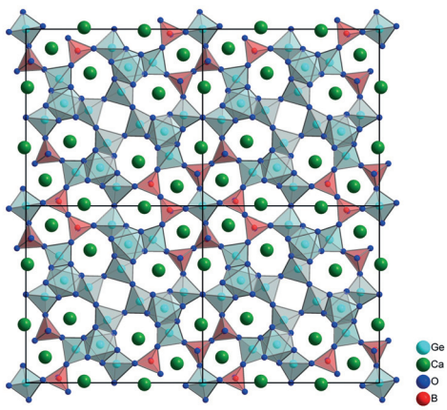

Figure 1.

[1] Y.-C. Hao, C.-L. Hu, X. Xu, F. Kong, J.-G. Mao, *Inorg. Chem.* **2013**, *52*, 13644.
[2] X. Xu, C.-L. Hu, F. Kong, J.-H. Zhang, J.-G. Mao *Inorg. Chem.* **2011**, *50*, 8861.

* Sebastian Bräuchle
E-Mail: Sebastian.Braeuchle@uibk.ac.at
[a] Institut für Allgemeine, Anorganische und Theoretische Chemie, Leopold-Franzens-Universität Innsbruck, Innrain 80/82, 6020 Innsbruck, Austria

 © 2016 WILEY-VCH Verlag GmbH & Co. KGaA, Weinheim

10.1002/zaac.201605088

Hexane-1,6-diammonium Hexane-1,6-bis(hydrogen phosphonate) – Another Salt with a Herringbone Motif Layer-Like Structure

Martin van Megen,*[a] Guido J. Reiss,[a] and Walter Frank[a]

Keywords: Alkane-*α*,*ω*-diammonium, Alkane-*α*,*ω*-bis(hydrogen phosphonate), Herringbone motif

The title compound, $[H_3N(CH_2)_6NH_3][HO_3P(CH_2)_6PO_3H]$, crystallises in the monoclinic space group $P2_1/c$ with a = 5.8824(2) Å, b = 20.2162(5) Å, c = 7.7574(2) Å, β = 98.090(3)°, V = 913.33(5) Å^3, Z = 2, R_1 = 0.0379, wR_2 = 0.0968 (1601 reflections; 103 parameters). The $–NH_3$ and $–PO_3H$ groups form two-dimensional networks in the *ac* plane *via* medium strong $N^+–H\cdots O$ and $O–H\cdots O^-$ hydrogen bonds. These networks are composed of ten- and twelve-membered rings (a third level graph set $R^3{}_3(10)$ and fourth level graph set $R^3{}_5(12)$, respectively). Along the *b* axis, these networks are connected with each other by the alkane-*α*,*ω*-diyl moieties of the anions and cations, respectively, resulting in a three-dimensional framework with a herringbone motif. This structural motif is well known for the alkane-*α*,*ω*-diamines[1,2] and alkane-*α*,*ω*-diphosphonic acids[3].

The title compound of this contribution is another example for the ability of the bis(hydrogen phosphonate) moiety to construct hybrid materials with discrete hydrophobic and hydrophilic regions[4].

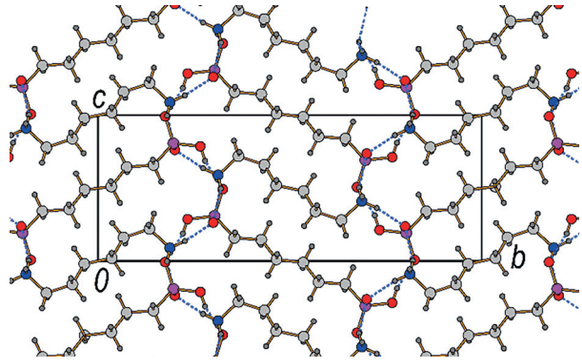

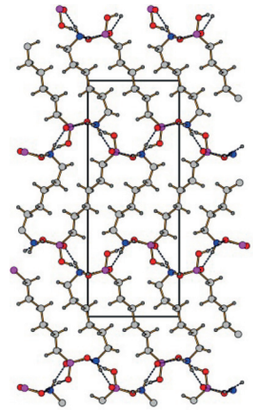

[1] G. J. Reiss, J. S. Engel, *CrystEngComm* **2002**, *4*, 155–161.
[2] V. R. Thalladi, R. Boese, H.-C. Weiss, *Angew. Chem. Int. Ed.* **2000**, *39*, 918–922.
[3] M. van Megen, W. Frank, G. J. Reiss, *Z. Kristallogr. – Cryst. Mater.* **2015**, *230*, 485–494.
[4] M. van Megen, W. Frank, G. J. Reiss, *CrystEngComm* **2016**, *18*, 3574–3584.

* Prof. Dr. M. van Megen
E-Mail: ac2@hhu.de
[a] Institut für Anorganische Chemie und Strukturchemie II
Heinrich-Heine-Universität Düsseldorf
Universitätsstraße 1
40225 Düsseldorf, Germany

 © 2016 WILEY-VCH Verlag GmbH & Co. KGaA, Weinheim

10.1002/zaac.201605089

Selective Alkane Oxidation on Catalysts $(V_{1-x}M_x)OPO_4$ (*M*: Mo, W)

Christian Schulz,[a] Subrata Chandra Roy,[b] Markus Weber,[b] Knut Wittich,[b] Robert Glaum,[b] and Frank Rosowski*[a,c]

Keywords: Selective oxidation; Metal oxides; Metal phosphates

Vanadyl pyrophosphate (VPP) is the state of the art catalyst in the selective oxidation of n-butane to maleic anhydride (MAN)[1]. Although the yield could be increased by a factor of 2-3, there was no substantial improvement in selectivity within 40 years of research. Consequently, there is a demand for alternatives to vanadyl pyrophosphate[2]. In this study, we present a new class of stable catalysts, which are active and selective in the oxidation of n-butane to maleic anhydride (Fig. 1). The solid solution $(V_{1-x}W_x)OPO_4$ with α_{II}-$VOPO_4$ structure type ($0.04 \leq x \leq 0.26$) was obtained from mixtures of β-V^VOPO_4 and W^VOPO_4 in sealed silica tubes. Synthesis is also possible by solution combustion synthesis (SCS) in air[3]. Members of the solid solution are semiconductors ($E_g \approx 1$ eV) with oxidation states $(V^{IV}{}_xV^V{}_{1-2x}W^{VI}{}_x)OPO_4$. All members of the solid solution were obtained as single phase powders. Performance data of selected catalysts can be found in Fig. 1. Solid solutions $(V_{1-x}Mo_x)OPO_4$ ($x < 0.3$) with β- and γ-$VOPO_4$ structure type can be obtained as metastable phases by SCS only. They show no activity in n-butane oxidation.

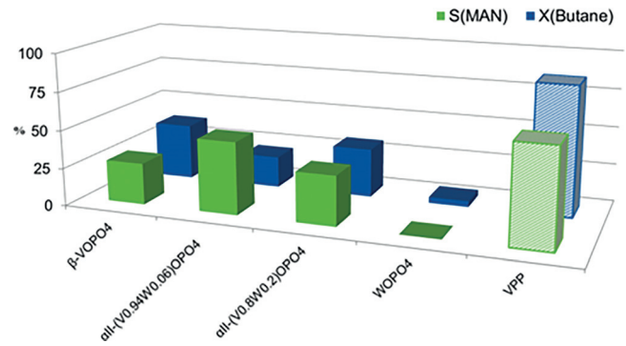

Figure 1 Activity (X) and selectivity (S) in n-butane oxidation of two members of the solid solution $(V_{1-x}W_x)OPO_4$. Results for β-$VOPO_4$, $WOPO_4$, and the technical VPP catalyst are given for comparison.

[1] R. Bergman, N. J. Princeton, N. Frisch, *U.S. Patent* 3,293,268, **1966**.
[2] A. Karpov, C.-K. Dobner, R. Glaum, S. Schunk, F. Rosowski, *Chem. Ing. Tech.* **2011**, *83*, 1.
[3] S. C. Roy, R. Glaum, D. Abdullin, O. Schiemann, N. Q. Bac, K.-H. Lii, *Z. Anorg. Allg. Chem.* **2014**, *640*, 1876.

* Dr. F. Rosowski
E-Mail: frank.rosowski@basf.com
[a] BasCat BASF UniCat JointLab, Hardenbergstr. 36
Sekr. EW K-01, 10623 Berlin, Germany
[b] Institute of Inorganic Chemistry, Gerhard-Domagk-Str. 1
53121 Bonn, Germany
[c] Process Research and Chemical Engineering – BASF SE,
Carl-Bosch-Str. 38, 67056, Ludwigshafen, Germany

 © 2016 WILEY-VCH Verlag GmbH & Co. KGaA, Weinheim

10.1002/zaac.201605090

Multinary Tungsten Phosphates with ReO_3 Structure Type: Synthesis and Catalyst Behavior

Knut Wittich,[a] Subrata Chandra Roy,[a] Christian Schulz,[b] Frank Rosowski,[b,c] and Robert Glaum*[a]

Keywords: Selective oxidation; Metal oxides

Via *solution combustion synthesis* (SCS)[1] access to a new class of multinary tungsten phosphates ($M_xW_yP_{1-x-y}O_{2.5+\delta}$) ($x + y \leq 0.5$)[2,3,4] is possible (ignition at 400 °C, subsequent heating in air at 600 °C). According to their X-ray powder diffraction pattern (Fig. 1) these metastable phases belong to the ReO_3 structure family. Upon heating $\vartheta > 800$ °C these phosphates transform into well-defined crystalline phases (e.g. $(V^{IV}_{0.25}W_{0.75}O_3)_8(PO_2)_4$ with $(WO_3)_8(PO_2)_4$ structure type[5]).

In catalyst tests for the selective oxidation of short chain hydrocarbons the vanadium containing phases with ReO_3 structure type, e. g. $(V_{0.167}W_{0.5}P_{0.333})O_{2.67+\delta}$), show selectivity and activity towards the formation of maleic anhydride (MAN) from n-butane[2].

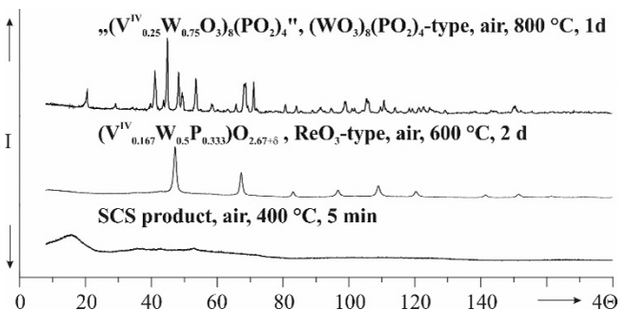

Figure 1. X-ray powder diffraction patterns of $(V_{0.167}W_{0.5}P_{0.333})O_{2.67+\delta}$ immediately after SCS and after subsequent heating at 600 and 800 °C.

[1] K. C. Patil, T. Mimani, *Mater. Phys. Mech.*, **2001**, *4*, 134.
[2] S. C. Roy, R. Glaum, F. Rosowski et al.; *European Patent Application filed*.
[3] S. C. Roy, *PhD thesis*, Univ. Bonn **2015**.
[4] K. Wittich, *part* of *planned PhD thesis*, Univ. Bonn.
[5] J. P. Giroult, M. Goreaud, P. Labbe, B. Raveau, *Acta Crystallogr., Sect. B* **1981**, *37*, 2139.

* Prof Dr. R. Glaum
E-Mail: rglaum@uni-bonn.de
[a] Institute of Inorganic Chemistry, Gerhard-Domagk-Str. 1
53121 Bonn, Germany
[b] BasCat BASF UniCat JointLab, Hardenbergstr. 36
Sekr. EW K-01, 10623 Berlin, Germany
[c] Process Research and Chemical Engineering – BASF SE
Carl-Bosch-Str. 38, 67056, Ludwigshafen, Germany

10.1002/zaac.201605091

Orthorhombic Lithium Tetrachloroaluminate and Lithium-bis(pentamethylbenzenium)-tris(tetrachloroaluminate)

Stephan W. Prömper[a] and Walter Frank*[a]

Keywords: Lithium tetrachloroaluminate; Polymorphism; Pentamethylbenzenium; Tris(tetrachloroaluminato)lithiate

An orthorhombic modification of lithium tetrachloroaluminate (**1**) is crystallized by dissolving lithium chloride and aluminium chloride in boiling *para*- or *meta*-xylene and keeping the colorless solution at room temperature. The new polymorph **1** crystallizes in the noncentrosymmetric spacegroup $Pmn2_1$ with a = 7.8150(5) Å, b = 6.4508(5) Å, c = 6.1234(4) Å, V = 308.70(4) Å^3, Z = 2, R_1 = 0.0264 and wR_2 = 0.0735 (878 reflections, 37 parameters). The chlorine atoms are slightly distorted hexagonal closest packed while the cations occupy half of the tetrahedral interstices of one kind (defect wurtz-stannite-type structure). The lithium cation site is half occupied.

Treating a yellow solution of pentamethylbenzenium tetrachloroaluminate in methylene chloride with lithium tetrachloroaluminate at −40 °C and cooling the solution to −78 °C leads to the second title compound (**2**). The substance crystallizes monoclinic ($P2_1/c$) with a = 9.7102(2) Å, b = 17.8382(5) Å, c = 21.5952(5) Å, β = 92.227(2)°, V = 3737.73(16) Å^3, Z = 4, R_1 = 0.0429 and wR_2 = 0.1159 (6578 reflections, 369 parameters) and consists of pentamethylbenzenium cations showing the expected cyclohexadienyl character referred to the C–C bond lenghts[1] and chiral, propeller-shaped moieties with tris-κCl,κCl'-tetrachloroaluminato coordinated lithium cations.

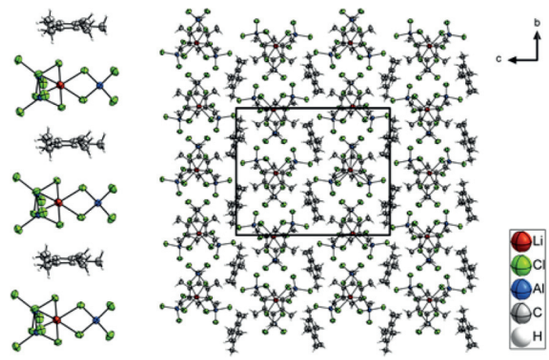

Figure 1. Chain of $C_{11}H_{17}^+$ and $[(AlCl_4)_3Li]^{2-}$ moieties along the a axis (left) and alternating layers of chains and cations (right).

[1] C. A. Reed, N. L. P. Fackler, Kee-Chan Kim, D. Stasko, D. R. Evans, *J. Am. Chem. Soc.* **1999**, *121*, 6314–6315.

* Prof. Dr. W. Frank
E-Mail: wfrank@hhu.de
[a] Institut für Anorganische Chemie und Strukturchemie II,
Heinrich-Heine-Universität, Universitätsstr. 1, 40225 Düsseldorf,
Germany

 © 2016 WILEY-VCH Verlag GmbH & Co. KGaA, Weinheim

10.1002/zaac.201605092

C-Type $LaTaO_4$ – A New Polymorph

Oliver Janka[a] and Thomas Schleid*[b]

Keywords: Lanthanum, Oxotantalates, Crystal Structure

Single crystals of a new polymorph of $LaTaO_4$, subsequently called *C*-type, have been obtained as by-product in attempts to synthesize CuLaOTe in sealed tantalum capsules. Like the *A*- and *B*-type representatives[1] also the new structure type contains no isolated $[TaO_4]^{3-}$ tetrahedra, in contrast to what is reported in common textbooks.[2] *C*-type $LaTaO_4$ crystallizes in the monoclinic crystal system with the space group $P2_1/n$ and lattice parameters of a = 539.37(4), b = 514.32(4), c = 1269.58(9) pm, β = 94.109(3)° for Z = 4. In its crystal structure, $[TaO_6]^{7-}$ octahedra form strands along [010] by condensation via *trans*-oriented edges. These corrugated strands are packed in a hexagonal closest arrangement of rods, whose cavities are filled with La^{3+} cations (Fig. 1). Within the octahedra typical Ta–O distances (d(Ta–O) = 188 – 215 pm) can be found. The La^{3+} cations are coordinated by 6+1 oxygen atoms (d(La–O) = 234 – 254 pm *plus* 294 pm) in the shape of distorted monocapped octahedra. This is in contrast to *A*- and *B*-type $LaTaO_4$, where eightfold coordination environments are found for the La^{3+} cations. When considering only the six closer contacts, the octahedra are condensed via two corners to form corrugated layers within the (001) plane. When also the seventh oxygen contact is included, the layers become connected along [001] to form a porous network.

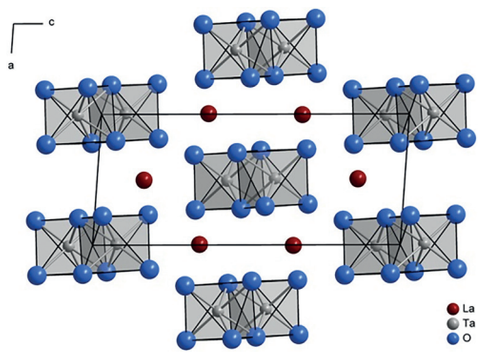

Figure 1: Extended unit cell of C-type $LaTaO_4$ along as viewed along [010]. The strands formed by *trans*-edge sharing $[TaO_6]^{7-}$ octahedra are highlighted.

[1] I. Hartenbach, F. Lissner, T. Nikelski, S. F. Meier, H. Müller-Bunz, Th. Schleid *Z. Anorg. Allg. Chem.* **2005**, *631*, 2377.
[2] A. F. Holleman, E. & N. Wiberg, *Lehrbuch der Anorganischen Chemie*, 101. Auflage, de Gruyter, Berlin, New York **1995**.

* Prof. Dr. Th. Schleid
E-Mail: schleid@uni-stuttgart.de
[a] Westfälische Wilhelms-Universität Münster,
Institut für Anorganische und Analytische Chemie
Corrensstrasse 28/30, 48149 Münster, Germany
[b] Universität Stuttgart, Institut für Anorganische Chemie
Pfaffenwaldring 55, 70569 Stuttgart, Germany

10.1002/zaac.201605093

On the Road to Pyrite-Type PdS_2 and $PdSe_2$ at High Pressures

Elisabeth Selb[a] and Gunter Heymann*[a]

Keywords: high-pressure, transition-metal chalcogenide, crystal structure, palladium

Under ambient conditions, PdS_2 and $PdSe_2$ crystallize in the PdS_2-type structure, space group *Pbca* (no. 61). The Pd-atoms are coordinated by four *Q*-atoms (*Q* = S, Se) in a square-planar geometry. The PdQ_4 units are interconnected *via* common corners to form jagged and well separated layers, held together by van der Waals forces. Investigations in diamond anvil cells by Soulard *et. al.* showed that the layers are pressed toward each other, until an octahedral coordination geometry at the Pd^{2+}-site is realized, as pressure is applied. As consequence the *c*-parameter decreases, and the pyrite-type structure (space group: $Pa\bar{3}$ no. 205) is adopted.[1,2] This phase transition is reported to be reversible. However, transition structures of PdS_2 and $PdSe_2$ could be stabilized *via* multianvil high-pressure/high-temperature syntheses at 5.5 GPa and 1200 °C, with a significant decrease in *c*-parameter. Single crystal analysis still indicates space group *Pbca* (no. 61) with lattice parameters and refinement results: *a*: 5.520(1) Å, *b*: 5.551(1) Å, *c*: 7.202(2) Å, *R1*: 0.0636, *wR2*: 0.0699 (all data) for PdS_2 and *a*: 5.887(1) Å, *b*: 5.940(1) Å, *c*: 6.851(1) Å, *R1*: 0.0222, *wR2*: 0.0397 (all data) for $PdSe_2$. The two axial positions of each square-planar Pd^{2+}-site are occupied by S- or Se-atoms, resulting in a 4+2 coordination. Atom distances between Pd-atoms and the axial atoms amounts 3.109(2) Å and 2.891(1) Å for PdS_2 and $PdSe_2$, respectively.

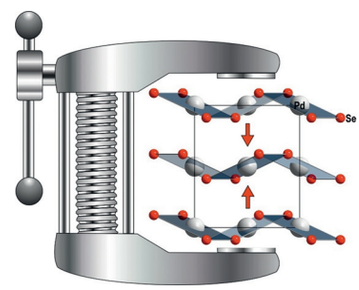

[1] C. Soulard, X. Rocquefelte, P. E. Petit, M. Evain, S. Jobic, J. P. Itié, P. Koo, H. J. Munsch, M. H. Whangbo, *Inorg. Chem.* **2004**, *43*, 1943–1949.
[2] F. Gronvold, E. Rost, *Acta Crystallogr.* **1957**, *10*, 329–331.

* Gunter Heymann
E-Mail: Gunter.Heymann@uibk.ac.at
[a] Institut für Allgemeine, Anorganische und Theoretische Chemie,
Universität Innsbruck
Innrain 80–82
6020 Innsbruck, Austria

 © 2016 WILEY-VCH Verlag GmbH & Co. KGaA, Weinheim

10.1002/zaac.201605094

Cubically Stabilized CeO_2–Er_6MoO_{12} and CeO_2–Yb_6MoO_{12} Solid Solutions

Daniel Schildhammer,[a] Gerda Fuhrmann,[a] Lucas L. Petschnig,[a] Michaela Kogler,[b] Herwig Schottenberger,[a] and Hubert Huppertz*[a]

Keywords: Fluorite-type structure, Rare earth molybdenum oxide, Ion conductivity

Fast oxide-ion conductors are important functional materials that can be used for many applications ranging from solid oxide fuel cells (SOFCs) to oxygen pumping devices.[1,2] Various systems of ternary rare earths oxides containing molybdenum were reported to show, when crystallizing in fluorite-type structures, high oxide ion conductivity with potential application in SOFCs.[3,4]

Here, the successful synthesis and stabilization of $Yb_5CeMoO_{12.5}$ and $Er_5CeMoO_{12.5}$ in a cubic defect fluorite *Fm*3 - *m* structure under ambient atmosphere at high temperatures is reported. Generally, rare earth molybdenum oxides RE_6MoO_{12} with smaller rare earths (*RE* = Er, Tm, Yb, Lu) crystallize in the rhombohedral *R*3 – defect fluorite structure. Through partial substitution of each sixth Yb^{3+} or Er^{3+} by Ce^{4+}, a phase transition from the rhombohedral to the cubic structure was achieved. The compounds were prepared by calcination at 1250 °C of a precursor obtained from a solution combustion reaction. The crystal structure analysis was performed by XPRD and Rietveld refinement.

Furthermore, characterization by electrochemical impedance spectroscopy was carried out revealing similar high electrical conductivities for the new cubic rare earth molybdenum oxides as for the conventional YSZ.

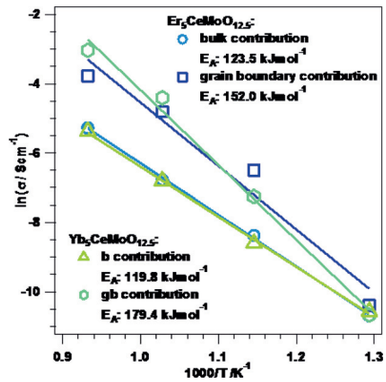

[1] B. C. H Steele, High Conductivity Solid Ionic Conductors, Recent Trends and Applications, **1989,** 402–446.
[2] J. C. Boivin, G. Mairesse, *Chem. Mater.* **1998**, *10*, 2870–2888.
[3] Q. Bo, J. Feng, P. Che, J. Wang, Q. Wang, X. Cao, J. Meng, *J. Phys.: Condens. Matter* **2003**, *15*, 5181–5190.
[4] M. Tsai, M. Greenblatt, W. H. McCarroll, *Chem. Mater.* **1989**, *1*, 253–259.

* Univ.-Prof. Dr. H. Huppertz
E-Mail: hubert.huppertz@uibk.ac.at
[a] Institut für Allgemeine, Anorganische und Theoretische Chemie, Leopold-Franzens-Universität Innsbruck, Innrain 80-82, 6020 Innsbruck, Austria
[b] Institut für Physikalische Chemie, Leopold-Franzens-Universität Innsbruck, Innrain 80-82, 6020 Innsbruck, Austria

 © 2016 WILEY-VCH Verlag GmbH & Co. KGaA, Weinheim

10.1002/zaac.201605095

In-situ Monitoring of Calcium Phosphate Phase Transitions: a Spectroscopic Approach

Anna-Maria Tsirigoni,[a] Laura Ruiz Arana,[a] Patric Lindenberg,[a] and Huayna Terraschke*[a]

Keywords: ILACS, calcium phosphates, *in-situ* luminescence, calcium hydroxylapatite, coordination sensors

Calcium phosphates (CaP) are major inorganic constituents of the human body, especially in bone and teeth minerals.[1] Understanding the transitions *in-situ* between the different phases of CaP offers new insights on comprehending the conversions between healthy and diseased tissues. In this work, the new *in-situ* luminescence analysis of coordination sensors (ILACS)[2] technique is employed, incorporating lanthanide ions as Ce^{3+} and Eu^{3+} to CaP and monitoring their spectroscopic changes during the conversion between e.g. $Ca_3(PO_4)_5OH$ (**1**), $CaHPO_4{\cdot}2H_2O$ (**2**), $CaHPO_4$ (**3**) and $Ca_8H_2(PO_4)_6{\cdot}5H_2O$ (**4**), under real reaction conditions (Fig. 1). Formation of **1** and its conversion to **2** were detected, for instance, through the strong increase and decrease on the intensity assigned to the f-d electronic transition of Ce^{3+}, respectively. No significant structural change was observed applying different types of coordination sensor (Eu^{3+} or Ce^{3+}), while doping concentrations above 3% caused shifts on the CaP phase transitions. Decreasing the total solution concentration from 0.15 M to ca. 0.05 M cause the conversion from **2** to **4** instead of from **2** to **3**. Hence, ILACS could successfully complement other *in-situ* methods for detecting CaP phase transitions.

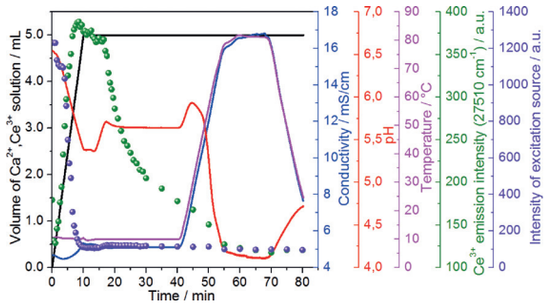

Figure 1. Phase transitions on CaP:Ce^{3+} monitored by *in-situ* luminescence (green curve, λ_{ex} = 310 nm), pH (red curve) and conductivity (blue curve).

[1] Q. Zhang, Y. Jiang, B. Gou, J. Huang, Y. Gao, J. Zhao, L. Zheng, Y. Zhao, T. Zhang, K. Wang, *Cryst. Growth Des.*, **2015**, *15*, 2204–2210.
[2] H. Terraschke, L. R. Arana, P. Lindenberg, W. Bensch, *Analyst,* **2016**, *141*, 2588–2594.

* Dr. H. Terraschke
E-Mail: hterrascke@ac.uni-kiel.de
[a] Institute of Inorganic Chemistry, Christian-Albrechts-Universität Kiel, Max-Eyth-Str. 2, 24118 Kiel, Germany

10.1002/zaac.201605096

Characterizing the Crystallization Kinetics of *Ln*(2,2′-Bipyridine)$_2$(NO$_3$)$_3$ (*Ln* = Eu, Tb) by New *in-situ* Luminescence Analysis Technique

Philipp Polzin,[a] Irma Vania Eliani,[a] and Huayna Terraschke*[a]

Keywords: ILACS, *in-situ* luminescence, lanthanides, crystallization kinetics, coordination sensors.

In-situ monitoring the formation of solid materials is essential to enable their rational synthesis and development of new compounds.[1] Hence, the new *in-situ* luminescence analysis of coordination sensors (ILACS)[2] utilizes the sensitivity of lanthanide (*Ln*) ions to the coordination environment to detect structural changes during crystallization processes. Here, the formation of [*Ln*(2,2'-bipyridine)$_2$(NO$_3$)$_3$] (*Ln* = Eu, Tb) was analysed by ILACS during co-precipitation synthesis. The gradual desolvation of the Ln^{3+} ions and attachment of ligands were detected by the exponential increase of the intensity of the $^5D_0 \rightarrow {}^7F_J$ (J = 0–4) and $^5D_4 \rightarrow {}^7F_J$ (J = 3–6) transitions (Fig. 1), additionally revealing similar crystallisation rates for Eu^{3+} and Tb^{3+} complexes, respectively. Moreover, the *in-situ* emission spectra show the decrease of crystallization rate and nucleation time in 1 min for reducing the concentration of the starting solutions e.g. in 1.2 mM, until ceasing crystallization at ca. 8 mM. Spontaneous nucleation is expected for initial concentrations of ca. 29.5 mM. Therefore, ILACS offers a promising method to monitor and predict crystal growth with a detection limit below 2 mM.

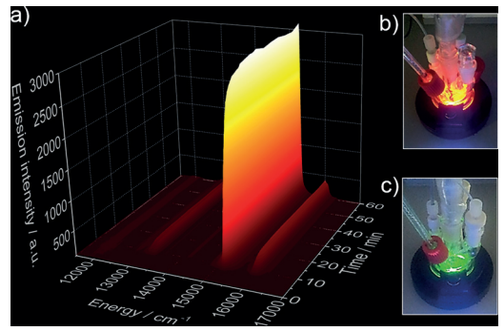

Figure 1. a) *In-situ* luminescence spectra (λ_{ex} = 365 nm) of [Eu(2,2'-bipyridine)$_2$(NO$_3$)$_3$]. b) Eu^{3+} red c) Tb^{3+} green emission of luminescent complexes during the synthesis reaction.

[1] N. Pienack, W. Bensch, *Angew. Chem., Int. Ed.*, **2011**, *50*, 2014–2034.
[2] H. Terraschke, L. R. Arana, P. Lindenberg, W. Bensch, *Analyst,* **2016**, *141*, 2588–2594.

* Dr. H. Terraschke
E-Mail: hterraschke@ac.uni-kiel.de
[a] Institute of Inorganic Chemistry, Christian-Albrechts-Universität Kiel, Max-Eyth-Str. 2, 24118 Kiel, Germany

 © 2016 WILEY-VCH Verlag GmbH & Co. KGaA, Weinheim

10.1002/zaac.201605097

Polymorphism and *in-situ* Detection of Reaction Intermediates on Eu(1,10-Phenanthroline)$_2$(NO$_3$)$_3$

Patric Lindenberg,[a] Laura Ruiz Arana,[a] Niclas Heidenreich,[a] and Huayna Terraschke*[a]

Keywords: reaction intermediates, *in-situ* luminescence, Eu(phen)$_2$(NO$_3$)$_3$, polymorphs, ILACS

Detailed analysis of reaction mechanisms by *in-situ* techniques are crucially important for identifying metastable intermediates, analysing polymorphic transitions and therefore for the discovery of new functional materials.[1] An example of functional material is the luminescent complex Eu(phen)$_2$(NO$_3$)$_3$ (**1**, phen = 1,10-phenanthroline, CSD ECABOZ02),[2] which potential ligand exchange processes upon the presence of other ligands e.g. acetylacetonate (acac) have been investigated here by the *in-situ* luminescence analysis of coordination sensors (ILACS) technique.[3] Complementary experiments at the beamline P07B (PETRA III, DESY) revealed that, for the synthesis conditions expected to lead to the formation of Eu(acac)$_3$phen (**2**), surprisingly, acac was not incorporated. Instead, it led to the formation of a polymorphic phase of **1** (CSD ECABOZ01)[2] and to a decrease of luminescence intensity (Fig. 1, λ_{ex} = 395 nm) at t = 0–7.5 min, indicating the formation of a pre-crystallization reaction intermediate. ILACS shows in addition that the increase of temperature e.g. from 25 °C to 60 °C do not influence the reaction kinetics or the structure of the formed product and represents therefore a powerful tool for monitoring reaction mechanisms.

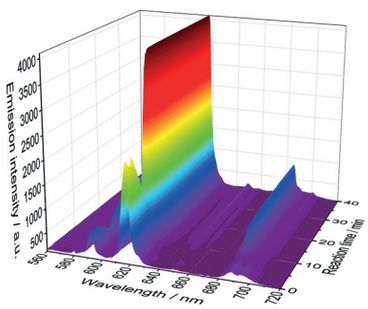

Figure 1. *In-situ* luminescence spectra of the [Eu(phen)$_2$(NO$_3$)$_3$] (λ_{ex} = 395 nm).

[1] N. Pienack, W. Bensch, *Angew. Chem., Int. Ed.* **2011**, *50*, 2014–2034.
[2] F. Werner, K. Tada, A. Ishii, M. Takata, M. Hasegawa, *CrystEngComm*, **2009**, *11*, 1197–1200.
[3] H. Terraschke, L. R. Arana, P. Lindenberg, W. Bensch, *Analyst,* **2016**, *141*, 2588–2594.

* Dr. H. Terraschke
E-Mail: hterrascke@ac.uni-kiel.de
[a] Institute of Inorganic Chemistry, Christian-Albrechts-Universität Kiel, Max-Eyth-Str. 2, 24118 Kiel, Germany.

10.1002/zaac.201605098

$Li_2Sr[Li_{0.5}Fe_{0.5}N]_2$ and Isotypic Phases: mm-Sized Single Crystals with Large Single-Ion Magnetic Anisotropy

Peter Höhn,*[a] Matej Bobnar,[a] Walter Schnelle,[a] Manuel Fix,[b] and Anton Jesche[b]

Keywords: nitridometalates, single crystals, magnetic materials

Low-valency nitridometalates of *d* metals M = Mn^{I} – Cu^{I} are characterized by complex anions $[MN_2]^{5-}$, chain fragments $[M_nN_{n+1}]^{(2n+1)-}$, or 1D chains $[MN]^{2-}$ and $[M_{1-x}Li_x]^{2-}$ with linear coordination of M.[1] Here we report on the investigations on large single crystals of the isotypic series $Li_2Sr[Li_{1-x}M_xN]_2$ ($I4_1/amd$, *#141*; M = Mn (x = 0.7, a = 380.87(3) pm, c = 28.334(4) pm), Fe,[2] Co (x = 0.25, a = 373.41(3) pm, c = 2793.2(5) pm), Ni,[3] Cu[4]) grown by HTCAF (high temperature centrifugation aided filtration).[5]
Magnetization measurements as a function of field and temperature were performed on single crystalline $Li_2Sr[Li_{0.5}Fe_{0.5}N]_2$ with the external field applied parallel and perpendicular to the crystallographic c-axis.
The temperature dependent magnetic susceptibility shows Curie-Weiss behavior with an effective moment of 3.7 μ_B/Fe. Isothermal measurements revealed a huge hysteresis with coercivity fields that exceed 7 Tesla for temperatures below 10 K, making the material one of the hardest ferromagnets known to date. In accordance, a large magnetic anisotropy with the easy axis pointing along the N-Fe-N molecular axis is observed. This indicates an orbital contribution to the magnetic moment in full analogy to $Li_2(Li_{1-x}Fe_x)N$ that shows a similar linear, two-fold coordination of Fe.[6]

[1] R. Kniep, P. Höhn, Comprehensive Inorganic Chemistry II, 2.06 Low-Valency Nitridometalates, Elsevier, **2013**, 137–160.
[2] J. Klatyk, R. Kniep, *Z. Kristallogr. NCS* **1999**, *214*, 449–450.
[3] G. Cordier, A. Gudat, R. Kniep, A. Rabenau, *Angew. Chem. Int. Ed.* **1989**, *28*, 1702–1703.
[4] J. Jäger, R. Kniep, *Z. Naturforsch.* **1992**, *47b*, 1290–1296.
[5] M. Boström, S. Hovmöller, *J. Alloys Compd.* **2001**, *314*, 154–159.
[6] A. Jesche, R. W. McCallum, S. Thimmaiah, J. L. Jacobs, V. Taufour, A. Kreyssig, R. S. Houk, S. L. Bud'ko, P. C. Canfield, *Nat Commun* **2014**, *5*, 3333.

* Dr. P. Höhn
E-Mail: hoehn@cpfs.mpg.de
[a] MPI-CPfS
Nöthnitzer Str. 40
01187 Dresden, Germany
[b] Universität Augsburg
Institut für Physik
Universitätsstraße 1
86135 Augsburg, Germany

 © 2016 WILEY-VCH Verlag GmbH & Co. KGaA, Weinheim

10.1002/zaac.201605099

$Li_{16}Sr_6M_6N$ (M = Ge, Sn, Pb) – Cubic Tetrelide-Nitrides with an Ordered Ir_4Sc_{11} Type Structure

Manisha Pathak,*[a] Matej Bobnar,[a] Walter Schnelle,[a] Peter Höhn,[a] and Yuri Grin[a]

Keywords: tetrelide-nitrides, crystal structure, structural relationship

Depending on preparation conditions and composition, the known phases in the quaternary systems Li–*AE*– *M* – N (*AE* = Ca, Sr, Ba; *M* = Ge, Sn, Pb) range from nitridotetrelates (e.g. $Ca_3[GeN_3]$[1]) via nitride-tetrelides (e.g. Sr_3SnN[2]) to intermetallic species.
Large single crystals of $Li_{16}Sr_6M_6N$ (M = Ge, Sn, Pb) were grown in lithium melts by modified high-temperature centrifugation aided filtration (HTCAF).
The phases crystallize cubic ($Fm\bar{3}m$ (#225); M = Ge: a = 1347.68(1) pm, Sn: a = 1406.40(1) pm, Pb: a = 1414.94 (1) pm). The crystal structure may be derived from $Sc_{11}Ir_4$[3] via $Ln_3Pd_8Sb_4$[4] and $U_6Fe_{16}Si_7C$[5] and described as $Sr_6Li_{16}M_6\square N$ exhibiting close relations to $Mn_{23}Th_6$.[6]
The Ge sample shows diamagnetism and a resistivity of about $1\cdot10^{-3}$ Ωm.

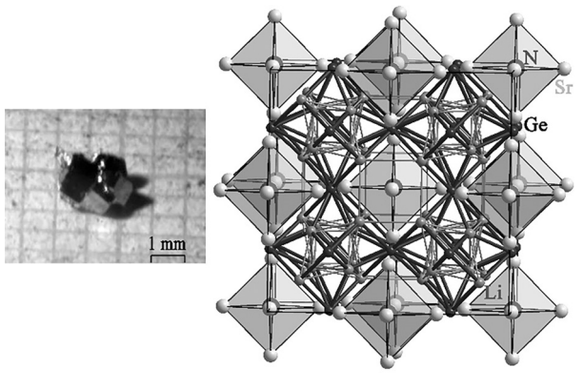

Figure 1. Crystal aggregate grown by HTCAF (left) and crystal structure (right) of $Li_{16}Sr_6Ge_6N$.

[1] M. Pathak et al., *ECSSC Proceedings* **2015**, *15*, 63–63.
[2] P. Höhn et al., *ECSSC Proceedings* **2015**, *15*, 189–189.
[3] B. Chabot, K. Cenzual, E. Parthe. *Acta Crystallogr., Sect. B* **1980**, *36*, 7–11.
[4] M. Zelinska et al., *J. Solid State Chem.* **2010**, *183*, 2121–2126.
[5] D. Berthebaud et al., *J. Solid State Chem.* **2007**, *180*, 2926–2932.
[6] J. V. Florio et al., *Acta Crystallogr.* **1952**, *5*, 449–457.

* Manisha Pathak
E-Mail: manisha.pathak@cpfs.mpg.de
[a] MPI-CPfS
Nöthnitzer Str. 40
01187 Dresden, Germany

10.1002/zaac.201605100

$Li_2Ag_7Sb_3S_9$ – A Compound in the Quasi-Binary System Li_3SbS_3 – Ag_3SbS_3

Thomas Rothenaigner[a] and Arno Pfitzner*[a]

Keywords: Crystal Structure, Ionic Conductor, Lithium Silver Antimony Sulfide

In literature there are many compounds known with the composition M_3SbS_3 (M = Ag[1], Cu[2,3], Li[4], Na[5], K[6] , Rb[6], Cs[6]). We investigated the quasi-binary section Li_3SbS_3 – Ag_3SbS_3 for new quaternary materials. $Li_2Ag_7Sb_3S_9$ has been synthesized by high temperature reaction of Li_2S, Ag_2S and Sb_2S_3. The crystal structure of $Li_2Ag_7Sb_3S_9$ was determined by single-crystal X-ray diffraction. The title compound crystallizes in the orthorhombic space group *Pnma* (No. 62) with a = 24.411(3) Å, b = 10.620(1) Å, c = 6.939(1) Å, V = 1798.9(5) Å^3, and Z = 4. The anionic substructure of $Li_2Ag_7Sb_3S_9$ consists of trigonal-pyramidal SbS_3, tetrahedral LiS_4 and trigonal-planar AgS_3 units. (Figure 1).
Thermal analysis revealed a reversible phase transition at 235°C and a melting point of 480°C.
The compound was further characterized by Raman spectroscopy. The Sb-S vibrations at 320 cm^{-1} and 287 cm^{-1} are in good agreement with data in literature[7]. Impedance spectroscopy shows an ionic conductivity of 10^{-7} S/cm at room temperature and 10^{-3} S/cm at 300°C.

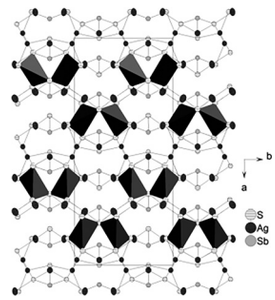

Figure 1. Section of the crystal structure of $Li_2Ag_7Sb_3S_9$. Lithium is located in the distorted tetrahedra.

[1] F. Laufek, J. Sejkora, M. Dusek, *J. Geosci.* **2010**, *23*, 21–26.
[2] E. Makovicky, T. Balic-Zunic, *Can. Mineral.* **1995**, *33*, 655–663.
[3] A. Pfitzner, *Z. Anorg. Allg. Chem.* **1994**, *620*, 1992–1997.
[4] S. Huber, C. Preitschaft, R. Weihrich, A. Pfitzner, *Z. Anorg. Allg. Chem.* **2012**, *638*, 2542–2548.
[5] C. Pompe, A. Pfitzner, *Z. Anorg. Allg. Chem.* **2013**, *639*, 296–300.
[6] L. Schindler, M. Schwarz, C. Röhr, *Z. Naturforsch.* **2013**, *68b*, 1295–1309.
[7] A. Pfitzner, *Chem. Eur. J.*, **1997**, *3*, 2032–2038.

* Prof. Dr. A. Pfitzner
E-Mail: arno.pfitzner@chemie.uni-regensburg.de
[a] Institut für Anorganische Chemie
Universität Regensburg
Universitätsstraße 31
93040 Regensburg, Germany

 © 2016 WILEY-VCH Verlag GmbH & Co. KGaA, Weinheim

10.1002/zaac.201605101

$ScCl[SeO_3]$: The Chloride Oxoselenate(IV) of the Smallest Rare-Earth Metal

Stefan Greiner[a] and Thomas Schleid*[a]

Keywords: Scandium, Oxoselenates, Chlorides, Pentagonal Bipyramid

The scandium chloride oxoselenate(IV) $ScCl[SeO_3]$ crystallizes in the orthorhombic space group *Pnma* with a = 702.48(5), b = 653.81(4), c = 838.74(6) pm and Z = 4 (CSD-430692). This composition MCl[SeO_3] is already known with M = Nd, Sm – Lu[1–3], and all representatives except for the neodymium compound exhibit the same HoCl[TeO_3]-type crystal structure[4]. The Sc^{3+} cations are surrounded by two chloride anions and five oxygen atoms, which belong to four ψ^1-tetrahedral $[SeO_3]^{2-}$ units, in the shape of a pentagonal bipyramid $[ScO_5Cl_2]^{9-}$ with $Sc^{3+}-O^{2-}$ distances between 203 and 222 pm. These values correlate well with those in $Sc_2[SeO_3]_3$[5]. Also the $Sc^{3+}-Cl^-$ distances ranging from 257 to 267 pm accord with those in $ScCl_3$[6,7]. The pentagonal bipyramids are connected via common O2···O2 edges to form chains with the formula •**FORMEL unleserlich!!!**•, which spread along the b-axis. For the connection of these polyhedra a rotation of 180° is necessary. The complete three-dimensional crystal structure is achieved by their linkage via common $[SeO_3]^{2-}$ tripods and Cl^- anions.

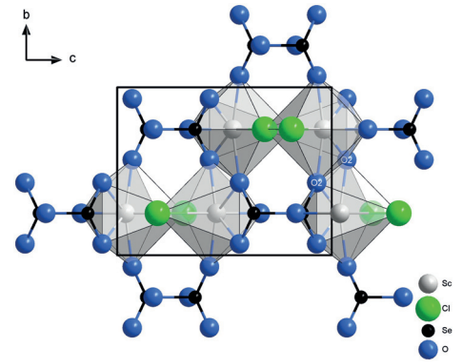

Figure 1. Fusion of the pentagonal bipyramids $[ScO_5Cl_2]^{9-}$ via common O2···O2 edges to •**FORMEL unleserlich!!!**• chains and their interconnection to a three-dimensional network via common $[SeO_3]^{2-}$ and Cl^- linkers.

[1] C. Lipp, Th. Schleid, *Z. Naturforsch.* **2008**, *63b*, 229−236.
[2] M. S. Wickleder, *Acta Crystallogr., Sect. E* **2003**, 59, i31−i32.
[3] M. S. Wickleder, *Z. Naturforsch.* **2002**, *57b*, 1414−1418.
[4] S. F. Meier, Th. Schleid, *Z. Anorg. Allg. Chem.* **2002**, *628*, 526−528.
[5] J. Wontcheu, Th. Schleid, *Z. Anorg. Allg. Chem.* **2003**, *629*, 1463−1465.
[6] W. Klemm, E. Krose, *Z. Anorg. Allg. Chem.* **1947**, *253*, 218−225.
[7] H. Fjellvåg, P. Karen, *Acta Chem. Scand.* **1994**, *48*, 294−297.

* Prof. Dr. Th. Schleid
E-Mail: schleid@iac.uni-stuttgart.de
[a] University of Stuttgart
Institute for Inorganic Chemistry
Pfaffenwaldring 55
70569 Stuttgart, Germany

 © 2016 WILEY-VCH Verlag GmbH & Co. KGaA, Weinheim

10.1002/zaac.201605102

Fluorine-Doped Layered Cathode Materials

Jan O. Binder,*[a] Ricardo Pinedo,[a] Dominik Weber,[a] Kai Weldert,[a] M. S. Friedrich,[a] Wolfgang Zeier,[a] and Jürgen Janek[a]

Keywords: NCM, Doping

High energy-density lithium ion batteries (LIBs) are in demand for electronic devices and electrical vehicles. Since the energy density of these batteries relies heavily on the cathode material, a great deal of attention is being focused on developing alternative materials. Layered Lithium nickel cobalt manganese oxides (NCM) can deliver high capacities at low costs. However, there are still problems associated with their cycle life, thermal stability, and safety[1].

The barrier for lithium migration through a 1-TM channel is correlated to the areal lithium–TM separation. This varies with the width of the Li layer (the distance between TM-O slabs), constraining the degree of local relaxation for the TM when lithium enters the activated state[2]. Nevertheless, the Li slab distance highly varies during discharge-charge processes leading to cell volume fluctuations which are considered a potential source of electrode degradation.

One approach to control the Li slab distance in high Ni materials is anionic substitution[3]. In this work, the effect of F doping is evaluated. The doping process was carried out by different post-calcination treatments in NCM materials, and a correlation between structural parameters and electrochemical performance has been established. By controlling the post-calcination parameters, the effect of F can be restricted to the materials surface. The stabilization of surfaces in NCM materials is a fundamental challenge in order to control the aging processes of these electrodes.

[1] L. Wu et al. *Chem. Mater.* **2011**, *23*, 3953.
[2] K. Kang et al. *Phys. Rev. B* **2006**, *74*, 094105.
[3] F. Kong et al., *J. Mater. Chem. A* **2015**, *3*, 8489.

* MSc. J. Binder
E-Mail: Jan.Binder@phys.chemie.uni-giessen.de
[a] Physikalisch-Chemisches Institut,
Justus-Liebig-Universität Gießen
Heinrich-Buff-Ring 17.
35392 Gießen, Germany

10.1002/zaac.201605103

Making the Most of Neutron-Diffraction Data: Lithium Diffusion Pathways in Ramsdellite-Like $Li_2Ti_3O_7$

Dennis Wiedemann,*[a] and Alexandra Franz[b]

Keywords: Neutron powder diffraction; Voronoi–Dirichlet partitioning; Procrystal void surface; Maximum-entropy methods

Ramsdellite-like $Li_2Ti_3O_7$ exhibits fast and strongly anisotropic lithium-ion conduction. Although proposed applications range from energy storage to lithium processing, the crucial diffusion pathways in this material have not yet been studied in depth; even aspects of its crystal structure are still under discussion. In our studies, we have examined $Li_2Ti_3O_7$ using variable-temperature neutron diffraction to probe its nontrivial lithium-ion distribution. At 24 °C, a Rietveld-refined structural model with anharmonic-anisotropic displacement parameters shows a statically disordered snapshot of the dynamic behavior during synthesis. Reconstruction of the scattering-length density *via* maximum-entropy methods (MEM) indicates successive partial relaxation and activation of lithium movement with increasing temperature in the metastability range. Using topological analyses of procrystal voids and Voronoi–Dirichlet partitioning (VDP), we have identified two pathways of lithium diffusion: interstitial migration along ribbons as the major, framework migration through vacancies as the most probable minor mechanism. Thus, we explain former empirical results and shed light on this paradigmatic lithium-ion conductor.

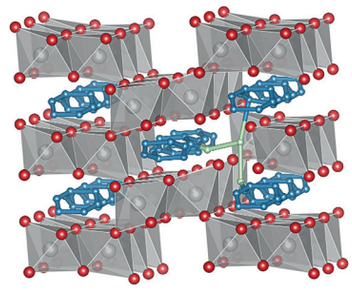

Figure 1. Void structure of the $Ti_3O_7^{2-}$ framework at 422 °C (VDP analysis). Gray: titanium, red: oxide ions; blue: preferred, green: probabilistic voids/channels.

* Dr. D. Wiedemann
E-Mail: dennis.wiedemann@chem.tu-berlin.de
[a] Institut für Chemie
Technische Universität Berlin
Straße des 17. Juni 135
10623 Berlin, Germany
[b] Abteilung Struktur und Dynamik von Energiematerialien
Helmholtz-Zentrum Berlin für Materialien und Energie
Hahn-Meitner-Platz 1
14109 Berlin, Germany

 © 2016 WILEY-VCH Verlag GmbH & Co. KGaA, Weinheim

10.1002/zaac.201605104

Synthesis of New Lanthanide Hydride Oxides *Ln*HO (*Ln* = Sm, Gd, Ho, Er)

Anton Werwein,*[a] Holger Kohlmann,[a] and Shaine Raseale[a]

Keywords: Rare earths; Hydride oxides

Lanthanide oxide fluoride are widely researched and the structures are well known.[1] LaOF crystalize in the fluorite structure type, with a statistical distribution, where the oxide and the fluoride atoms are in mixed anion position. But about Hydride oxides in general are not known so much. The compound LaHO was first synthesized by Malaman and resemble a ordered fluorite type, where the lanthanide atoms are arranged at three different positions.[2] Other hydride oxides known so far are *Ln*HO (*Ln* = Ce, Nd), which are isotype to LaHO.[3,4] The synthesis of four new lanthanide hydride oxide was successfully achieved for the lanthanides Sm, Gd, Ho, Er. The compounds were made by the reaction of the oxides Ln_2O_3 and the corresponding hydride LnH_3 at 550 °C and 20 bar hydrogen pressure in an Inconel autoclave. The colorless products were characterized by X-ray powder-diffraction. The compounds crystallize in the tetragonal space group *P*4/*nmm* and are also isotypic to LaHO. According to Rietveld refinement oxygen atoms are surrounded by a distorted tetrahedral arrangement of *Ln* atoms (Tab.1). The Lattice parameters reflects the lanthanide contraction.

Table 1. *Ln*–O bond lengths.

Compound	a /Å	c /Å	d *Ln*–O /Å
SmHO	7.7381(2)	5.4614(4)	Sm1 2.250(6)Sm2 2.359(4)Sm3 2.336(5)
GdHO	7.65286(15)	5.4116(3)	Gd1 2.217(8)Gd2 2.334(5)Gd3 2.308(7)
HoHO	7.4724(3)	5.3034(4)	Ho1 2.263(7)Ho2 2.30(1)Ho3 2.202(6)
ErHO	7.4099 (12)	5.2588 (19)	Er1 2.263(8)Er2 2.293(6)Er3 2.218(6)

[1] W. Klemm, H. A. Klein, *Z. Anorg. Allg. Chem.* **1950**, *248*, 167–171.
[2] B. Malaman, J.F. Brice, *J. Solid State Chem.* **1984**, *53*, 44–54.
[3] M. Tellefson, E. Kaldis, E. Jilek, *J. Less-Common-Met.* **1985**, *110*, 107–117.
[4] M. Wideroe *et al*, *J. Solid State Chem.* **2011**, *184*, 1890–1894.

* Prof. Dr. H. Lohlmann
E-Mail: holger.kohlmann@uni-leipzig.de
[a] Institut für Chemie
Universität Leipzig
Johannisallee 29.
04103 Leipzig, Germany

10.1002/zaac.201605105

Modulated Vacancy Ordering in $SrGe_{6-x}$

Lev Akselrud,[a] Aron Wosylus,[a] Rodrigo Castillo,[a] Bernhard Wahl,[b] Thomas Doert,[b] and Ulrich Schwarz*[a]

Keywords: high-pressure synthesis, germanium, incommensurate modulation

Synthesis of tetrel-rich compounds at extreme conditions opens a pathway to new network patterns with often unfamiliar coordination environments and unusual topology. An earlier study on the metastable high-pressure phase $SrGe_{6-x}$ (x = 0.5) reported a $EuGa_2Ge_4$–type[1,2] crystal structure comprising disordered defects at one of the three symmetry independent germanium network positions[3]. However, a more recent investigation on the corresponding barium compound $BaGe_{5.5}$[4] evidenced incommensurate ordering of the defects resulting in a modulated super-structure.
This finding motivated a reinvestigation, and samples of the phase $SrGe_{6-x}$ ($x \approx 0.5$) were synthesized at 5 GPa and annealed at 1200 K for several hours before quenching to ambient conditions. This procedure yields single crystals which exhibit distinct reflections indicating an ordered superstructure of the $EuGa_2Ge_4$ aristotype. A detailed analysis reveals an incommensurately modulated ordering of vacancies in the germanium network. Based on powder X-ray diffraction data, four-dimensional indexing yields space group *Cmcm*[00*s*] with lattice parameters a = 4.1036(2), b = 11.1814(6) and c = 12.6934(6) with a modulation vector q = [0.5510(1), 0, 0] in which the first component deviates significantly from the rational value 5/9 = 0.5555. Physical measurements reveal that the compound exhibits metal-type electrical conductivity.

[1] J. D. Bryan, G. D. Stucky, *Chem. Mater.* **2001**, 13, 253–257.
[2] W. Carrillo-Cabrera, S. Paschen, Yu. Grin, *J. Alloys Compd.* **2002**, 333, 4–12.
[3] H. Fukuoka, S. Yamanaka, E. Matsuoka, T. Takabatake, *Inorg. Chem.,* **2005,** *44,* 1460–1465.
[4] L. Akselrud, A. Wosylus, R. Castillo, U. Aydemir, Yu. Prots, W. Schnelle, Yu. Grin, U. Schwarz, *Inorg. Chem.* **2014**, 53, 12699–12705.

* Dr. Ulrich Schwarz
E-Mail: schwarz@cpfs.mpg.de
[a] MPI für Chemische Physik fester Stoffe
Nöthnitzer Str. 40
01187 Dresden, Germany
[b] Technische Universität Dresden
Institut für Anorganische Chemie
Bergstraße 66
01062 Dresden, Germany

 © 2016 WILEY-VCH Verlag GmbH & Co. KGaA, Weinheim

10.1002/zaac.201605106

Zr-Metal-Interactions in Thin Film and Intermetallic Compound Systems in Fuel Reforming Processes

Norbert Köpfle,*[a] Lukas Mayr,[a,b] Xue-Rong Shi,[a] Dmitry Y. Zemlyanov,[b] Johannes Bernardi,[c] Sabine Schwarz,[c] Marc Armbrüster,[d] Simon Penner,[a] and Bernhard Klötzer[a]

Keywords: ((MSR, $Cu/Cu_{51}Zr_{14}$ pre-catalyst, inverse Pd-ZrO_xH_y and Cu-ZrO_xH_y model catalysts))

An in situ activating bimetallic $Cu/Cu_{51}Zr_{14}$ pre-catalyst for hydrogen generation from methanol and water, prepared by intermetallic co-melting, yields very high CO_2-selectivity (>99.9 %) and thus H_2 yields. Evolution of structural activation monitored by X-ray diffraction (XRD), X-ray photoelectron spectroscopy (XPS) and electron microscopy indicates transformation of the initially bimetallic $Cu/Cu_{51}Zr_{14}$ pre-catalyst into an active, selective and self-stabilizing state with coexistence of dispersed Cu and partially hydroxylated tetragonal ZrO_2. The outstanding performance is assigned to the presence of a high interface site concentration following in situ decomposition of the intermetallic compound. The active interfacial sites result from a teamwork of Cu, responsible for methanol activation, and tetragonal ZrO_2, activating water via surface hydroxylation.

Beyond intermetallic melt preparation, inverse Pd-ZrO_xH_y and Cu-ZrO_xH_y model catalysts were prepared by chemical vapor deposition (CVD) using a zirconium-t-butoxide (ZTB) precursor. Depending on post-treatments, either ZrO_xH_y or ZrO_2 overlayers or Zr as sub-nanometer metal clusters could be obtained. As a practical consequence of Zr redox activity, the initially bimetallic Pd-Zr precatalysts showed pronounced activity for dry reforming of methane, which is attributed to the synergistic bifunctional cooperation of Pd and ZrO_xC_y surface species.

[1] L. Mayr, B. Klötzer, D. Schmidmair, N. Köpfle, J. Bernardi, S. Schwarz, M. Armbrüster, S. Penner, *ChemCatChem* **2016**, *8*, 1778–1781.

* N. Köpfle
E-Mail: norbert.koepfle@uibk.ac.at
[a] Institute of Physical Chemistry, University of Innsbruck
Innrain 80–82, 6020 Innsbruck, Austria
[b] Birck Nanotechnology Center, Purdue University
1205 West State Street, West Lafayette, IN 47907, USA
[c] USTEM, TU Wien
Wiedner Hauptstraße 8-10/052, A-1040 Wien, Austria
[d] Faculty of Natural Science, Institute of Chemistry
Materials for Innovative Energy Concepts,
Technical University of Chemnitz, D-09107 Chemnitz, Germany

 © 2016 WILEY-VCH Verlag GmbH & Co. KGaA, Weinheim